Transmucosal delivery of insulin for diabetes therapy: Development and evaluation of a mucoadhesive buccal patch comprising insulin loaded transfersomes

NAJMA EASA

A thesis submitted in fulfilment of the requirements for the degree of

Doctor of Philosophy,

Kingston University London, United Kingdom

NOVEMBER 2020

Abstract

Background and Aim: The International Diabetes Federation suggests in 2017, around 451 million adults around the globe were affected by diabetes mellitus. Worldwide, invasive subcutaneous injection devices remain the standard for diabetes treatment. To increase patient adherence, and to help reduce the anxiety of painful daily administration of insulin this study investigated the prospect of using ultradeformable vesicles, known as transfersomes, to act as carriers and permeation enhancers for the delivery of insulin. The overall aim was the development of a double-layered patch, in which the transfersomes were embedded in the mucoadhesive layer, and the presence of an outer impermeable layer enabled the formation of a novel unidirectional immobilized delivery system for buccal delivery of insulin.

Methods: A reverse phase HPLC method was developed and validated, according to ICH guidelines, for the detection and quantification of insulin. Vesicles were formed using a thin-film hydration technique with bath sonication, and manual extrusion was used for further downsizing. Throughout the project, vesicles were evaluated for particle size, polydispersity index, zeta potential and insulin encapsulation efficiency (EE, %). Permeability of insulin was studied across TR146 buccal cell line, and sulforhodamine B (SRB) assay was used for in-vitro cytotoxicity screening. Minitab factorial design was employed to optimise mucoadhesiveness of lyophilised patches.

Results and Discussion: Analysis and quantification of insulin with HPLC demonstrated insulin to degrade much faster in acidic conditions. Preliminary studies led to the selection of Span 60, which was combined with the phospholipid DPPE (1,2-dipalmitoyl-3-sn-phosphatidylethanolamine) to produce transfersomes. Membrane

fluidity was enhanced by the addition of Tween 80 and reduction of cholesterol content. Based on toxicity studies, the two promising formulations consisted of Span 60 (40%), DPPE (20%), Tween 80 (20%), cholesterol (15%), with either 5% dicetyl phosphate (D5E) or 5% sodium glycodeoxycholate (S5E). Insulin release from patch S [sodium alginate (2% w/v), HPMC (0.5% w/v), Sorbitol (5% w/v) and PEG 400 (0.25% w/v)] was found to occur as burst release with 75% of the total insulin being released in the first 30 minutes. The most promising percentage drug release (66.5%), in 6 hours, was with patch S containing the transfersomal formulation D5E.

Conclusion: This thesis demonstrated an excellent approach in delivering insulin via a non-invasive route by combining novel transfersomes as permeation enhancers within an optimised mucoadhesive buccal patch. Furthermore, the project led to the generation of new data and observations concerning the influence of extrusion and vortexing on vesicle size, use of CytoSMART for cell imaging, use of actinomycin D as positive control in SRB cytotoxicity assays with TR146 cells and influence of the cryoprotectant sorbitol on mucoadhesion combined with HPMC, sodium alginate and chitosan in freeze-dried patches.

Keywords: Insulin, diabetes, buccal, non-invasive, transfersomes, vesicles, TR146 cells, HPLC, patch, mucoadhesion

Dedication

I dedicate this thesis to my parents, who through their hard work, have been my beacon of encouragement. I cannot thank them enough for their support, trust, and everything that they have done for me.

Acknowledgements

Firstly, I thank the Almighty for the strength and the will to complete my research and this thesis. I am particularly thankful for my first Supervisor Dr Anil Vangala for his continuous support, guidance, experience, and encouragement with all aspects of my PhD. I am also grateful for my co-supervisors Professor Raid G. Alany and Dr Mark Carew for their knowledge and involvement.

Furthermore, I am very thankful for the continuous assistance and ideas from Dr Siamak Soltani, Dr Ali Al-Kinani, Dr Amanda Munasinghe, and Amtul Bhunnoo throughout my project.

I would also like to express my gratitude to Dr Lauren Mulcahy-Ryan, Professor Mehmet Dorak, Professor Peter J. Foot, and Richard Giddens for their assistance in the various areas of my project.

Finally, I am ever grateful for my friends and family solely for their presence and encouragement for me to complete my research successfully.

List of publications and presentations

1. Poster presentation at the annual SEC conference, May 2018, Kingston University, London, UK. Attained 1st prize.

2. Oral presentation at the 3-Minute Thesis competition, June 2018, Kingston University, London, UK. Attained 2nd prize.

3. Poster presentation at the Academy of Pharmaceutical Sciences (APS) conference, September 2018, Hilton Hotel, Glasgow, UK.

4. A keynote review published with Drug Discovery Today titled "A review of non-invasive insulin delivery systems for diabetes therapy in clinical trials over the past decade", (https://doi.org/10.1016/j.drudis.2018.11.010) [1].

5. Oral presentation at the annual Science, Engineering and Computing (SEC) conference, April 2019, Kingston University, London, UK.

6. Poster presentation at the United Kingdom and Ireland Controlled Release Society's (UKICRS) Symposium, June 2019, John Moores University, Liverpool, UK.

Contents

List of figures

List of tables

List of abbreviations

ACN	Acetonitrile
APS	Academy of Pharmaceutical Sciences
AUC	Area under the curve
CEO	Chief executive officer
cm	Centimetre
CMC	Carboxymethylcellulose
Da	Dalton
DCCT	Diabetes control and complications trial
DCP	Dicetyl phosphate
DLS	Dynamic light scattering
DMSO	Dimethyl sulfoxide
DOE	Design of experiment
DPI	Dry powder inhaler
DPPE	1,2-dipalmitoyl-3-sn-phosphatidylethanolamine
DSC	Differential scanning calorimetry
EDTA	Ethylenediaminetetraacetic acid

EE	Encapsulation efficiency
ELISA	Enzyme-linked immunosorbent assay
EMA	European Medicine Agency
ER	Endoplasmic reticulum
EU	European Union
FBS	Fetal bovine serum
FDA	Food and Drug Administration
FDKP	Fumaryl diketopiperazine
FITC	Fluorescein isothiocyanate
GI	Gastrointestinal
GIPET	Gastrointestinal permeation enhancement technology
GIT	Gastrointestinal tract
GNP	Gold nanoparticle
GRAS	Generally recognised as safe
GTP	Guanosine-5-triphosphate
HBSS	Hank's balanced salt solution

HDV	hepatocyte directed vesicle
HEC	Hydroxyethylcellulose
HEPES	Hydroxyethylpiperazine ethane sulfonic acid
HLB	Hydrophilic lipophilic balance
HPC	Hydroxypropyl cellulose
HPLC	High-performance liquid chromatography
HPMC	Hydroxypropyl methylcellulose
HTM	Hepatocyte-targeting molecule
ICH	International Conference on Harmonization
IND	Investigational new drug
IS	Internal standard
IU	International unit
kDa	Kilodalton
LC	Loading capacity
LDE	Laser doppler electrophoresis
LMW	Low molecular weight
LOD	Limit of detection

LOQ	Limit of quantification
LUV	Large unilamellar vesicles
MHRA	Medicines and Healthcare products Regulatory Agency
mg	Milligram
Min	Minute
mL	Millilitre
mm	Millimetre
MLV	Multilamellar vesicles
MS	Mass spectrometry
NA	Not applicable
NCEs	New chemical entities
NCT	National clinical trial
nm	Nanometre
PAA	Poly (acrylic acid)
PBS	Phosphate buffered saline
PDI	Polydispersity index

PDM	Personal diabetes manager
PE	Phosphatidylethanolamine
PEG	Polyethylene glycol
PLGA	Poly (lactic-co-glycolic acid)
POD	Protein Oral Delivery^{TM}
QC	Quality control
RI	Refractive index
RHI	Recombinant human insulin
RP-HPLC	Reverse-phase HPLC
RSD	Relative standard deviation
sc	Subcutaneous
SD	Standard deviation
SEC	Science, Engineering and Computing
SEM	Scanning electron microscopy
SGDC	Sodium glycodeoxycholate
SRB	Sulforhodamine B
SRP	Signal recognition particle

SUV	Small unilamellar vesicles
T1DM	Type 1 diabetes mellitus
T2DM	Type 2 diabetes mellitus
TCA	Trichloroacetic acid
TEER	Transepithelial electrical resistance
TFA	Trifluoroacetic acid
T_{max}	Maximum serum insulin
UK	United Kingdom
UKICRS	UK & Ireland Controlled Release Society
USA	United States of America
U-Strip	Ultrasonic Strip
UV	Ultraviolet
WHO	World Health Organisation
XRD	X-ray diffraction
µg	Microgram
µL	Microlitre
µm	Micrometre

1. Introduction

1.1 Overview of diabetes mellitus and insulin

Diabetes mellitus (DM) affects a considerable proportion of the population worldwide. It is estimated, by the International Diabetes Federation, that in 2017 this metabolic disease affected 451 million adults around the globe, and they are projecting the numbers to reach 693 million by 2045 [2]. According to the 1999 WHO criteria, a fasting blood plasma glucose of $\geq$ 7 mmol/L or $\geq$ 126 mg/dL is accepted for diagnosis of diabetes [3]. The condition can be very burdensome to both patients and the healthcare system if it is not controlled effectively. Uncontrolled diabetes in the short-term can result in serious complications such as hypoglycaemia (< 4 mmol/L), hyperosmolar hyperglycaemic state (often > 40 mmol/L) and diabetic ketoacidosis as it can lead on to other major health issues such as renal failure, cardiovascular disease, neuropathy and amputations [4]. Even though many new therapies are available for type 2 diabetics (T2DM), such as the glucagon-like peptide-1 analogues (e.g. dulaglutide), insulin is still one of the main treatments for patients with DM; particularly those with type 1 diabetes (T1DM).

Presently, for insulin-dependent diabetic patients, the primary route of insulin administration is the parenteral route. Thus, for individuals to maintain the correct level of blood glucose in many cases, this requires them to regularly administer multiple daily injections of either long-acting, intermediate-acting, short-acting, and/or rapid-acting insulin via the subcutaneous route. To increase patient compliance, and to help reduce the anxiety of painful daily administration of insulin, numerous researchers are working on the development of novel carrier systems for the safe and effective delivery

of insulin via non-invasive routes, which mainly include; buccal, oral, pulmonary, nasal and transdermal systems. Thus to gain an overview, a comprehensive review was completed of formulations and delivery systems that have had some success in the area of non-invasive delivery of insulin [1].

1.1.1 Diabetes mellitus

DM is classified by WHO into type 1, type 2, gestational diabetes and intermediate conditions such as impaired glucose tolerance and impaired fasting glycaemia, which can progress into diabetes [4]. The two main types of diabetes mellitus are T1DM and T2DM. The aetiology of both types are complex, and based on current evidence involves both genetic and environmental factors [5]. T1DM, also known as early-onset, is caused by an absolute deficiency of insulin due to autoimmune destruction of the insulin-producing beta-cells in the pancreas. Roughly one-tenth or less of all people with DM are classified as type 1 diabetics and are diagnosed commonly in early childhood or as young adults. T2DM is the most common form of diabetes, which is responsible for almost all the other cases of diabetes and is caused as a result of insulin resistance and relative insulin deficiency [1].

1.1.2 Insulin structure
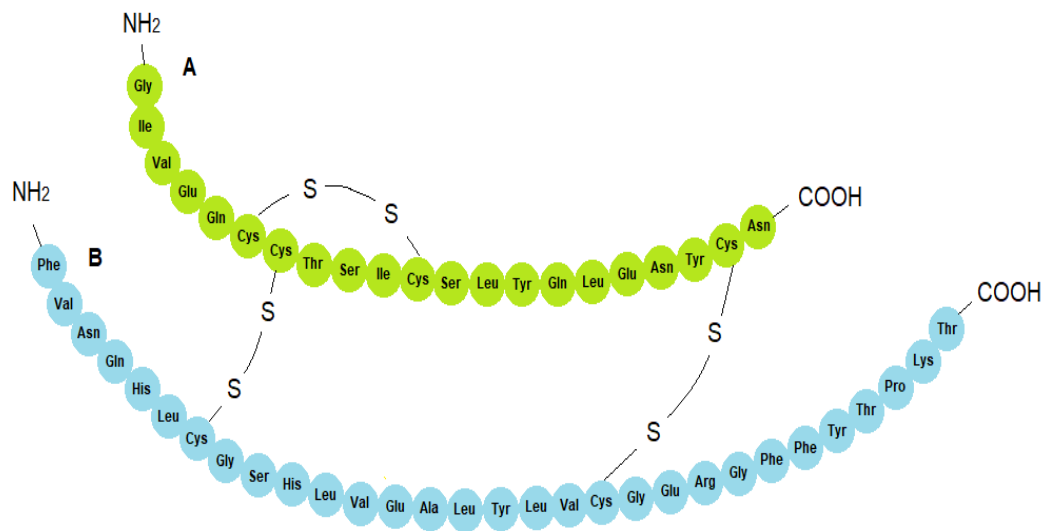
Figure 1.1: Schematic representation of human insulin [1].

As shown in Figure 1.1, monomeric human insulin comprises 51 amino acids, which is in the form of an A chain of 21 amino acids and a B chain of 30 amino acids. It has a molecular weight of 5.8 kDa and consists of two disulphide bonds that connect the A and B chains (A7-B7 & A20-B19), and one disulphide linkage that is present within the A chain (A6-A11) [6].

1.1.3 Insulin in clinical practice

The goal for insulin treatment would be to accomplish plasma insulin levels that mimic as closely as possible the normal secretion of insulin in non-diabetic people. This includes covering baseline insulin, which is usually in the range of 5 to 15 microunits per millilitre and the insulin released in response to meal intake, which generally results in insulin levels of 60 to 80 microunits per millilitre [7], [8]. The primary method for insulin administration is via subcutaneous (sc) injections. Disposable injection pens

such as FlexPen® by Novo Nordisk A/S are commonly used in practice [9]. The main benefits of these devices include the high bioavailability, the controlled onset of action and flexibility in dosing. The disadvantages include the bruising of injection sites, lipodystrophy, weight gain and variations in absorption when the injected limb is used for vigorous exercise. Short-acting insulin formulation act within 30-60 minutes, with maximal effect occurring 2-4 hours, and lasts up to 8 hours. Intermediate-acting formulations and long-acting preparations have an onset of 1-2 hours, levels peak around 4–12 hours, and have a duration of action of 16–42 hours [10].

1.2 Evaluation of insulin delivery via non-invasive routes

As part of initial research, a review was completed, which covered non-invasive insulin delivery formulations that have managed to enter the different stages of clinical trials in the past decade. The data was primarily based on the database, ClinicalTrials.gov and results shown in Table 1.1 below [11]. The advantages and disadvantages of the various non-invasive insulin delivery routes are outlined in Figure 1.2 below.

Buccal Delivery
- ✓ Good patient acceptability
- ✓ Convenient and easily removed in the event of adverse reactions, side-effects or over dosage
- ✓ Low enzymatic activity compared to GIT
- ✓ Highly vascularized absorptive surface area
- ✓ Fast flowing blood supply (2.4ml/min/cm²)
- ✓ Direct access to the systemic circulation
- ✓ Potential bypass of hepatic first pass metabolism through the internal jugular vein
- ✓ Short recovery time after trauma or injury
- ✓ Tolerant to possible allergens due to low number of Langerhans cells
- X Small surface area for absorption
- X Low permeability
- X Saliva secretions can vary (excessive secretion can dilute the drug or cause wearing away of formulation & too little maybe inadequate to cause dissolution of the formulation)
- X Taste of drug can be an issue
- X Possible choking hazard due to unintentional swallowing of formulation
- X Food consumption may dislodge delivery system
- X Drinking hot, cold or acidic liquids may alter drug absorption from formulation

Nasal Delivery
- ✓ Potential bypass of hepatic first pass metabolism
- ✓ Low enzymatic activity
- X Small surface area
- X Possible irritation
- X Irreversible damage to the cilia after long-term administration
- X Variability in absorption due to differences in mucus composition and characteristics

Pulmonary Delivery
- ✓ Large surface area for drug absorption (50-140 m²) with around 500 million alveoli
- ✓ Highly vascularized
- ✓ Thin alveolar-capillary barrier hence small barrier for drug permeation
- ✓ Low enzymatic activity
- ✓ Higher bioavailability (4-40 fold increase) compared to most other transmucosal routes e.g. buccal and nasal delivery
- X Variable bioavailability affected by respiratory factors such as: inspiration effort, tidal volume and peak flow
- X Cough is a common side-effect
- X Possible long-term damage to the lungs
- X Clearance by alveolar macrophages

Oral Delivery
- ✓ Most patient friendly route of drug delivery
- ✓ Convenient administration hence possible improvement in compliance
- ✓ More reflective of physiological insulin delivery
- ✓ Reduced peripheral hyperinsulinemia
- ✓ Possibly reduced chance of weight gain
- X Low stomach pH leading to insulin degradation
- X Low permeability
- X Enzymatic degradation in the GIT
- X Variability of drug absorption in the GIT depending on location of release in the GIT, the fed and fasted state and transit time
- X First pass hepatic insulin extraction leading to degradation of 50% or more of insulin that enters hepatocytes

Transdermal Delivery
- ✓ Convenient administration
- ✓ Large surface area
- ✓ Bypass of hepatic first pass metabolism
- ✓ Less likely to result in fluctuating insulin levels
- ✓ Possibility of terminating drug dosing by removal of delivery device
- X Very low permeability hence mechanisms of enhancing absorption required
- X Possible irritation
- X Allergic contact hypersensitivity may occur
- X Skin reactions can arise due to occlusion by the delivery device

Figure 1.2: Advantages and disadvantages of various non-invasive delivery routes for insulin [1].

Summary from the following resources [12]–[20]

Table 1.1: A summary of clinical trials submitted in the clinicalTrials.gov website involving pulmonary, buccal, oral, and nasal insulin delivery systems, for type 1 & 2 diabetes mellitus, with the trial start date being between January 2008 and December 2017. No trials recorded for transdermal delivery in the past decade [1], [21].

Pulmonary Insulin Delivery					
Product Name	Company	Technology	Year Trial Started	Phase	NCT Number
Dance-501	Dance Biopharm	Inhaled insulin administered using the Adagio-01 inhaler device (also known as dance-501). The device uses a vibrating mesh micropump technology developed by Aerogen.	2013	1 & 2	NCT02713841
			2016	1 & 2	NCT02716610
Afrezza®	Mannkind Corporation & Sanofi	Technosphere® Insulin SAR439065 Afrezza®. Technosphere® particles are formed using the carrier fumaryl diketopiperazine (FDKP). Insulin is adsorbed onto the particles (around 2 µm in size), forming Technosphere® insulin.	2008	1	NCT00673621
				2	NCT00662857
				1	NCT00674050
				2	NCT00747006
				3	NCT00700622
			2009	3	NCT00642616
			2010	3	NCT01196104
			2011	3	NCT01451398
				3	NCT01445951
			2012	1	NCT01544881
			2015	1	NCT02485327
				1	NCT02470637
				2	NCT02527265
			2017	1 & 2	NCT03234491
				3	NCT03324776
				4	NCT03143816
				4	NCT03313960
Buccal Insulin Delivery					
Product Name	Company	Technology	Year Trial Started	Phase	NCT Number
Oral-lyn™	Generex Biotechnology Corp.	Formulation contains surfactants as absorption enhancers by forming insulin-containing micelles. Generex Oral-lyn™ delivers	2008	3	NCT00668850

Product Name	Company	Technology	Year Trial Started	Phase	NCT Number
		insulin via a device known as RapidMist™.			
Oral Insulin Delivery					
GIPET® I	Novo Nordisk	GIPET® I tablet preparation consists of micelles formed with the aid of patented absorption enhancers.	2013	1	NCT01809184
			2013	1	NCT01796366
				1	NCT01931137
			2014	1	NCT02304627
			2015	2	NCT02470039
				1	NCT02479022
ORMD-0801	Oramed, Ltd. & Integrium	ORMD-0801 consists of an enteric-coated capsule that encompasses insulin along with protease inhibitors and absorption enhancers that aid delivery in the small intestine.	2008	2	NCT00867594
			2013	2	NCT01889667
			2014	2	NCT02094534
			2015	2	NCT02535715
				2	NCT02496000
			2016	2	NCT02954601
Oshadi Oral Insulin	Oshadi Drug Administration	Oshadi carrier contains a mixture of pharmacologically inert silica nanoparticles with a hydrophobic surface and a branched polysaccharide. Insulin is suspended, embedded or dispersed in oil or mixture of oils	2010	1	NCT01120912
		Oshadi Icp (insulin, proinsulin and C-peptide in Oshadi carrier)	2013	1&2	NCT01772251
				2	NCT01973920
HDV Insulin	Diasome Pharmaceuticals & Integrium	In the HDV (hepatocyte directed vesicle) insulin gel capsule, the insulin is bound to HDV. The HDV vesicle is less than 150 nm in diameter, and the phospholipid bilayer has specific hepatocyte-targeting molecule (HTM), which in the latest preparation is biotin-phosphatidylethanolamine (biotin-PE).	2008	2&3	NCT00814294
			2016	2	NCT02794155

Product Name	Company	Technology	Year Trial Started	Phase	NCT Number
IN-105	Biocon Limited	The tablet formulation IN-105 oral insulin (now known as Tregopil) is a modified form of human insulin where the free amino acid group on the Lys-β29 residue has been covalently bonded via a non-hydrolysable amide bond to a small polyethylene glycol (PEG) molecule. This modification offers better stability and reduced degradation in the presence of enzymes in the GIT.	2010	1	NCT01035801
ORA2	Bows Pharmaceuticals AG	Insulin in a dextran matrix capsule.	2009	1&2	NCT00990444
			2010	1	NCT01114750
Nasal Insulin Delivery					
Product Name	Company	Technology	Year Trial Started	Phase	NCT Number
Nasulin™	CPEX Pharmaceuticals Inc.	The intranasal insulin spray contains cyclopentadecalactone (CPE-215), which is the main excipient in the permeation enhancement technology of CPEX.	2009	2	NCT00850161
				2	NCT00850096

1.2.1 Pulmonary insulin delivery

So far only two products, both dry powder inhaler (DPI) insulin systems, have secured FDA approval; one being Exubera, which also had the EMA (European Medicine Agency) approval, and Afrezza® [22]–[24]. Although the product was unsuccessful, the approval of Exubera in 2006, demonstrated some level of optimism for the possibility of non-invasive insulin formulations [23]. Afrezza® is an inhaled human insulin product, which was approved in June 2014 for T1DM and T2DM, but in the UK and Europe, it is still in phase 3 clinical trials [22], [25], [26]. The insulin is a dry powder formulation, which is contained in single-use cartridges and consists of 4, 8 or 12 unit doses of insulin [27]. Upon inhalation, the Technosphere® insulin particles are aerosolized and delivered to the lung alveoli [28].

Technosphere® insulin is formed through the adsorption of insulin to the carrier fumaryl diketopiperazine (FDKP), which under acidic conditions, self-assembles into microparticles of ~2 µm [26]. After crossing the alveoli into the bloodstream, the FDKP molecule remains unchanged and is eliminated by the kidneys [28]. Although patients will still need to administer their basal insulin, Afrezza® can replace meal-time insulin [29]. As shown in Figure 1.2, there are many benefits to delivering insulin via the pulmonary route. Still, some disadvantages also exist, including being inappropriate for patients with chronic lung disease, owing to the risk of acute bronchospasm. Also, it is not suitable for smokers or those who have lately quit smoking [22].
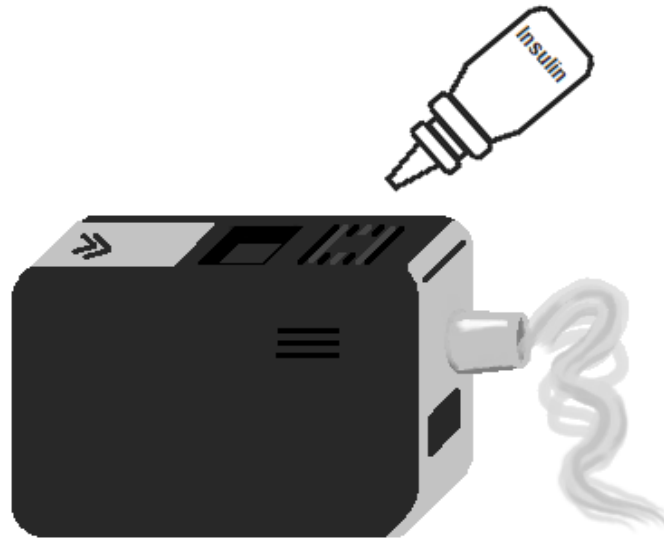
Figure 1.3: Simplified image of the Dance-501 device with separate insulin container.
Adapted from [24].

Another inhaled insulin product, which has completed phase 2 clinical trials, is the pocket-sized insulin inhaler device Dance-501 [24]. The device, shown in Figure 1.3, developed by Aerogen, uses a vibrating mesh micropump technology. The advantages of this device are that it is discrete, compact and battery-operated, and hence the developers have overcome the disadvantages faced with Exubera [24]. Moreover, the incidence of coughs is lower in comparison to DPI systems, due to the formulation being a liquid aerosol system [24].

The insulin release is breath actuated, which, requires initial patient training, which could result in variable bioavailability similar to current problems faced with such inhaler devices used for respiratory conditions. Another drawback is that insulin from a separate container is required to be dispensed into the inhaler reservoir, which adds an extra step to the administration process, and the manual work could be an issue for arthritic and elderly patients.

1.2.2 Buccal insulin delivery

A buccal insulin product, Generex Oral-lyn™ spray, developed by Generex Biotechnology, for use as prandial insulin in T1DM and T2DM has been approved for clinical use in Ecuador and Lebanon, however, in Canada, the US and Europe the product is still in phase 3 clinical trials [15], [30], [31]. The FDA has approved the product only for the treatment of patients under the Investigational New Drug (IND) program. This enables accessibility of the device to patients that suffer from severe or life-threatening T1DM and T2DM who are not eligible for the phase 3 clinical trials, and there is also no other alternative acceptable treatment [30].

The device used for insulin delivery by Generex Oral-lyn™ is known as RapidMist™. The critical component of this system is insulin-containing micelles, which are used as absorption enhancers. Still, the formulation also consists of small amounts of other excipients that are classified by the FDA as generally recognised as safe (GRAS) [15], [32]. The insulin-containing micelles (> 7 μm) are too big to travel to the alveoli thus are impacted in the oral cavity. Each canister holds 400 units of human insulin, and while 1 puff consists of 10 units of insulin, only 1 tenth of the drug is absorbed; therefore with each spray, only 1 unit of insulin is delivered to the blood circulation [15], [33]. Rationally, many patients require ten units or more of postprandial insulin, some considerably more, consequently using the device to dispense ten or more puffs each time can become undesirable and may not be feasible for chronic use. In a study with T1DM patients, it was observed that insulin delivery with Oral-lyn™ was much faster compared to sc injections and within 10 minutes insulin levels could be detected in the blood circulation [34]. Moreover, Oral-lyn™ insulin reached peak insulin levels at 0.5 hours, while sc injections were much slower in contrast. This small study also showed

buccal insulin could possibly be more reflective of the normal insulin response to meal intake in non-diabetic individuals, as, at 2.5 hours, Oral-lyn™ insulin had almost reached baseline, compared to sc injection, which had a slower onset and greater duration [34]. Although there are several benefits to the Oral-lyn™ device and formulation, the low bioavailability of the formulation can be the main drawback for the product in obtaining worldwide approval.

Another buccal insulin product of interest was developed by the joint partnership of MonoSol Rx and Midatech Ltd [20]. Midatech's gold nanoparticle (GNP) technology was combined with MonoSol's PharmFilm drug delivery technology, to form a buccal soluble film product called MidaForm® Insulin PharmFilm [35], [36]. In this formulation, the recombinant human insulin (RHI) is bound to glycan-coated gold nanoparticles through non-covalent binding and embedded in a polymeric mucoadhesive film for delivery of insulin via the buccal mucosa. It is suggested by Midatech Pharm that the gold nanoparticle technology aids the permeability of drugs through membranes and leads to an increase in stability. The particles are also inert and biocompatible [37]. The core of the GNPs is formed from gold metal atoms, which are attached via gold sulphur bonds to an organic layer of glycans. During the self-formation process insulin, can attach to the gold core (1-2 nm). In Phase I clinical trials, using insulin aspart, the formulation was shown to be both well tolerated and safe [20]. Additionally, owing to their small size GNPs are believed to be eliminated via the liver and kidneys. Although the technology looks promising, and the company has facilities to scale up the production of the formulation, Midatech announced in May 2016 that the results of the Phase 2a clinical trials (MTD101) demonstrated low bioavailability for the transbuccal film insulin compared to sc insulin [38]. Hence, the company were evaluating their

options. The product is not on the pipeline list of products for Midatech or MonoSol Rx, now renamed as Aquestive. It is less likely that the development of MidaForm® Insulin PharmFilm will be advanced.

1.2.3 Oral insulin delivery

Novo Nordisk, in partnership with Merrion Pharmaceuticals, is developing the GIPET (gastrointestinal permeation enhancement technology) system for oral delivery of insulin in the form of a tablet [39]. The oral preparation consists of micelles formed with the aid of patented absorption enhancers, which have the purpose of increasing absorption across the GI tract. The main product is known as GIPET I (OI338GT or NN1953), a long-acting insulin analogue, which has managed to reach phase 2 clinical trials. Novo Nordisk is also using the GIPET technology to develop oral formulations of two other insulin analogues known as insulin 287 and insulin 320 (OI320GT or NN1957), which have both completed phase 1 clinical trials [40]. Other than the basic information not much can be found about the GIPET formulation or the results of the trials.

Oramed Pharmaceuticals have an oral insulin formulation, known as the ORMD-0801 capsule, which is being tested in several phase 2 clinical trials in both T1DM and T2DM patients [41]. Oramed Pharmaceuticals' Protein Oral Delivery™ (POD) technology consists of an enteric-coated capsule that encompasses insulin along with protease inhibitors and absorption enhancers that aid delivery in the small intestine. In the phase 2 trial (NCT00867594), eight T1DM patients, with uncontrolled blood glucose levels (HbA1c: 7.5-10%), were trialled with the ORMD-0801 capsules containing 8mg of insulin in each capsule [42]. In this trial, the patients were asked to self-administer the

ORMD-0801 capsules three times a day, 45 minutes before their meals, in addition to their standard insulin therapy. Although the study included a small number of individuals and a short treatment period of 10 days, the outcome was significantly reduced glycaemia throughout the day. Additionally, the formulation was tolerated well by individuals with no hypoglycaemic episodes or adverse events. One of the potential drawbacks to this formulation is the administration of a large amount of insulin, and, surprisingly, no hypoglycaemic incidents occurred within the study. Still, the study was small, and the effects of interindividual variability will more likely be experienced in more extensive studies.

Diasome pharmaceuticals have designed an oral HDV (hepatocyte-directed vesicle) insulin gel capsule, in which all the insulin is bound to HDV. The HDV vesicle is less than 150 nm in diameter, and the phospholipid bilayer has specific hepatocyte-targeting molecule (HTM), which in their latest preparation is biotin-phosphatidylethanolamine (biotin-PE), incorporated within its structure [43]. As reviewed by Geho et al. (2009), this formulation not only improves oral insulin delivery by shielding insulin from proteolytic enzymes in the upper GI tract but is also more able to mimic physiological insulin delivery via HTM guidance towards hepatocytes. This novel carrier system looks promising, and the FDA has approved it for initiation of phase 3 clinical trials based on the effectiveness of the delivery system in phase 2 human studies. In comparison to other possible oral insulin formulations, one of the most promising aspects of this formulation is the amount of insulin contained in each capsule, which can be as little as 5 units [15], [44]. Accuracy of dosing is highly essential with insulin treatment. One of the main disadvantages with insulin being given orally is the possibility that interindividual variability can lead to overdosing, due to both

genetic variations in individuals but also factors such as food and transit time in the GI tract. In theory, the risk would be much lower with formulations containing smaller amounts of insulin; such as with HDV oral insulin, compared to formulations with 150 units or more per dose, such as Capsulin[TM] IR designed by Diabetology [45].

Oshadi Drug Administrations' newest formulation is in phase II clinical trials, and it has been called Oshadi Icp, as it is a combination of insulin, proinsulin and C-peptide. In 2010, the company made a patent application for their oral insulin formulation in which it is stated that the preparation comprises "a particulate non-covalently associated mixture of pharmacologically inert silica nanoparticles having a hydrophobic surface, a branched polysaccharide, and insulin suspended, embedded or dispersed in an oil or mixture of oils" [46]. The diameter of the nanoparticles is in the range of 1-100 nanometres. Other than the information obtained from the patent (20100278922) there is very little information published by the company. The possible reasoning behind the combination of insulin, proinsulin and C-peptide in the formulation is to reflect a delivery system similar to endogenous insulin release particular as orally delivery insulin reaches the circulation via the hepatic portal vein [47].

Biocon Limited's oral insulin tablet IN-105, now known as Tregopil, is a novel insulin analogue [48]. Tregopil is a modified form of human insulin where the free amino acid group on the Lys-β29 residue has been covalently bonded via a non-hydrolysable amide bond to a small PEG molecule [49]. This modification, in comparison to the original human insulin, has the advantage of better stability and reduced degradation in the presence of enzymes in the GIT, possibly due to steric hindrance. The water solubility of the insulin analogue is also improved and is most likely attributed to the presence of the PEG modification. Furthermore, in phase I study, it was found that the

amount of insulin absorbed was adequately significant to cause reductions in plasma glucose levels, which indicated that the alteration aided absorption of the intact insulin peptide in the GIT. After administration, based on the initial studies, it was observed that insulin levels peaked at around 20 minutes and returned to baseline after 1 hour and 20 minutes, which indicates Tregopil could possibly be useful for control of postprandial glucose levels [49].

Diabetology is also one of the companies that are developing an oral insulin product, known as Capsulin™ IR (insulin replacement), which is in the phase 2 stage of clinical trials [50]. The formulation is a simple mixture, with unmodified insulin (150U or 300U), contained in a standard enteric-coated capsule [45]. The oral formulation uses the company's in-licensed Axcess™ drug delivery technology, which includes a solubiliser and absorption enhancer but does not include any new chemical entities (NCEs) and has demonstrated effectiveness in delivering peptides such as insulin [51]. The main excipients are both pharmacopoeial, and GRAS listed and included an aromatic alcohol and dissolution aid. The whole formulation has been designed to bypass the harsh pH conditions of the stomach and to rapidly dissolve in the small intestine (jejunum), allowing all the components to meet the surface of the intestinal wall.

Bows Pharmaceutical AG was also developing an oral insulin formulation consisting of insulin in a dextran matrix capsule. Still, it appears that they are no longer active in promoting the product with the last update being November 2010 [11].

As insulin is hydrophilic, the main route of permeation in the GI tract is via the paracellular route [52]. It is a relatively high molecular weight drug, and without any absorption enhancement, the permeability, as well as oral bioavailability, is likely to be

extremely low [53]. Therefore, most of the oral insulin formulations being developed include absorption enhancers, but the possible toxicity of such products is a concern in the long term.

1.2.4 Nasal insulin delivery

CPEX Pharmaceuticals Inc. has developed an intranasal insulin spray, containing regular short-acting human recombinant insulin, given the trade name Nasulin™. The main excipient in the nasal insulin formulation is the cyclopentadecalactone (CPE-215), which according to the company has been proven to enhance absorption and is known as the permeation enhancement technology of CPEX [54], [55]. CPE-215 is a naturally occurring compound obtained from the plant *Angelica archangelica* and is contained in many everyday use products including food ingredients, cosmetics and personal hygiene. The other components of the formulation include polysorbate 20, sorbitan monolaurate and cottonseed oil. During the initial studies in healthy volunteers, it was found that the normal physiological nasal cycle did not result in clinically significant alterations in insulin absorption. Still, the absorption of insulin was decreased by roughly 50% in those individuals that were affected by total nostril blockage [56]. Insulin levels peak at around 10-20 minutes post-administration, and hence the formulation is suitable for prandial glucose control. Nasulin™ is generally well tolerated although transient side-effects such as irritation, tickling sensation and sneezing do occur but tend to disappear on continued dosing. In the study by Stote et al. (2011) it was concluded that overall, the intrasubject variability of insulin administered using Nasulin was approximately 40%, which is comparable to that of regular sc administration of insulin.

1.2.5 Transdermal insulin delivery
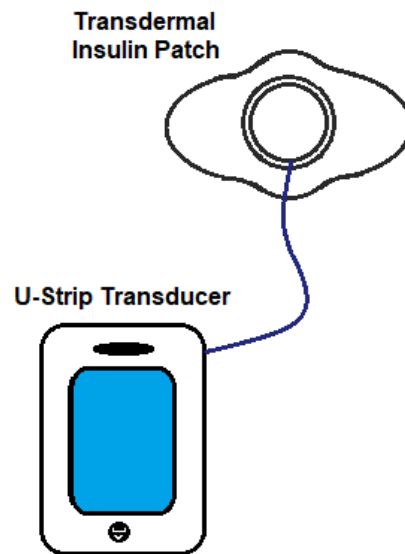
Figure 1.4: Schematic diagram of the two-component system: U-Strip transdermal insulin patch attached to the U-Strip transducer or controller.

Notes: Adapted from [57]

In transdermal insulin delivery systems, the product of interest is the non-invasive U-Strip (Ultrasonic Strip) transdermal patch designed by Transdermal Specialities, which can be used by both type 1 and type 2 diabetics [58]. As shown in Figure 1.4, it is a two-component system, consisting of the insulin patch, which uses an absorbent pad containing up to 150 units of insulin, that is attached to the second component the U-Strip controller, which is a transducer device that generates a unique alternating ultrasonic transmission [57]. The U-Strip system utilises two types of ultrasonic waveforms; initially, sawtooth waveforms are used to expand the pore diameter from roughly 50 µm to 110 µm to facilitate the penetration of large molecules, such as insulin. Square waveforms are emitted to actively force insulin through the enlarged pores into the dermis and the blood circulation. The U-Strip device is portable, battery-operated, and designed to release insulin, specifically insulin lispro, only when the

ultrasound is activated. It is also programmable, can be worn on either one of the arms or on the belt, and has a touch screen to enable patients to control both dosage levels and frequency. Additionally, the device can store data, which is transferable via the internet and hence can be a useful record for the management of patient's treatment and compliance by their healthcare team. Considering that 12 human clinical trials have been completed successfully and an additional 500 patient experiment is underway, the technology looks promising, and it will be interesting to see further developments in the future.

1.3 Introduction to the project

Upon completion of the review and literature search, it was clear several different paths could be explored to deliver insulin via a non-invasive route, all of which had both advantages and disadvantages, as shown in Figure 1.2 [1]. The pulmonary route was one possible direction, as it already has a successful formulation and has benefits such as extensive surface area and a small barrier for drug permeation. But there are disadvantages such as variability of absorption, as a result of respiratory factors, and there are the unknown risks of using insulin long-term in the lungs [17]. The oral route would be the most convenient and patient-friendly path and possibly more reflective of physiological insulin delivery. However, insulin is a protein, and after oral intake, travelling down the gastrointestinal tract (GIT), the low stomach pH will lead to degradation of the protein. Even if this is overcome, further challenges in the GIT include enzymatic degradation, low permeability and variability of drug absorption by the presence or absence of food [15]. These issues, combined with insulin being a narrow therapeutic index drug, even if the formulation has sufficient bioavailability,

there is a significant risk that the variations can lead to greater episodes of hypoglycaemia.

Taking all factors into consideration, the best route for insulin delivery appeared to be via the buccal cavity, particularly as Oral-lyn™, a buccal formulation, has already achieved reasonable success and approval. Also, it has good patient acceptability and short recovery time (4-14 days cellular turnover time), which means the use of permeation enhancers can be safer compared to other mucosae such as GI [59], [60]. On completion of the review, the inspiration emerged to produce insulin-containing vesicles that will be embedded in a mucoadhesive buccal patch formulation. This motivation mainly stemmed from the following two products; the MidaForm Insulin PharmFilm® in developed by MonoSol Rx and Midatech and HDV insulin produced by Diasome Pharmaceuticals [36], [43], [61].

1.3.1   Overview of the buccal cavity

The oral cavity consists of several parts: lips, tongue, gingiva, hard palate, soft palate, cheek and the floor of the mouth [62]. The oral mucosa is composed of several structures an outermost layer of stratified squamous epithelium, followed by the basement membrane, the lamina propria and then the submucosa [13], [63]. In terms of drug delivery, the two most important areas are identified as sublingual, which consists of the floor of the mouth under the tongue and the buccal mucosa, which is the inner lining of the cheek [64]. In the buccal mucosa, the epithelium is roughly 40-50 cell layers thick (0.5-0.8 mm), and there are slightly fewer layers in the sublingual area [13], [64]. These two regions are the most permeable areas of the oral cavity and consist of non-keratinised mucosae [12]. Keratinised and non-keratinised mucosae

vary in the composition of intercellular lipids, as well as how the lipids are packed [64], [65]. In keratinised tissue, such as the gingivae and hard palate, the intercellular space contains neutral lipids (e.g. ceramides and acylceramides), and are in a more ordered, lamellar state [13]. Whereas in non-keratinised mucosa the lipids are in a more amorphous state, with intermittent short stacks of lipid lamellae. Acylceramides are absent in non-keratinised tissue, and they only contain small amounts of ceramides and neutral but polar lipids (mainly cholesterol sulphate and glucosylceramides) [66]– [68]. Consequently, non-keratinised tissue offers less hindrance in the diffusion of molecules compared to keratinised mucosa [64].

1.3.2 Transport pathways

In the buccal mucosa, drugs can permeate via two pathways [13]. As reviewed by Rathbone and Tucker, the diffusion can occur either through the paracellular pathway (via intercellular space between the cells) or the transcellular pathway (intracellularly across epithelial cells) depending on the physicochemical properties of the diffusing molecule [69]. It has been suggested that both hydrophilic and lipophilic molecules can permeate via either of the pathways and even simultaneously [13], [69]. Hydrophilic drugs may traverse through the transcellular pathway by utilizing the aqueous pores in the plasma membrane of epithelial cells [69]. Once inside, the drug can cross the cell; either by simple diffusion or using specialised transport mechanisms. Lipophilic drugs, on the other hand, would penetrate transcellularly using the lipid bilayer of the plasma membrane. However, the paracellular route is the predominant transport pathway for many drugs [69]. Lipid soluble drugs cross via the paracellular way by diffusing through intercellular lipids. While water-soluble drugs utilise aqueous channels in the intercellular space [69]. It is proposed peptides and proteins, such as insulin, permeate

via the intercellular route due to their higher solubility in the aqueous fluids of the intercellular spaces [64].

1.3.3 Saliva and enzymatic activity

Saliva secretion occurs mainly by the parotid, submaxillary and sublingual glands, which are the major salivary glands but also via the buccal or minor salivary gland [70]. At rest, the pH of the saliva is around 6.6, which is slightly acidic, but upon stimulation, it increases to approximately 7.4 due to a rise in bicarbonate ion concentration [71]. Although enzymes, inorganic salts, lipids and mucin are present in saliva, water (95-99% per weight) is the main component [64]. The presence of saliva usually is beneficial in keeping the buccal cavity lubricated. Still, in terms of drug delivery, the presence of excess saliva can lead to a reduction in the contact time of drugs by removal of drug/formulation from the site of absorption [72], [73]. The buccal cavity, in comparison to the GIT, has less enzymatic activity, which provides a more favourable environment for the delivery of peptide and proteins, such as insulin, which are susceptible to enzymatic degradation [59], [62], [64]. However, the enzymatic activity cannot be disregarded; hence the use of bioadhesive devices/formulations which can help with exposure to enzymes and saliva by protecting the drug for a more extended period and increasing drug contact time at the site of absorption [64], [74].

1.4 Delivery of insulin via the buccal mucosa

For small molecular weight drugs, such as glyceryl trinitrate, the sublingual mucosa can be seen as a more favourable region compared to the buccal mucosa due to the higher permeability and more rapid absorption [12], [13]. But for many drugs, the location is unsuitable due to the difficulty of finding sufficient smooth surface area and

achieving reasonable contact time, due to absence of immobile mucosa and the frequent washing of the region by saliva [13]. Although the buccal mucosa is thicker, it has an expanse of smooth muscle, to enable placement of formulation, and the area is reasonably immobile, which can make it suitable for retentive devices [13], [75]. Hence the buccal mucosa can be a possible target for delivery of drugs, such as insulin, via a controlled release formulation.

The advantage of the buccal mucosa is that it is a highly vascularized surface and drug delivery generally occurs through simple diffusion via the paracellular route. Once peptides and proteins permeate the buccal mucosa, via the intercellular spaces, they enter the lamina propria, the connective tissue, which has a network of capillaries [64], [76]. When the drug reaches the blood, this route provides direct access to the systemic circulation via the jugular vein, which enables bypass of hepatic first-pass metabolism [59], [60], [75], [76]. In the buccal cavity, other routes such as pinocytosis, active transport, and passage through the aqueous pores do exist but usually play minor roles in drug transport across the mucosa [75]. Although permeability is higher in the buccal mucosa, compared to skin, it is still a significant barrier for proteins crossing the buccal membrane [76]. As the paracellular pathway is suggested to be the main route utilised by proteins, the foremost hurdle to buccal mucosal permeation, is the intercellular lipids. However, factors such as saliva and enzymatic activity in the oral cavity must also be taken into consideration in the formulation design.

Permeability is one of the main barriers for drug delivery of proteins across mucosal membranes, such as in the buccal cavity. Hence to increase the likelihood of proteins permeating the oral mucosa permeation enhancers need to be present in the formulation. As comprehensively reviewed by Verma et al. (2011) there are many

classes of permeation or penetration enhancers including surfactants, bile salts, chelating agents, monohydric alcohols, liposomes and cationic polymers (e.g. chitosan) [77]. The mechanism of penetration differs depending on the type of enhancer. Chelating agents, such as sodium citrate and EDTA, are suggested to act by interfering with calcium in the membrane. Positively charged polymers, e.g. chitosan possibly acts via ionic interaction with the negatively charged mucosal surface. The primary mechanism for surfactants, e.g. Tweens, Spans and bile salts, is thought to be the perturbation of intercellular lipids [77].

1.5 Lipid-based vesicles as delivery systems

The ability of lipid-based vesicles to enhance drug delivery is possibly due to the synergistic effect of being drug carriers as well as permeation enhancers [78]. Niosomes, liposomes and transfersomes are examples of lipid-based vesicles. One of the main advantages of these vesicles compared to polymeric nanoparticles is their ability to encapsulate both hydrophilic and hydrophobic drugs [79]. Ordinarily, hydrophilic drugs are entrapped within the aqueous interior of these vesicles, while lipophilic drugs are embedded in the bilayers [78], [80]. Drug entrapment occurs during the self-assembly stage when the non-ionic surfactants or phospholipids form closed bilayered structures to achieve the most thermodynamically stable state [81]. This happens due to the inclination for the hydrophobic chains to minimise contact with the aqueous media and hence vesicles are formed with the hydrophilic or polar head group facing the aqueous bulk and the hydrophobic chains facing each other within the bilayer. Generally, energy from heat or agitation is required in forming bilayered structures [82]. The composition of niosomes/liposomes can affect their physicochemical properties such as morphology, charge, lamellarity and elasticity.

Other than the surfactant niosomes and liposomes can include other components such as cholesterol and charged molecules.

1.5.1 Advantages and disadvantages

Other than the incorporation of both hydrophobic and hydrophilic drugs, these vesicles, as reviewed by Sharma et al. 2019, can offer many other advantages to the delivery of pharmaceutical products [80]. Benefits include improving solubility, reducing the rate of degradation, enhancing drug permeation, prolonging of drugs within the circulation, and overall, there is flexibility in their design based on desired therapeutic outcomes. There are also some possible disadvantages such as low drug entrapment and stability issues, which can lead to problems of drug leakage during storage and transport. But it has been suggested that these vesicles are more stable encapsulating macromolecules, such as insulin, compared to low molecular weight drugs [83].

1.5.2 General preparation techniques

1.5.2.1 Thin layer hydration (or hand-shaking method)

This method involves all the ingredients (surfactants/lipids) being dissolved in volatile organic solvents (e.g. chloroform/methanol) in a round bottom flask. Then the organic solvent is evaporated, under vacuum (i.e. reduced pressure), by using a rotary evaporator. This leaves a thin surfactant/lipid film on the wall of the round bottom flask, which is hydrated with an aqueous solution (with or without drug). To form niosomes/liposomes/transfersomes the hydration step needs to be carried out at a temperature above the phase transition temperature of the phospholipids/surfactants

and with gentle agitation for a specified period [81], [84]. This method has been used to form insulin-containing niosomes [85].

1.5.2.2 Reverse phase evaporation

In this procedure, initially, the surfactants/lipids are dissolved in an organic solvent while the drug is dissolved in an aqueous phase. Then a mechanical or sonication method is used to emulsify the two phases and create a water-in-oil emulsion. Subsequently, the slow elimination of the organic solvent, under reduced pressure, leaves a gel-like mixture. Sometimes further hydration of the mixture is required to form a dispersion of large vesicles [83], [86].

1.5.2.3 Ethanol injection

This method firstly requires dissolution of the drug and lipids/surfactants in ethanol. Successively, the mixture is rapidly injected into the aqueous phase (60°C) under magnetic stirring. To remove the residual ethanol, the product is then transferred to a rotary evaporator (60°C), and the ethanol is evaporated under vacuum. This results in the production of the vesicles.

1.5.2.4 Ether injection

This technique involves the lipids/surfactants being dissolved in either diethyl ether or a combination of ether and methanol, which is slowly injected into the aqueous solution containing the drug to be encapsulated. This is done while maintaining the temperature above the boiling point of the organic solvent. The removal of the organic solvent leads to the formation of niosomes/liposomes [87].

1.5.2.5 Trans-membrane pH Gradient Method

This technique is similar to the hand-shaking method. The main difference is being, after rotary evaporation of the organic solvent, the surfactant/lipid film is hydrated, by vortex mixing with an acidic solution; commonly citric acid (pH 4). This results in the formation of multilamellar vesicles, which are put through freeze-thaw cycles and subsequently sonicated. To encapsulate a drug, first, the vesicle dispersion is mixed with the aqueous drug solution, then a pH gradient is created by the addition of a base (e.g. disodium phosphate) [88]. Increasing the pH to 7-7.2 in the aqueous surrounding the vesicles results in the formation of protonated as well as unprotonated drug. The unprotonated neutral drug can permeate and enter niosomes/liposomes. After entry into the acidic environment, the drug becomes protonated and is confined within the vesicles. This form of entry continues until an equilibrium of drug concentration is achieved [81].

1.5.3 Liposomes

Liposomes, discovered in 1965, are closed bilayered structures formed using phospholipids such as phosphatidylcholine and phosphatidylethanolamine [89], [90]. The benefits of liposomes, as drug carriers, include their low toxicity profile, their biodegradability, and biocompatibility [91]. The first such product to obtain FDA approval was the liposomal formulation of doxorubicin, Doxil®, in 1995 [92]. As reviewed by Bulbake et al. (2017), due to the advantages offered by these vesicles, there are numerous drugs encapsulated in liposomal formulations that are now approved and available for human use [90]. These formulations have been taken advantage of in many areas of therapy particularly in cancer with products like

DaunoXome® (daunorubicin) and Onivyde® (a combination of 5-fluorouracil and leucovorin) but also other areas, such as Ambisome® (amphotericin B), for the treatment of fungal infections [90].

1.5.4 Niosomes

Niosomes are bilayered vesicular systems, similar in structure and function to liposomes, but are formed from the self-assembly of non-ionic surfactants in aqueous media instead of phospholipids [81], [93]. Niosomes, likewise to liposomes, can be categorised into three groups based on their size: small unilamellar vesicles (25-50 nm, SUV), multilamellar vesicles (≥ 50 nm, MLV) and large unilamellar vesicles (≥ 100 nm, LUV) [88]. The diameter of MLVs are expected to be between 100 and 1000 nm, while LUVs are roughly around 100 to 250 nm [94].

1.5.5 Transfersomes
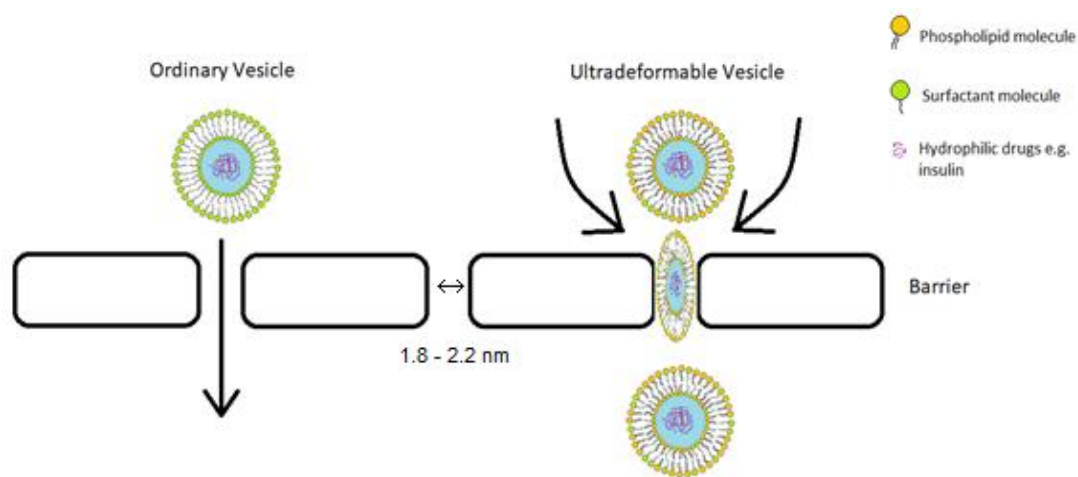
Figure 1.5: A schematic diagram representing the mechanism of permeation enhancement of water-soluble drugs by transfersomes across membranes.

Notes: Modified from [95] for buccal delivery and information for the radius of the pore size of porcine buccal mucosa (1.8-2.2 nm) obtained from [96].

Numerous vesicular systems have been investigated to increase the permeability of proteins, such as insulin, across the buccal membrane; the mechanism is shown in Figure 1.5. Transfersomes (also known as flexible liposomes, elastic liposomes or ultradeformable liposomes), are relatively novel drug delivery systems, in which the bilayer consists of a combination of phospholipids and edge activators. As reviewed by Abdelkader et al., (2014) the concentration of edge activator can vary from 20-50% (mol/mol) [97]. The advantage of these vesicles compared to ordinary liposomes and niosomes is that they are metastable. This allows them to be highly or ultra-deformable and hence able to squeeze through pores, under non-occlusive conditions, up to one-tenth smaller than their size. As a result, particles of 200-300 nm can penetrate the intact skin [98]–[101]. A substantial number of studies are related to the use of transfersomes to enhance drug delivery across the skin. Still, fewer studies can be found that have investigated the mechanism of such vesicles for improving drug delivery in the buccal cavity. In theory, the structure of the skin closely resembles the buccal membrane, but with better permeability, thus greater enhancement of drug delivery may be possible [102]. In transfersomes, the surfactant (or edge activator) is an essential component in achieving membrane deformability by destabilizing the bilayer and lowering the interfacial tension. These are often single-chain surfactants such as Span 80/60 and Tween 80/60 [103].

1.5.6   Other components in nanovesicles

1.5.6.1   Cholesterol

The presence of cholesterol can affect the fluidity and permeability of the bilayer and influence the size and entrapment efficiency of the vesicles. Cholesterol is one of the

ingredients most frequently found in niosomes and liposomes [83]. This is because, for some lipids and surfactants, the inclusion of cholesterol is essential for vesicles to be formed. For example, a study found in the absence of cholesterol Span 60 niosomes created a gel, whereas, in its presence, a homogenous niosomal dispersion was formed [104]. The presence of cholesterol in the formulation requires a balance. This is because studies suggest the inclusion of cholesterol in vesicles leads to an increase in encapsulation efficiency (EE); however, it can also result in an increase in the hydrodynamic diameter of the vesicle and increase rigidity. This increase in rigidity is due to cholesterol being a lipid that fills empty spaces within the bilayer and acting like a "mortar", which may benefit the stability and leaking of the drug. Still, it can also mean a reduction in the release rate of the encapsulated drugs [88], [97].

1.5.6.2   Charged molecule

To increase stability and prevent aggregation, charged molecules are sometimes included, as additives, in the formation of vesicle [105]. The improvement in stability occurs via electrostatic repulsion as; theoretically, all the vesicles will be of similar charge, positive or negative; thus adjacent vesicles will repel each other and remain discrete preventing their aggregation and fusion [105]. As reviewed by Yeo et al. 2018, dicetyl phosphate (DCP) is a well-known negatively charged molecules used in niosomal preparations while stearylamine and cetylpyridinium chloride are common positively charged molecules [82].

1.5.6.3   Polyethylene glycol

PEGylation, as the name suggests, is the covalent linkage of PEG to a targeting moiety. PEGylation of liposomes aims to develop delivery systems that enhance the

drug half-life of liposomes by hindering their recognition by phagocytic cells [90], [106]. Furthermore, this process leads to alterations in the physicochemical properties of liposomes, such as particle size, which can also affect their clearance by the renal system and hence further prolong drug circulation time [90].

1.6 Buccal patches/films as delivery systems

Formulating a patch for drug delivery in the buccal cavity requires several considerations, although the most critical factors are the projected time of action and the drug dosage. Still, other factors also need to be well-thought-out such as physical appearance and drug stability [107]. For a buccal formulation, the maximum duration should be around 4-6 hours [77]. This suggestion is reasonable as any patch that must be maintained in the mouth for longer than 6 hours would likely cause discomfort for the patient and may result in reduced patient compliance. The primary purpose of using a patch is to deliver, as well as increase contact time for the drug at the site of absorption. Several drugs in the European market are available in buccal film formulations, which are designed for systemic drug delivery; such as fentanyl (Breakl) for pain relief, nicotine (Niquitin) for smoking cessation, and the antiemetic ondansetron (Setofilm) [61]. However, these are all small active pharmaceutical ingredients, and yet there are no buccal films approved for delivery of large macromolecules, such as insulin [61]. Thus, this indicates the production of a successful buccal formulation, will require not only greater contact time for drug absorption but also permeation enhancers to assist in the penetration of insulin.

1.6.1 Methods of forming patches

1.6.1.1 Solvent or film casting method

This method is the most popular for buccal film production, which is possibly due to the ease and low cost of processing, as well as the ability to produce films with uniform thickness [108]. The method involves creating a homogeneous solution or suspension by dissolving or mixing the excipients and the drug in a solvent, such as water or ethanol [61]. This step is then followed by degassing to remove the entrapped air. The solution or mixture is then transferred to a mould and dried. After drying the film is ready and removed from the mould [61]. In this technique, the choice of solvent is important, as using water may not be suitable for heat-sensitive drugs, such as proteins, as the temperature to evaporate water can denature proteins. But the use of more volatile solvents also needs to be carefully considered as there is potential for trace amounts of the solvent remaining in the formulation and even the risk of occupational solvent exposure during manufacture [61].

1.6.1.2 Hot-melt extrusion

In this method, the drug and excipients are weighed and then loaded into one or more hoppers, which leads into the extruder [109]. The screws present within the extruder move the material towards the heated section, which results in both the mixture melting and mixing. The extrudate is then put through a flat die to form films. Elongation rollers and cooling elements are used to control factors such as film thickness [61]. This method is mainly used for small molecule drugs. Due to the exposure of the ingredients, including the drug, to elevated temperatures and high pressure the use of this method with proteins is likely to lead to their denaturation [61].

1.6.1.3   Freeze-drying

The use of freeze-drying as a process to form films or patches is less common, compared to the previously mentioned methods, thus not often referred to in reviews. Lyophilization or freeze-drying as the name suggests is the removal of solvents from frozen solutions or suspensions, which contain both the drugs and the excipients [107]. The advantage of the method, particularly for heat sensitive drugs such as proteins, is that the whole process is carried out in the absence of elevated temperatures. Another benefit may also be the formation of films that comprise of glassy amorphous structures, which can improve the drug dissolution rate [107]. Several studies have formed buccal patches/wafers/films/sponges, using this method, and a few of the studies were in particular related to protein delivery systems [107], [110], [111].

1.6.2   Mucoadhesive polymers

1.6.2.1   Mucoadhesion

Mucoadhesion is a term used to describe the adhesion between a synthetic surface and a mucosal membrane [112]. As summarized by Smart (2005) and Shaikh et al. (2011), there are six theories to explain the phenomenon of mucoadhesion: adsorption, diffusion, electronic, fracture, mechanical and wetting theory [113]. In the adsorption theory, the main contributors to adhesion are hydrogen bonding and van der Waals' forces. The diffusion theory involves the interdiffusion of polymer chains across an adhesive surface; thus, the process is affected by the accessibility of molecular chain lengths and their mobilities. The electronic theory is suggested to occur owing to differences in the electronic structure of the adhering surfaces, which results in the transfer of electrons upon the interaction of the surfaces [114]. The fracture theory

varies from all the other theories, as it describes the adhesive strength based on the forces required for the two surfaces to be detached. The mechanical theory is the assumption that adhesion develops as a result of interlocking of liquid adhesive into irregularities on a surface [113]. The wetting theory, mainly involving liquid systems, is the capability of a liquid to spontaneously spread onto a surface for adhesion to occur [113]. Mucoadhesion, however, is a complex phenomenon and often cannot be simply described by one theory. Particularly as in the oral cavity, the dry or partially dry oral dosage form may encounter mucous membranes that have thin and discontinuous mucus layers.

Generally, two steps are involved between the mucoadhesive device and the mucous membrane; an intimate contact stage (wetting) and a consolidation stage (physicochemical interactions) [113]. Mucoadhesive formulations adhere most strongly, only after initial activation by moisture, to solid dry surfaces [113], [115]. The presence of moisture is critical to enable the mucoadhesive molecules to move spontaneously, adapt to the structure of the surface, and bond using forces such as van der Waals' and hydrogen bonding. Moisture essentially acts as a plasticiser [113]. Generally, although hydrogen bonding is valuable, the bonding implicated in mucoadhesion is heterogeneous, hence challenging to identify the exact bonds and groups involved [116]. The standard film-forming polymers (also known as first-generation mucoadhesive polymers) include chitosan, hydroxypropyl methylcellulose (HPMC), methylcellulose, pullulan, polyacrylate and polymethacrylate derivatives and sodium alginate [61].

1.6.2.2 Cellulose derivatives

A wide variety of cellulose derivates exist, but a few are commonly used for their mucoadhesive properties. One prevalent derivative, which is indicated to have the best mucoadhesive characteristics is the anionic carboxymethylcellulose (CMC) [115]. CMC is also biocompatible and has excellent stability properties. Other mucoadhesive derivatives are the following non-ionic forms of cellulose: hydroxyethyl cellulose (HEC), hydroxypropyl cellulose (HPC) and HPMC [117]. HPMC is suggested to have moderate mucoadhesive properties [117]. However, in a study comparing several polymers, including sodium carboxymethyl cellulose and HPMC, it was found that although CMC had excellent mucoadhesiveness, the excessive swelling resulted in volunteers complaining due to the formulation causing difficulty in speaking [118]. The optimum mucoadhesive formulation in the study contained HPMC as the main component [118].

1.6.2.3 Chitosan

Chitosan is a polysaccharide, derived from the deacetylation of chitin; it is one of the most extensively researched cationic polymers [117], [119]. In terms of chemical structure, chitosan comprises of D-glucosamine with occasional N-acetyl-D-glucosamine units, which are held together via β(1→4) linkage [120]. The physical properties of the polymer are affected by the degree of deacetylation. The mucoadhesion properties of chitosan is a combination of hydrophobic interactions as well as ionic and/or hydrogen bonding with the negatively charged mucous surface [121]. The advantages of using chitosan are that it is biodegradable, biocompatible and has low toxicity [117]. Although not yet FDA approved for oral drug delivery, chitosan

has been approved by the FDA and EU for other purposes. Thus, the likelihood of approval is strong if a successful formulation is produced [120], [121].

1.6.2.4 Alginates

Alginates are anionic and are found to have excellent mucoadhesive properties [122]. They are natural polymers, which are biodegradable and biocompatible, sourced from algae, bacteria, and seaweed [117]. These are linear polysaccharides composed of varying ratios of mannuronic acid and guluronic acid units [122]. It has been found that the extent of interaction of these polymers with mucin, which consequently affects their mucoadhesive properties, is determined by their chain flexibility and their molecular weight [123].

1.6.2.5 Polyacrylates

These are acrylic acid polymers that are cross-linked with polyalkenyl ethers or divinyl glycol [117]. There is a wide range of these synthetic polymers available, and their popularity is due to their excellent mucoadhesive characteristics, non-toxic nature and they are also classified as GRAS ingredients by the FDA [117]. The mucoadhesive properties of poly (acrylic acid) (PAA) is due to possession of carboxylic groups, which enables them to form hydrogen bonds with the oligosaccharide chains of mucin [117]. Additionally, the mucoadhesion is enhanced by the physical entanglement that occurs between the PAA and the mucus layers. Thus, a combination of hydrophobic interactions and adhesive forces (i.e. hydrogen bonding and van der Waals) is involved in the adhesion process. Two types of derivatives of PAA that are highly studied regarding their mucoadhesive properties is polycarbophil (Noveon®) and carbomer (Carbopol®) [124]. Mucoadhesive carbomers, like Carbopol® 934P, 971P and 974P,

have no residual benzene content, which enables them to be used to produce oral formulations [117]. Carbopol offers advantages in sustained drug delivery and formation of pH-sensitive delivery systems. This is the result of the carboxyl groups of the polymer, which at highly acidic environments (pH 1.2) do not dissociate. Still, at pH values nearing neutrality (pH 6.8) the carboxyl groups dissociate producing swollen gels [125]. Although this can be useful for oral formulations designed to bypass the stomach, in the buccal cavity, the swelling may cause discomfort for patients and cause potential compliance issues [117].

1.6.3 Cryoprotectants

Proteins and delivery systems, such as liposomes and nanoparticles, can be unstable in the liquid state. Freeze-drying can be a valuable method to stabilize both proteins and liposomes, through the formation of a solid dosage form [126], [127]. However, a cryoprotectant/ lyoprotectant may be required, to protect the liposomes and the protein against morphological changes during the freezing process as well as sublimation [126]. The role of cryoprotectants is particularly crucial for proteins, as they are needed to replace the hydrogen bonding of the protein, which is lost on the removal of water molecules [127]. Thus, incorporation of insulin-containing liposomes within the patch requires the presence of cryoprotectants such as trehalose, sucrose, glucose, fructose or sorbitol [128]. In a study, working with insulin loaded poly (lactic-co-glycolic acid) (PLGA) nanoparticles found the presence of a cryoprotectant before freeze-drying increased insulin structural stability by up to 79% [128]. In this study, sorbitol was found to be highly aiding in the stabilisation of insulin during storage.

1.6.4 Organoleptic

Numerous drugs substances, in their natural state, are unpalatable and unattractive [129]. Thus, they may necessitate supplementation with flavours and/or colours. Taste buds of the tongue react rapidly to flavours; hence the taste of formulations is particularly important for material delivered via the buccal cavity. The addition of flavours can help disguise specific tastes of drugs; for example, citrus flavours can help mask sour or acid-tasting drugs while bitter taste can be masked with sweetening agents. There are several sweetening agents available such as sucrose and sodium saccharin, but the agent recommended that diabetic individuals are sorbitol. Furthermore, if the formulation is to be used by children, they generally prefer a sweet taste [129].

1.6.5 Plasticisers

In some formulations, the presence of plasticisers is necessary to enable the dosage form to have flexibility and resistance [112]. Additionally, these additives aid the mechanical properties of films by improving factors such as tensile strength [61]. Common plasticisers include triethyl citrate, PEG, castor oil, glycerol, and sorbitol. In literature PEG 400 has been incorporated in formulations both as a plasticiser, to improve the flexibility of films, but also to aid in the removal of films from moulds [107].

1.6.6 Drug release: application of mathematical modelling

Often the data obtained from *in vitro* release studies from the patch formulation can be correlated to various kinetic models, which can help to understand the mechanism of drug release from the formulation [130].

Equation 1.1

$$Q_t = Q_0 + K_0 t$$

Zero-order release kinetics is explained by Equation 1.1, where Q_t is the amount of drug dissolved in time t, Q_0 is the initial amount of drug in solution and the zero-order release constant is represented by K_0[131]. Fitting data into zero-order release kinetics can be done by plotting the cumulative amount of drug released versus time [130]. As suggested by Jain and Jain (2016), zero-order drug release kinetics may be desirable for formulations intended for slow and prolonged release drug delivery [132].

Equation 1.2

$$Log\ C = Log\ C_0 - Kt/2.303$$

First-order drug release is represented by Equation 1.2, where C_0 is the initial drug concentration, K is the first-order rate constant, and t is the time [131]. Fitting of release data in a first-order model is via plotting of cumulative log percentage of drug remaining versus time. This model can be used to express the release of water-soluble drugs from porous matrices [133].

Equation 1.3

$$Q_t = K_H \times t^{1/2}$$

The simplified Higuchi model can be expressed by Equation 1.3, where Q_t is the amount of drug released at time $t^{1/2}$ and K_H is the Higuchi rate constant [131]. To fit data to this model, the cumulative percentage drug release against the square root of time is plotted. In this model a few assumptions are made (i) the initial concentration of the drug is higher in the matrix in comparison to drug solubility; (ii) Drug diffusivity

is constant; (iii) the size of particles are smaller compared to the thickness of the system; (iv) there is negligible polymer swelling, and dissolution; (v) drug diffusion only occurs in one dimension; and (vi) sink conditions are maintained in the release environment [131]. This model, proposed by Higuchi in 1961, was the first to describe drug release from sustained-release medication in particular solid drugs dispersed in solid matrices [134]. However, the model has been applied to many types of systems, and numerous studies, as summarised by Jain and Jain (2016), have related the Higuchi model to the mechanism of drug release from liposomal formulation [132].

Equation 1.4

$$\frac{M_t}{M_\infty} = Kt^n$$

The Korsmeyer-Peppas model is described by Equation 1.4, where M_t/M_∞ is the fraction of drug released, K is the kinetics constant, t is the release time, and n is the diffusional release exponent [131], [135]. The exponent n characterizes the mechanism of release and for cylindrically shaped devices when n is 0.45 the mechanism of release is Fickian diffusion release, $0.45 < n < 1.00$ is Anomalous (non-Fickian) diffusion (both phenomenon of diffusion and polymer relaxation). When n is 1 it represents zero-order release [131], [136]. To fit data into this model, typically, the initial 60% drug release is plotted [132]. This model was initially used to study the mechanism of drug diffusion from polymeric systems; however, many researchers have reported the fitting of this model to drug release for many types of delivery systems [132], [135].

1.7 Aim and objectives

The primary purpose of this research was to produce a novel insulin delivery system that accomplished the ideal characteristics summarised by Verma et al. (2011). These characteristics include fast adherence to the buccal mucosa, enhanced insulin absorption, the unidirectional release of the drug, safe and does not aid or cause infections such as dental caries, and will not cause obstruction to regular activity in the buccal cavity, [77].
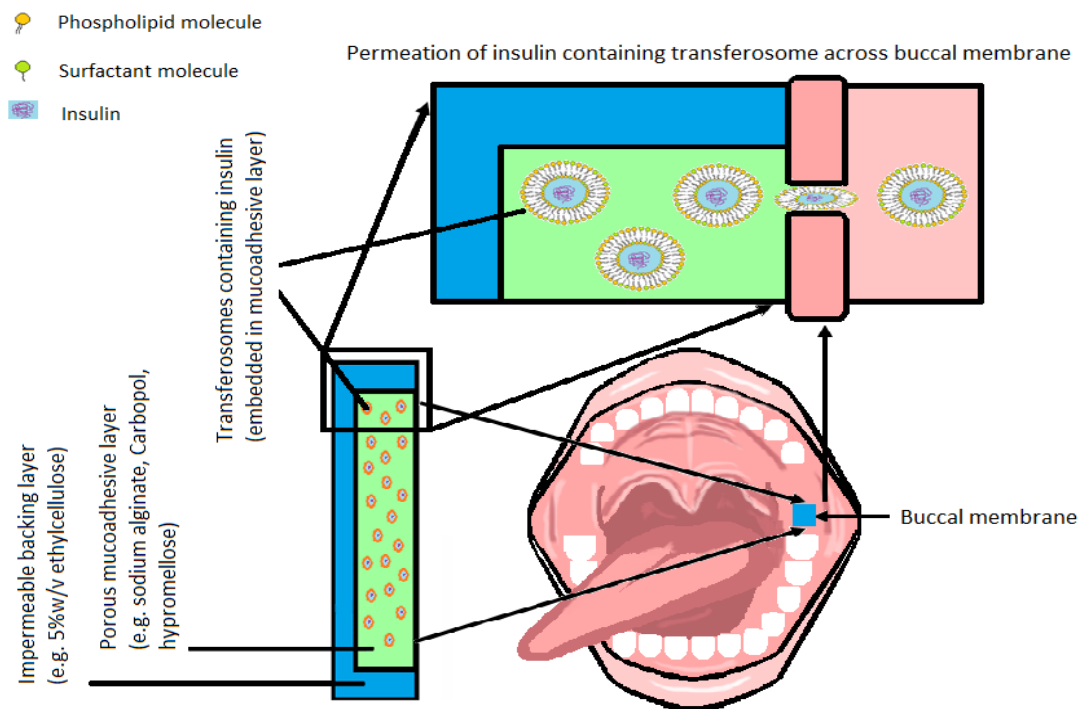
Figure 1.6: Schematic diagram of two-layered patch consisting of a mucoadhesive layer containing transfersomes, which will attach to the buccal membrane, and an impermeable backing layer that will protect the mucoadhesive layer from exposure to the conditions in the mouth. The image also displays the direction of patch attachment and permeation of insulin-containing transfersomes across the buccal membrane.

Hence the overall aim of this research was to attempt delivery of insulin via the buccal mucosa through the preparation of a double-layered patch, consisting of a mucoadhesive layer and an impermeable backing layer. The mucoadhesive layer, as

shown in Figure 1.6, would have insulin incorporated ultradeformable vesicles, i.e. transfersomes, embedded inside.

Overall objectives:

- Development and validation of analytical methods (high-performance liquid chromatography, HPLC) for the identification and quantification of insulin and atenolol (control)

- Formation of niosomes for selection and optimisation of cholesterol, charged molecule and Span content (Spans 20, 40, 60, or 80) for the production of transfersomes

- Development of transfersomes with an optimised combination of non-ionic surfactants, phospholipid, cholesterol and charged molecule or bile salt

- Testing the final transfersomal formulations for toxicity and permeability studies using TR146 buccal cells.

- Assessment and selection of polymers to form the mucoadhesive layer optimised to create aesthetically appealing patches after freeze-drying and to include an appropriate concentration of cryoprotectant

- The final transfersomal formulations combined with the optimised patches and tested for release studies (including mathematical modelling) and characterisation studies such as X-ray diffraction (XRD) and differential scanning calorimetry (DSC).

2. Analytical method development for insulin and atenolol

2.1 Introduction

Human insulin is typically preferred, over porcine and bovine insulin, as the latter two differ slightly by a few amino acids, and thus side reactions are more common [137]. It is a protein; hence it is a relatively large molecule with a molecular weight of 5808 Da [137]. There are three forms of analytical techniques that we can use to detect and analyse insulin. As reviewed by Shen et al. (2019), these are immunoassays, the newer techniques known as electrochemical biosensors and the popular chromatographic methods [138].

Enzyme-linked immunosorbent assay (ELISA) is an important type of immunoassay that works by the detection of a target antigen (analyte) within samples, which in this case is insulin [139]. One widely known ELISA assay for insulin is the sandwich ELISA, which quantifies the amount of insulin bound between a matched pair of antibodies [138]. In this method, the insulin-specific capture antibody is pre-coated in the wells so that when insulin-containing samples are added, they bind to the immobilized antibody. A second detection antibody is then added to form a sandwich, and any unbound antibody is washed off. Subsequently, a chromogenic substrate solution is mixed with the insulin complex, and an acid is added for termination of the reaction. The colour produced at the end of the assay is measured using a spectrophotometer to quantify the amount of insulin [138], [140]. Although this type of assay can be highly specific and can detect and quantify insulin at low concentrations, there are also disadvantages to this type of technique. Downsides can be high cost, antibody instability and thorough optimisation is required; to prevent false positive or negative results due to influence

of background noise reactions [139], [141]. Other modified ELISA assays have also been developed, such as the amplified luminescent proximity homogenous assay (AlphaLISA) and another known as homogeneous time-resolved fluorescence (HRTF). A few other types of immunoassays that have shown good insulin selectivity include chemiluminescence immunoassay (CLIA), radioimmunoassay (RIA), and on-chip immunoassay.

Electrochemical biosensors consist of four parts: the analyte (e.g. insulin), the bio-recognition element, the transducer and the instrumentation [142]. The bio-recognition element enables the selective identification of insulin. When an analyte binds to the bio-recognition element, the transducer, in the device, converts the interaction to an electrical signal (i.e. electrical current or voltage) [142]. The final essential component, which acquires and records the electrical signals from the transducer, is the instrumentation. There are different types of biosensors, and one method of their classification is via the type of response generated: potentiometric (DC electrical potential), amperometric (DC response current) and impedimetric (AC signals). Advantages of these electrochemical biosensors are that they can be robust, cost-effective and can be less susceptible to interferences from non-specific binding [142].

One of the most common methods for insulin detection and quantification is chromatographic analysis. The advantage of this type of analysis is also the capability to detect degradation products. Hence the method can be stability indicating, which is vital for proteins, as they are highly susceptible to degradation, particularly in aqueous solutions [143]. Reversed-phase HPLC (RP-HPLC) is a popular chromatographic method for insulin and is generally combined with a detector to generate quantitative

data. Conventional detectors include ultraviolet (UV), diode array and mass spectrometry (MS).

2.1.1 Reverse-phase high-performance liquid chromatography

RP-HPLC, operates through a combination of nonpolar stationary phase and a polar mobile phase, hence the separation and elution time of the molecule depends on the hydrophobic nature of the molecule [144], [145]. The hydrophobic environment of the column, i.e. the stationary phase, is formed by the bonding of inert silica to hydrocarbon chains. This leads to the column having a higher affinity for hydrophobic compounds. Thus, when molecules, contained in the aqueous phase, pass through the column, the more hydrophobic molecules adsorb on to the stationary phase, and the more hydrophilic molecules pass through the column and are eluted first. Therefore, the elution of the molecule will depend on the polarity of the molecule and the polarity of the mobile phase. The less polar the molecule, the greater the interaction with the stationary phase. Hence, a higher concentration of organic solvent (e.g. acetonitrile, ACN) would be required to reduce the interaction and for the molecule to elute. RP-HPLC can be via either an isocratic method (the ratio of organic solvent is maintained the same throughout) or via gradient method (the concentration of organic solvent is increased over a specified time) [144]. Other factors that can affect separation include the organic solvent composition, temperature and ionic modifiers [146]. Although there are a few ion-pairing agents available such as formic acid, phosphoric acid and acetic acid the additive trifluoroacetic acid (TFA), is a more commonly used agent with proteins due to its volatility [144]. Based on the literature, a popular column used for insulin is the C-18 (octadecyl carbon chain) bonded to silica, and this, together with the other chromatographic conditions, is summarized in Table 2.1. Overall, there are many

advantages to RP-HPLC such as high recovery, reproducibility and the stability of the column over a wide variety of mobile phase conditions [144].

2.1.2   International Conference on Harmonisation guidelines

For the development of a reliable and accurate analytical procedure, it is important to validate the method according to a relevant guideline, such as the International Conference on Harmonisation (ICH). The validation should take into consideration possible uses of the analytical procedure. The validation characteristics, covered by ICH, include specificity, accuracy, precision, repeatability, intermediate precision, detection limit, quantification limit, linearity, and range [147], [148].

The specificity of a method to an analyte is the ability of the method to distinguish and quantify the analyte even in the presence of other possible impurities or degradants in the sample.

Accuracy of a procedure conveys how close in agreement a calculated value is to either a theoretical value or a reference standard. Precision portrays the closeness of agreement between a series of measurements of the same sample. There are different forms of precision and includes repeatability (also known as intra-assay precision) and in intermediate precision (e.g. interday precision).

Detection limit or limit of detection (LOD) is the lowest concentration of an analyte, which can be identified but not necessarily quantified as an exact value. It can be calculated using the standard deviation (SD) of the response and the slope of the calibration curve (Equation 2.1).

Equation 2.1

$$LOD = \frac{3.3\,\sigma}{S}$$

Where

σ = the SD of the response

S = the slope of the calibration

Quantification limit or limit of quantification (LOQ) is the lowest concentration of an analyte that can be quantified with the method with appropriate precision and accuracy. It can be calculated using the SD of the response and the slope of the calibration curve (Equation 2.2).

Equation 2.2

$$LOQ = \frac{10\,\sigma}{S}$$

Where

σ = the SD of the response

S = the slope of the calibration curve

Linearity is expressed by a method, over a certain range, when the response produced is directly proportional to the analyte concentration present in the sample. The range is the lower and upper concentration of analyte that the method demonstrates linearity but also accuracy and precision.

Table 2.1: A summary of RP-HPLC-UV methods for insulin from literature.

Ref	Column	Mobile phase	Elution type	Detection (nm)	Flow rate (mL/min)	Elution time (min)	LOD & LOQ	IS
[143]	Hypersil RP-C18 column (3 µm, 4.6 mm x 100 mm)	KH_2PO_4 buffer (0.1M), ACN, & methanol (62:26:12, v/v). Final pH adjusted to 3.1.	Isocratic	214	1	7.9	2.93 µg/mL & 9.78 µg/mL	2-nitrophenol
[149]	Xterra RP-C18 (5 µm, 4.6 mm x 250 mm) with Guard column	ACN & deionized water with 0.1% TFA. [First 30:70 (v/v) linear change to 40:60 (v/v) over 5 min next 40:60 (v/v) retained from 5 to 10 min]	Gradient first 5 min then isocratic for 5 min	214	1	5.6	0.24 µg/mL & 0.72 µg/mL	NA
[150]	Phenomenex RP-C18 (5 µm, 4.6 mm x 150 mm) with Guard column	0.2M sodium sulphate anhydrous (pH 2.3 with ortho phosphoric acid) & ACN (74:26, v/v)	Isocratic	214	1.2	10.2	0.35 µg/mL & 0.7 µg/mL	Methylparaben
[151]	Phenomenex RP-C18 (5 µm, 4.6 mm x 150 mm)	ACN with 0.1% TFA & deionized water with 0.1% TFA (30:70, v/v)	Isocratic	215	1.5	8.5	10 µg/mL & 60 µg/mL	NA

Abbreviations: Reverse-phase high-performance liquid chromatography (RP-HPLC), the limit of detection (LOD), the limit of quantification (LOQ), ultraviolet (UV), TFA (trifluoroacetic acid), acetonitrile (ACN) and internal standard (IS)

2.2 Chapter aims

➢ Develop an HPLC method for insulin, which is stability-indicating.

➢ Validate the method according to ICH guidelines and apply the analytical method for the detection and quantification of insulin under various conditions such as in the presence of transfersomal formulations.

➢ Develop and validate an HPLC method for atenolol for determination and quantification of atenolol in permeation studies.

2.3 Materials

RHI (27.5 IU/mg), 2-Nitrophenol, atenolol and phosphate-buffered saline (PBS, pH 7.4) were all purchased from Sigma-Aldrich (Merck KGaA, Darmstadt, Germany). HPLC grade TFA (99+%), methanol and ACN purchased from Fischer Scientific (Leicestershire, UK). MilliQ® water was obtained internally.

2.4 Insulin method validation

2.4.1 Preparation of the insulin standard and quality control solutions

A standard stock solution of RHI was prepared in PBS at a concentration of 1.5 mg/mL in a 50 mL volumetric flask. This was then diluted, if required, with PBS to produce the following concentration of insulin for the calibration curve: 1.5 mg/mL, 0.9 mg/mL, 0.75 mg/mL, 0.6 mg/mL, 0.3 mg/mL, 0.1 mg/mL, 0.06 mg/mL, 0.03 mg/mL, 0.01 mg/mL and 0.005 mg/mL. These ten concentrations were then used to construct a calibration graph for RHI using HPLC. Separately, three quality control (QC) samples were chosen at concentrations of 1.44 mg/mL, 1.2 mg/mL and 0.96 mg/mL. For stability testing the samples were stored in PBS solution in the refrigerator (2-8°C) and

analysed daily for a total of 5 consecutive days (1.2 mg/mL) and after one month (stock solution 1.5 mg/mL). For both the inter-day and intra-day analysis, the stock solutions were prepared just before the HPLC analysis was to be carried out.

2.4.2 Preparation of the internal standard and HPLC vial preparation

Fresh stocks of the internal standard (IS, 2-nitrophenol) was prepared daily at a concentration of 0.2 mg/mL. In the HPLC vials, the IS to insulin concentration was maintained in the ratio of 1:4, respectively (e.g. 200 µL of IS and 800 µL of insulin). Hence the concentration of IS was maintained as 0.04 mg/mL in all the runs.

2.4.3 Results and discussion

2.4.3.1 Method development and optimisation

Insulin detection and quantification were conducted using the Shimadzu LC-2010A HT unit (Kyoto, Japan). The system consists of a degassing unit, quaternary low-pressure gradient unit, pump unit, mixer, autosampler, column oven, and a UV-VIS detector with a thermostatted flow cell. The column used was a SphereClone™ C-18 (150 x 4.6 mm, 5 µm), which was combined with a security guard column and cartridge kit, all purchased from Phenomenex (Cheshire, UK). The LabSolutions software was used to analyse the chromatograms. Initially, a method was developed that did not include an internal standard, and although relatively sharp peaks were produced, there was some interday variability in the results (Figure 2.1). This was particularly true, after a few weeks of inactivity, even with the same HPLC instrument and column. In this isocratic method the two solvents used were 30% of 0.1% (v/v) TFA in ACN (solvent A) and 70% 0.1% (v/v) TFA in MilliQ® water (solvent B) [151]. The method was then adjusted

to include an IS, which led to the selection of 2-nitrophenol, which has been used with insulin in previous literature [143]. This directed to the mobile phase comprising of 33.5% of solvent A [0.1% (v/v) TFA in ACN] and 66.5% of solvent B [0.1% (v/v) TFA in MilliQ® water]. The solvents for the mobile phase were prepared on the day of analysis. The flow rate was set as 1 mL per minute. The temperature was maintained at 25 ˚C. The wavelength of the UV detector was set at 215 nm. An injection volume of 10 µL was used for all samples. Each sample was run for 10 minutes and the peak for insulin was observed between 3.5-4.5 minutes. 2-Nitrophenol was used as an IS, concentration maintained as 0.04 mg/mL, which was observed between 7.5-8.5 minutes.
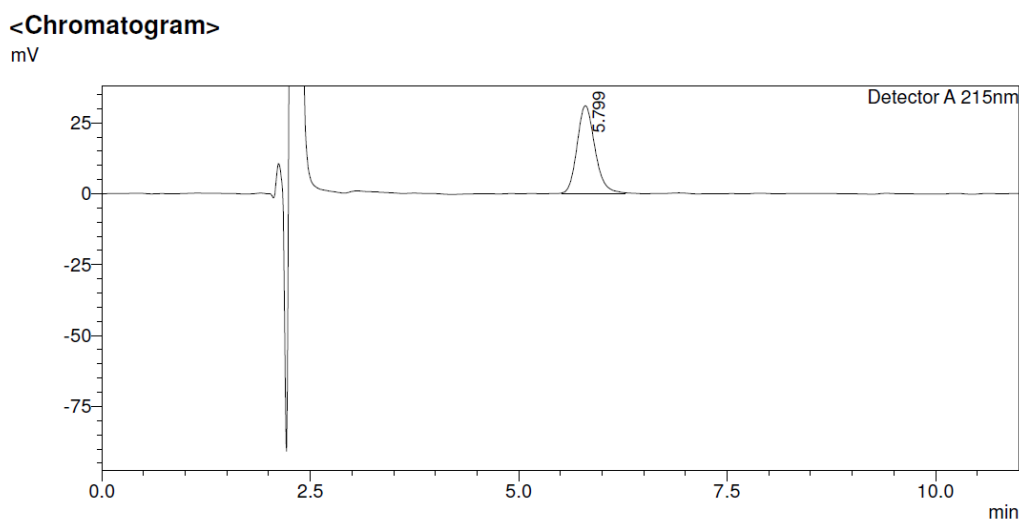
Figure 2.1: Chromatogram of insulin produced using 30% ACN with 0.1% (v/v) TFA and 70% MilliQ® water with 0.1% (v/v) TFA.

Abbreviations: Acetonitrile (ACN) and trifluoroacetic acid (TFA)

2.4.3.2 Accuracy and intraday precision

Table 2.2: Intraday repeatability and precision parameters for insulin in PBS

Theoretical Concentration (mg/mL)	Concentration Ratio	Response Ratio	Calculated Concentration (mg/mL)	% Recovery	% RSD
0.96	19.2	4.33	0.95	99.31	1.13
0.96	19.2	4.40	0.97	100.82	
0.96	19.2	4.43	0.97	101.52	
1.20	24.0	5.54	1.22	101.40	0.82
1.20	24.0	5.60	1.23	102.43	
1.20	24.0	5.63	1.24	103.05	
1.20	24.0	5.56	1.22	101.67	
1.20	24.0	5.66	1.24	103.51	
1.20	24.0	5.70	1.25	104.23	
1.44	28.8	6.46	1.42	98.39	1.12
1.44	28.8	6.59	1.45	100.44	
1.44	28.8	6.57	1.44	100.12	

Notes: Concentration of internal standard (2-Nitrophenol) was maintained constant as 0.04 mg/mL.
Abbreviations: Relative standard deviation (RSD) and phosphate-buffered saline (PBS)

The accuracy and intraday precision (repeatability) of the method was demonstrated by injecting three times the low and high QCs (0.96 mg/mL and 1.44 mg/mL) and six times the main QC (1.2 mg/mL). Results are shown in Table 2.2 above. The average accuracy for the intraday results was found to be 101.41 ± 1.72%, compared to the theoretical concentration, and the mean % relative standard deviation (RSD) value 1.02 ± 0.18%. These results show the method is both accurate and repeatable.

Table 2.3: Intraday and interday repeatability and precision parameters for insulin in PBS

Day	Theoretical Concentration (mg/mL)	Calculated Concentration (mg/mL)	% Recovery	% RSD
1	0.96	0.97	100.55	0.79
2	0.96	0.95	99.04	
3	0.96	0.95	99.25	
1	1.20	1.23	102.72	0.75
2	1.20	1.20	99.58	
3	1.20	1.19	99.19	
1	1.44	1.44	99.65	0.76
2	1.44	1.41	98.20	
3	1.44	1.42	98.44	

Notes: Concentration of internal standard (2-Nitrophenol) was maintained constant as 0.04 mg/mL. Results represent mean [(n=3) for 0.96 mg/mL & 1.44 mg/mL and (n=6) 1.20 mg/mL]. Abbreviations: Relative standard deviation (RSD) and phosphate-buffered saline (PBS)

The intermediate precision (interday repeatability) was demonstrated by repeating the injection of the three QCs, same as for intraday, over three consecutive days (Table 2.3). In the interday repeatability calculations, the average % recovery was found to be 99.62 ± 1.35%, with % RSD of 0.77 ± 0.39%. These values meet the ICH guidelines in demonstrating intermediate precision as the results show a high level of accuracy and repeatability.

2.4.3.3 Linearity and range

Table 2.4: Insulin calibration curve data.

Insulin concentration (mg/mL)	Concentration Ratio	Response Ratios			% Recovery	% RSD
0.005	0.1	0.017	0.016	0.015	107.11	2.95
0.01	0.2	0.045	0.041	0.042	103.53	2.94
0.03	0.6	0.148	0.150	0.151	102.60	0.86
0.06	1.2	0.313	0.311	0.313	102.72	0.27
0.1	2.0	0.489	0.502	0.495	96.46	1.29
0.3	6.0	1.517	1.533	1.536	97.53	0.68
0.6	12.0	3.172	3.151	3.134	100.17	0.60
0.75	15.0	3.918	3.945	3.880	99.42	0.83
0.9	18.0	4.820	4.840	4.821	102.12	0.24
1.5	30.0	7.796	7.823	7.914	99.46	0.78

Notes: Concentration of internal standard (2-Nitrophenol) was maintained constant as 0.04 mg/mL.
Abbreviation: Relative standard deviation (RSD).
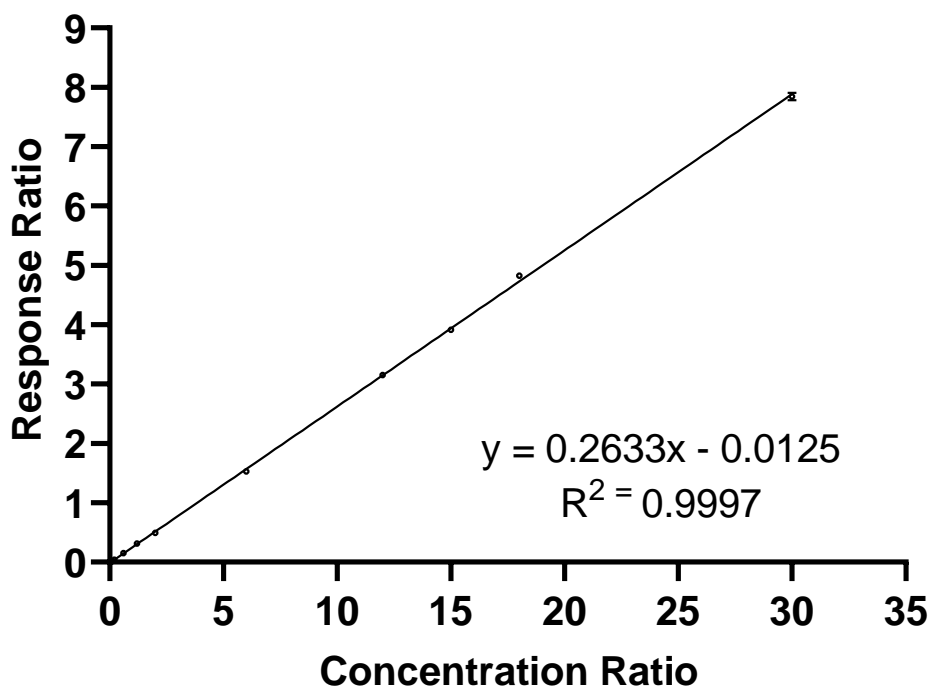
Figure 2.2: Calibration curve for insulin displaying linearity across all concentrations tested 0.005 mg/mL to 1.5 mg/mL.

Notes: Concentration of internal standard (2-Nitrophenol) was maintained constant as 0.04 mg/mL. Results represent mean ± SD (n=3). See Table 2.4 for insulin concentration and concentration ratio.

Linearity is the ability of the method to demonstrate a direct proportional response to the increase in analyte concentration (i.e. insulin). It can be observed based on Table 2.4 and Figure 2.2 that between the range of 0.005 mg/mL to 1.5 mg/mL a linear response is achieved (R^2 >0.999), with precision and accuracy across all values.

2.4.3.4   Detection and quantification limit

LOD and LOQ were calculated according to the ICH guidelines using Equation 2.1 and Equation 2.2, respectively, based on the calibration curve and regression analysis. LOD was found to be 0.005 mg/mL, displayed in Figure 2.3, and LOQ was found to be 0.016 mg/mL.

<Chromatogram>
mV

Detector A 215nm
7.969
3.510

100—

0—

-100—

0.0   2.5   5.0   7.5   10.0
                                                      min
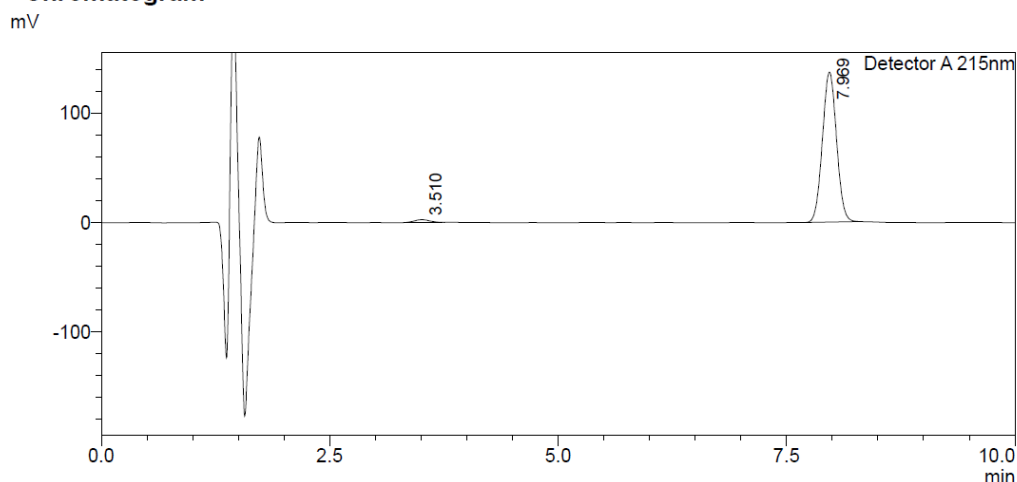
Figure 2.3: Chromatogram of LOD (0.005 mg/mL) concentration in PBS.

Notes: Concentration of internal standard (2-Nitrophenol) was maintained constant as 0.04 mg/mL. Abbreviation: phosphate-buffered saline (PBS)

2.4.3.5   Specificity and stability

It is essential to develop a method that is specific to insulin and is stability-indicating, as storage in aqueous solutions can lead to possible hydrolytic reactions or polymerisation of insulin [143]. Storage in media of neutral and alkaline pH (such as PBS pH 7.4) can enable deamidation to take place at residue asparagine B3 (AsnB^3) [152]. Although deamidation can take place in neutral formulations, it takes place at a slower pace than in acidic conditions [152]. Hence deamidation wasn't observed during storage in PBS (pH 7.4), or water but it was seen when insulin was stored at room temperature (21-23°C) after 24 hours storage in 1% (v/v) acetic acid (pH 2.9). It can be seen from the chromatogram (Figure 2.4) a second peak (at 4.128 minutes) has appeared just after the regular insulin peak. This is likely to be the peak for insulin as a result of deamidation of asparagine at residue A21, as this is the expected hydrolytic degradation product of insulin in acidic conditions [152], [153].
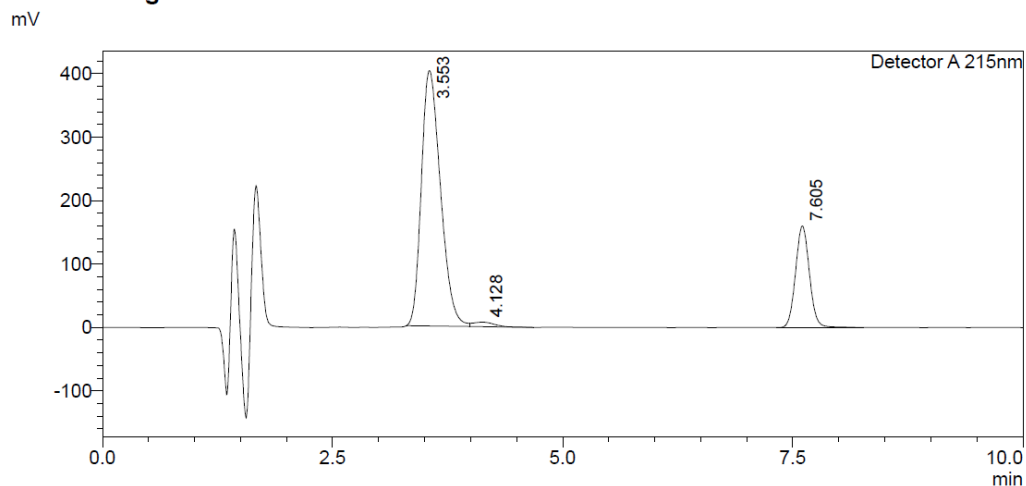
Figure 2.4: Chromatogram of insulin after storage in 1% acetic acid (pH 2.9) for 24 hours at room temperature (21-23°C).

Notes: Concentration of internal standard (2-Nitrophenol) was maintained constant as 0.04 mg/mL.

Table 2.5: Stability of insulin in PBS solution stored in a fridge (2-8°C, n=6).

Days in Fridge	Theoretical Conc. (mg/mL)	Conc. Ratio	Response Ratio	Calculated Conc. (mg/mL)	Precision (% Recovery)	% RSD
0	1.20	24	5.61	1.23	102.72	0.82
1	1.20	24	5.31	1.17	97.20	0.42
2	1.20	24	5.49	1.21	100.43	0.58
3	1.20	24	5.20	1.14	95.17	0.35
4	1.20	24	4.98	1.09	91.21	0.30
30	1.50	30	4.98	0.95	73.00	0.51

Notes: Concentration of internal standard (2-Nitrophenol) was maintained constant as 0.04 mg/mL. Abbreviations: Relative standard deviation (RSD) and phosphate-buffered saline (PBS)

It has been found that insulin stored in solution is susceptible to dimerisation, particularly when shaking is applied [154]. Monomeric insulin is the biologically active form of insulin; hence it is essential to detect any such changes during storage and production of formulations [155]. Analysis of insulin during storage in PBS solution (pH

7.4) in the fridge (2-8°C) resulted in a reduction of insulin to 91.21% after four days compared to the original stock (Table 2.5). After 30 days of storage, the concentration of insulin was reduced to 70.00%. It can be seen from the chromatogram (Figure 2.5) below that at 30 days a second peak has appeared at 3.542 minutes just before the regular insulin peak, which is likely to be the result of insulin dimer formation [154]. The peak at 2.744 minutes is possibly the result of tetrameric insulin due to the absence of Zn^{2+} in the solution to form hexamers [153], [156].
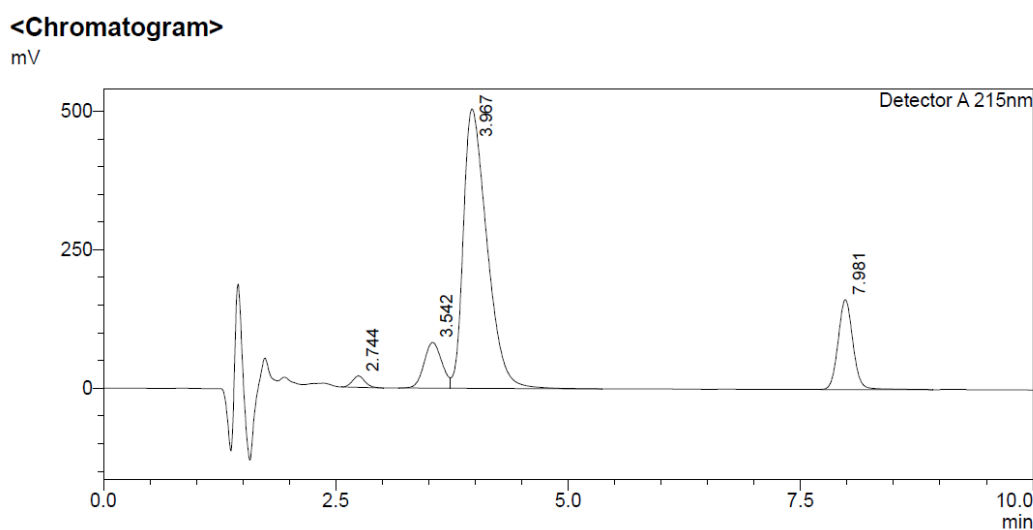
Figure 2.5: Chromatogram of insulin in PBS solution (pH 7.4) after 30 days of storage in the fridge (2-8°C).

Notes: Concentration of internal standard (2-Nitrophenol) was maintained constant as 0.04 mg/mL. Abbreviation: Phosphate-buffered saline (PBS)

Hence throughout all the steps of transfersome production stability was assessed, such as during heat and bath sonication, and only when no significant difference in the percentage recovery was seen compared to freshly prepared insulin samples was the step approved and continued. Additionally, the chromatograms were observed to confirm the absence of peaks that could indicate degradation products.

2.4.3.6   Specificity and application

\<Chromatogram\>

mV

Detector A Channel 1 215nm

a.

\<Chromatogram\>

mV

Detector A Channel 1 215nm

8.101

b.

\<Chromatogram\>

mV

Detector A 215nm

3.956

7.918

c.
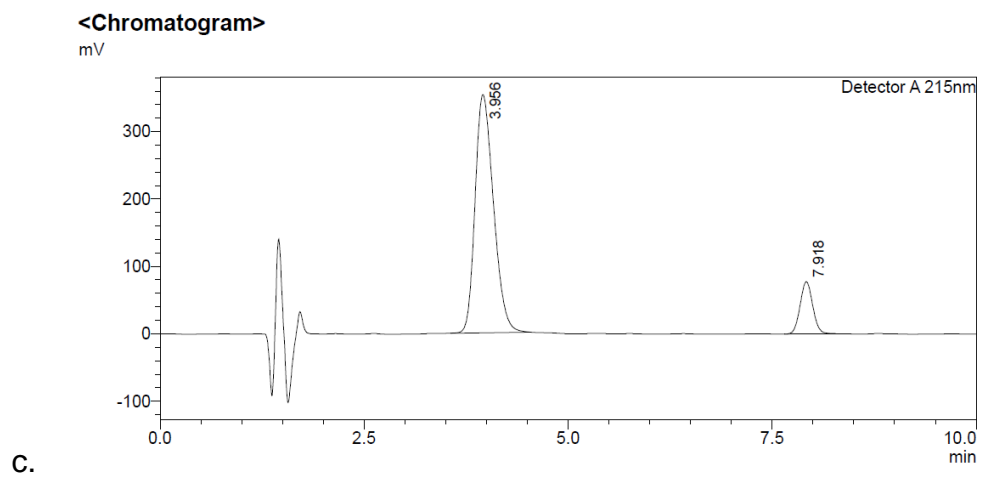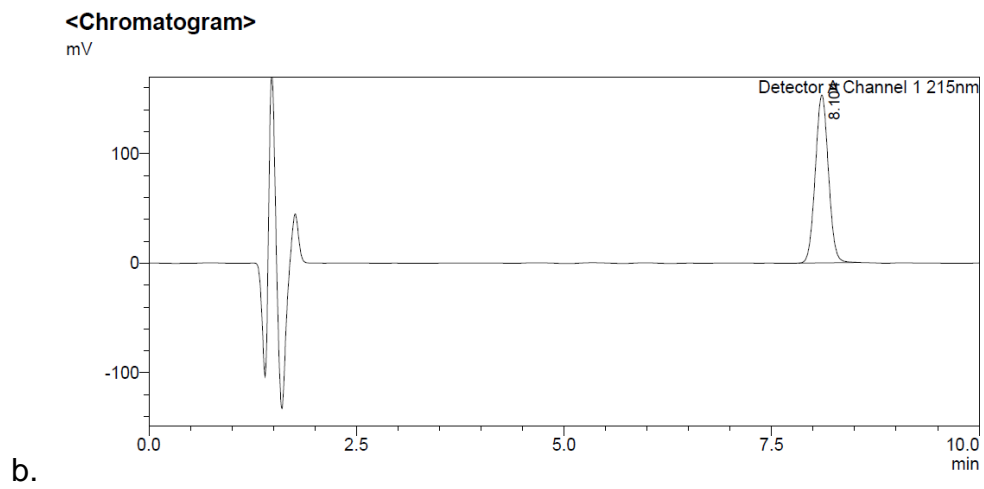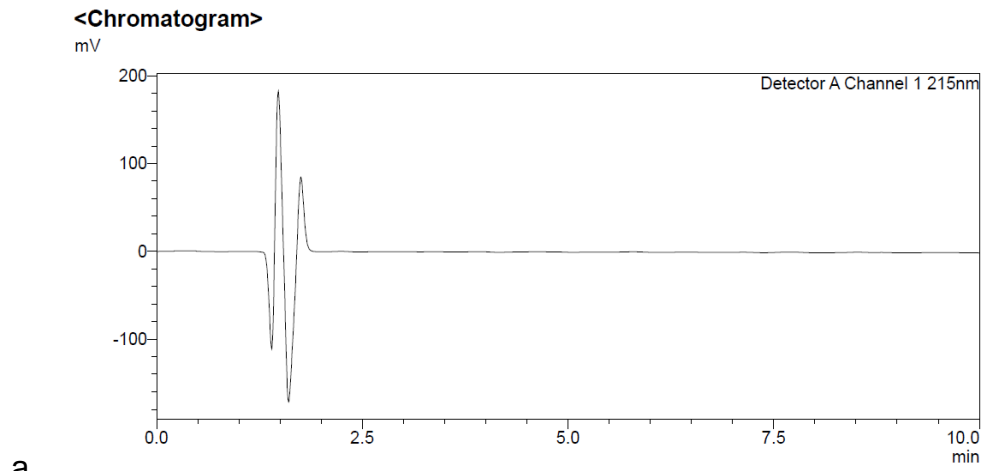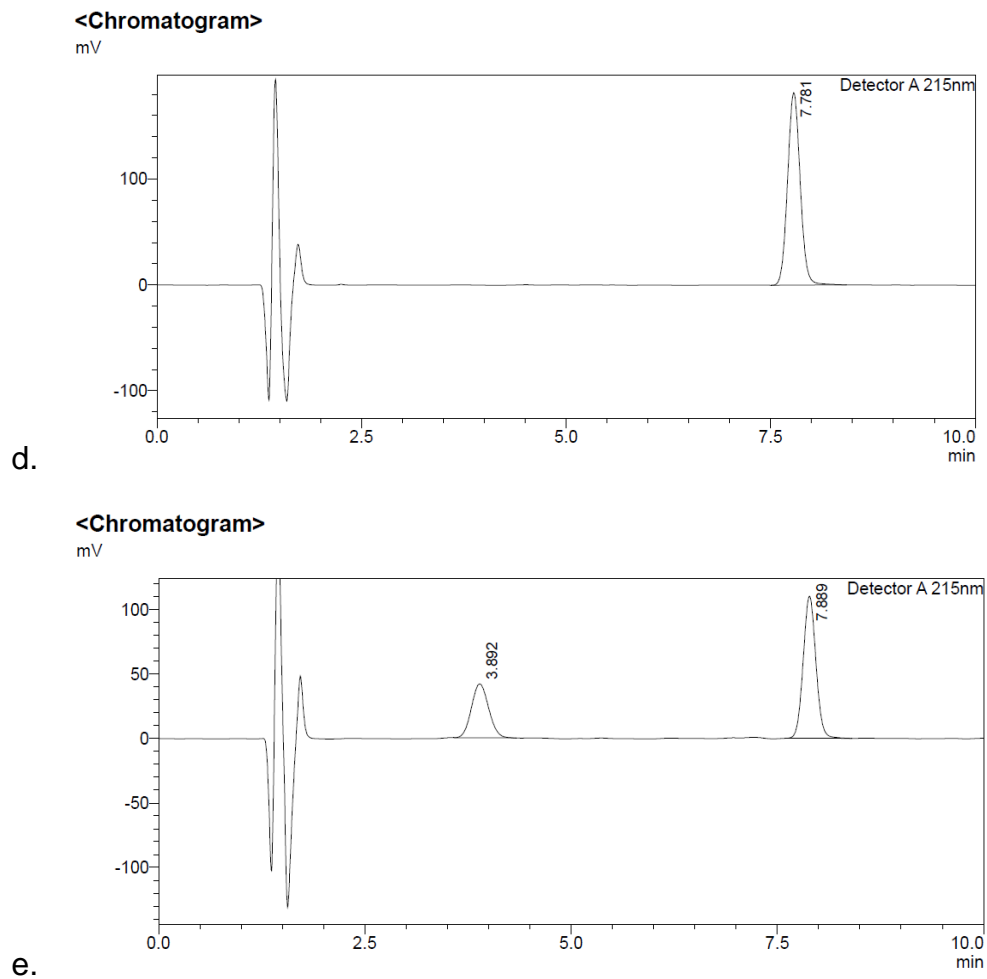
Figure 2.6: Chromatograms of (a) blank PBS only, (b) internal standard only (0.04 mg/mL), (c) insulin (1.2 mg/mL) with internal standard (0.04 mg/mL) in PBS, (d) unloaded supernatant of a transfersomal formulation, and (e) insulin in supernatant of a transfersomal formulation.

Abbreviation: Phosphate-buffered saline (PBS)

Specificity of the method to insulin is vital to ensure other impurities do not interfere with the results. It can be seen from Figure 2.6, that the method is specific to insulin as the insulin peak only appears in the solutions that insulin was expected to be present (c & e) and absent in the solutions that do not contain insulin (i.e. a, b & d). Additionally, no interfering peaks can be observed that can influence the peak for insulin.

2.5 Atenolol method validation

2.5.1 Preparation of the atenolol standard and quality control solutions

A standard stock solution of atenolol was prepared in PBS at a concentration of 1 mg/mL in a 50 mL volumetric flask. This was then diluted, if required, with PBS to produce the following concentration of insulin for the calibration curve: 1 mg/mL, 0.6 mg/mL, 0.4 mg/mL, 0.1 mg/mL, and 0.03 mg/mL. These five concentrations were then used to construct a calibration graph for atenolol using HPLC. Separately, three quality control (QC) samples were chosen at concentrations of 0.8 mg/mL, 0.2 mg/mL and 0.05 mg/mL. For both the inter-day and intra-day analysis, the stock solutions were prepared just before the HPLC analysis was to be carried out.

2.5.2 Results and discussion

2.5.2.1 Method development and optimisation

An isocratic RP-HPLC method was developed for atenolol detection and quantification. It was conducted using the Shimadzu LC-2010A HT unit (Kyoto, Japan). The column a SphereClone™ C-18 (150 x 4.6 mm, 5 µm). The mobile phase consisting of two solvents; 19% of solvent A [0.1% (v/v) TFA in methanol] and 81% of solvent B [0.1% (v/v) TFA in MilliQ® water]. The solvents for the mobile phase were prepared on the day of analysis. The flow rate was set at 0.5 mL per minute. The temperature was maintained at 25 ˚C. The wavelength of the UV detector was set at 276 nm. An injection volume of 10 µL was used for all samples. Each sample was run for 10 minutes, and the peak for atenolol was observed between 7.0-8.0 minutes.

2.5.2.2   Specificity and accuracy

a.

\<Chromatogram\>

mV

Detector A 276nm

\<Peak Table\>
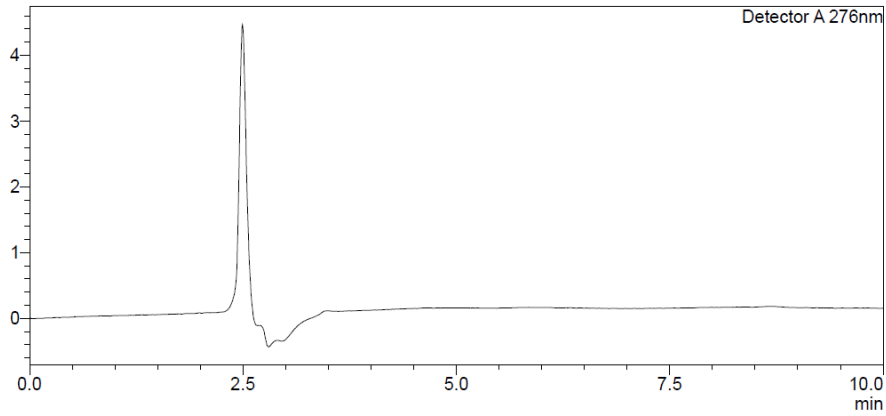
Detector A 276nm

Peak#	Ret. Time	Area	Height	Conc.	Unit	Mark	Name
Total							

b.

\<Chromatogram\>

mV

7.098

Detector A 276nm

\<Peak Table\>
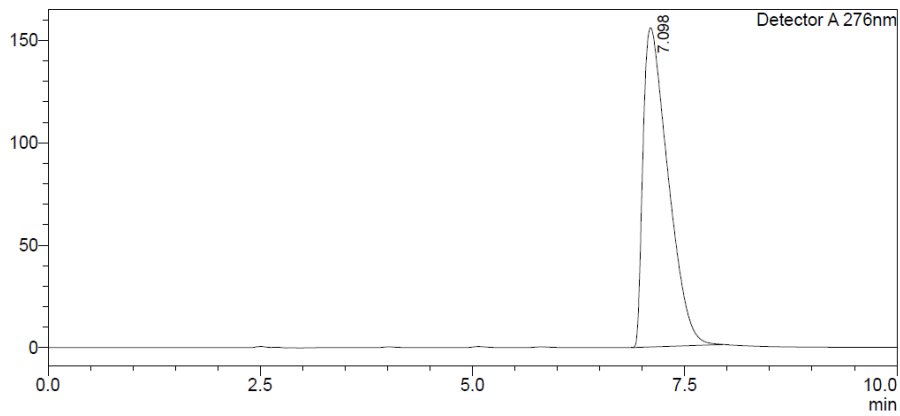
Detector A 276nm

Peak#	Ret. Time	Area	Height	Conc.	Unit	Mark	Name
1	7.098	3191275	155927	0.800	mg/L		Atenolol
Total		3191275	155927				

Figure 2.7: Chromatograms of (a) blank PBS only, and (b) atenolol (0.8 mg/mL) in PBS.

Abbreviation: Phosphate-buffered saline (PBS)

It can be seen from Figure 2.7 that the peak is specific for atenolol as the blank PBS solution (a) displays only the solvent peak and no other peaks, while (b) shows only the peak for atenolol. The accuracy of the method can also be observed as; theoretically, the concentration of atenolol should be 0.8 mg/mL, and this is demonstrated to be true in Figure 2.7; calculated with the LabSolutions software.

2.5.2.3   Accuracy and intraday precision

Table 2.6: Intraday repeatability and precision parameters for atenolol in PBS

Theoretical Concentration (mg/mL)	AUC	Calculated Concentration (mg/mL)	% Recovery	% RSD
0.05	194985	0.05	101.49	0.05
0.05	194968	0.05	101.48	
0.05	194812	0.05	101.40	
0.20	793750	0.20	100.28	0.10
0.20	794955	0.20	100.44	
0.20	793499	0.20	100.25	
0.80	3214200	0.81	100.78	0.27
0.80	3204160	0.80	100.46	
0.80	3192845	0.80	100.11	
0.80	3193325	0.80	100.12	
0.80	3195677	0.80	100.20	
0.80	3192282	0.80	100.09	

Abbreviations: Relative standard deviation (RSD) and phosphate-buffered saline (PBS)

The accuracy and intraday precision (repeatability) of the method was demonstrated by injecting three times the low and medium QCs (0.05 mg/mL and 0.2 mg/mL) and six times the main QC (0.8 mg/mL). The average accuracy for the intraday results was found to be 100.59 ± 0.56%, compared to the theoretical concentration, and the mean

% RSD value 0.14 ± 0.12% (Table 2.6). These results show the method is both highly accurate and repeatable.

Table 2.7: Interday repeatability and precision parameters for atenolol in PBS

Day	Theoretical Concentration (mg/mL)	Calculated Concentration (mg/mL)	% Recovery	% RSD
1	0.05	0.05	101.46	0.14
2	0.05	0.05	98.42	
3	0.05	0.05	100.10	
1	0.20	0.20	100.32	0.09
2	0.20	0.20	99.35	
3	0.20	0.20	100.06	
1	0.80	0.80	100.29	0.21
2	0.80	0.81	100.65	
3	0.80	0.81	101.07	

Notes: Results represent mean [(n=3) for 0.05 mg/mL & 0.2 mg/mL and (n=6) 0.8 mg/mL]. Abbreviations: Relative standard deviation (RSD) and phosphate-buffered saline (PBS)

The intermediate precision (interday repeatability) was demonstrated by repeating the injection of the three QCs, same as for intraday, over three consecutive days (Table 2.7). In the interday repeatability calculations, the average % recovery was found to be 100.19 ± 0.90%, with % RSD of 0.15 ± 0.06%. These values meet the ICH guidelines in demonstrating intermediate precision as the results show a high level of accuracy and repeatability.

Table 2.8: Atenolol calibration curve data.

Atenolol concentration (mg/mL)	AUC			Calculated concentration (mg/mL)	% Recovery	% RSD
0.03	114962	115275	114947	0.03	102.49	0.16
0.1	394151	394766	393833	0.10	100.61	0.12
0.4	1580431	1581523	1578621	0.40	99.34	0.09
0.6	2391124	2393732	2394889	0.60	100.13	0.08
1.0	3990738	3989233	3991862	1.00	100.05	0.03

Abbreviations: Area under the curve (AUC) & relative standard deviation (RSD)

The calibration curve shows: $y = 3996441x - 7812$, $R^2 = 1.00$
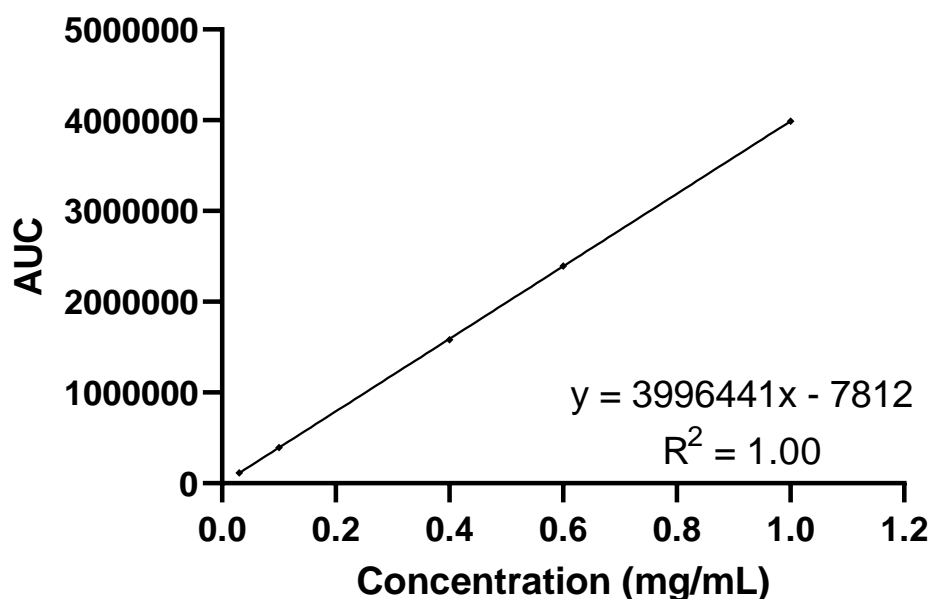
Figure 2.8: Calibration curve for atenolol displaying linearity across all concentrations tested 0.03 mg/mL to 1.0 mg/mL.

Notes: Results represent mean ± SD (n=3). Abbreviation: Area under the curve (AUC).

Linearity is the ability of the method to demonstrate a direct proportional response to the increase in analyte concentration (i.e. atenolol). It can be observed based on Table

2.8 and Figure 2.8 that between the range of 0.03 mg/mL to 1 mg/mL a linear response is achieved ($R^2 > 1$), with precision and accuracy across all values.

2.5.2.5 Detection and quantification limit

LOD and LOQ were calculated according to the ICH guidelines using Equation 2.1 and Equation 2.2, respectively, based on the calibration curve and regression analysis. LOD was found to be 0.001 mg/mL, displayed in Figure 2.3, and LOQ was found to be 0.004 mg/mL.

2.5.2.6 Stability of atenolol

Table 2.9: Stability of atenolol in PBS solution stored in a fridge (2-8°C, n=6).

Days in Fridge	Theoretical Conc. (mg/mL)	AUC	Calculated Conc. (mg/mL)	% Recovery	% RSD
0	0.8	3198748	0.802	100.29	0.27
1	0.8	3203513	0.804	100.44	0.05
2	0.8	3196136	0.802	100.21	0.10
3	0.8	3196069	0.802	100.21	0.13
4	0.8	3191371	0.801	100.06	0.07

Abbreviations: Area under the curve (AUC), relative standard deviation (RSD) and phosphate-buffered saline (PBS)

It is crucial to detect any changes in the % recovery of drugs during use to determine how long a solution will be stable and can be used for studies. Based on the results of 5 days storage of atenolol in PBS solution in the fridge (2-8°C), it can be confirmed that atenolol is stable during this period, and can be used for studies without the requirement to prepare fresh batches daily (Table 2.9).

2.6 Conclusion

In summary, two new, reliable, and accurate methods have been developed for both the detection and quantification of insulin and atenolol and validated according to ICH guidelines. Although the ICH guideline does not specify exact acceptance limits the % recovery and the % RSD values attained are satisfactory and comparable to existing literature validated according to the same guideline [157]. The validated method for insulin was used for quantification of insulin in calculating EE (%), loading capacity (LC, %), release studies and permeation studies. The method for atenolol was used for quantification of atenolol in permeation studies.

3. Formulation and characterisation of niosomes: screening of surfactant

3.1 Introduction

Niosomes are formed using non-ionic surfactants. They are becoming more extensively studied as substitutes to liposomes due to their greater stability as well as cost-effectiveness [83], [104]. Further advantages these systems offer include being non-immunogenic, biocompatible and biodegradable [94]. Several types of non-ionic surfactants are used to form niosomes but commonly include esters of fatty acids, alkyl ethers, alkyl amides and alkyl esters [158]. Alkyl ethers can be an option for entrapping proteins due to their high stability compared to alkyl esters. Still, the latter is less toxic than the former as the esterase enzymes in the body can degrade the ester bonds in the surfactants [88]. Hence for a chronically administered drugs, such as insulin, the ester-linked surfactants are a safer option as carriers for drug delivery. The sorbitan esters (Spans) are particularly favourable as they are commonly used in the food and pharmaceutical industry and are on the GRAS ingredients list [104].

A parameter that is a good indicator of surfactants forming niosomes is the hydrophilic-lipophilic balance (HLB), which as the name suggests describes the balance between the hydrophilic and hydrophobic portion of the surfactant [83], [159]. In non-ionic surfactants, the HLB ranges from 0-20, and the higher the HLB value, the more hydrophilic the surfactant [159]. The HLB of Spans are as follows; Span 20 (8.6), Span 40 (6.7), Span 60 (4.7), and Span 80 (4.3) [104]. It has been found that Spans with HLB values between 4-8 are compatible with the formation of vesicles [83]. Hydrophilic surfactants (HLB 14-17) are generally not considered suitable for the production of

bilayered structures due to their high aqueous solubility; however, they can sometimes form niosomes in the presence or optimum concentrations of cholesterol [159], [160]. Cholesterol can act as a bilayer membrane stabilisers [97].

As discussed by Israelachvili (1976), the packing properties of surfactants is also an essential factor to take into account when developing niosomes [161]. The formation of bilayers occurs when the packing parameter falls between ½ and 1. It has been found that primarily the formation of the smallest structures is more likely when amphiphiles aggregate; however, the size and shape of the structures is restricted by the packing. Thermodynamically the development of spherical vesicles is favoured over planar bilayers, and commonly sonication is a method used for their formation [161].

The phase transition temperature of surfactants also affects the characteristics of niosomes. In the gel state, the alkyl chains are ordered structures, while in the liquid state, the bilayer is in a more disordered arrangement [88]. It has been observed that Spans can form liposome like vesicles [104].

Aggregation of vesicles can be a problem in some formulations. Hence often it is important to include a charged molecule in the niosomal formulation, such as the positively charged stearylamine or the negatively charged DCP, which can reduce or prevent aggregation through electrostatic stabilisation [83].

For the selection of the correct Span and cost efficiency, it was opted to initially form niosomes, to optimise factors such as cholesterol content and presence or absence of charged molecule before production of transfersomes.

3.2 Chapter aims

- To prepare niosomes using sorbitan esters (Span 20, Span 40, Span 60 and Span 80).

- To determine particle size and zeta potential.

- To optimise cholesterol content in the niosomal formulations.

- To study the effects of the charged molecules (DCP) on the properties of niosomes.

- To analyse insulin EE (%) of niosomes using previously validated HPLC.

3.3 Materials and methods

RHI (27.5 IU/mg), sorbitan laurate (Span 20), sorbitan monopalmitate (Span 40), sorbitan monostearate (Span 60), sorbitan monooleate (Span 80), cholesterol, DCP and PBS (pH 7.4) were all purchased from Sigma-Aldrich (Merck KGaA, Darmstadt, Germany). Chloroform and HPLC grade TFA and ACN were purchased from Fischer Scientific (Leicestershire, UK). MilliQ® water was obtained internally using a Merck Millipore Direct-Q® 3UV water purification system (Billerica, MA, USA). All other chemicals and reagents used were of analytical grade.

3.3.1 Niosome preparation and optimisation

Insulin is a protein, hence the stability of the drug is a key factor to consider during niosomal preparation. Thus for initial development, the method was followed based on a previous study working with insulin, which produced niosomes using the four types of Spans (Span 20, 40, 60 & 80) [162]. After preliminary tests, some adjustments were

made, including bath sonication, to both reduce the size and aid uniformity of the formed niosomes.

3.3.2   Thin-film hydration method

Niosomes were prepared using 300 micromoles of surfactant/cholesterol or surfactant/cholesterol/DCP dissolved in 10 mL of chloroform: methanol (9:1 v/v) in a 100 mL round-bottom flask in compositions shown in Table 3.1. The organic solvents were removed at 50˚C, under vacuum, using a RE300 rotary evaporator at speed 10 rotation. The process lasting around 15 minutes. The dried surfactant/lipid film was then hydrated with 5 ml PBS (pH 7.4) or 5 mL PBS containing insulin (20 units/mL) in a Fisherbrand bath sonicator (FB15047) at 55-60˚C for 15 minutes. A temperature of 55˚C was chosen, which increased to around 60°C during sonication. The temperature was set above the phase transition temperature of the non-ionic surfactants. The highest phase transition temperature being 50˚C belonging to Span 60 [104]. The resulting product was then left to cool and stored in a refrigerator (2-8˚C) until further studies were carried out. All samples were produced in triplicates.

Table 3.1: Composition of surfactant (Span 20,40,60 or 80), cholesterol and DCP in niosomes (total 60 µmoles/mL).

Formulation	Surfactant (% mol)	Cholesterol (% mol)	DCP (% mol)
70:30	70	30	0
60:40	60	40	0
50:50	50	50	0
65:30:5	65	30	5
55:40:5	55	40	5
50:45:5	50	45	5
60:30:10	60	30	10
50:40:10	50	40	10

3.3.3   Centrifugation and resuspension

To separate the unentrapped drug from the entrapped drug the niosomal sample volume was diluted 20 times in PBS and centrifuged at 30,000 g for 30 minutes (4°C) using a Sigma 3-30 KS Centrifuge (SciQuip, Shropshire, UK). The supernatant was then filtered through a 0.22 µm pored filter and analysed using HPLC (method described in Chapter 2). The pellet was resuspended in PBS using a vortex machine for 5 minutes and used for further studies or stored in the fridge (2-8°C) for further analysis. Experiments generally completed within three days of niosome formation.

3.4 Characterisation studies of niosomes

3.4.1   Particle size and polydispersity index analysis

The particle size of the niosomes was analysed by dynamic light scattering (DLS) using Malvern Zetasizer Nanoseries MR30717 (Malvern Instruments Limited, Worcestershire, UK). The niosome samples (diluted 1 in 10 in MilliQ® water) were analysed in disposable polystyrene cuvettes at 25°C. Due to the mixed composition of the niosomes the particle size and polydispersity index (PDI) was measured using intensity distribution, which enables the samples to be analysed using the same refractive index (RI) as PBS (RI=1.330) and absorption of 0.01. All triplicate samples were additionally analysed in triplicates within the instrument settings.

3.4.2   Zeta potential determination

The zeta potential of the niosome samples was measured using laser doppler electrophoresis (LDE) with the instrument Malvern Zetasizer Nanoseries MR30717 (Malvern Instruments Limited, Worcestershire, UK). For each run, 0.6 mL of sample,

diluted 1 in 10 in MilliQ® water, was injected into the disposable folded capillary cells (DTS1070). The analysis was carried out using the Smoluchowski model with the measurement duration being set as automatic (10 runs minimum & 100 runs maximum). All triplicate samples were additionally analysed in triplicates within the instrument settings.

3.4.3 The encapsulation efficiency (%) of insulin

The percentage of drug encapsulated within the vesicles can be determined by calculating the EE. After centrifugation of the niosomal dispersion, the supernatant was separated from the pellet, filtered through a 0.22 µm filter, and subsequently analysed for insulin content using HPLC (method discussed in Chapter 2). To quantify the insulin EE (%), Equation 3.1 and LC (%),   Equation 3.2 were used:

Equation 3.1

$$Encapsulation\ efficiency\ (\%) = \frac{Total\ amount\ of\ insulin - free\ insulin}{Total\ amount\ of\ insulin}\ x\ 100$$

Equation 3.2

$$Loading\ capacity\ (\%) = \frac{Total\ amount\ of\ insulin - Free\ insulin}{Weight\ of\ transferosomes} \times 100$$

3.4.4 Statistical analysis

All the values are expressed as the mean ± SD. Two-way ANOVA tests were performed on the obtained results, if the criteria were met, using GraphPad Prism 8. On some data, one-way ANOVA was more suitable, and where this is the case, it is

stated under the relevant data. Also, on the appropriate data, Tukey's multiple comparisons test was used to compare the means of the results, unless otherwise indicated. P-value of less than 0.05 was considered statistically significant. Table 3.2 shows the symbols used to represent significance levels on graphs/charts.

Table 3.2: Symbols representing the level of significance.

Symbol	Meaning
ns	$p \geq 0.05$
*	$p < 0.05$
**	$p < 0.01$
***	$p < 0.001$
****	$p < 0.0001$

3.5 Results and discussion

3.5.1 Preliminary findings

Aggregation of vesicles can be a problem in some formulations. Hence it is important to investigate the effects of a charged molecule in the niosomal formulation, which can reduce or prevent aggregation through electrostatic stabilisation [83]. Stearylamine is a positively charged molecule, which can be used. Still, in preliminary studies, it was tested with the Spans and found not to have favourable effects on the zeta potential. Aggregation was observed in the formulations during production with large variations in particle size. Hence DCP was used, which was found to form more stable milky dispersions, and aggregates could not be observed with the naked eye. Also, it has been used previously with the Spans and found to be compatible and valuable for stability [104].

Several methods can be used for size reduction of niosomes, one of which is probe sonication. However, using probe sonication, the tip of the probe is directly submerged into the niosomal dispersion, which results in high energy input in the dispersion as well as possible contamination of the solution [163]. It was found with insulin, even at the lowest amplitude, the solution frothed up, overheating occurred and analysing the solution with HPLC showed a broad distorted peak. Another option is bath sonication, where the niosomal formulation is in a tube or round bottom flask and placed into a bath sonicator. This method has advantages such as greater control of temperature, no contamination and less energy input [163]. Hence insulin stability was not affected for the short period of sonication.

The hydration medium often used with vesicles is phosphate buffer of varying pH. The pH is routinely chosen based on the solubility of the drug [94]. Phosphate buffer (pH 7.4) has been used in previous studies with insulin, and in this study, insulin achieved good solubility at this pH. Thus was chosen as the hydration medium [164].

3.5.2 The particle size of niosomes

3.5.2.1 Effect of sonication
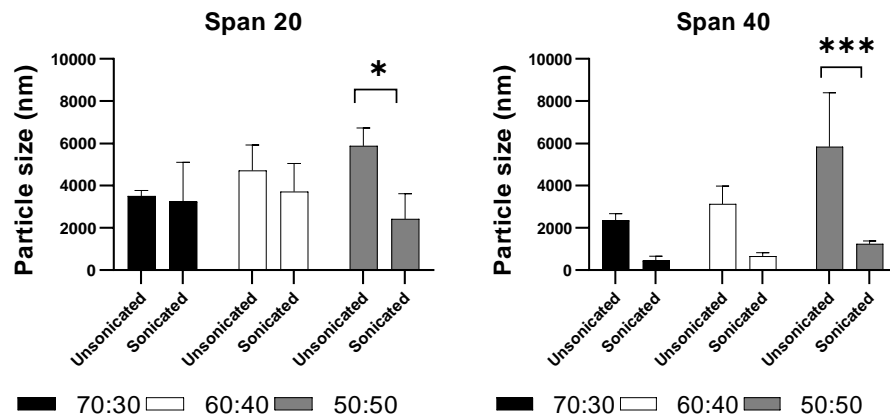
Figure 3.1: Analysis of particle size of 3 ratios (%) of surfactant and cholesterol of unloaded niosomal preparations of Span 20 and Span 40 with and without sonication using DLS.

Notes: Results represent mean ± SD (n=3). Two-way ANOVA analysis revealed a significant reduction ($p < 0.05$) in particle size for both Span 20 and Span 40 after sonication. Specifically, Sidak's multiple comparisons test showed significant difference (* = $p < 0.05$) in Span 20 and (** = $p < 0.001$) in Span 40 niosomes after bath sonication in the combination with 50:50 ratio of surfactant: cholesterol. Abbreviation: Dynamic light scattering (DLS)

Particle size plays a crucial role in influencing the delivery of drugs across mucosal membranes. As summarised by Ucheghu et al. (1998), niosomes prepared without a size reduction step results typically in production of niosomes in the micron size range [83]. This was found to be accurate, and it can be seen in Figure 3.1, the vesicles formed without a sonication step, just using the method by Varshosaz et al. (2003), both Span 20 and 40, have produced niosomes that are around 2 μm or greater [162]. However, for buccal delivery, the particles need to be as small as possible, ideally much less than 1 μm, to possibly achieve permeation through the buccal membrane. Performing two-way ANOVA analysis of the results for particle size, before and after bath sonication, in the 50:50 ratio of surfactant: cholesterol for both Span 20 and Span 40, a significant reduction ($p < 0.05$) in size was observed after the sonication step.

Although the 70:30 and 60:40 ratios did not show statistical significance, due to the large variations in particle size, the mean data reveals that the particle sizes are much smaller after sonication. Thus, the niosomal preparation method was modified to incorporate 15 minutes of sonication, using a sonicator bath at 55°C.

3.5.2.2 Effect of the cholesterol content on particle size
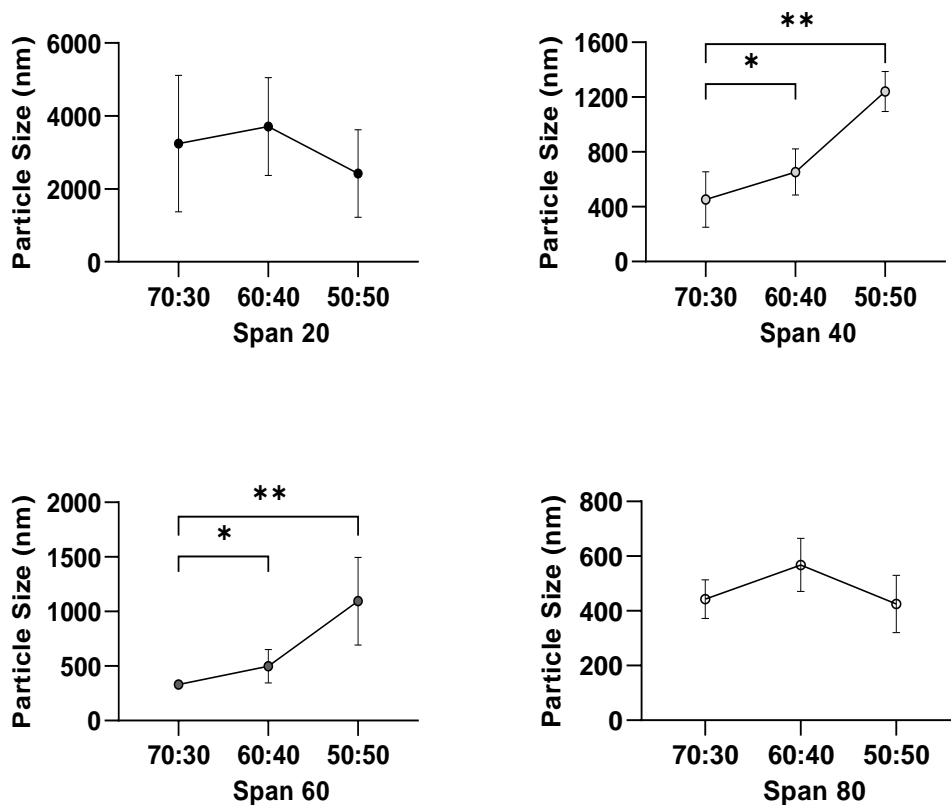
Figure 3.2: Effect of the cholesterol content on the particle size of Span 20, 40, 60 and 80 niosomes.

Notes: Results represent mean ± SD (n=3). Two-way ANOVA analysis showed no significant difference (p > 0.05) in particle size between the different Spans across the different compositions. Tukey's multiple comparisons test of Span 20 and 80 showed no significant difference between the different concentrations of cholesterol. Tukey's multiple comparisons test of Span 40 and 60 showed significant difference (** = p < 0.01) between the 70:30 cholesterol ratio and the 50:50 ratio and significant difference (* = p < 0.05) between the 70:30 and 60:40 cholesterol ratio.

In general, it has been known that the inclusion of cholesterol in vesicles increases the particle size [88]. In XRD studies, carried out by McIntosh (1978), it was observed that the presence of cholesterol led to an increase in the width of the phospholipid bilayers [165]. Examining the trend in particle size of niosomes in Figure 3.2 reveals increasing cholesterol content from 30% to 40% and 50%, with Span 40 and 60 leads to significant increase in particle size. The increase in particle size was also found in other studies and could be due to an increase in the bilayers and rigidity of the niosomes [105], [162], [166], [167]. Still, little difference was observed with Span 20 and Span 80. This is possibly due to Span 40 and 60, being gel-type surfactants, whereas Span 20 and 80 are liquid state [162]. The cholesterol in vesicles requires optimisation as the greater rigidity can lead to a reduction in the release rate of the encapsulated drug [88].

3.5.2.3　Effect of the charged molecule on particle size
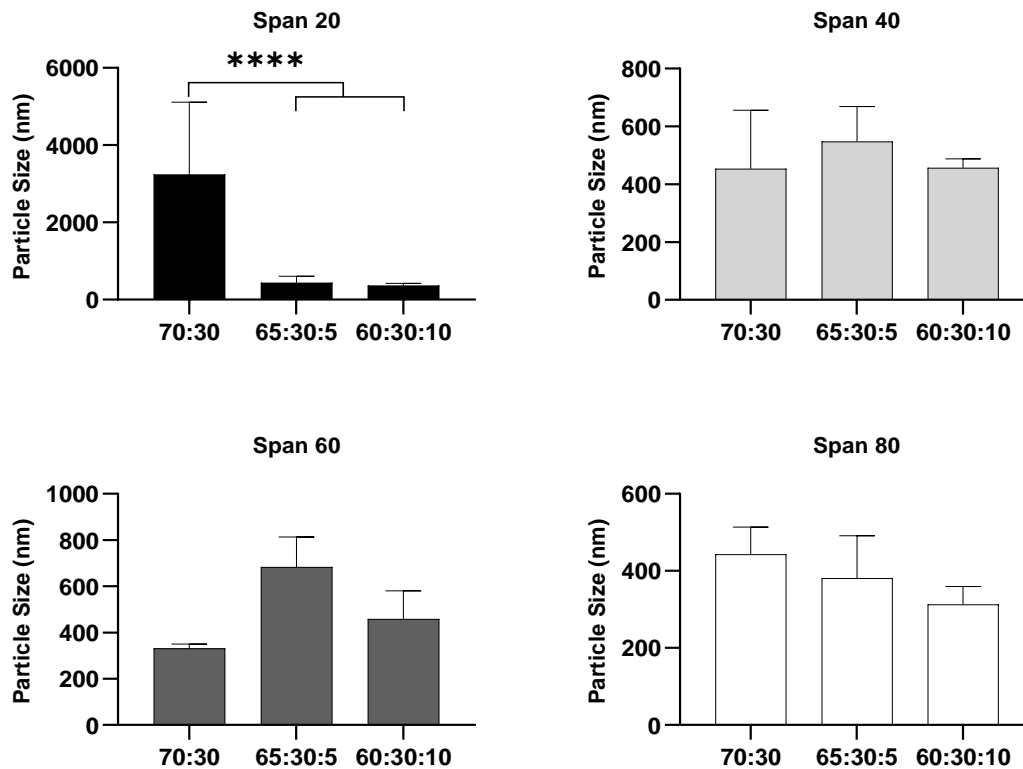
Figure 3.3: Effect of absence and increasing concentrations of DCP on the particle size of Span 20, 40, 60 and 80 niosomes.

Notes: Results represent mean ± SD (n=3). Two-way ANOVA analysis revealed a significant difference ($p < 0.01$) in the different combinations. Specifically, Tukey's multiple comparisons tests showed a significant reduction (**** = $p < 0.0001$) in particle size of Span 20 niosomes in the presence of 5% and 10% DCP. Abbreviation: Dicetyl phosphate (DCP)

A close comparison of the effect of the negatively charged molecule on the particle size of niosomes in Figure 3.3 demonstrates significant reduction ($p < 0.0001$) in particle size between Span 20 niosomes with DCP compared the niosomes without DCP. This is similar to the results observed by previous studies as charged molecules can act as stabilizing or flocculating agents through electrical repulsion. Thus, the absence of such molecules leads to greater coalescence resulting in size variation [162], [168]. In the study carried out by Varshosaz et al. (2003), a decrease in size was also observed for Span 80, but the size of Span 40 and 60 niosomes increased in the

presence of DCP. In multilamellar vesicles, such as these, the presence of charged molecules can create an expansion in the interlamellar distance among successive bilayers, which subsequently results in greater overall volume [104]. But in this study, results shown in Figure 3.3, the inclusion of DCP in the Span 40, 60 and 80 niosomes did not make a significant difference in particle size. This difference in results is possibly due to the incorporation of sonication in our study, which, as shown in Figure 3.1, can have a significant influence on the particle size of niosomes. Hence even though in the Span 80 niosomes it can be seen that the mean size of niosomes is decreasing, with increasing concentration of DCP, due to the reduction of particles by sonication and the variation in the size of the particles the difference is not statistically significant (Figure 3.3).

3.5.2.4 Selection based on particle size

a.

b.
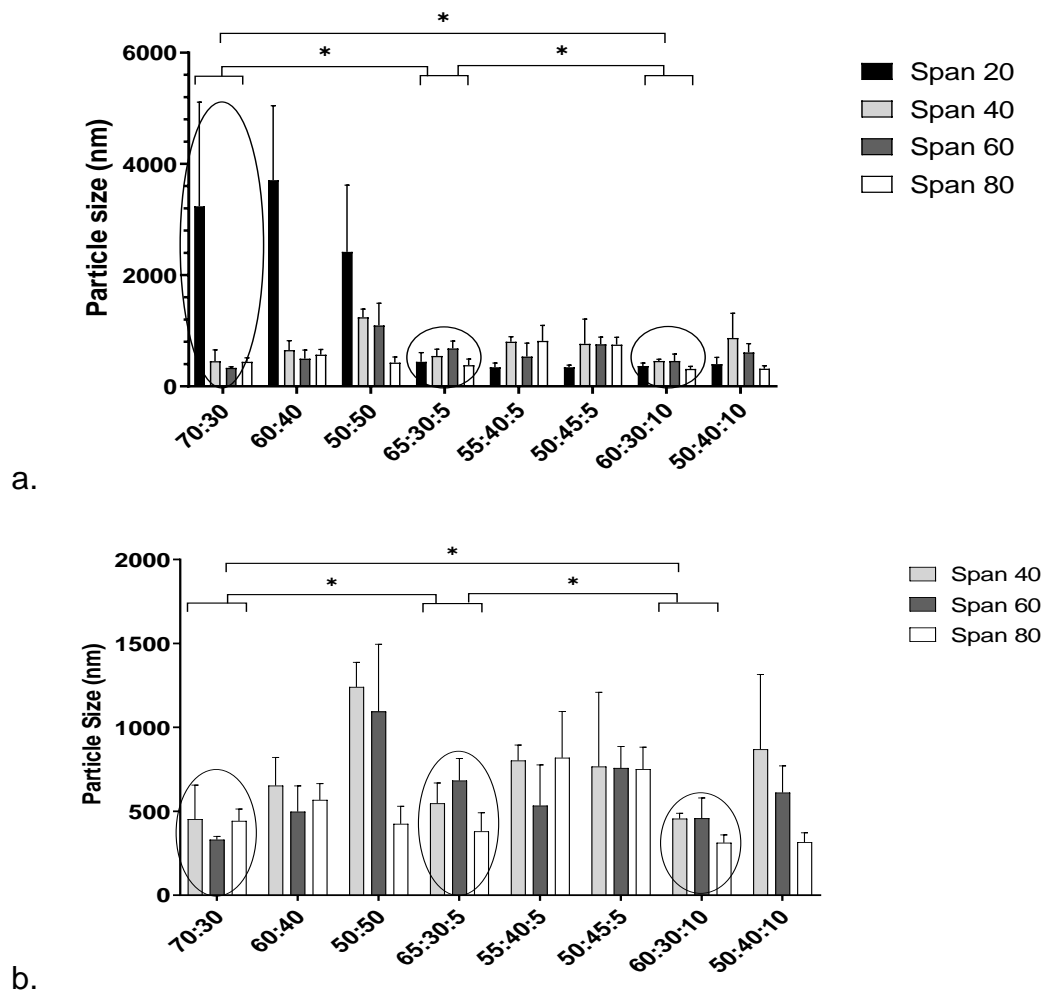
Figure 3.4: a. Comparison of particle size of empty niosomes produced using Span 20, 40, 60 and 80 with different (%) ratios of cholesterol with or without DCP. b. Comparison of particle size of empty niosomes produced using Span 40,60 and 80 with different (%) ratios of cholesterol with or without DCP.

Notes: The circles and * represent the concerned formulations that are significantly different ($p < 0.05$). Results represent mean ± S.D., n = 3. Abbreviation: Dicetyl phosphate (DCP)

Figure 3.4 has been displayed as part a and b. The particle size of the Span 20 niosomes without DCP are much larger than the other Span. Hence for better visual comparison of the particle size and the error bars results for Span 20 is only presented in part a. Similar to the outcomes observed by Varshosaz et al. (2003), the niosomes formed with Span 20, without the charged molecule, resulted in large and highly varied

particle sizes [162]. One explanation is that the presence of the charged molecule would typically help increase stability in the system through electrical repulsion, but in its absence can lead to greater aggregation and coalescence resulting in size variation and larger particle sizes [162]. Thus, in Span 20 niosomes, the presence of the charged molecule leads to a decrease in particle size both at 5 and 10% DCP.

Another factor, as observed by Nowroozi et al. (2018), is that surfactants with higher HLB values tend to form niosomes with greater particle size, and Span 20 has an HLB of 8.6, which is the highest HLB of all the Spans tested [169]. This is because, with an increase in the hydrophilicity of the surfactant, there is an increase in surface free energy [104].

The aim of analysing particle size using DLS was to narrow down the different ratios of surfactant, cholesterol with or without DCP from eight different ratios to three or four, which would then be tested and further analysed for insulin encapsulation. To narrow down the number of ratios, the combined results for particle size of all the Spans but at the different ratios, were statistically compared using two-way ANOVA and statistical significance ($p < 0.05$) was found between the surfactant: cholesterol: DCP ratios 70:30, 65:30:5 and 60:30:10 as shown circled in Figure 3.4. Looking carefully at these results, they all contain 30% cholesterol. Generally, the particle sizes for these ratios is the smallest for all the Spans, except for Span 20 (Figure 3.4, b).

Table 3.3: Comparison of PDI of unloaded niosomes produced using Span 20, 40, 60 and 80 with different ratios of cholesterol with or without DCP.

Formulations	Span 20	Span 40	Span 60	Span 80
70:30	0.7 ± 0.1	0.7 ± 0.2	0.6 ± 0.1	0.7 ± 0.1
60:40	0.9 ± 0.2	0.9 ± 0.1	0.8 ± 0.1	0.6 ± 0.1
50:50	0.9 ± 0.1	0.9 ± 0.1	1.0 ± 0	0.5 ± 0.1
65:30:5	0.6 ± 0.3	0.9 ± 0.1	1.0 ± 0	0.7 ± 0.1
55:40:5	0.5 ± 0.2	0.9 ± 0	0.8 ± 0.1	0.9 ± 0
50:45:5	0.6 ± 0.1	0.8 ± 0.1	1.0 ± 0	0.8 ± 0
60:30:10	0.7 ± 0.1	0.8 ± 0.1	0.8 ± 0.1	0.6 ± 0.1
50:40:10	0.8 ± 0.1	0.9 ± 0	0.9 ± 0	0.6 ± 0.1

Notes: Results represent mean ± SD (n=3). Abbreviations: polydispersity index (PDI) and dicetyl phosphate (DCP)

Generally analysing the PDI, the aim would be to observe values of less than 0.5, which would indicate a suitable size distribution within the sample [170]. The closer the PDI value is to zero, the more homogenous the samples [167]. But looking at the results in Table 3.3, the results vary mostly between 0.6 to 1, which indicates the particle sizes are varied and not homogenous. As found by Yoshioka et al. (1994), the size distribution of niosomes tends to be relatively wide. However, it was suggested this could be altered through adjustments in the hydration time and extent of shaking [104]. Hence in further studies, change is required in the method to increase vesicle size homogeneity.
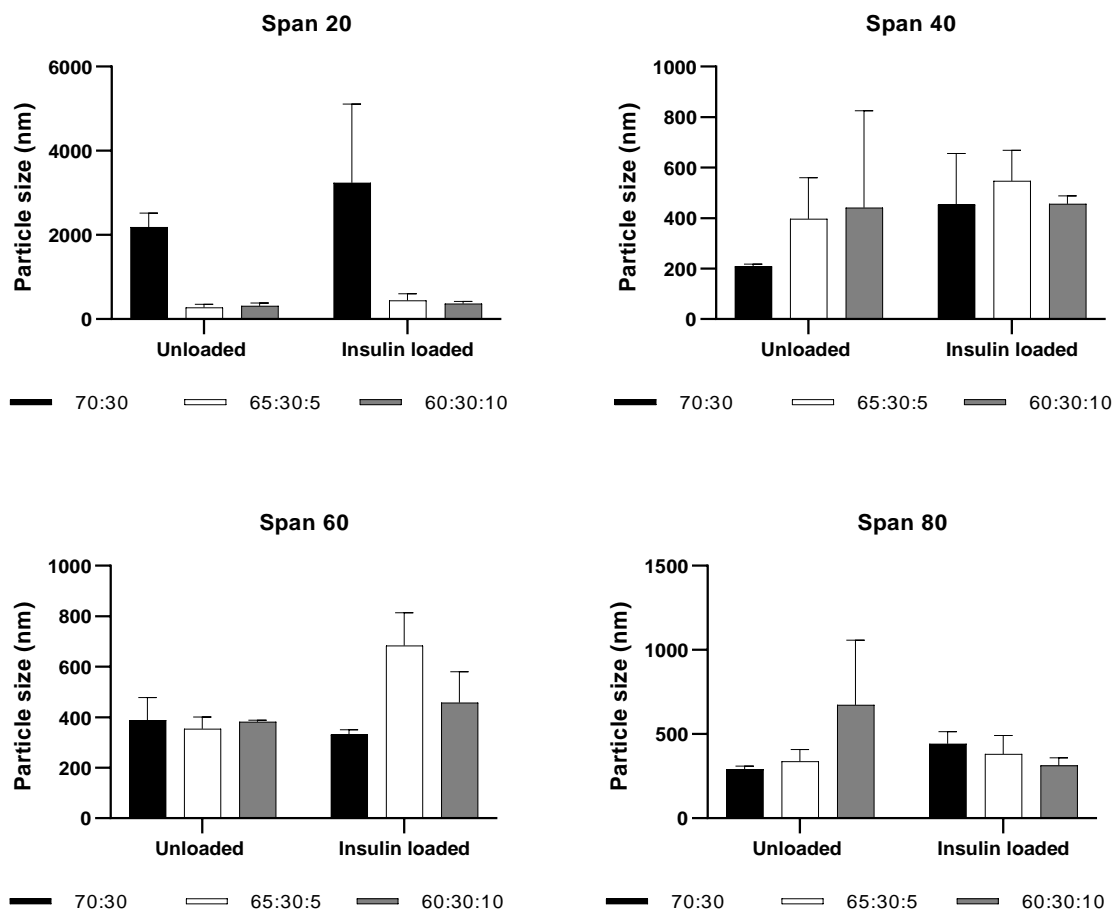
Figure 3.5: The effect of insulin incorporation on the particle size of niosomes in the three formulations with different surfactants prepared by the thin-film hydration method and analysed using DLS.

Notes: Results represent mean ± SD (n = 3). Two-way ANOVA analysis showed no significant difference $(p > 0.05)$ in particle size with and without insulin. Abbreviation: Dynamic light scattering (DLS)

Overall, in Figure 3.5, no significant $(p > 0.05)$ difference was observed in the size of the particles with or without insulin incorporation as confirmed with statistical analysis using two-way ANOVA.

3.5.3 Zeta potential
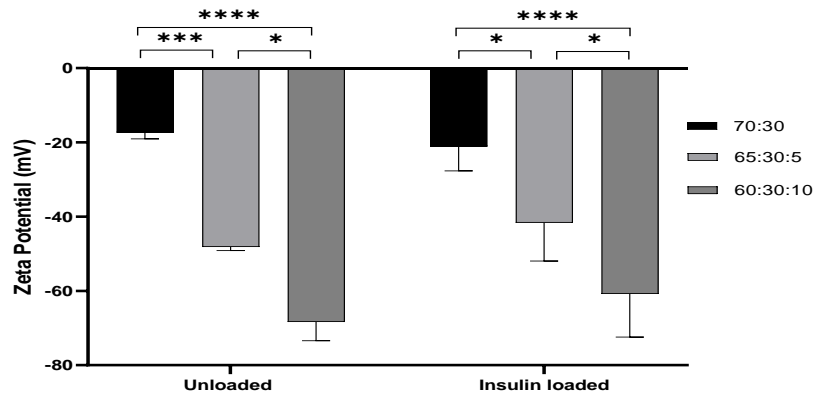
Figure 3.6: Effect of DCP and insulin incorporation on the zeta potential of Span 20.

Notes: Results represent mean ± SD (n = 3). Two-way ANOVA analysis showed no significant difference ($p > 0.05$) between the unloaded and insulin loaded formulations. Analysis using Tukey's multiple comparisons test (* = $p < 0.05$, *** = $p < 0.001$ and **** = $p < 0.0001$). As shown by **** the effect of DCP on the zeta potential is particularly significant ($p < 0.0001$) between the means of the uncharged formulations, either with or without insulin, and the charged formulations containing 10% DCP. Abbreviation: Dicetyl phosphate (DCP)

The zeta potential is an essential factor in determining the stability of colloidal dispersions as it is the electric potential at the boundary of the double layer on the surface of particles [171]. The degree of electrostatic repulsion between adjacent similarly charged vesicles is reflected by the magnitude of the zeta potential [172]. Systems with high zeta potential typically confer stability as the forces of repulsion exceed the attractive forces while it is vice versa for low zeta potential systems, and thus, these may flocculate or coagulate [172]. The zeta potential was measured using LDE. Two-way ANOVA analysis of the results for the zeta potential depicted in Figure 3.6 showed no significant difference ($p > 0.05$) between the niosomal formulations of Span 20 unloaded and loaded with insulin but demonstrated significant difference ($p < 0.05$) between the different formulation ratios. In general, although non-ionic surfactants typically do not hold any charge, the uncharged niosome was observed to

possess a slightly negative zeta potential (-17.4 ± 1.7 unloaded and 21.0 ± 6.6 insulin loaded Figure 3.6). Similar observations have been made in another study, also working with Spans [105]. As expected, as the concentration of the negatively charged DCP molecule is increased, the zeta potential becomes more negative (Figure 3.6). Another study looking at the effects of DCP on surface charge acquired similar results, with a greater negative zeta potential being obtained in the presence of a higher concentration of DCP [173]. According to the Tukey's multiple comparisons test the effects of DCP on the zeta potential is particularly significant ($p < 0.0001$) between the means of the uncharged formulations either with or without insulin, and the charged formulations containing 10% DCP. Colloidal systems that have zeta potential values less than -30mV or greater than +30mV are considered highly dispersed [171]. Hence, since DCP in the formulation at either concentration (5% or 10%) results in zeta potential less than -30mV, it will be beneficial to include in the formulation to increase system stability.

3.5.4 Percentage insulin encapsulation efficiency and loading capacity
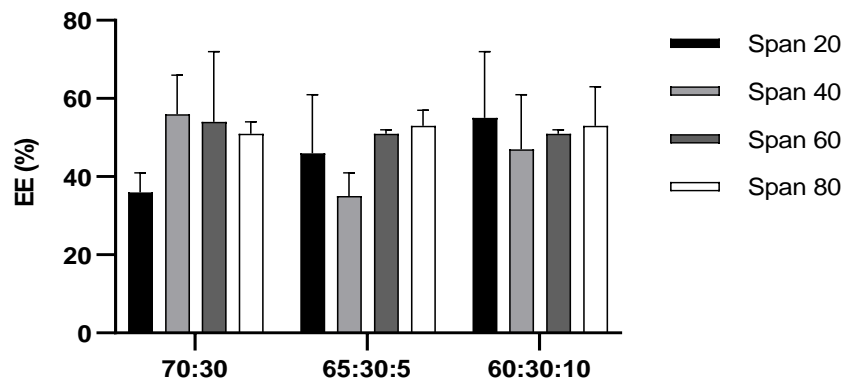
Figure 3.7: Results for EE (%) of three different ratios (%) of Span 20, Span 40, Span 60 & Span 80.

Notes: Results represent mean ± S.D (n = 3). Abbreviation: Encapsulation efficiency (EE)
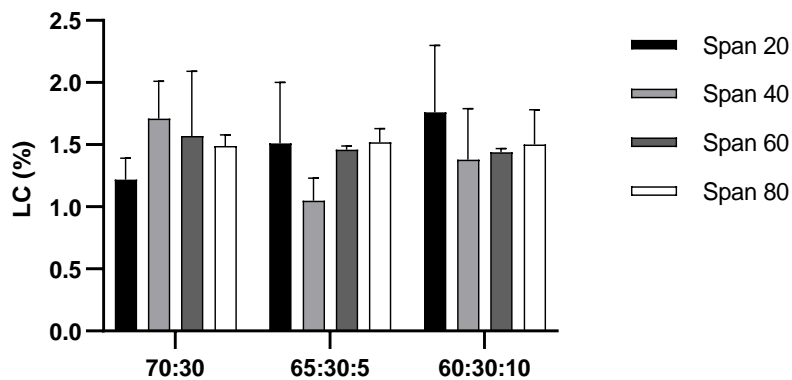
Figure 3.8: Results for LC (%) of three different ratios (%) of Span 20, Span 40, Span 60 & Span 80.

Notes: Results represent mean ± S.D (n = 3). Abbreviation: Loading capacity (LC)

The HLB of the surfactant is typically found to influence the EE; however, the lipophilicity or hydrophilicity of the encapsulated drug also has an effect [79], [174]. It is suggested that using surfactants with high HLB values achieves greater entrapment

with hydrophilic drugs [79]. Nevertheless, there are conflicting results in this regard. As a study, testing Span 85, Span 80, sodium cholate, sodium deoxycholate and Tween 80, found the EE to be the highest with Span based vesicles (transfersomes) even though they have low HLB values [175].

In addition to HLB, the physical state of the surfactant could influence the EE. For example, Span 40 and 60 are gel-type surfactants, whereas Span 20 and 80 are liquid state, and surfactants in gel form accomplished niosomes with better EE [79], [162]. This is possibly due to the gel state surfactants forming bilayers with well-ordered alkyl chains compared to the more disordered arrangement formed with liquid state surfactants [88]. Statistical analysis of the results for EE and LC of niosomes, displayed in Figure 3.7 and Figure 3.8 respectively, showed no significant difference ($p > 0.05$) between the different surfactants or the varying ratios of surfactant, cholesterol and DCP. However, looking at the results, Span 60 niosomes containing 5% and 10% DCP, achieved the best results in terms of SD with 51 ± 1% EE. Homogeneity of vesicles in terms of EE is important, as insulin is a narrow therapeutic drug. Hence it is essential to have consistent EE, to increase the likelihood of predictable therapeutic effect and possible scale-up. Additionally, Span 60 has the highest phase transition temperature, surfactants with higher transition temperatures are found to provide better entrapment [88], [104]. Although the results look reasonably good with Span 80, the surfactant was very difficult to work with, in terms of separating the entrapped drug in niosomes from the unentrapped drug in solution. After centrifugation, the contents of the pellet tend to seep into the supernatant; hence separation was difficult and increasing the centrifugation timing to 2 hours and increasing the speed to 50, 000 g did not improve

the situation. This is possibly related to the physical state of Span 80, which is initially liquid.

3.6 Conclusion

In summary, much of the initial focus has been on looking at both improving the method used to prepare the niosomes but also testing the stability of insulin at each step to make sure the protein maintained its integrity during the processes. The focus was also on finding the combination of surfactant, cholesterol with or without DCP, which not only would result in production of particle sizes in the nanoparticle size range (1-1000 nm) but also make sure particle sizes are reproducible, and the EE (%) is high. The confirmation so far in this study has been that a cholesterol content of 30% molar ratio would be the best to take forward, based on particle size (mean with insulin 458 nm). Also in terms of EE, Span 60 containing 10% DCP, was able to achieve one of the highest with 51 ± 1% EE. Hence the Span 60 niosomal formulation of surfactant: cholesterol: DCP comprising of 60:30:10 was carried forward for further studies.

Particle size reproducibility can be difficult with a bath sonicator as both human factors are involved, such as the time and angle of rotation in the bath sonicator, and also the bath sonicator itself can result in variability due to the sonication being quite varied in the different areas of the bath. However, based on literature, the use of a bath sonicator, during the hydration stage of the thin film hydration method, can result in greater sample homogeneity and achieve a decrease in PDI compared the niosomes produced without sonication [169]. Hence, it is possible for more homogeneous samples to be produced with the method but requires further optimisation in future studies.

4. Formulation and characterisation of transfersomes

4.1 Introduction

Transfersomes are bilayered structures, comprising of phospholipids and a surfactant or edge activator, which enables transfersomes to have membrane flexibility and to permeate through pores that are smaller than their own size [98]. The possible mechanism of permeation is displayed in Figure 4.1. An early study looking at the epicutaneous application of insulin-containing transfersomes (also known as transfersulin) were able to demonstrate spontaneous transport of insulin into the body across the skin [98]. In mice, the use of transfersomes showed a significant reduction in blood glucose by 20-30%, within 2-4 hours. In contrast, simple lipid suspensions and drug solutions were not able to induce a considerable response [98]. After application of non-occluded transfersomes on the skin, evaporation of water occurs, which enables the hydration gradient to influence the vesicles [78]. The enhanced elasticity together with the hydro-affinity facilitates the drug-loaded vesicles to squeeze between the cells along the intercellular lipids of the stratum corneum [78], [176]. Hence it has been suggested transfersomes should not be administered under occlusion as this would reduce the hydration gradient, which usually drives the vesicles across the skin [177]. Additionally, after application of insulin-containing transfersomes on the skin, it was observed that the formulation acted as an epicutaneous reservoir, prolonging the hypoglycaemic action [98].
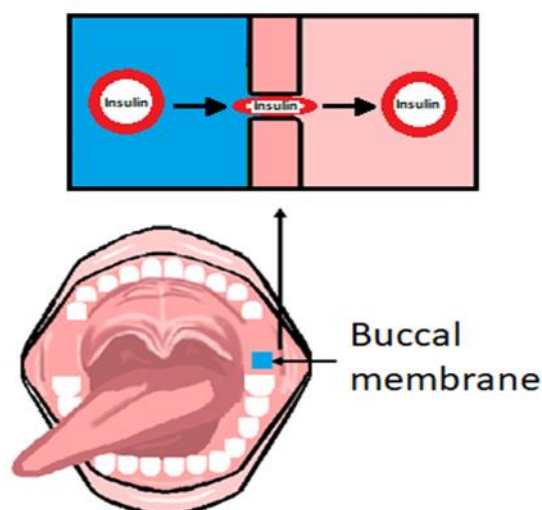
Figure 4.1: Schematic representation of the mechanism of permeation by transfersomes.

In the buccal mucosa, permeation is likely to be via the intercellular lipids of the epithelial membrane. Thus, the ingredients of transfersomes can be designed and optimised specifically for individual drugs, taking into consideration the overall formulation and route of delivery [78]. In transfersomes, the surfactant (or edge activator) is an essential component in achieving membrane deformability by destabilizing the bilayer and lowering the interfacial tension [103]. Examples of edge activators include bile salts (sodium cholate and sodium deoxycholate), polyoxyethylene sorbitan fatty acid esters (Tweens 80 and Tween 20) and sorbitan fatty acid esters (Spans 40, Span 60, and Span 80). As reviewed by Khan et al. (2015), surfactants, such as Tween 80 are also often used in parenteral protein formulations, as they can prevent protein aggregation when exposed to freeze-thaw stress and vortexing [178], [179].

The ability of transfersomes to enhance drug delivery is suggested to be due to the combined effect of the vesicles being ultradeformable carriers as well as permeation

enhancers [78]. The composition of transfersomes can have a significant influence on their physicochemical properties and thus, their effectiveness as drug carriers [180]. The critical packing parameter of the chosen surfactant, Span 60, falls between ½ and 1, which means it can form bilayered spherical vesicles [181]. Additionally, double-chained amphiphiles, such as phospholipids, often with the use of sonication, are found to form bilayers with very homogenous structures [161]. Thus, combined with the presence of cholesterol, which acts as a bilayer membrane stabiliser, the formulation is likely to form homogenous bilayered vesicles.

In a normal cell, membrane fluidity is of vital significance for adequate diffusion of membrane components, including lipids and proteins [182]. It also affects the flexibility of the membrane in morphological transformations, one of which is an adaptation to the environment [183]. Cholesterol is one of the factors regulates membrane fluidity in mammalian cells by interfering with the packing of acyl chains and thus increasing the rigidity of the membrane [184].

Phosphatidylcholine and phosphatidylethanolamine are the two most abundant phospholipids in mammalian cell membranes [185]. Often in the formation of liposomes and transfersomes, phosphatidylcholine is used, however, based on the potent nature of HDV insulin (discussed in chapter 1), which contains a form of phosphatidylethanolamine it may offer more favourable characteristics [43].

The goal in this chapter was to optimise the ingredients of the transfersomal formulation in terms of characteristics such as particle size, PDI and EE (%) as well as test for release studies. Simultaneously the formulations were tested for toxicity and permeability studies using TR146 buccal cells detailed in Chapter 5.

4.2 Chapter aims

➢ To determine the optimum ratio of phospholipid to be incorporated with Span 60, cholesterol and DCP using factorial design (Minitab).

➢ To enhance membrane elasticity by modifying ratios of cholesterol and the addition of Tween 80.

➢ To further reduce the size of vesicles using extrusion.

➢ To determine the value of using a bile salt (e.g. sodium glycodeoxycholate) within the formulation versus DCP.

➢ To compare the impact of 1,2-dipalmitoyl-3-sn-phosphatidylethanolamine (DPPE) versus soybean lecithin as the phospholipid.

➢ To carry out release studies on the two formulations, which demonstrate excellent results in the toxicity studies.

4.3 Materials and methods

RHI (27.5 IU/mg), sorbitan monostearate (Span 60), cholesterol (C8667), DCP, polysorbate 80 (Tween 80), sodium glycodeoxycholate (SGDC), PBS (pH 7.4), and Avanti® Mini-Extruder (fitted with 0.4-micrometre polycarbonate membrane and with heating block) were all purchased from Sigma-Aldrich (Merck KGaA, Darmstadt, Germany). DPPE and soybean lecithin was obtained from Tokyo Chemical Industry (UK). HPLC grade ACN and TFA (99+%) were both purchased from Fischer Scientific (Leicestershire, UK). MilliQ® water was obtained internally using a Merck Millipore Direct-Q® 3UV water purification system (Billerica, MA, USA). All other chemicals and reagents used were of analytical grade.

4.3.1 Thin-film hydration method

Transfersomes were prepared using the traditional thin-film hydration technique combined with down-sizing methods to reduce particle size. The formulation composition for the transfersomal formulations vary and are shown in Table 4.1, Table 4.2 and Table 4.3 but consists of a mixture of the following: cholesterol, Span 60, Tween 80, soybean lecithin, DPPE, DCP and sometimes SGDC. The correct quantity of components was dissolved in 10 mL of chloroform: methanol (9:1) in a round-bottom flask. The organic solvents were removed at 50°C, under vacuum, using a rotary evaporator. The dried surfactant/lipid film was then flushed with nitrogen gas for several minutes before being hydrated with 5 mL of PBS (pH 7.4) containing RHI (0.73 mg/mL or 1.5 mg/mL) in a bath sonicator at 55-60°C for 10 minutes (optimised at 3 minutes manual rotation and 7 minutes on stand without rotation). The samples were stored in a refrigerator (2-8°C) and used for studies within three days. All samples were produced in triplicates unless stated otherwise.

4.3.2 Centrifugation and resuspension

To separate the unentrapped drug from the entrapped drug the niosomal samples were diluted ten times in PBS and centrifuged at 50,000 g for 60 minutes (4°C) using a Sigma 3-30 KS Centrifuge (SciQuip, Shropshire, UK). The supernatant then filtered through a 0.22 µm pored filter and analysed using HPLC (see chapter 2). Depending on the experiment, the pellet was resuspended in PBS (pH 7.4) (unless stated otherwise) using a vortex machine for 5 minutes and then used for further studies.

4.3.3 Extrusion of transfersomes

To form more homogenous and smaller transfersomes, the hydrated solutions were extruded ten times at 55-58°C using an Avanti® Mini-Extruder (fitted with 0.4 micrometre polycarbonate membrane). The resulting product was then left to cool and stored in a refrigerator (2-8°C) until further studies were carried out. All samples were produced in triplicates unless stated otherwise. The samples extruded are compositions shown in Table 4.2 and Table 4.3.

4.3.4 Stability studies during regular storage

The samples were stored in the refrigerator (2-8°C), in clear glass vials, for three months and then analysed for particle size and PDI. They were also observed for any physical or colour changes during storage.

4.3.5 Release studies

The release study was adapted from literature [186]. The release of insulin from the transfersomes was carried out in 4 mL of PBS (pH 7.4) and 1% v/v acetic acid (pH 2.9) over 6 hours. The calculated amount of transfersomes were transferred into the correct liquids, magnetic stirring initiated, and at each time point (0.5, 1, 2, 4, and 6 hours) samples of 0.8 mL was transferred to allocated 1.5 mL Eppendorf tubes and replaced with fresh 0.8 mL of each liquid [this loss was taken into account in the release profile calculations (Equation 4.1)]. The samples were then centrifuged at 13.3 rpm for 30 minutes at 4°C using a Micro Star 17R centrifuge (VWR international, Leicestershire, UK). The supernatant was then analysed for insulin content using HPLC (method see chapter 2). The release studies were performed on the final transfersomes D5E (total

insulin 0.467 mg in 4mL) and S5E (total insulin 0.353 mg in 4 mL), detailed in Table 4.3.

Equation 4.1

$$Mt = Vr \times Ct + Vs \times \Sigma(Ct)$$

Where

M_t = mass of insulin released at each time interval

V_r = volume in the receptor compartment

Ct = concentration of insulin at each time interval

Vs = sample volume

$\Sigma(Ct)$ = cumulative insulin concentration at each time interval

4.3.6   Morphology of transfersomes

The morphological examination of transfersomes was carried out using a ZEISS EVO 50 tungsten source scanning electron microscopy (SEM, Germany). Samples were diluted 1 in 1000 in MilliQ® water and a drop of the formulation transferred to specimen stubs and air dried for a few hours. The transfersomes were then coated with gold/palladium under vacuum with a Polaron SC7640 sputter coater (Quorum Technologies LTD, Kent, UK) before being imaged.

4.3.7 Experimental design

Factor	Name	Type	Low	High
A	Span 60	Numeric	60	120
B	Phospholipid	Numeric	60	120

Figure 4.2: Displays the low and high levels of the two factors (Span 60 and phospholipid, μmoles).

A two factor, two-level factorial design (2^2) was created, for the optimisation of the molar ratio of Span 60 and the phospholipid (DPPE) in the transfersomes. The design was chosen to include 1 centre point per block. The two levels for Span 60 and the phospholipid are shown in Figure 4.2, with both low being 60 μmoles and high 120 μmoles. The software Minitab 19 (USA) was used to both generate and evaluate the results for particle size and EE (%). For each combination, a total of 6 replicates were carried out. The combinations were hydrated with 5 mL of insulin 0.73 mg/mL.

Table 4.1: Composition of phospholipid & Span 60 preparations generated by Minitab factorial design in combination with cholesterol (90 μmoles) and DCP (30 μmoles). Total 5 mL hydration liquid (insulin 0.73 mg/mL).

Formulation	Phospholipid (μmoles, P)	Span 60 (μmoles, S)
P60S60	60	60
P60S120	60	120
P90S90	90	90
P120S60	120	60
P120S120	120	120

Abbreviation: Dicetyl phosphate (DCP)

4.4 Characterisation studies of transfersomes

Particle size, PDI, zeta potential, EE (%), LC (%) and statistical analysis were all carried out based on the methods described in chapter 3.

4.5 Results and discussion: optimisation of phospholipid content

4.5.1 Particle size and polydispersity index analysis
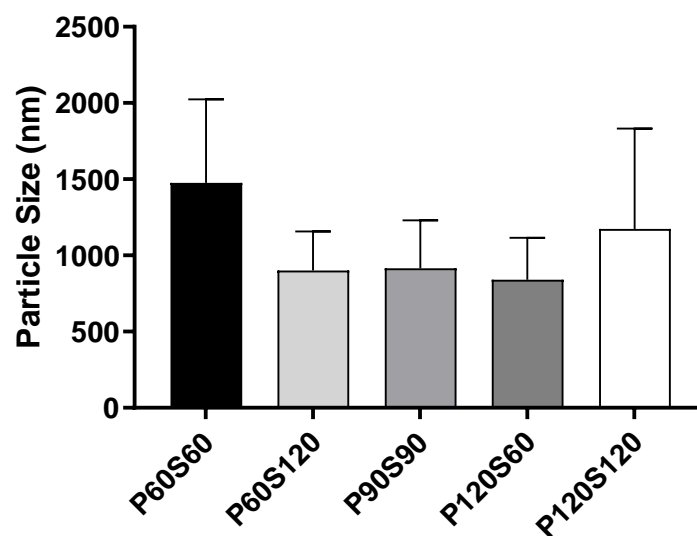
Figure 4.3: Analysis of the particle size of 5 ratios of phospholipid (P) and Span 60 (S) preparations using DLS.

Notes: Results represent mean ± S.D (n = 6). One-way ANOVA analysis showed no significant difference *(p > 0.05)* in particle size between the different compositions. Abbreviation: Dynamic light scattering
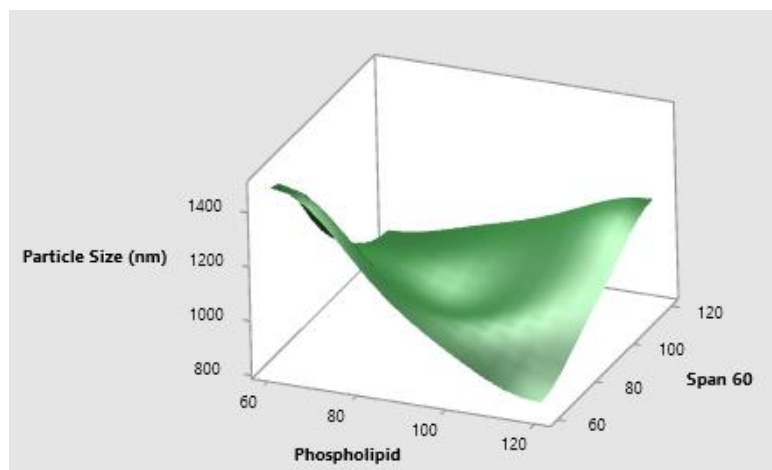
Figure 4.4: Surface plot of particle size (nm) versus Span 60 and phospholipid, analysed using Minitab (n=6).

Particle size is a critical parameter regarding both the physical properties of vesicles and that of the encapsulated drug as well as their biological fate [187], [188]. A study looking at oral administration of griseofulvin loaded liposomes found liposomes of smaller size (< 400 nm) were able to achieve greater bioavailability compared to vesicles above 800 nm [189]. The particle size of vesicles can also influence toxicity as a study found the larger sized liposomes of amphotericin B were more toxic in comparison to the smaller sized vesicles [190]. They can also affect membrane permeability, particularly in transfersomes, as it can determine their ability to enter the paracellular pathway [105]. Looking at the results for particle size, Figure 4.3, there is no significant difference ($p > 0.05$) in the results between the different compositions of phospholipid and Span 60, mainly due to the substantial variation in particle size. However, looking at the surface plot, analysed using Minitab, it can be observed the three compositions P60S120, P90S90 and P120S60 are responsible in forming multilamellar vesicles in the lower size range (Figure 4.4). This can be justified by the fact that in all the formulations, the cholesterol and DCP components are equivalent while only changing the phospholipid and Span 60 molar ratio. The composition

P60S60 results in larger particle size due to the greater impact of the negatively charged molecule, which exerts electrostatic repulsion and hence enlargement between the interlamellar distance among successive bilayers [104]. In the same formulation cholesterol also has a more significant impact and is known to contribute in increasing the size of vesicles, due to insertion of cholesterol within bilayers, which strengthens the nonpolar tail of the surfactant and phospholipids and increases rigidity [105], [162]. The larger particle size of P120S120 formulations is likely to be due to the greater overall molar ratio of constituents in this composition in comparison to the others. Overall, even in the lower size range, the particles are large around 900 nm, thus unlikely to achieve permeation via the buccal mucosa. This is taking into consideration that vesicles of 600 nm or above typically are not able to deliver their entrapped drug into deeper layers of the skin, whereas those 300 nm or below can do so, and this could be reflective of the situation in the buccal mucosa [191], [192]. Therefore, the formulation is likely to require further adjustment in components and possibly another downsizing method such as extrusion.

Figure 4.5: Analysis of PDI of 5 ratios of phospholipid (P) and Span 60 (S) preparations using DLS.

Notes: Results represent mean ± S.D (n = 6). One-way ANOVA analysis showed no significant difference ($p > 0.05$) in PDI between the different compositions. Abbreviation: Polydispersity index (PDI)

Additional to particle size, the PDI is an essential parameter in drug delivery as it can affect product performance, stability, efficacy, safety and the bulk properties of products [191]. Like the results for particle size, one-way ANOVA analysis showed insignificant difference ($p > 0.05$) in the PDI of the different compositions (Figure 4.5). The PDI value ranges from 0 to 1, and the closer the value is to 1, the greater the particle size distribution [191]. The PDI value for all the compositions can be observed to be around 0.6, which indicates the samples are relatively heterogenous, as the value is close to 0.7. Samples with PDI values greater than 0.7 show broad particle size distribution [191]. Further work is required in this area to optimise the method to reduce the PDI, as summarised by Danaei et al. (2018), for nanovesicles a PDI of 0.3 and below, indicates the formation of homogenous samples [191].

4.5.2 Zeta potential
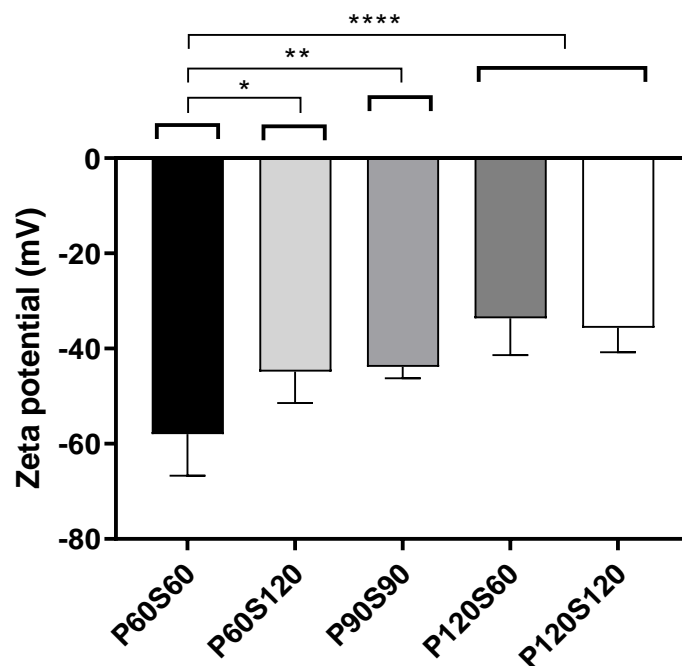
Figure 4.6: Analysis of the zeta potential of 5 ratios of phospholipid (P) and Span 60 (S) preparations using Malvern Zetasizer.

Notes: Results represent mean ± S.D (n = 6). Tukey's multiple comparisons test and One-way ANOVA analysis showed significant difference ($p < 0.05$) in zeta potential between the P60S60 and the other compositions (* = $p < 0.05$, ** = $p < 0.01$ and **** = $p < 0.0001$).

Charged molecules, such as DCP, are included in formulations to increase vesicle stability and prevent aggregation [105]. The results for the zeta potential demonstrate formulation P60S60 has the highest negative zeta potential, and it is significantly different to all the other compositions (Figure 4.6). This can be expected as the molar concentration of cholesterol and DCP are maintained constant thus in the overall ratio of components within the P60S60 transfersome the negatively charged DCP molecule will have greater influence compared to P120S120 where the molar concentration of the phospholipid and surfactant is much higher in the total composition. The two compositions, with the lowest negative zeta potential, P120S60 and P120S120 can be

explained by the fact that DPPE is a cationic phospholipid and these compositions comprise the highest molar ratio of the phospholipid, thus reducing the negative effects of DCP [193]. This also supports the greater negative zeta potentials of formulations P90S90 and P60S120 as the molar ratio of DPPE is less compared to P120S60 and P120S120. However, the zeta potential of all the formulations was found to be around -30 mV or lower; therefore, should offer sufficient stabilisation [194].

4.5.3   The encapsulation efficiency of insulin

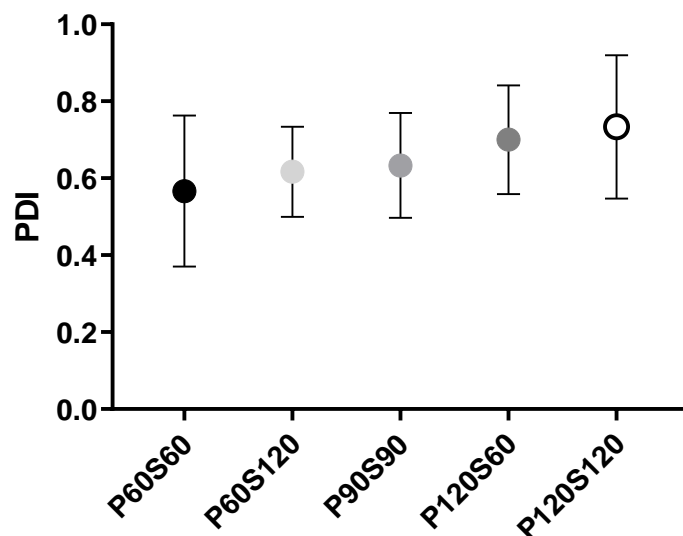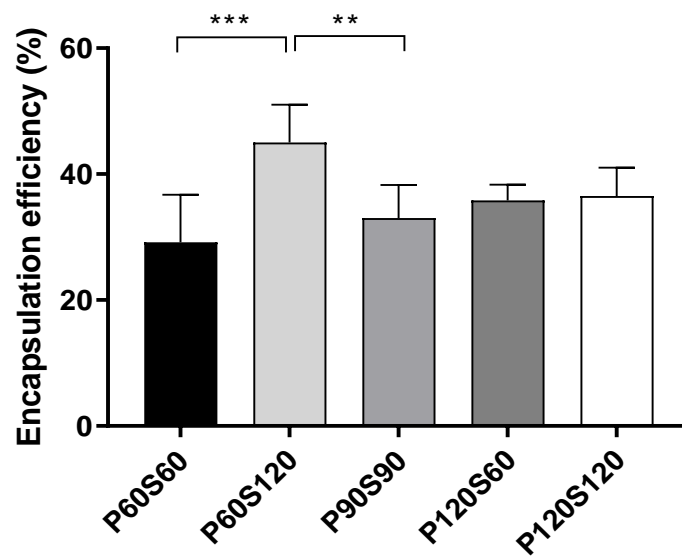**Figure 4.7: Analysis of the EE (%) of 5 ratios of phospholipid (P) and Span 60 (S) preparations using HPLC.**

Notes: Results represent mean ± S.D (n = 6). One-way ANOVA analysis showed a significant difference ($p < 0.05$) in EE (%) of insulin between the sample means. Tukey's multiple comparisons test showed significant difference ($p < 0.001$) between P60S120 and the P60S60 ratio and a significant difference ($p < 0.01$) with the P90S90 composition.
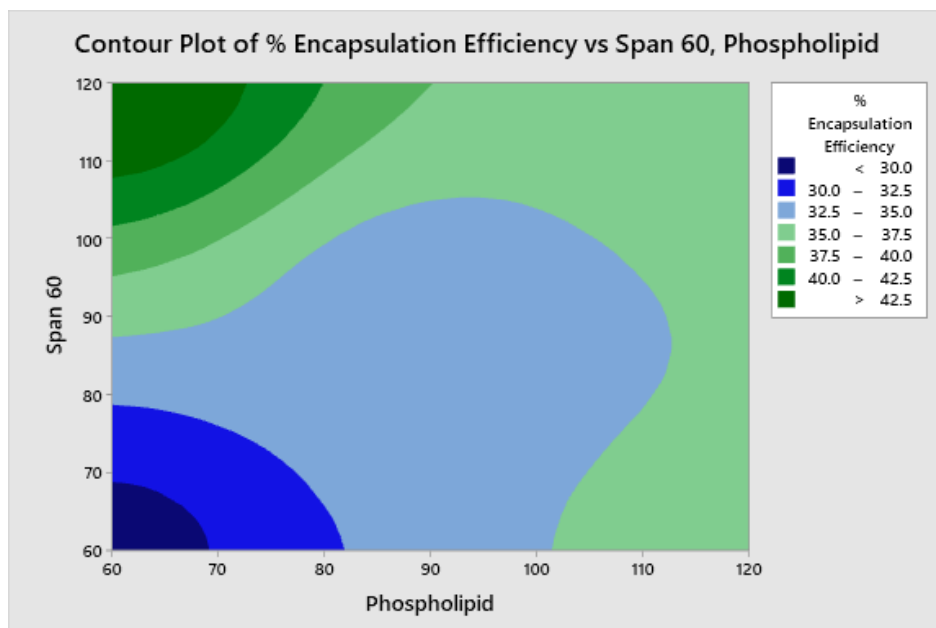
Figure 4.8: Contour plot for EE (%) of 5 ratios of phospholipid (P) and Span 60 (S) preparations using Minitab.

Notes: Results represent mean ± S.D (n = 6).

The results show, based on the darkest green patches on the contour plot, the highest percentage encapsulation (> 42.5) is obtained when phospholipid concentration is between 60-72 μmoles, and Span 60 concentration is between 108-120 μmoles (Figure 4.8). This is consistent with, Figure 4.7, which shows the formulation P60S120 achieved the highest EE of 45 ± 6% and the result was significantly higher than the EE (%) of P60S60 and P90S90.

4.5.4   Summary

The data on EE (45 ± 6%) and particle size (~900 nm) indicate the formulation P60S120 containing DCP (30 μmoles), DPPE (60 μmoles), cholesterol (90 μmoles), and Span 60 (120 μmoles) would be the most promising combination to be considered for further studies. This formulation was tested for release studies and permeation across TR146 buccal cells, and the results showed the release and permeation to be

undetectable after 6 hours of study. This could be due to several factors, such as the large particles size, as well as in studies of liposomes it has been shown that both phosphatidylethanolamine and cholesterol can increase the rigidity of the bilayer [182]. In effect, this rigidity could be to the extent that the insulin molecule is not able to permeate across the vesicle bilayer [83]. Thus, as well as reducing the particle size, the concentration of cholesterol possibly needs to be reduced to enable the insulin to release and permeate. Additionally, Span 60 (C_{18}) is one of the least leaky surfactants, due to the high phase transition temperature, which may benefit EE (%) but can hinder drug release [83], [104]. Hence the inclusion of a more hydrophilic surfactant can aid drug release. In several studies of lipid-based vesicles, it has been found the presence of increasing concentrations of Tween 80 (HLB 15) has led to enhancements in the release or permeability of the encapsulated drugs [195], [196]. Furthermore, in a study comparing Tween 80 to bile salts and the more lipophilic Spans, revealed Tween 80 to have the highest level of deformability [175]. This is due to the presence of the hydrophilic surfactant forming transient holes within the bilayer and thus enhancing membrane fluidity [175].

4.6 Results and discussion: influence of Tween 80

Table 4.2 shows the composition of Tween 80 and cholesterol that were tested in attempts to increase the release and permeability of transfersomes. This composition was also exposed to extrusion as a further downsizing method. The effects of these changes were investigated on particle size, PDI, zeta-potential and % EE. The effect of increasing the concentration of insulin from 0.73 mg/mL to 1.5 mg/mL in the hydration media was also observed on the % EE and % LC. The results of the % viability assays are discussed in chapter 5.

Table 4.2: Composition of Tween 80 and cholesterol in the transfersomal formulations in combination with Span 60 (120 µmoles), DPPE (60 µmoles) and DCP (30 µmoles). Total 5 mL hydration liquid (insulin 1.5 mg/mL).

Formulation	Cholesterol (µmoles, C)	Tween 80 (µmoles, T)
C90T0	90	0
C90T45	90	45
C45T0	45	0
C45T45	45	45

Abbreviations: 1,2-dipalmitoyl-3-sn-phosphatidylethanolamine (DPPE) and dicetyl phosphate (DCP)

4.6.1   Particle size and polydispersity analysis
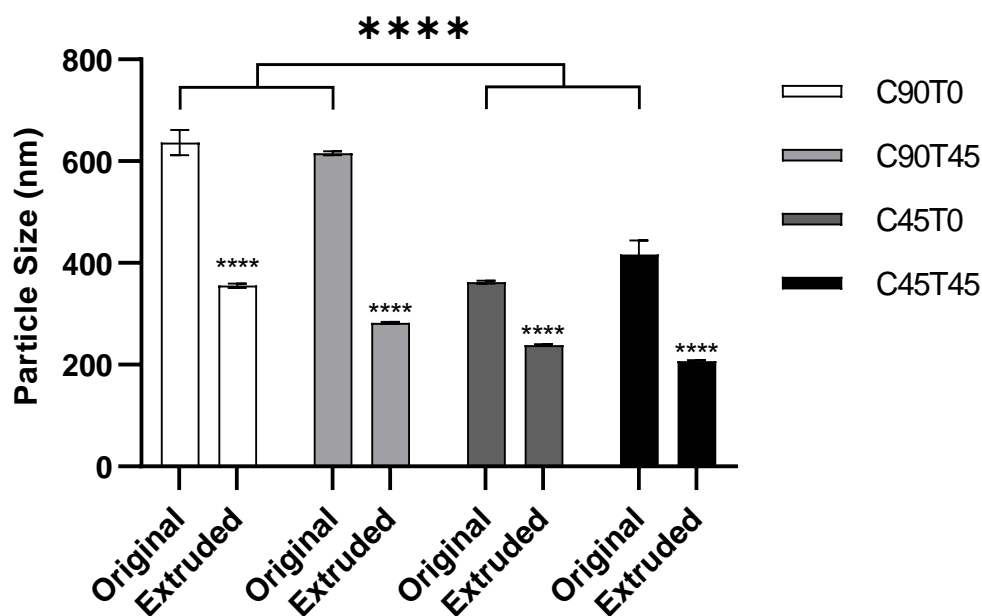
Figure 4.9: The influence of Tween 80 and cholesterol on particle size before and after extrusion.

Notes: Results represent mean ± SD (n=3). Two-way ANOVA analysis showed a significant difference ($p < 0.0001$) in particle size between the original and the extruded samples across all compositions (demonstrated by **** above the bars). Tukey's multiple comparisons test showed no significant difference (ns = $p > 0.05$) between C90T0 and C90T45. Significant difference (** = $p < 0.01$) observed between C45T0 and C45T45. Significant difference (**** = $p < 0.0001$) also observed between C90T0 and C90T45 with C45T0 and C45T45.
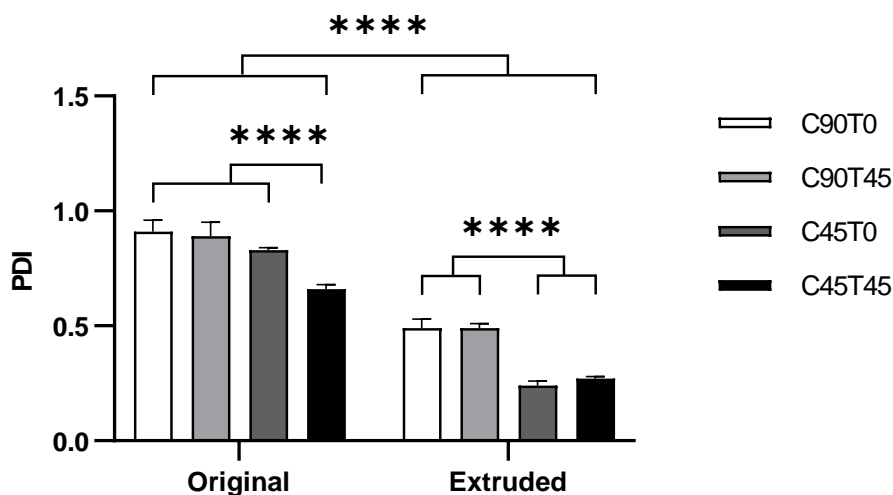
Figure 4.10: The influence of Tween 80 and cholesterol on PDI before and after extrusion.

Notes: Results represents mean ± SD (n=3). Two-way ANOVA analysis showed a significant difference (**** = $p < 0.0001$) in PDI before and after extrusion across all compositions. Tukey's multiple comparisons tests showed a significant difference (**** = $p < 0.0001$) in the original samples between C90T0, C90T45, C45T0 compared to C45T45. In the extruded samples, a significant difference (**** = $p < 0.0001$) was observed between C90T0 and C90T45 with C45T0 and C45T45.

In a study carried out on niosomes looking at the best method of downsizing found extrusion to be a useful technique for relatively fluid surfactants such as Tween 60, for both reducing particle size and achieving a narrow PDI [169]. In the same study, probe sonication was found to be more suitable for niosomes composed of Span 60, as it is a more rigid surfactant. When investigating the possible use of probe sonication in preliminary studies, insulin was found to not be stable during the process with a lot of frothing produced and a broad peak observed in HPLC analysis. Additionally, there were also possibilities of introducing impurities during the process [163]. Therefore, in this study, extrusion was chosen as the downsizing method, as Tween 80 in the formulation is a relatively fluid surfactant, even if Span 60 is more rigid.

Hence an extruder kit was purchased, which included 0.1 micrometre pore membranes. Using the manual extruder when it was attempted to extrude the

formulations through the 0.1 micrometre membrane at 55-58°C, it was impossible to extrude. Hence 0.4 μm membrane was attempted next and was successful. Once it had been extruded through the 0.4 μm membrane, it was again attempted to extrude through the 0.1 μm membrane but was still unsuccessful. Hence the final procedure for the formation of the transfersomes was modified to include extrusions via the 0.4 μm membrane only, which was optimised to ten extrusions.

As anticipated, it can be seen from, Figure 4.9 and Figure 4.10 above, across all the compositions the size and PDI of the vesicles, were significantly reduced ($p < 0.0001$) after the extrusion process. The percentage reductions in particle size were most significant with the Tween 80 containing formulations 54.1% (C90T45) and 50.4% (C45T45) followed by 44.2% (C90T0) and 34.0% (C45T0). This phenomenon was observed in another study, where inclusion of Tween 80 resulted in the reduction of particle size. Additionally, as expected based on previous studies, there is a significant reduction ($p < 0.0001$) in the particle size with a decrease in cholesterol content comparing compositions with 90 μmoles (C90T0 and C90T45) and those with 45 μmoles (C45T0 and C45T45). Thus, as anticipated C45T45, with Tween 80 and the lowest concentration of cholesterol, had the smallest average size of 206.7 nm ± 2.69 nm, which would be used for further studies. After extrusion, the PDI is less than 0.5 across all the formulations, but the most homogeneous samples are C45T0 and C45T45, with PDI values of 0.24 ± 0.02 and 0.27 ± 0.01, respectively.

4.6.2 Zeta potential determination
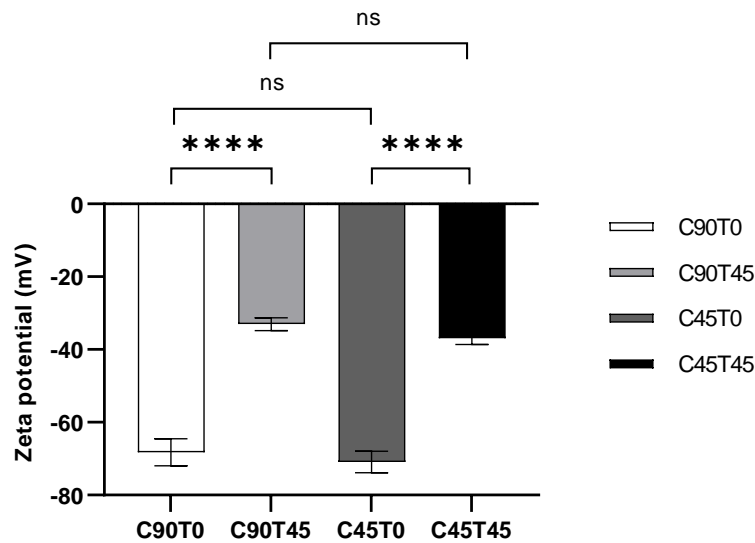
Figure 4.11: The influence of Tween 80 and cholesterol on the zeta potential.

Notes: Results represents mean ± SD (n=3). One-way ANOVA analysis showed significant difference (**** = $p < 0.0001$) among the mean values. Tukey's multiple comparisons test showed significant difference (**** = $p < 0.0001$) in zeta potential between C90T0 and C90T45. Significant difference (**** = $p < 0.0001$) was also observed between C45T0 and C45T45. No significant difference (ns = $p > 0.05$) was observed between C90T0 and C45T0. Also, no significant difference (ns = $p > 0.05$) was observed between C90T45 and C45T45.

Usually, for electrostatic stabilisation of vesicle, as summarised by Ge et al. 2019, the zeta potential needs to be above +30 mV or below -30 mV and based on these results all the formulations offer sufficient stability [194]. But it is noticeable, in Figure 4.11, there is a significant reduction in zeta potential in the formulations containing Tween 80 (C90T45 and C45T45). This is similar to a study looking at vesicles formed using Tween 80 and curcumin (as a substitute to cholesterol) it was also observed when the ratio of Tween 80 was gradually reduced the zeta potential becomes more negative [197]. Another study working with Tween containing transfersomes found them to exhibit positive zeta potentials with those of higher HLB values demonstrating greater positive zeta potential [198]. Additionally, it can also be due to Tween 80 being a non-

ionic surfactant with a sizeable hydrophilic head group, which is capable of interfering with the surface charge much more compared to the cholesterol, which is embedded in the bilayer.

4.6.3 Encapsulation efficiency of insulin
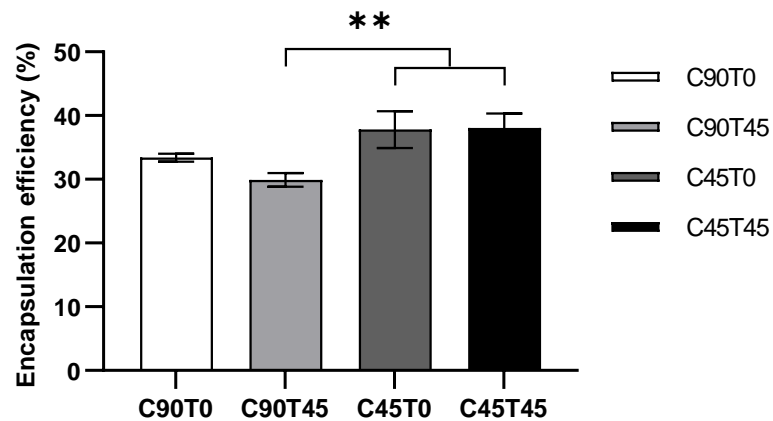
Figure 4.12: The influence of Tween 80 and cholesterol on the EE (%).

Notes: Results represents mean ± SD (n=3). One-way ANOVA analysis showed significant difference (**** = $p < 0.0001$) between the mean values. Tukey's multiple comparisons tests showed a significant difference (** = $p < 0.01$) in EE (%) between C90T45 compared to C45T0 and C45T45. Abbreviation: Encapsulation efficiency (EE)

The EE (%) of vesicular systems, as summarised by Ge et al. (2019), is often around 10 to 40%, although can reach up to 90% for some drugs, depending on the components of the system [194]. Thus, the results for all the formulations (Figure 4.12) are within acceptable limits, although the better EE (%) results were achieved by the Tween 80 containing formulations (C45T0 and C45T45). The significant increase in EE (%) in the presence of Tween 80 is possibly due to the presence of its long alkyl chains [199]. It was expected that the reduction in cholesterol would result in a significant decrease in EE (%), but this was not observed, possibly due to the

cholesterol content still being within the optimum range to provide enough rigidity to the structure, to maintain the drug entrapment.
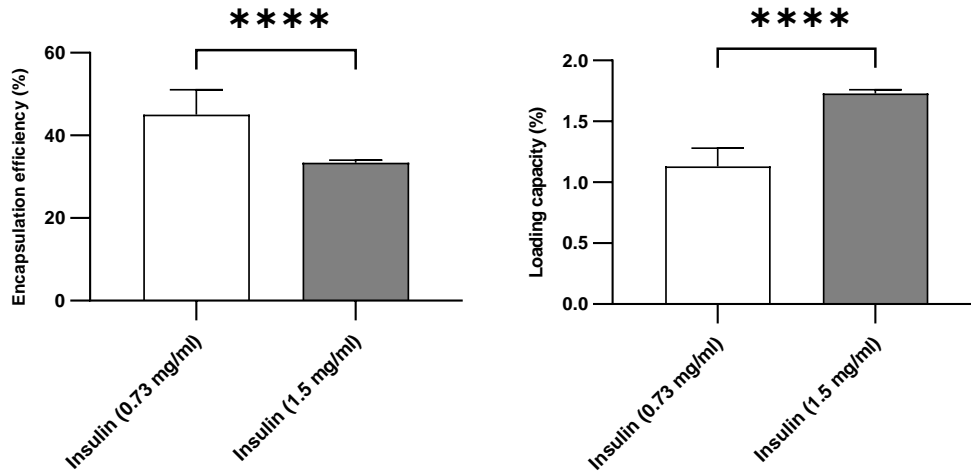
Figure 4.13: Shows EE (%) and LC (%) of insulin in formulation C90T0.

Notes: Results represents mean ± SD (n=6). One sample t-test, assuming Gaussian distribution, showed significant difference (p <0.0001) in EE (%) and LC (%) due to an increase in the concentration of insulin, from 0.73 mg/mL to 1.5 mg/mL, in the hydration media. Abbreviations: Encapsulation efficiency (EE) and loading capacity (LC)

Comparison of the formulation C90T0, with the molar ratio of vesicle components, kept constant, in the presence of an increasing concentration of insulin from 0.73 mg/mL to 1.5 mg/mL led to a significant decrease ($p < 0.0001$) in EE (%) Figure 4.13. However, the results show a significant increase ($p < 0.0001$) in LC (%). This is comprehensible as there is only a specific volume or space available within the aqueous compartment of the vesicles; thus, only a certain amount of the hydrophilic drug can be accommodated within the volume. This means although there is less drug encapsulated, the loading is higher and thus greater insulin content in ratio to the transfersomes.

4.6.4 Summary

Based on the outcome of the characterisation studies and the toxicity study (see chapter 5) the formulation (C45T45), consisting of 40% Span 60, 20% DPPE, 15% cholesterol, 15% Tween 80, and 10% DCP, was found to be promising and taken forward for further studies.

4.7 Results and discussion: determining effect of phospholipid and bile salt on transfersomes

The main results and discussion in this section are based on the ten transfersomal formulations, shown in Table 4.3, which consists of Tween 80 and Span 60 with a combination of either lecithin or DPPE with DCP or SGDC or both. The bile salt SGDC was chosen as a possible additional permeation enhancer, to be incorporated within the transfersomal formulation, as it has been shown in studies to have the ability to enhance the permeability of insulin and other hydrophilic macromolecules across TR146 buccal cells and porcine mucosa, respectively [60], [64]. Based on previous results, 60 micromoles of each transfersomal formulation was produced per mL of hydration liquid, and the ratio of cholesterol was retained as 15% and Span 60 as 40%. Figure 4.18 shows the appearance of the produced transfersomal suspensions.

Table 4.3: Percent composition of the different components in each transfersomal formulations tested (total 60 µmoles/mL).

Formulation	Cholesterol (% mol)	Span 60 (% mol)	Tween 80 (% mol)	DCP (% mol)	SGDC (% mol)	DPPE (% mol)	Lecithin (% mol)
*D5E	15	40	20	5		20	
D10E	15	40	15	10		20	
*S5E	15	40	20		5	20	
S10E	15	40	15		10	20	
D5S5E	15	40	15	5	5	20	
D5L	15	40	20	5			20
D10L	15	40	15	10			20
S5L	15	40	20		5		20
S10L	15	40	15		10		20
D5S5L	15	40	15	5	5		20

Abbreviation: Dicetyl phosphate (DCP), sodium glycodeoxycholate (SGDC), and 1,2-dipalmitoyl-3-sn-phosphatidylethanolamine (DPPE). * = formulations carried forward.

4.7.1 Particle size and polydispersity index analysis

a.

b.

c.
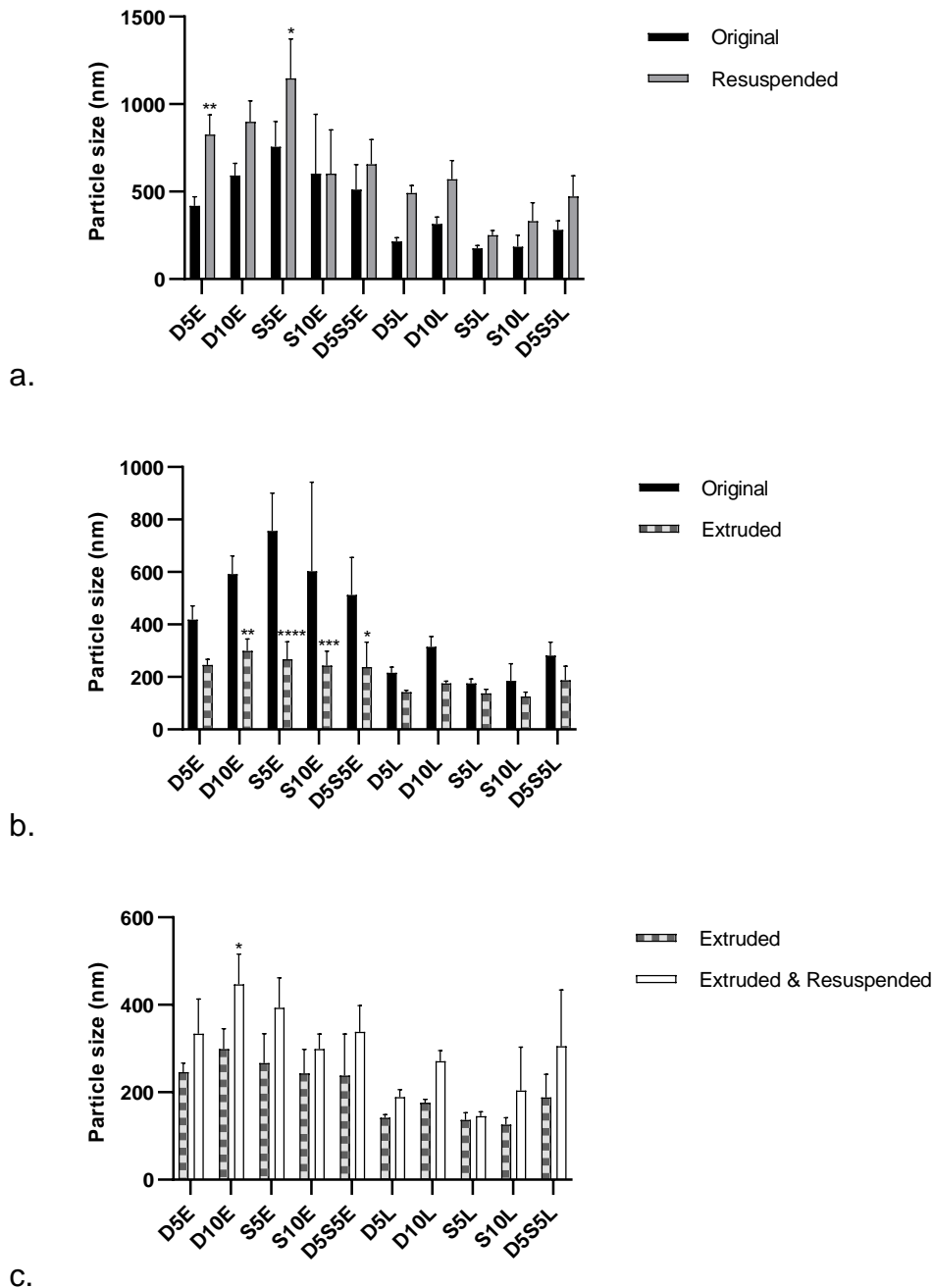
Figure 4.14: Comparing the effect of extrusion and resuspension of vesicles using vortexing on particle sizes of transfersomes.

Notes: Results represents mean ± SD (n=3). Two-way ANOVA analysis showed significant difference (**** = $p < 0.0001$) between the mean values of (a) original vs resuspended, (b) original vs extruded, and (c) extruded vs extruded and resuspended. Sidak's multiple comparisons test showed significant difference (a) D5E (** = $p < 0.01$) and S5E (* = $p < 0.05$), (b) D10E (** = $p < 0.01$), S5E (**** = $p < 0.0001$), S10E (*** = $p < 0.001$), D5S5E (* = $p < 0.05$), and (c) D10E (* = $p < 0.05$).
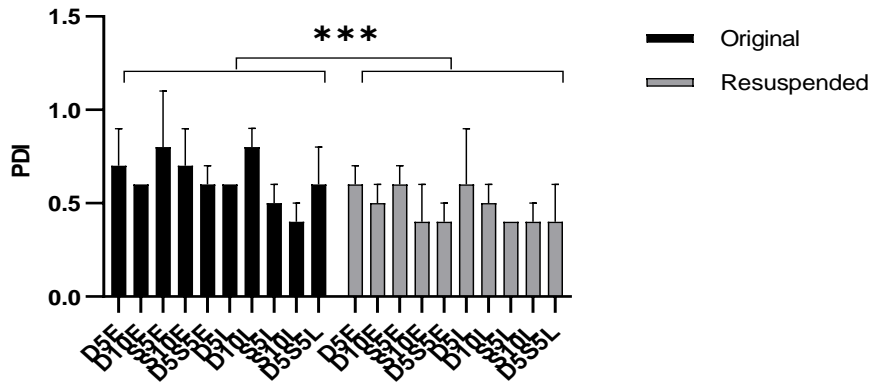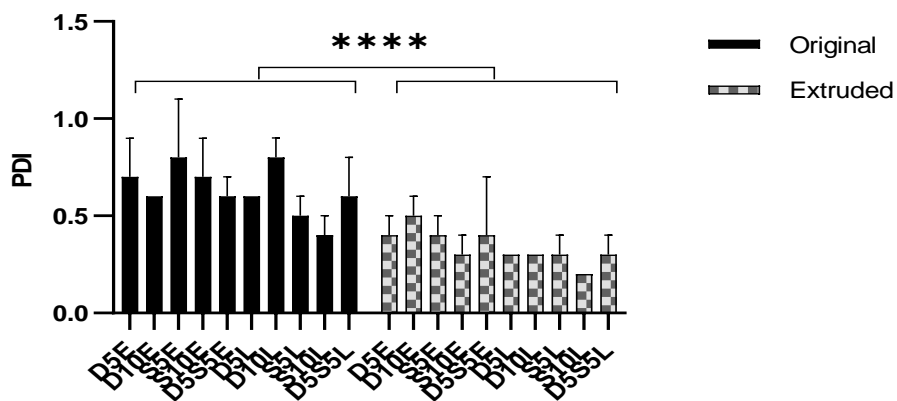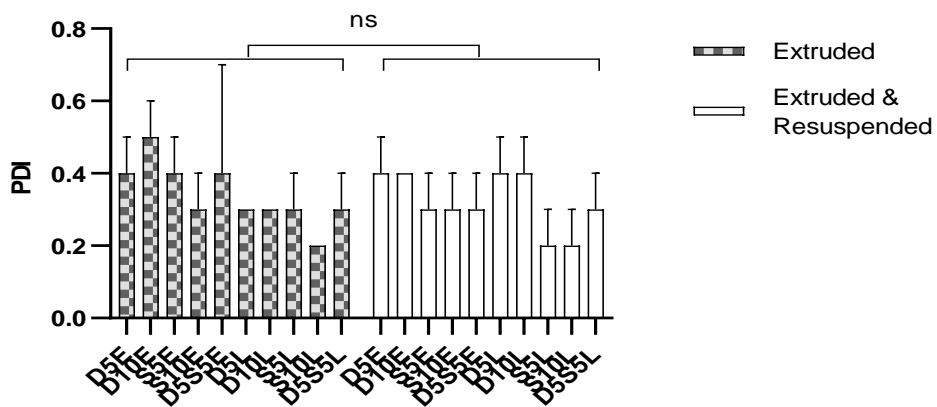
Figure 4.15: Comparing the effect of extrusion and resuspension of vesicles using vortexing on PDI of transfersomes.

Notes: Results represents mean ± SD (n=3). Two-way ANOVA analysis showed a significant difference (*** = $p < 0.001$) between the mean values of original vs resuspended (a). Also showed significant difference (**** = $p < 0.0001$) between the mean values of original vs extruded (b). But no significant difference (ns = $p > 0.05$) between the means of extruded vs extruded and resuspended was observed.

Particle size and PDI, as highlighted by Nowroozi et al. (2018), are very influential in the final characteristics and properties of vesicles [169]. Thus, it needs to be monitored and optimised to achieve the best possible performance in drug delivery. Forming smaller vesicles using bath sonication and extrusion may lead to greater instability of transfersomes. This is because thermodynamically a higher input of energy is required to form smaller vesicles. Thus these vesicles contain surplus energy that can lead to greater instability compared to bigger transfersomes [83]. Hence the particle size of the transfersomes was analysed during the production and size reduction to observe the effects of the procedure on the vesicles and their homogeneity.

Two-way ANOVA analysis showed a significant difference between the mean of the particles produced originally (just after bath sonication) compared to the resuspended vesicles, i.e. samples centrifuged then pellet resuspended via vortexing [Figure 4.14 (a)]. It can be observed that the particle size, of all the formulations, are larger after resuspension compared to the original samples. However, with further statistical testing using Sidak's multiple comparisons test only formulations D5E ($p < 0.01$) and S5E ($p < 0.05$) were affected individually. The PDI of the resuspended particles is overall lower compared to the original particles [Figure 4.15 (a)]. This is possibly the result of the formation of more thermodynamically stable particle size upon vortexing compared to the original, which had been exposed to bath sonication during production.

Two-way ANOVA analysis also showed a significant difference between the mean of the particles produced compared initially to the extruded particles [Figure 4.14 (b)]. The results show all the extruded vesicles are much smaller in size compared to the original samples, but with further statistical analysis (Sidak's multiple comparison's tests)

mainly the formulations containing DPPE are significantly smaller in size, except for D5E. Extrusion is generally a suitable method for size reduction of vesicles and improvement of homogeneity of particle size, i.e. PDI [169], [200]. In Figure 4.15, the PDI of the extruded particles is overall significantly lower compared to the original particles, which is expected as the particles are smaller and more uniform in size.

Two-way ANOVA analysis also showed a significant difference between the mean of the particles extruded compared to the particles that were extruded and resuspended (after centrifugation) [Figure 4.14 (c)]. However, on individual analysis, only formulation D10E was significantly higher in vesicle size ($p < 0.05$). There was no significant difference observed between the PDI of the extruded particles versus the extruded and resuspended particles (Figure 4.15). Commonly, the aim would be to observe PDI values of less than 0.5, which would indicate a suitable size distribution within samples. However, the lower, the better, and it can be seen from the results after extrusion all the sample means are less than or equal to 0.5 [170].

Looking at the particles containing lecithin, they are much smaller compared to those containing DPPE, which is likely due to the physical nature of the phospholipids as DPPE is solid at room temperature whereas lecithin is liquid. This reduced particle size may offer advantages in permeability studies. But looking at the extruded vesicles the particles are mostly below 400 nm; thus most of the formulations will be suitable for further studies based on the particle size and PDI.
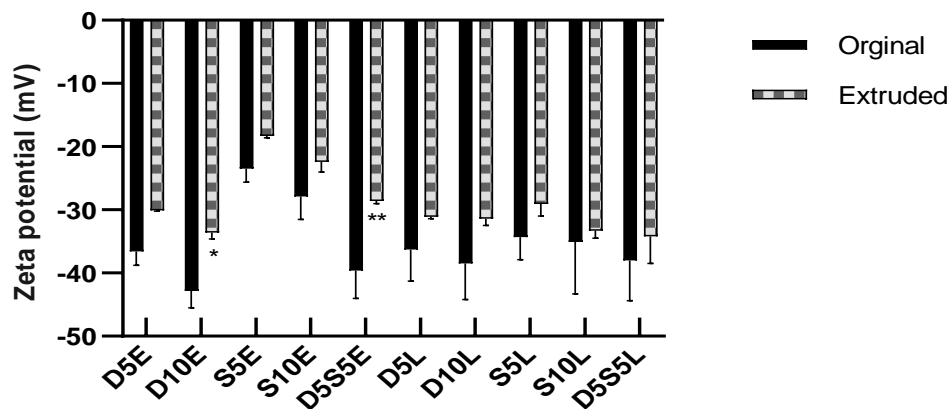
Figure 4.16: Zeta potential of the ten transfersomal formulations before and after extrusion.

Notes: Results represents mean ± SD (n=3). Two-way ANOVA analysis showed significant difference (**** = $p < 0.0001$) between the mean values of original vs extruded. Sidak's multiple comparisons test showed significant difference (* = $p < 0.05$) D10E and (** = $p < 0.01$) D5S5E compared to the original zeta potential.

The mean zeta potential of the extruded transfersomes is significantly less negative compared to the original samples (Figure 4.16). However, most of the formulations, except for S5E and S10E, are still within the optimum range of -30 mV or below, which means the samples should be stable colloidal systems and have reduced chance of aggregation during storage [194]. Based on the literature, it is known that cholate based transfersomes have negative zeta-potentials thus it was presumed DCP was unlikely to be required to provide the electrostatic stabilisation in the formulation [79]. However, it can be seen from Figure 4.16 that although the negative charge is sufficient in the presence of lecithin, in the presence of the positive phospholipid DPPE, the zeta potential is less negative compared to the DCP formulation and it is around -18 mV (S5E). In literature, an increase in the cholate bile salt led to greater negative surface charge (-26.4 ± 2.5 mV to -34.9 ± 2.2 mV), which was also observed in this study with the formulation S10E having a more negative zeta potential than S5E [198]. But both

formulations (S5E and S10E) still have zeta potentials less negative than -30 mV and not above +30 mV; hence if these formulations were chosen for further studies, the stability needs to be monitored.

4.7.3   Encapsulation efficiency of insulin
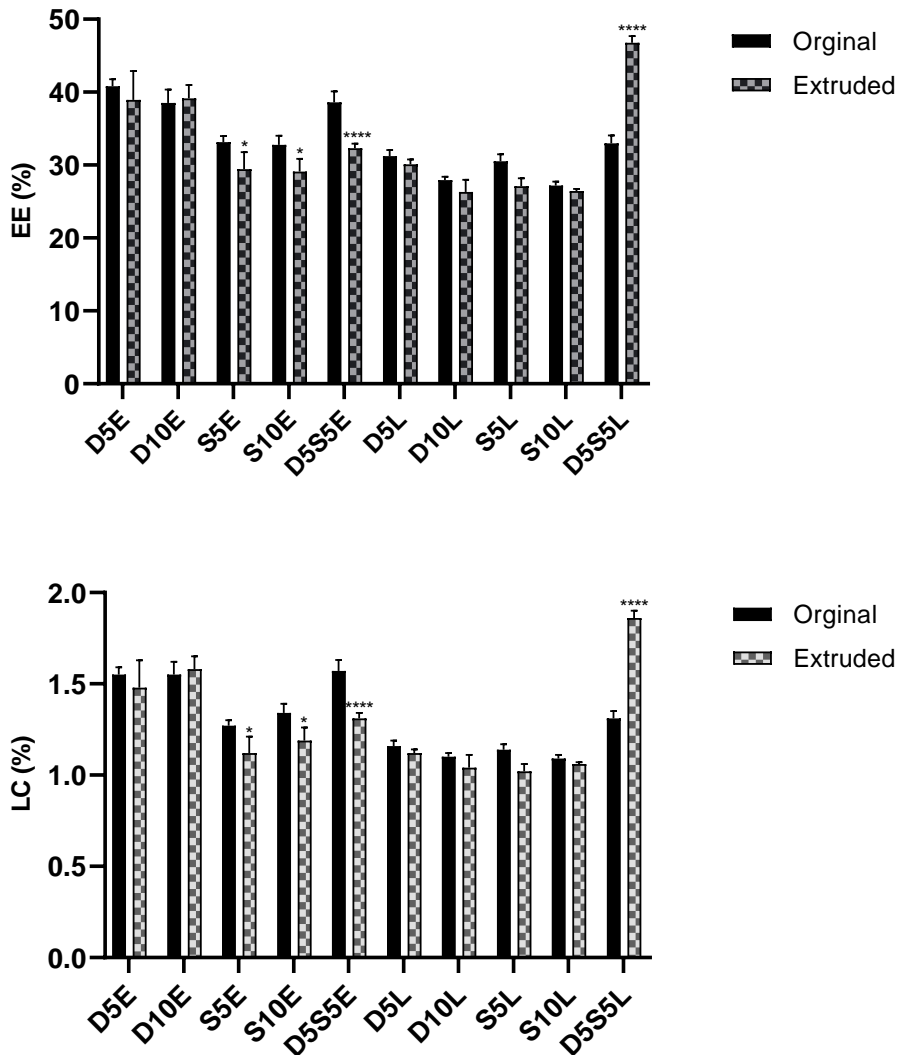
Figure 4.17: Comparison of EE (%) and LC (%) of the ten transfersomal formulations before and after extrusion.

Notes: Results represents mean ± SD (n=3). Two-way ANOVA analysis of the mean values of original vs extruded showed significant difference (**** = $p < 0.0001$) in the EE (%) but no significant difference ($p > 0.05$) in LD (%). But both EE (%) and LC (%) results in the Sidak's multiple comparisons analysis showed significant difference (* = $p < 0.05$) with S5E and S10E and (**** = $p < 0.0001$) with D5S5E and D5S5L.

Looking at the individual results, comparing EE (%) and LC (%), the results appear very similar (Figure 4.17). Statistical analysis (Sidak's multiple comparisons test) of the effect of extrusion showed a significant reduction of EE and LC for three of the formulations (S5E, S10E and D5S5E), all of which contain the bile salt SGDC and the phospholipid DPPE. These results correlate highly with the significant reduction in particle size after extrusion. In another study, this phenomenon was also observed with the EE decreasing upon decrease of particle size after extrusion [200]. This is possibly due to the lower volume available to contain the drug within the vesicle bilayers, which also explains the similarity of the LC results. The anomaly is formulation D5S5L, which after extrusion resulted in a significant increase in the EE and LC. This is possibly due to the particle size of this formulation being the highest among the lecithin containing vesicles and lecithin is a more fluid phospholipid compared to DPPE, thus during extrusion, the process may have aided drug entry within the fluid membrane of the vesicle. Based on these results, after extrusion, the formulations with the best EE and LC are D5E, D10E and D5S5L.

4.7.4　Summary

Figure 4.18: Displays the transfersomal suspensions (from left to right D5E, D10E, S5E, S10E, D5S5E, D5L, D10L, S5L, D10L, S5L, S10L and D5S5L) produced using Table 4.3.

The ten transfersomes produced using compositions suggested in Table 4.3 and displayed in Figure 4.18 all showed optimistic results, after extrusion, in the characterisation studies. In terms of particle size, all except (D10E) formed particles < 400 nm. However, the lecithin containing formulations were overall were much smaller in size. PDI was also satisfactory with all formulations achieving a PDI of 0.4 or less. The zeta potential was optimal (-30 mV or below surface charge) for most formulations, except for S5E, S10E, D5S5E and S5L. In terms of EE (%) and LC (%), all compositions achieved between 26-47% and 1-1.9%, respectively. Nevertheless, the promising formulations in terms of EE (%), were D5S5L (46.8%), D10E (39.2%) and D5E (39.0%). However, after carrying out viability assays (discussed in chapter 5), the safest formulations were D5E and S5E. Thus, these two formulations would be taken forward for further studies. Although D5E is the more favourable formulation, due to the higher EE and optimal zeta potential S5E (29.4% EE) would be a good comparison for permeability studies as it contains the bile salt (SGDC).

4.7.5 Morphological studies
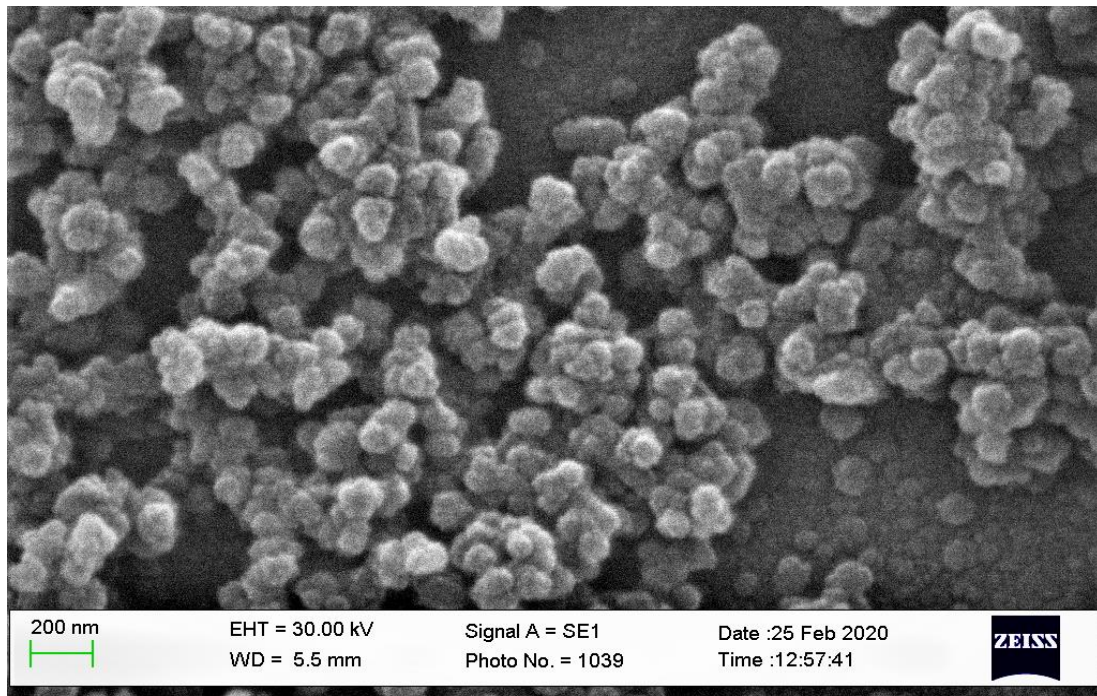
Figure 4.19: SEM image of transfersomes (D5E).

The morphological analysis of transfersomes with SEM showed the particles to be relatively spherical (Figure 4.19). However, some have aggregated together during drying, and the observation is similar to the image of Tween 80 containing liposomes seen in another study using SEM [201]. Observing the particle size based on Figure 4.19, most of the vesicles are less than 200 nm in size. This is much smaller than the DLS measurement of the particle size; however, this is understandable as DLS measures the hydrodynamic vesicle size and for SEM the particles are dried under vacuum before imaging. Thus, there is a loss of liquid from the vesicle, which would lead to the vesicles shrinking in size. The lack of correlation of SEM with DLS measurements has been observed in other studies [202]. Lyophilization of the transfersomes before SEM was considered and tested, but it was found, similar to another study, that it did not depict the correct morphology of the actual transfersomes [198].

4.7.6 In-vitro release studies
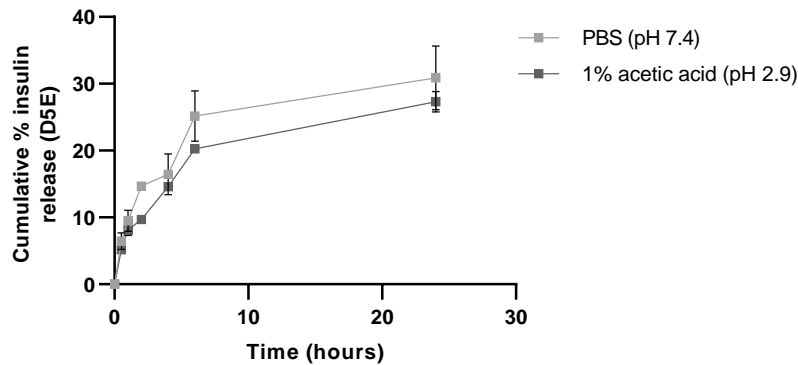
Figure 4.20: Cumulative % insulin release from transfersome D5E in PBS (pH 7.4) and 1% v/v acetic acid (pH 2.9).

Notes: Results represent mean ± SD (n=3). Two-way ANOVA analysis with Geisser-Greenhouse correction showed insignificant difference ($p > 0.05$) between the release of insulin from D5E transfersomes in PBS and 1% acetic acid. Abbreviation: Phosphate-buffered saline (PBS)
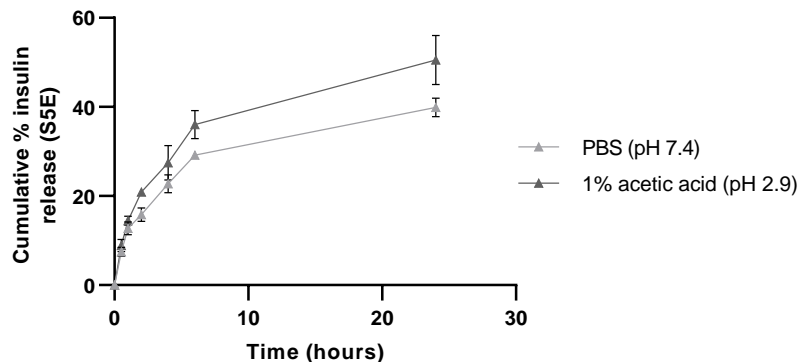
Figure 4.21: Cumulative % insulin release from transfersomes S5E in PBS (pH 7.4) and 1% v/v acetic acid (pH 2.9).

Notes: Results represent mean ± SD (n=3). Two-way ANOVA analysis with Geisser-Greenhouse correction showed a significant difference (* = $p < 0.05$) between the release of insulin from S5E transfersomes between in PBS compared to 1% acetic acid. Sidak's multiple comparisons test comparing each time point of insulin release from S5E showed no significant difference ($p > 0.05$) across all time points. Abbreviation: Phosphate-buffered saline (PBS)
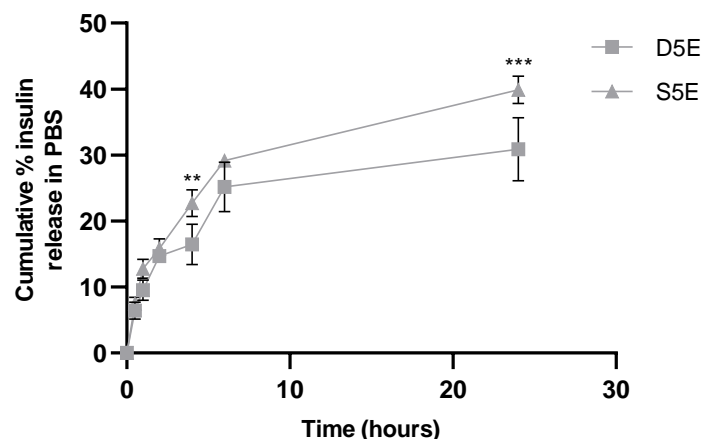
Figure 4.22: Comparison of cumulative % insulin release from transfersomes D5E and S5E in PBS (pH 7.4).

Notes: Results represent mean ± SD (n=3). Two-way ANOVA analysis showed a significant difference (**** = $p < 0.0001$) between the release of insulin from D5E transfersomes compared to S5E in PBS (pH 7.4). Sidak's multiple comparisons test comparing each time point release of insulin from D5E and S5E showed significant difference (** = $p < 0.01$) at 4 hours and (*** = $p < 0.001$) at 24 hours of release. Abbreviation: Phosphate-buffered saline (PBS)

Most of the release studies are carried out in PBS pH 7.4, as upon stimulation, due to the presence of the patch, this is the likely pH in the buccal cavity [71]. However, in literature, some liposomal formulations have been unstable in the presence of low acidic temperatures (pH 2) [203], [204]. Thus, as the transfersomes will be incorporated in buccal patches produced using chitosan, dissolved in 1% acetic acid (pH 2.9), it is essential to test the release and determine if at this pH there are any significant differences or burst release of insulin during the formation of the patch.

Comparing the release of insulin from the D5E transfersome in PBS (pH 7.4) and 1% acetic acid (pH 2.9), no significant difference was observed (Figure 4.20). Thus, showing the formulation is relatively stable at this pH for the duration tested. Two-way ANOVA analysis of the formulation S5E showed the release in 1% acetic acid to be significantly higher than in PBS (Figure 4.21). However, further statistical analysis

showed no significant difference in the release of insulin when the release was compared individually at each time point. But to be precautious, it is crucial when the transfersomes are incorporated in the patch formulations that they should be placed soon after in the freezer to prevent drug release from the transfersomes before freeze-drying.

As shown in Figure 4.22 insulin release after 6 hours was 25.2 ± 3.8% (D5E) and 29.2 ± 0.3% (S5E) and after 24 hours 30.9 ± 4.8 (D5E) and 39.9 ± 2.1% (S5E). Based on the release studies S5E overall achieved significantly higher percentage drug release compared to D5E, and this is possibly due to the greater leakage offered by the hydrophilic bile salts, by forming transient pores within the bilayer, compared to DCP [175]. Between 6 hours and 24 hours, the difference in the release is small and resembles prolonged drug release. This phenomenon has been observed in other studies looking at liposomes. Specifically, Span 60-based vesicles for delivery of drugs such as doxorubicin and ketoprofen, which can be of therapeutic benefit if an extended drug release is desired [205], [206]. This difference in the rate of release is explained in literature as possible loose drug depots on the surface of the vesicles as well as in the interphase between lipid tails and polar headgroups of the bilayer [132].

Furthermore, since the release from both transfersomal formulations (D5E and S5E) does not reach even 50% of the total amount of insulin in 24 hours there is the possibility that the indirect quantification of insulin encapsulation using the supernatant may not be entirely representative of the total insulin encapsulated as discussed by Hussain et al. (2019) [207]. However, often proteins are quantified indirectly, because unlike small molecular weight drugs, solubilisation of protein containing vesicles could compromise the protein molecule's structural integrity leading to misleading and

inaccurate results. Additionally, a study looking at protein quantification and interference of liposomes found that solubilisation of anionic and neutral liposomal formulations presented greater interferences in the results compared to cationic liposomes [207]. Thus, further work would be required to optimise and develop an accurate method of quantifying insulin directly.

4.7.7 Stability of transfersomes

a.   b.
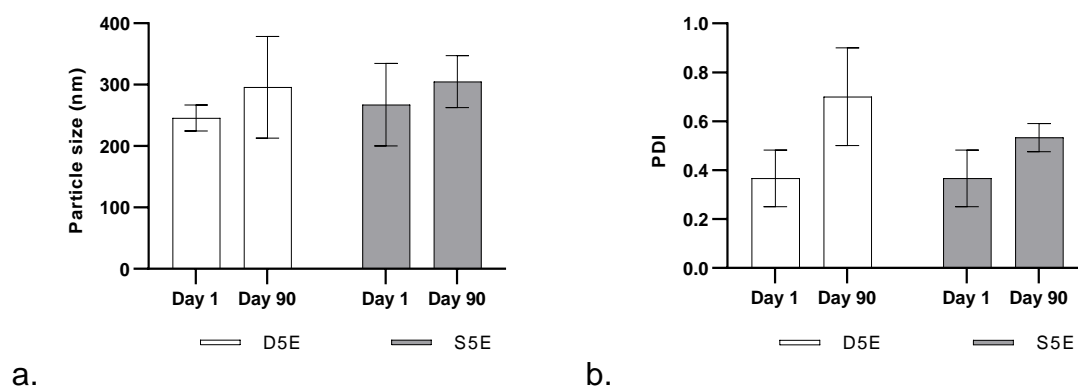
Figure 4.23: Stability of formulations D5E and S5E after three months of storage in the fridge (2-8°C). (a) Particle size and (b) PDI.

Notes: Results represent mean ± SD (n=3). Two-way ANOVA analysis showed insignificant difference ($p > 0.05$) in particle size after three months of storage in the fridge in PBS (pH 7.4) for both D5E and S5E (a). Two-way ANOVA analysis showed a significant difference (* = $p < 0.05$) in PDI after three months of storage in the fridge. Tukey's multiple comparisons test comparing each formulation D5E and S5E showed insignificant difference ($p > 0.05$). Abbreviation: Phosphate-buffered saline (PBS)

The vesicles were formed using bath sonication and extrusion, and thermodynamically a greater input of energy is required to form smaller vesicles, thus contain surplus energy, which over time can lead to greater instability compared to larger transfersomes [83]. Looking at Figure 4.23 (a), in terms of particle size, statistical analysis did not show any significant difference in size before and after storage (3 months 2-8°C). Two-way ANOVA analysis of PDI, however, did show the statistically significant difference before and after storage. Individual analysis, using Tukey's

multiple comparisons test, showed an insignificant difference for both D5E and S5E. Although statistically, the results may not be significant, due to the high error bars, it can be seen, particularly for D5E, that the mean particle size is larger and there is much higher variation within the results hence for D5E PDI is around 0.7 compared to 0.4 initially. Stability issues were expected for S5E, which initially had a zeta potential of -18.3 ± 0.3 mV. But the outcome is unexpected for D5E, which formerly had a zeta potential of -30.1 ± 0.1 mV and thus based on previous studies was meant to be stable.

4.8 Conclusion

In summary, two novel transfersomal formulations were formulated, and insulin release after 6 hours was found to be 25.2 ± 3.8% (D5E) and 29.2 ± 0.3% (S5E). The work on these vesicles led to the development of an optimised, efficient, and inexpensive procedure for producing vesicles and reducing particle size using a combination of the standard thin-film hydration technique, bath sonication and manual extrusion. Although the release studies were carried out for 24 hours, for observation purposes, the maximum intended duration of action would be 6 hours, as keeping formulations in the buccal cavity for greater than 6 hours would likely cause discomfort for patients [77]. Hence further release and permeation studies of D5E and S5E were carried out for 6 hours. The chosen formulations were also tested for toxicity and permeability studies (see chapter 5) and incorporated in mucoadhesive buccal patches and tested for release studies (see chapter 6).

5. Cell culture studies

5.1 Introduction

Porcine buccal mucosa has been suggested to be a good representation of the human buccal mucosa. Still, based on literature and experience, there is a lot of variation in the thickness of the mucosa, which makes it difficult for repeatability and consistency in permeability experiments. Even when extreme care is taken during tissue preparation, it is difficult to maintain the viability and integrity of the porcine buccal mucosa [208]. Therefore TR146 buccal cells were selected for *in vitro* tests as they can form stratified squamous epithelium similar to normal human buccal epithelium [209], [210].

Studying permeability of drugs using an *in vitro* cell models, such as TR146, has the advantage of being relatively simple but more importantly, a reproducible method of predicting *in vivo* drug permeation. The cells are seeded in permeable supports and allowed to grow in monolayers. The cells can form 4 to 7 layers between 3-4 weeks and can display the ultrastructural characteristics similar to that of the average human buccal mucosa [211], [212]. These characteristics include the presence of multilaminar bodies, desmosomes, intermediate filaments, and microvilli-like processes. They also lack tight junctions [211].

5.2 Chapter aims

> To carry out toxicity studies on the final ten transfersomes using SRB toxicity assay.

> To study the permeability capability of the top two transfersomal formulations across TR146 buccal cells.

> To see if the presence of bile salt in the formulation will have any impact on the permeation of insulin.

> To image the cells before and after permeation studies to observe any changes in cell viability and morphology.

5.3 Materials and methods

5.3.1 Materials

RHI (27.5 IU/mg), sorbitan monostearate (Span 60), cholesterol (C8667), DCP, polysorbate 80 (Tween 80), SGDC, dimethyl sulfoxide (DMSO), hydroxyethylpiperazine ethane sulfonic acid (HEPES) solution (1M), atenolol, FITC-Dextran (20kDa), Actinomycin D (2 mg/mL), Sulforhodamine B (SRB), PBS (pH 7.4), Corning® 96 well TC-treated microplates, and Avanti® Mini-Extruder (fitted with 0.4-micrometre polycarbonate membrane and with heating block) were all purchased from Sigma-Aldrich (Merck KGaA, Darmstadt, Germany). DPPE and soybean lecithin were purchased from Tokyo Chemical Industry (UK). The TR146 (ECACC 10032305), human buccal mucosa cells, were obtained from Public Health England (London, UK). Gibco™ Ham's F-12 Nutrient Mix, Gibco™ Fetal Bovine Serum (FBS), Gibco™ L-Glutamine (200 mM), Gibco™ Hank's balanced salt solution (HBSS, pH 7.4), Gibco PBS (pH 7.4), Gibco™ trypsin-ethylenediaminetetraacetic acid (EDTA; 0.25%), and

Gibco™ Penicillin-Streptomycin (10,000 units/mL) were all purchased from Fischer Scientific (Leicestershire, UK). Sarstedt TC-inserts (polyethylene terephthalate membrane bottom with a pore size of 0.4 μm and surface area of 1.1 cm^2) were purchased from (Numbrecht, Germany). MilliQ® water was obtained internally using a Merck Millipore Direct-Q® 3UV water purification system (Billerica, MA, USA). All other chemicals and reagents used were of analytical grade.

Transfersomes were prepared using the traditional thin-film hydration technique, discussed in chapter 4. The composition of transfersome content shown in Table 5.1 is only for viability assays looking at the influence of cholesterol and Tween 80.

Table 5.1: Composition of Tween 80 and cholesterol in the transfersomal formulations in combination with Span 60 (120 μmoles), DPPE (60 μmoles) and DCP (30 μmoles). Total 5 mL hydration liquid (insulin 1.5 mg/mL).

Formulation	Cholesterol (μmoles, C)	Tween 80 (μmoles, T)
C90T0	90	0
C90T45	90	45
C45T0	45	0
C45T45	45	45

Abbreviation: 1,2-dipalmitoyl-3-sn-phosphatidylethanolamine (DPPE) and dicetyl phosphate (DCP)

The main results and discussion in this section are based on the ten transfersomal formulations, shown in Table 5.2 below, which consists of Tween 80 with a combination of either lecithin or DPPE with DCP or SGDC or both. Based on previous results, 60 micromoles of each transfersomal formulation was produced per mL of hydration liquid, and the ratio of cholesterol was retained as 15% and Span 60 as 40%.

Table 5.2: Percentage of the different components in each transfersomal formulation tested (total 60 µmoles/mL).

Formulation	Cholesterol (% mol)	Span 60 (% mol)	Tween 80 (% mol)	DCP (% mol)	SGDC (% mol)	DPPE (% mol)	Lecithin (% mol)
D5E	15	40	20	5		20	
D10E	15	40	15	10		20	
S5E	15	40	20		5	20	
S10E	15	40	15		10	20	
D5S5E	15	40	15	5	5	20	
D5L	15	40	20	5			20
D10L	15	40	15	10			20
S5L	15	40	20		5		20
S10L	15	40	15		10		20
D5S5L	15	40	15	5	5		20

Abbreviation: Dicetyl phosphate (DCP), sodium glycodeoxycholate (SGDC), and 1,2-dipalmitoyl-3-sn-phosphatidylethanolamine (DPPE)

5.3.2 SRB cell viability assay

Firstly around 2×10^4 cells were added to 96-well plates in 200 µL growth medium and allowed to attach and grow. After 24 hours, the media was removed, and the correct amount of formulation added with growth media and left for incubation for 24 hours. The assay included the following as controls: (1) culture media only (without cells); (2) culture media with only cells; (3) cells in the presence of two concentrations of the cytotoxic actinomycin D as a positive control. After 24 hours of exposure, the formulations were washed off five times with PBS and 100 µL of media added to each well. Then 33 µL of cold 40% (w/v) trichloroacetic acid (TCA) was added to all wells and placed in the fridge for 1 hour. The wells were then washed four times with distilled water and left on the bench to dry overnight. Next day 100 µL of SRB solution (0.4% w/v in acetic acid) was added to each well and left at room temperature for 30 minutes. Next, to remove the unbound dye, the wells were washed four times with 1% (v/v)

acetic acid and allowed to dry overnight. Subsequently, 100 µL of 10mM Tris buffer (pH 10) was added to each well and left for 30 minutes to solubilize the protein-bound dye. Finally, the optical density (OD) of each 96-well plate was read at 554 nm using a microplate reader. To calculate cell cytotoxicity, first, the values must be corrected, by subtracting the OD of the background control well (containing only media and no cells) from all the ODs of the sample readings, then apply Equation 5.1 shown below. Subsequently, to calculate (%) cell viability Equation 5.2 is applied.

Equation 5.1

$$Cytotoxicity\ (\%) = \frac{Control\ Cells - Tested\ Cells}{Control\ Cells} \times 100$$

Equation 5.2

$$Cell\ Viability\ (\%) = 100 - \%\ Cytotoxicity$$

5.3.3 CytoSMART Omni live cell imaging

To monitor and capture images of the TR146 cells during growth and viability studies the novel CytoSMART Omni system was used, which is produced by CytoSMART Technologies (Eindhoven, Netherlands). The system is connected to a windows-based computer and works from inside standard CO_2 incubators. It uses automated inverted bright-field microscopy for imaging of cells in well plates [213]. The images are uploaded and analysed using CytoSMART ™ Cloud. The magnification used in the system is equivalent to a typical 10x objective of a standard bright field microscope. Before the formulation and controls were added, the cells were given time to adhere and grow over 18 hours, and the growth was monitored during this period. The study was carried out in Corning® 96 well TC-treated microplates, and except for the blank wells, all the other wells had 2×10^4 cells added. The controls included blank wells, wells with only cells and actinomycin D (0.1 g/mL & 2.5 g/mL) as positive control. The toxicity of the positive control was monitored over 24 hours. The test formulations (Table 5.2) were all tested, but due to their opaque nature, images were only taken after the 24-hour viability studies. The formulations were removed, the wells washed five times with HBSS, then growth media added and 96 well plate placed back in the incubator for imaging.

5.3.4 Teer measurement for TR146 cells

TEER measurements were assessed using a Merck Millipore Millicell ERS (electrical resistance system) Voltohmmeter (Billerica, MA, USA). The TEER was measured to test the integrity of the epithelial cells cultured on permeable filter inserts, before and after permeability studies, and to monitor growth over 30 days. TEER ($\Omega.cm^2$) was calculated using Equation 5.3.

Equation 5.3

$$Teer = (Resistance_{\text{inserts with cells}} - Resistance_{\text{inserts without cells}}) \times Surface\ Area\ of\ inserts$$

5.3.5 Permeation studies
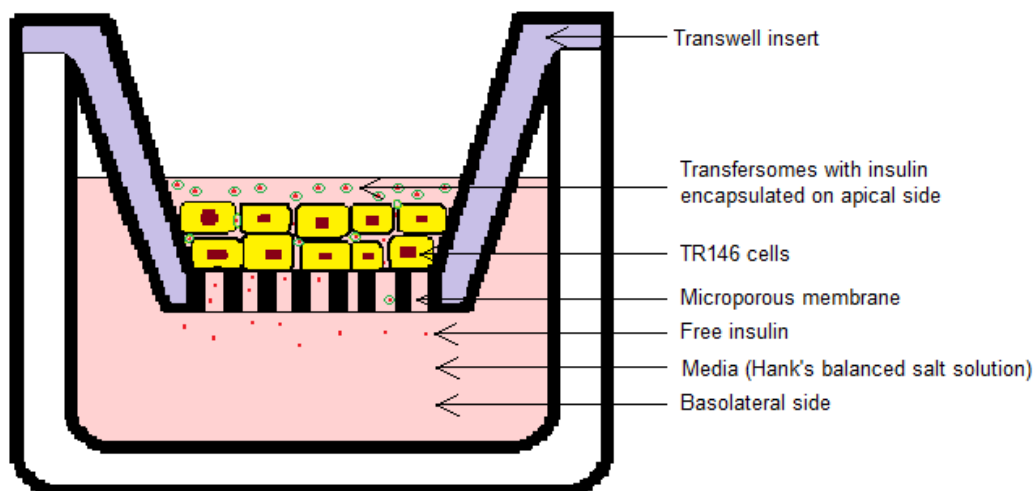
Figure 5.1: Schematic illustration of the permeation of insulin across TR146 cell layers on a transwell insert.
Adapted from [60]

Permeability studies were carried out over 6 hours using TR146 buccal cell line (passage 14-20). It was performed according to Bashyal et al. (2018) but with some

modifications, illustrated in Figure 5.1 [60]. TR146 cell, at a density of 2 x 10^4 cells/filter, were seeded and cultured in 12-well Corning® culture plates with Sarstedt TC-inserts and incubated at 37°C and 5% CO_2. The media was changed every 2-3 days until the TEER measurement reached around 55 Ω.cm^2. This indicated the cells were ready for permeation studies, and this was usually around day 28-30, which corresponds with previous literature [210]. For permeation studies, a total of 0.8 mL of HBSS with 25 mM HEPES, with or without drug/formulation, was added to the apical membrane and the inserts were then placed on the wells containing 1.2 mL of buffer in each well (basolateral side). Samples (200 µL) were collected from the basal side, and replaced with new buffer, at 30 minutes, 1 hour, 2 hours, 4 hours and 6 hours [the loss taken into consideration in the permeability calculations (Equation 5.4)]. Studies were carried out as five replicates for the formulations, and three replicates for the controls. The amount of insulin loaded transfersomes was 8mg in 0.8ml, with insulin LC (%, SD) of 1.48 ± 0.15 [D5E (total insulin 0.117 mg)] and 1.12 ± 0.09 [S5E (total insulin 0.090 mg)]. The concentration of the controls was as follows: atenolol (0.125 mg/mL), dextran (0.125 mg/mL) and insulin (0.1125 mg/mL). Also, controls with no cells and with cells only were present throughout the experiment.

Equation 5.4

$$Mt = Vr \times Ct + Vs \times \Sigma(Ct)$$

Where

M_t = mass of insulin permeated at each time interval

V_r = volume in the receptor compartment (basolateral side)

Ct = concentration of insulin at each time interval

Vs = sample volume

$\Sigma(Ct)$ = cumulative insulin concentration at each time interval

The permeability parameters; steady-state flux (Js), permeability coefficient (Kp), and enhancement ratio (ER) were calculated from the linear part of the permeation curve [214]. They were calculated using Equation 5.5, Equation 5.6, Equation 5.7, respectively.

Equation 5.5

$$J_s = \frac{Q_t}{A.t} \ (\mu g.\,cm^{-2}.\,s^{-1})$$

Where Q_t is the total permeated drug, A is the cross-sectional diffusion area (cm^2), and t is the time of exposure (seconds, s).

Equation 5.6

$$K_p = \frac{J_s}{C_0} \ (cm.\,s^{-1})$$

Where C_0 is the initial donor concentration (µg.cm^{-3})

Equation 5.7

$$ER = \frac{K_p \ (insulin \ in \ test \ formulation)}{K_p \ (insulin \ control)}$$

5.4 Results and discussion

5.4.1 SRB cell toxicity assay
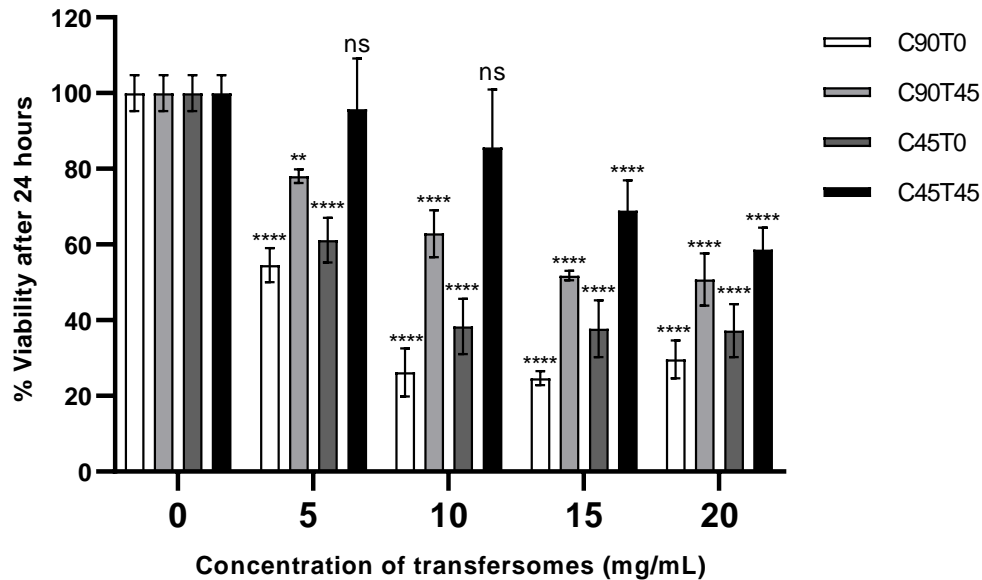
Figure 5.2: The influence of Tween 80 inclusion and cholesterol reduction on cell viability.

Notes: Results show sample mean ± SD (n=3). Two-way ANOVA showed significant difference (**** = $p < 0.0001$) between the sample means. Dunnett's multiple comparisons test showed significant reduction (**** = $p < 0.0001$) in % viability across all concentrations of the transfersomal formulations C90T0, C45T0 and C90T45 (except at 5 mg/mL, ** = $p < 0.01$) compared to the control (0, cells only no formulation). No significant difference (ns = $p > 0.05$) was observed with C45T45 at concentrations of 5 mg/mL and 10 mg/mL, but significant reduction (**** = $p < 0.0001$) was observed at concentrations of 15 mg/mL and 20 mg/mL.

The concentration of transfersomal formulations chosen for the study was based on preliminary studies, as well as the calculation of the amount of insulin contained, which would be necessary to have a reasonable therapeutic effect. Thus, the higher the concentration of transfersome that is safe and non-toxic to cells, the higher the amount of insulin that is available for permeability studies, and to exert medicinal effect if the product is successful. The results in Figure 5.2 show the level of toxicity is generally C45T45 < C90T45 < C45T0 and C90T0 across all concentrations, although there is less variation between C45T0 and C90T0. Thus, the results demonstrate the presence

of Tween 80 has some protective effect on the cell viability, which may not be surprising as Tween 80 is sometimes used as a stabilising agent for proteins in *in vivo* studies [215]. This result is also supported by another study, which found Tween 80 was safer at much higher concentrations on human fibroblast cultures, compared to the other surfactants tested [216]. This observation may explain why Tween 80 is one of the most extensively used surfactants in parenteral protein formulations [178]. As expected, similar to other studies on surfactants, all the formulations demonstrated concentration-dependent cell toxicity, particularly for C45T45, which is insignificantly different to the viability of the control (cells only) at 5 mg/mL and 10 mg/mL. Still, at the higher concentrations, the viability is significantly lower than the control [217]. Thus, this shows the presence of Tween 80 will be useful in the formulation, but further studies need to be carried out to investigate variation.
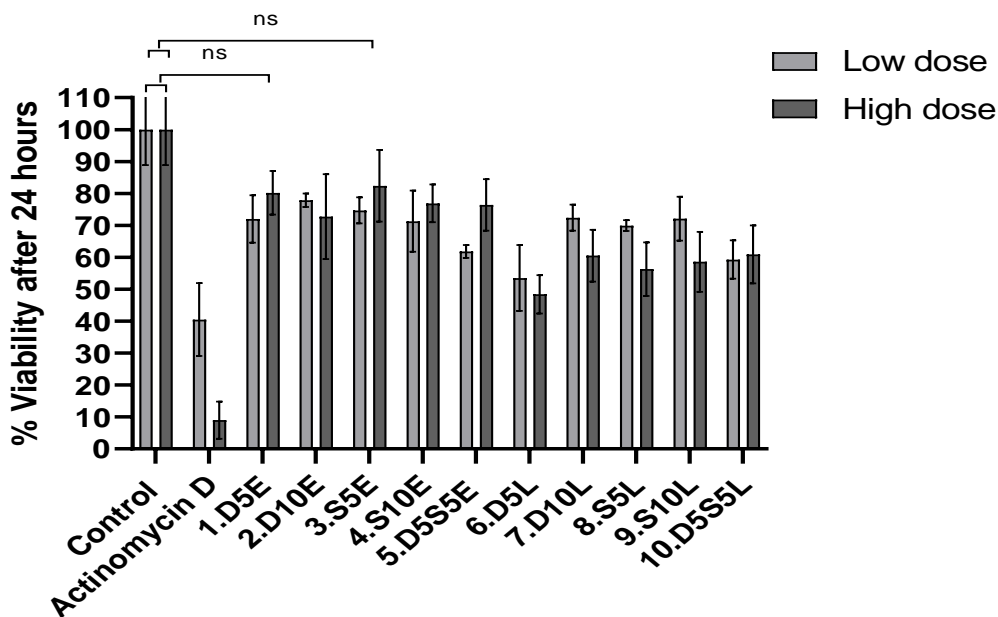
Figure 5.3: % Viability of TR146 cells after 24-hour exposure to two concentrations of the positive control and the test transfersomes.

Notes: Results represent mean ± S.D. (n = 3). Note that control [(cells only) low & high represents 100%]. Two-way ANOVA analysis showed insignificant difference ($p > 0.05$) between the low and high dose of formulations but showed significant difference (**** = $P < 0.0001$) between the means of the formulations and the positive control actinomycin D (low 0.1 µg/mL & high 2.5 µg/mL). Dunnett's multiple comparisons test comparing formulations 1-10 (low 5 mg/mL & high 10 mg/mL) compared to the control all showed significant difference (* = $p < 0.05$) except formulation D5E and S5E (highlighted as ns = $p > 0.05$).

The *in vitro* cell viability of the ten insulin loaded transfersomes was tested at two different concentrations (5 and 10 mg/mL) on TR146 buccal cells, and Figure 5.3, represents the results. When carrying out cytotoxicity assays, if a tested compound decreases the viability of the cells to less than 70% of the control group, which is set as 100% (the cells in the presence of culture medium alone), then the compound has the cytotoxic potential [218]. Actinomycin D, a potent inducer of cell apoptosis, was used as a positive control, as it has been found to block the transcription of all RNA synthesis at doses greater than 1 µg/mL [219], [220]. Looking at the results for actinomycin D, the SRB study can demonstrate concentration-dependent cytotoxicity.

2-way ANOVA analysis of the results for both the low (0.1 µg/mL) and high (2.5 µg/mL) actinomycin D dose resulted in significant ($P < 0.0001$) reduction in cell viability compared to the control and much lower viability than 70%. Only two formulations, D5E and S5E, at the higher concentrations, were found to have % viability not significantly different from the control (cells only) and above 70% viability. Looking at Figure 5.3 it can be observed that the formulations containing DPPE (both at 5 mg/mL and 10 mg/mL) are mainly around 70% while the results for Lecithin are approximately 60%. To confirm these observations, the mean average and SD of the results of DPPE and lecithin were calculated and found to be 74.6 ± 3.7 (n = 30) and 61.2 ± 2.7 (n = 30) respectively. This suggests the use of DPPE could be a safer to use as a phospholipid in these formulations compared to lecithin. Although the composition of these transfersomes differ, in a study looking at elastic bilosomes, SGDC, (15% w/w) in combination with soy lecithin (85% w/w), was found to be safe to use at a concentration of 1.25 mg/mL based on the *in vitro* viability studies [60]. In comparison to this study, the mass of SGDC in the 5 mg/mL is comparable to the 1.25 mg/mL, and the 10 mg/mL concentration is relative to the 2.5 mg/mL. The lecithin formulation used with the same amounts of SGDC in our study showed significant toxicity ($p < 0.001$) at both concentrations; however, the presence of the other ingredients (Span 60, Tween 80 and cholesterol) must be taken into consideration. Additionally, not all lecithin has the same composition and ratios of the different types of phospholipids, which may also influence the formulation [221]. On the other hand, with DPPE at the higher concentration, the difference between the control and formulation S5E was found not to be significant ($P \geq 0.5$), and separate comparison of the low and high dose also showed insignificance. These results led to the transfersomal formulations, D5E and S5E, being carried forward for permeability studies.

5.4.2 CytoSMART live cell imaging
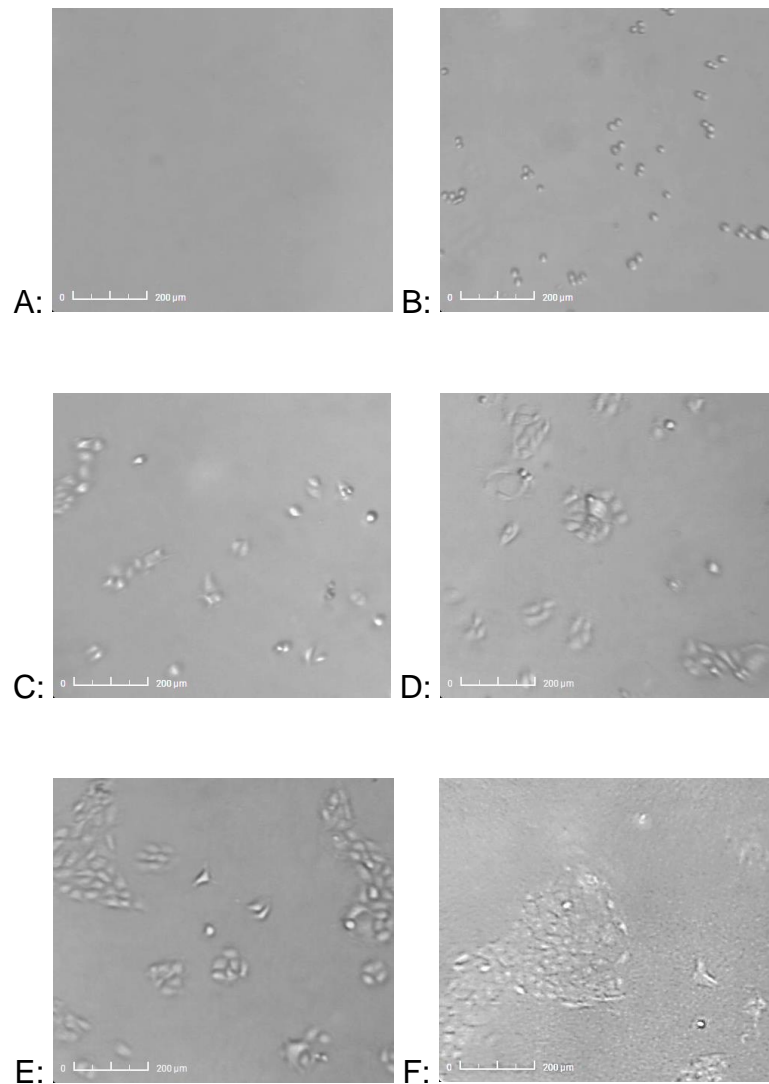
Figure 5.4: CytoSMART images showing the growth of TR146 cells over 42 hours.

Notes: (A) Blank no cells; (B) cells just added; (C) 6 hours growth; (D) 12 hours growth; (E) 18 hours growth; and (F) 42 hours growth.
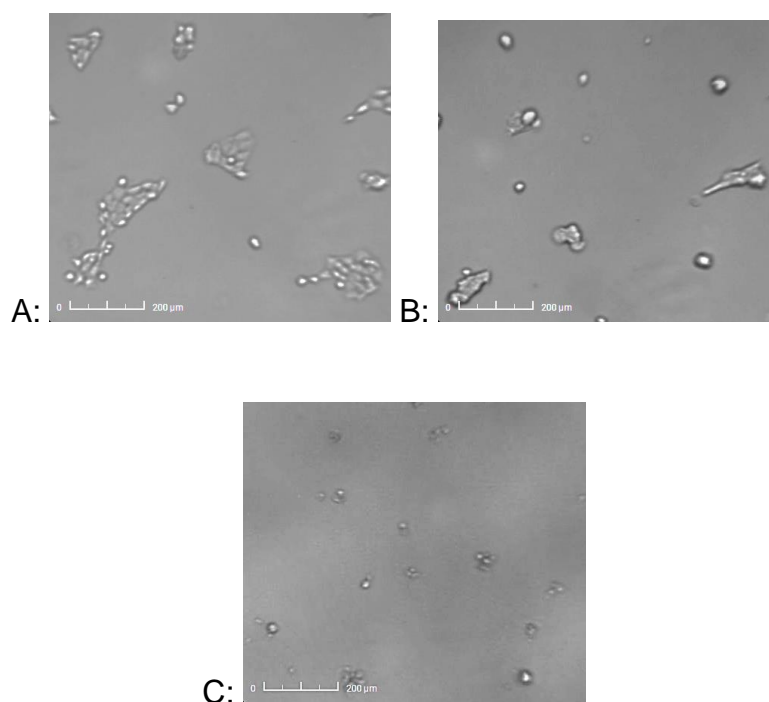
Figure 5.5: CytoSMART images showing the effect of actinomycin D (2.5 µg/mL) on TR146 cells over 24 hours.

Notes: (A) After 18 hours of cell growth Initial addition of actinomycin D (AD); (B) 1 hour after AD addition; and (C) 24 hours after AD addition.

It can be seen from Figure 5.4 initially the cells are free in solution then slowly they are adhering to the bottom of the well and multiplying, and at 18 hours they are mainly adherent. After 42 hours it can be observed they have contentedly increased in numbers. After 18 hours of growth, the formulations, and the positive control actinomycin D is added to the wells. Figure 5.5 shows the effect of the presence of the positive control, which is a potent inducer of cell apoptosis [219]. As soon as it is added the cells start to shrink (A) and just after 1 hour there is a clear difference in morphology, and the cells appear to detach from the bottom of the wells. After 24 hours, the cells look almost wholly diminished and dead. This is supported with the SRB viability assay, which indicated at this concentration the cell viability to be 9 ± 5.8% after 24 hours.
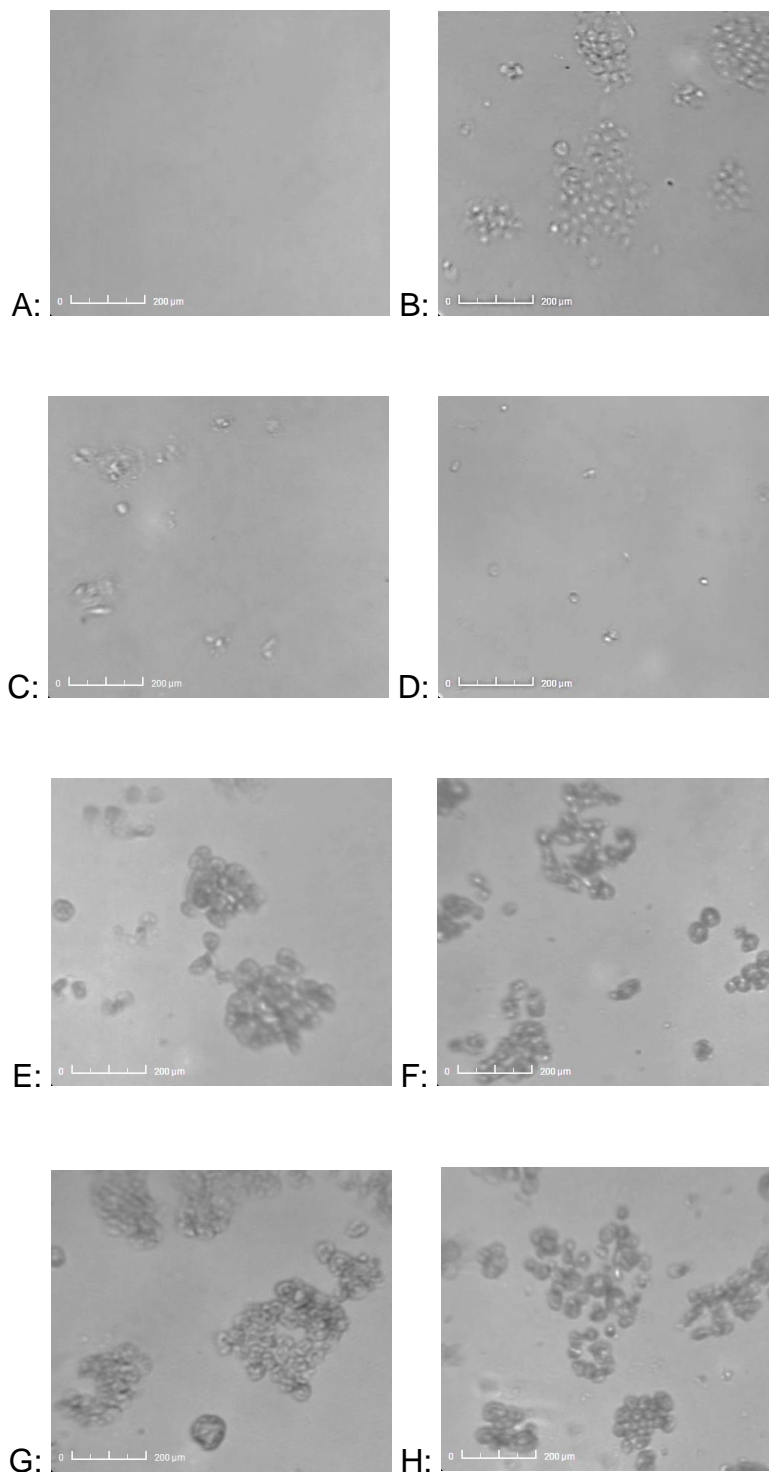
Figure 5.6: CytoSMART images of TR146 cells following removal of formulations and replacement of media after 24 hours.

Notes: (A) Control no cells; (B) Control cells only; (C) Actinomycin D 0.1 µg/mL); (D) Actinomycin D 2.5 µg/mL; (E) D5E 5 mg/mL; (F) D5E 10 mg/mL; (G) S5E 5 mg/mL; and (H) S5E 10 mg/mL.

After 18 hours of cell attachment and growth, the positive control and the transfersomal formulations were added to the wells for monitoring of their effect on cell viability and morphology. Figure 5.6 represents the cells, washed, and media replaced, after 24-hour exposure of the cells to the transfersomal formulations and the positive control. Looking at Figure 5.6, it can be seen, there is a clear difference, in the number and morphology of the cells, between the cells exposed to the positive control compared to the formulations D5E and S5E at both low and high concentrations. At both concentrations of actinomycin D it can be observed that there are very few cells left, which is expected at small doses (<0.1 g/mL) it causes preferential inhibition of ribosomal RNA synthesis while at doses greater than 1 µg/mL it causes blockage of transcription of all RNA species [219], [220], [222]. The images of the cells after exposure to D5E and S5E are more pronounced and bolder compared to the cells only control, but this may be due to incomplete washing of the cells or some formulation trapped between cells. It can be noticed, however, that cells have more significant space or are not as tightly clustered in the cells exposed to the transfersomes compared to the control. This supports the results from the TEER studies, which suggested that the transfersomes affected the integrity of the cells.

5.4.3 TEER measurement across TR146 cells

To confirm the integrity of the TR146 cells, before and after permeation studies, TEER measurements were carried out. These results are similar to the initial TEER values seen in the study on elastic bilosomes [60]. TR146 cells generally have lower TEER measurements, compared to intestinal cell lines such as Caco-2 (~260 $\Omega.cm^2$). This is possibly due to the lack of tight junctions in these cells, which is reflective of their absence in the normal human buccal epithelium [211]. No significant difference was seen in the TEER measurements between the controls, but the two tested formulations did result in significantly lower TEER values, which are displayed in Table 5.3 below. This indicates that the formulations have some effect on the integrity of the TR146 cells, which could be related to the extraction of intercellular lipids by the transfersomes, as this is a possible mechanism by which these molecules act as penetration enhancers in the buccal mucosa [223].

Table 5.3: TEER measurements across TR146 cells before and after permeability studies.

Treatment	Before permeability studies TEER ($\Omega.cm^2$)	After permeability studies TEER ($\Omega.cm^2$)
Control	55.7 ± 2.3	53.2 ± 5.5
Insulin only	56.5 ± 4.4	52.8 ± 2.2
D5E	55.4 ± 3.5	45.8 ± 2.8*
S5E	56.1 ± 3.8	42.2 ± 2.8**

Notes: Control (cells only) and results represent mean ± S.D., (n = 3).

5.4.4 *In vitro* permeation studies

Table 5.4: Permeation parameters calculated from *in vitro* permeation of TR146 cells.

Drug	J_s (µg.cm^{-2}.s^{-1}) x 10^{-4}	K_p (cm.s^{-1}) x 10^{-6}	ER insulin
FITC-Dextran	3.22 ± 0.09 ****	2.57 ± 0.07****	NA
Atenolol	7.78 ± 0.59	6.22 ± 0.47	NA
Insulin	7.03 ± 0.59	6.25 ± 0.52	1.00
Insulin in D5E	4.99 ± 1.04**	3.38 ± 0.70****	0.54
Insulin in S5E	3.35 ± 1.22****	2.98 ± 0.11****	0.48

Notes: Results represent mean ± S.D., (n = 3 for control insulin, dextran and atenolol and n = 5 for insulin from D5E & S5E). ** $p < 0.01$ versus control insulin & **** $p < 0.0001$ versus control insulin.
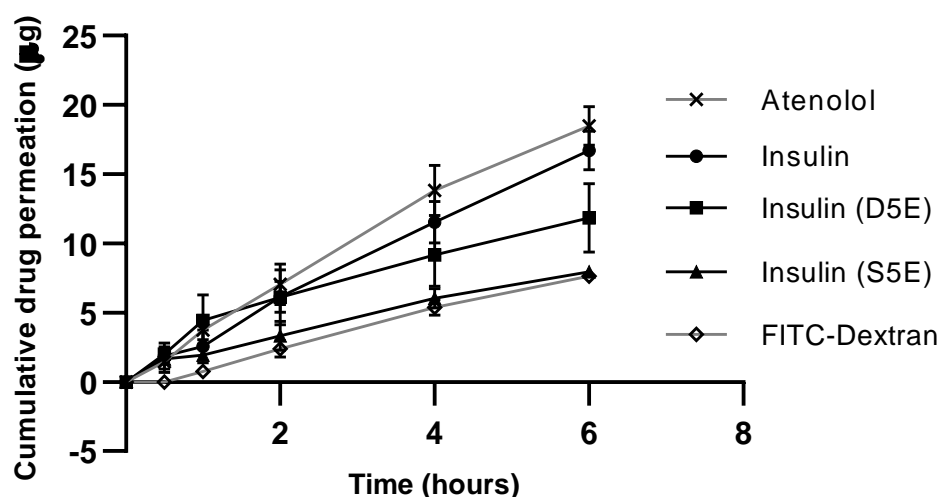
Figure 5.7: Cumulative drug permeation (µg) of atenolol, insulin (control), insulin (D5E), insulin (S5E) and FITC-Dextran across TR146 cell layer.

Notes: Results represent mean ± S.D., (n = 3 for insulin control, atenolol and FITC-Dextran) and [n = 5 for insulin (D5E) and insulin (S5E)].

The cumulative permeation profile (µg) of the controls (insulin, atenolol and FITC-dextran) and the insulin-containing transfersomes, across the TR146 cell layers, were calculated against each time point and is displayed in Figure 5.7. The capacity for the

controls and insulin from the test transfersomal formulations to traverse the TR146 cell layers over six hours was evaluated by calculation of the steady-state flux (J_s) and the permeability coefficient (K_p) (Table 5.4). The enhancement ratio for the tested transfersomes versus the control insulin was also calculated and is shown in Table 5.4 above. Atenolol was used as a control as it is a small hydrophilic drug, with molecular weight (Mw) of 266 Da, and it has been previously tested for permeability across the TR146 cells. FITC-Dextran was used as a second control as it is a large (Mw 20,000 Da) hydrophilic molecule, compared to insulin (Mw 5808 Da) [98]. In a previous study looking at the permeation of FITC-Dextran molecules weighing from 4,000 to 40,000 Da, it was demonstrated that the K_p decreased linearly with increasing Mw [212]. Hence the prediction was that the atenolol would achieve the highest K_p, as small hydrophilic molecules (Mw ≤ 300 Da) can traverse the cell layers via passive paracellular diffusion, then insulin and finally FITC-Dextran [224]. As expected, the results in Table 5.4, shows FITC-Dextran attained significantly ($p < 0.0001$) lower K_p than both insulin and atenolol. But surprisingly insulin and atenolol both achieved high K_p with no significant difference between the two.

In another study, the apparent permeability coefficient of atenolol was found to be 2.2 x 10^{-6}. Still, this lower result is possibly related to the higher initial TEER of the cells (247 ± 70 $\Omega.cm^2$) compared to TEER of ~ 55 $\Omega.cm^2$ in this study [225]. Again, this difference in TEER may also explain the high permeability of the control insulin as reduced integrity may allow for the greater crossing of bigger molecules. Another possible explanation is that a study looking at the mechanism and route of insulin permeation, involving the use of FITC-insulin and confocal microscopy, observed that insulin could traverse TR146 cell layers via both passive and active transport [226].

Hence possible use of the combined route could have led to the greater permeability of insulin, but further investigations of this potential are required. Looking at the ER of the two test transfersomes (D5E and S5E), and the drug permeation profile, neither managed to enhance the permeability of insulin compared to the control within the 6 hours of the study. This could be for the reason that during epicutaneous application the penetration is suggested to occur as a result of the difference in osmotic gradient between the surface of the skin and the intercellular lipids but using the TR146 cell model the cells have to be maintained hydrated with HBSS. Thus, the hydration gradient is absent, and this would be similar to applying drug-containing transfersomes under occlusion, which has been shown to disable these ultradeformable carriers by removing the main driving force in crossing membranes [177]. Thus, the primary mechanism of permeation across the TR146 cells, in this study, is possibly permeation via fusion of the transfersomes with the buccal membrane [227], [228]. Additionally, the hydration of cells could loosen the interstices, which could result in the accumulation of insulin within the cell layers and thus prolong its permeation across the cells [228]. In another study, the presence of SGDC, with lecithin, managed to achieve an ER of 5.24 [60]. But in this study in combination with DPPE, cholesterol, Tween 80, and Span 60, it was unable to perform as well. This may also be due to the difference in particle size as SGDC with lecithin is around 146 nm while S5E is approximately 267 nm; hence the larger particle size can reduce the permeability capability.

5.5 Conclusion

Although the results for permeability are not as hoped, the results may not represent the *in vivo* condition, and either of the formulations (D5E or S5E) may still be capable

of enhancing the permeability of insulin *in vivo*. Particularly as SGDC is a dihydroxy bile salt, and there are indications that it may have the ability to reduce degradation of proteins/peptides through inhibitory effects on peptidases on the buccal membrane [64]. The reduction in TEER values, and the CytoSMART images of the cells exposed to the formulations, indicate application *in vivo*, can result in some tissue damage, but this usually is reversible in the buccal mucosa and may not be as significant compared to other mucosa in the body [60]. Additionally, a decrease in formulation concentration, maybe the solution to the disturbance of tissue integrity as in previous literature [60]. Also, further investigations are required to examine the exact permeation pathway of both insulin and the transfersomes. As being deformable, and the integrity of the cells disturbed, it may be possible for the transfersomes to have crossed the cell layers intact without releasing insulin. Additionally, it is feasible that the transfersomes may have entered the buccal cells and remained within the cells if entry was via the transcellular pathway, and thus resulting in low permeation.

These studies demonstrated SRB toxicity assays to be a reliable study with TR146 buccal cells, and actinomycin D was found to be an excellent concentration-dependent positive control. These to my knowledge have not been investigated with TR146 buccal cells previously. CytoSMART is also a relatively novel imaging technique, which has not been used in this manner but again exhibited suitability for the purpose.

6. Formulation and characterisation of a mucoadhesive buccal patch

6.1 Introduction

The rationale for designing a mucoadhesive buccal patch was to provide a carrier as well as greater contact time for the drug at the site of absorption and permeation. Freeze-drying was chosen as the drying method as both insulin and lipid vesicles can have stability issues, such as the formation of aggregates and sometimes drug leakage [229]. Although a cryoprotectant is needed to minimise such drawbacks in the formulation. A study found the addition of sorbitol to the formulation was able to offer proper protection for preventing structural changes to insulin during freeze-drying and increased stability overall in the tested storage conditions [39].

As reviewed by Shaikh et al. (2011), the most common technique for assessing bioadhesion is using tensile strength method [114]. Several studies have been carried out using texture analysers to measure the force necessary to detach bioadhesive films from excised tissue *in vitro* to assess bioadhesion [230], [231].

Ethylcellulose is a polymer that is often used for the production of impermeable backing layers for patches [232], [233]. This is because it is a water-insoluble polymer that is biocompatible and non-allergenic [234]. It also has an excellent safety profile as it is FDA approved and a GRAS ingredient [234]. It is particularly favourable for buccal delivery as it is both tasteless and odourless. It is soluble in a variety of organic solvents, such as ethanol and chloroform, and is stable across a wide range of acidic and alkaline environments (pH 3-11).
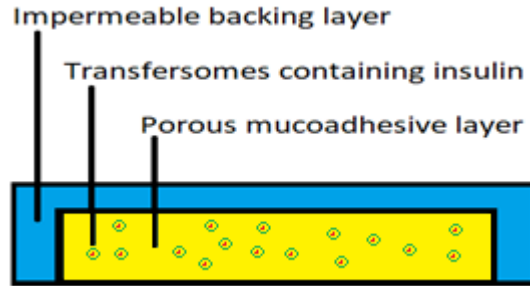
Figure 6.1: Schematic representation of the double-layered patch consisting of a mucoadhesive layer (with transfersomes) and an impermeable backing layer.

In this chapter, the overall goal was to evaluate the appearance as well as mucoadhesive properties of several polymers, plus a cryoprotectant, after freeze-drying, for a buccal patch formulation for the incorporation of insulin-containing transfersomes (Figure 6.1).

6.2 Chapter aims

- Selection and optimisation of cryoprotectant (sorbitol or trehalose).

- Use of factorial design for the preparation and evaluation of experimental factors.

- Maximisation of mucoadhesiveness of freeze-dried patches in the presence of the cryoprotectant.

- Optimisation of polymers to produce compact, flexible and aesthetically appealing lyophilised patches.

- Embed the final transfersomes in the optimised patches and analyse physicochemical properties using DSC and XRD.

- Combine mucoadhesive layer with impermeable backing layer and carry out insulin release studies of the final patches with transfersomes embedded.

6.3 Materials and methods

6.3.1 Materials

Sodium alginate (12,000-40,000 Da), low molecular weight chitosan (50,000-190,000 Da), hydroxypropyl methylcellulose (HPMC, viscosity 40-60 cp, 2% in H_2O), D-sorbitol (≥ 98%), glycerol (≥ 99%), trehalose, ethylcellulose, cyanoacrylate adhesive (medium viscosity), RHI (27.5 IU/mg), sorbitan monostearate (Span 60), cholesterol (C8667), DCP, polysorbate 80 (Tween 80), SGDC, and PBS (pH 7.4) were all purchased from Sigma-Aldrich (Merck KGaA, Darmstadt, Germany). 1,2-dipalmitoyl-3-sn-phosphatidylethanolamine (DPPE) was purchased from Tokyo Chemical Industry (UK). HPLC grade ACN, TFA (99+%) and Silicagel orange (ACROS Organics™) were purchased from Fischer Scientific (Leicestershire, UK). Porcine buccal tissue was obtained from Jennings C D & Sons (Surbiton, UK). MilliQ® water was obtained internally using a Merck Millipore Direct-Q® 3UV water purification system (Billerica, MA, USA). All other chemicals and reagents used were of analytical grade.

6.3.2 Minitab experimental design

The development and evaluation of pharmaceutical formulations have traditionally been through monitoring the effects of one variable at a time, which can be time-consuming [235]. Additionally, this strategy can exclude observations of combined effects of ingredients, particularly in complex formulations with multiple ingredients such as patches. To study the influence of several polymers (HPMC, sodium alginate and Low MW chitosan), the cryoprotectant sorbitol, and the plasticiser PEG 400 on mucoadhesion Minitab design of experiment (DOE) was used. For all the experiments, general full factorial designs were created with either 2 or 3 factors and levels varying

from 2-4 levels for each factor. These designs are shown in the appropriate discussion sections (Figure 6.5, Figure 6.9 and Figure 6.11). All were completed in triplicates with randomised runs.

6.3.3 Method of patch preparation

The method was adapted from previous literature [110]. The correct amount of constituents (chitosan, sodium alginate, HPMC, sorbitol, trehalose and sometimes PEG 400) as suggested by the DOE, were dissolved in water (or 1% acetic acid for chitosan containing mixtures) in a glass vial or beaker under magnetic stirring. Once all the constituents were dissolved aliquots of 2 mL of each formulation transferred to the allocated wells of a 12-well plate. To produce transfersome/insulin-containing patches, these were added and gently mixed with the polymer solution prior to well transfer. Once all wells were settled and bubble-free, the lid was placed back on the plates and transferred to a -20°C freezer; to enable the samples to freeze slowly overnight (minimum 18 hours). Subsequently, the lids of the plates were removed, the plates wrapped in a layer of cling film, and one hole pierced above each well. Next, samples were moved to a BenchTop Pro with Omnitronic freeze dryer (SP Scientific, SP industries Inc, Missouri, USA). To ensure complete drying, the freeze-drying process was carried out for 48 hours. The sample was then ready for studies, and any unused patches were placed in the -20°C freezer for storage. Experiments were typically completed within three days of patch production.

6.3.4 Preparation with a backing layer

The backing layer was produced by dissolving ethyl cellulose (5% w/v), under magnetic stirring, in a solution of glycerol (10% v/v) in ethanol. 1.5 mL of this solution was

transferred to each well of a 12-well plate solution and left overnight in a fume hood to dry. Once dry, the backing layer was attached to the freeze-dried mucoadhesive layer, by applying a thin coating of cyanoacrylate adhesive between the two layers.

6.3.5 Stability studies of buccal patches

During studies, it was observed that the patches were hygroscopic. Hence the final formulations of patches with or without insulin/transfersomes were stored both in a desiccator and the freezer for two months (2mo) to see if there was any changes in the amorphous crystalline structure of the patches during storage using XRD studies. Samples in the desiccator were stored in the presence of silica gel orange.

6.3.6 *Ex vivo* testing of mucoadhesion

The formed patches were tested for mucoadhesiveness using a TA.XT Plus Texture Analyser (Stable Micro Systems, Surrey, UK). The Exponent software was used for data collection as well as setting up and running the experimental method (Stable Micro Systems, Surrey, UK). A technique in literature was adapted and optimised to test the patches with the aim of drug delivery via the buccal mucosa [236]. The method was set up with the following parameters: pre-test speed 0.5 mm/s, test speed 0.5 mm/s, post-test speed 10mm/s, applied force of 20 g (or 0.196 N), return distance of 15 mm, a contact time of 60 s, trigger force of 5 g (or 0.049 N) with trigger type being set as auto. The patches were cut to size (10 mm x 10 mm) and attached to a cylindrical probe (P/10, 10 mm in diameter) using double-sided adhesive tape. The probe, with a patch attached, was then tested for mucoadhesiveness by slowly approaching the porcine buccal mucosa or solidified gelatine (6.5% w/v) (both thinly wetted with PBS)

maintaining contact (60 s) and detaching (Figure 6.2). On completion of each run, the

key result generated by the software was the peak force (adhesiveness, N).
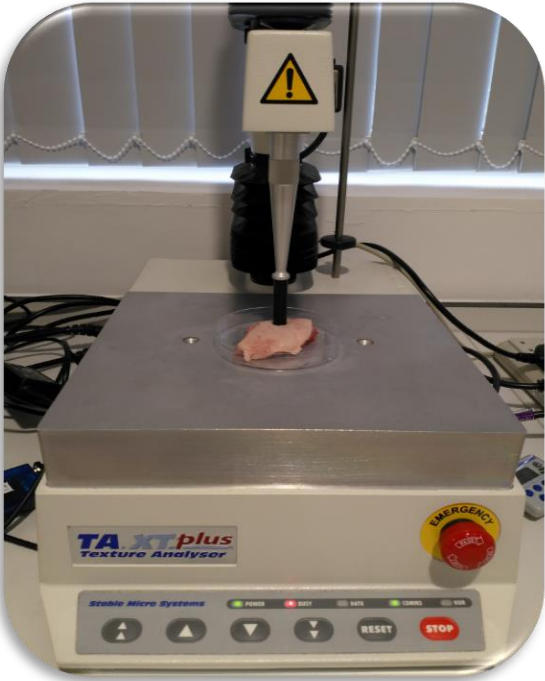
a.

b.
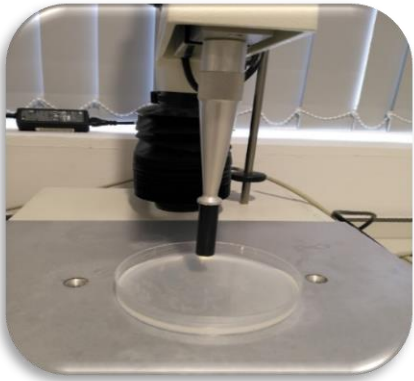
c.

Figure 6.2: Testing mucoadhesiveness on porcine buccal mucosa using a TA.XT Plus Texture Analyser (a & b). Testing mucoadhesiveness on solidified gelatine (c).

6.3.7 *In vitro* release studies
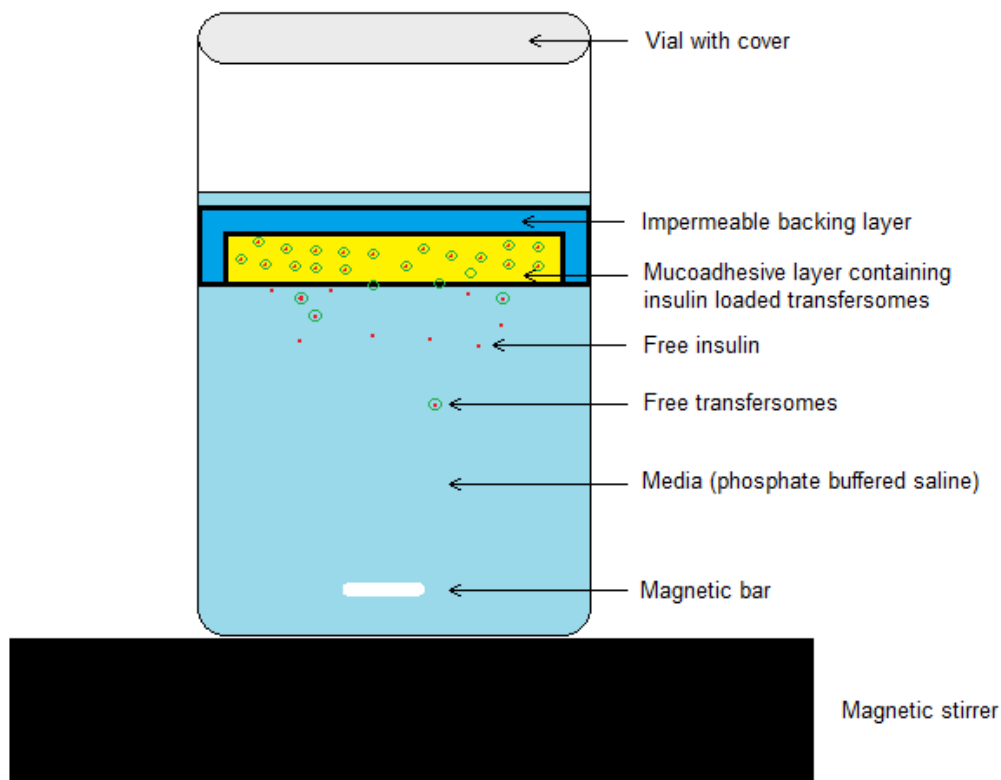
Figure 6.3: Schematic illustration of the release of insulin in release studies from the insulin containing transfersomes in the double-layered mucoadhesive patch.

Method adapted from previous literature [110]. The release of insulin from the patches was carried out in 4 mL of PBS (pH 7.4) at 23°C, over 6 hours. The patches were placed at the surface of the liquid with the mucoadhesive layer submerged in the PBS (shown in Figure 6.3). At each time point (0.5, 1, 2, 4, and 6 hours) samples of 0.8 mL was transferred to allocated 1.5 mL Eppendorf tubes and replaced with fresh 0.8 mL of PBS [this loss was taken into account in the release profile calculations (Equation 4.1)]. The samples were then centrifuged at 13.3 rpm for 30 minutes at 4°C using a Micro Star 17R centrifuge (VWR international, Leicestershire, UK). The supernatant was then analysed for insulin content using HPLC (see chapter 2). As suggested in the method, the release was carried out at 23°C instead of 37°C to reduce the occurrence

of insulin self-aggregation [110], [237]. The release studies were performed on the final patches S and C, detailed in Table 6.1. The release study included control patches containing insulin (0.36 mg/patch), transfersomes D5E (total insulin 0.467 mg in 4mL) and S5E (total insulin 0.353 mg in 4 mL), detailed in Table 6.2.

6.3.8 Thickness, surface pH and swelling studies

The thickness of the patches (3.5 cm^2) was measured using a digital calliper, by measuring at the centre point. The wetted surface pH was tested using colour-fixed pH indicator sticks (pH 4.5-10, Fisherbrand, Fisher Scientific, Leicestershire, UK). Six samples of each were measured. Swelling studies were attempted, according to previous literature; however, the patches could not be weighed accurately as upon wetting they patches disintegrated [110].

6.3.9 Morphology of patches

The morphological examination of the patches was carried out using a ZEISS EVO 50 tungsten source scanning electron microscopy (SEM, Germany). Samples were prepared on specimen stubs and coated with gold/palladium under vacuum with a Polaron SC7640 sputter coater (Quorum Technologies LTD, Kent, UK) before being imaged.

6.3.10 X-ray diffraction analysis

X-ray diffraction (XRD) was carried out using a Bruker-AXS diffractometer (model D8, Bruker AXS GmbH, Karlsruhe, Germany). The x-ray wavelength was set up as 0.1542 nm (or 1.542 Angstrom). The samples (~0.5 g) were scanned between the ranges of 5°-50° (2θ), with increments of 0.1° at step time of 2 seconds (Temp 20°C).

6.3.11 Thermal analysis

Thermal analysis was recorded using differential scanning calorimetry (DSC, Mettler Toledo DSC822^e, Mettler-Toledo Ltd, Leicester, UK). 3-5 mg of the freeze-dried patches or raw powdered ingredients were weighed and transferred to 40 µL aluminium pans. The pan was then sealed with an aluminium lid, which was subsequently pierced to produce a tiny hole on the lid. The sample pan and the empty aluminium reference pan were placed in the instrument and the method initiated. The method consisted of 10 °C per minute heating rate over the range of 25-350 °C. The thermograms were analysed using the software STAR^{e}SW 10.
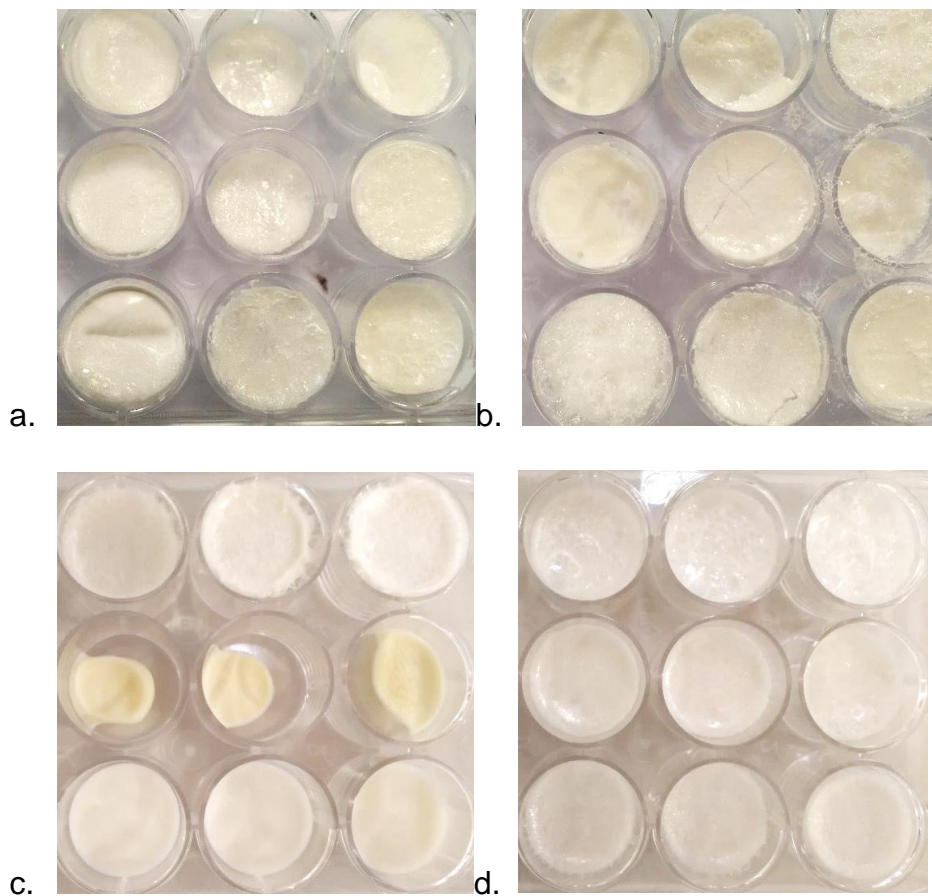
Figure 6.4: Images of freeze-dried patches produced using HPMC (0.5% w/v) with different ratios of cryoprotectant and polymer [row 1 cryoprotectant (3% w/v) and polymer (0.5% w/v), row 2 cryoprotectant (1% w/v) and polymer (1% w/v), and row 3 cryoprotectant (3% w/v) and polymer (1% w/v)]. (a) Trehalose and Chitosan and (b) Trehalose and Sodium alginate (c) Sorbitol and Chitosan and (d) Sorbitol and Sodium alginate.

One of the preliminary steps in the choice of polymers was to freeze-dry several combinations of polymers (HPMC, chitosan and sodium alginate) with different ratios of either sorbitol or trehalose as a cryoprotectant, and examine the patches in terms of appearance, uniformity of appearance, softness and rigidity. In the patches that contained only HPMC, with a cryoprotectant, the products showed signs of phase

separation as the final products formed two distinct layers with one layer being rigid and another layer that appeared as solid froth. This resulted in varied outcomes for mucoadhesiveness. Hence, HPMC was used in combination with other polymers to form patches. After many initial attempts with the two cryoprotectants, it can be seen from Figure 6.4, with the exception of row 2 (c), the patches containing sorbitol (c and d) have rows of patches that are generally more aesthetically appealing, more uniform, have a smooth surface, absence of fractured surfaces and appear typically more robust compared to the trehalose containing patches (a and b). Thus, sorbitol was chosen to be used for further studies.

6.5 Results and Discussion: Comparison of gelatine and porcine buccal mucosa in mucoadhesive experiments

Porcine buccal tissue is often used in studies to represent the human buccal mucosa [238], [239]. However, the surface of porcine buccal mucosa, shown in [(b) Figure 6.2], is not entirely smooth and can vary slightly depending on the different regions and also between different batches. To confirm the use and reliability of the porcine buccal mucosa, the same factorial design (Figure 6.5) was repeated but using solidified gelatine in a petri dish [(c) Figure 6.2] to mimic the mucosa and provides a repetitive smooth surface. The mucoadhesive strength of the formulations was measured and compared mainly using the maximum force required for detachment of the applied patch from the buccal mucosa or gelatine (labelled Peak Force (Adhesiveness, N) in the analysis), which provides an insight into the retention of the film in the buccal cavity [240].

Factor	Name	Type	Levels	Level Values			
A	Sorbitol	Numeric ▾	4	0	1	3	5
B	HPMC	Numeric ▾	3	0	0.5	1	
C	Chitosan	Numeric ▾	2	0.5	1		

Figure 6.5: Image showing the level and level values of a general factorial design used for the formation of mucoadhesive patches with sorbitol, HPMC and chitosan.
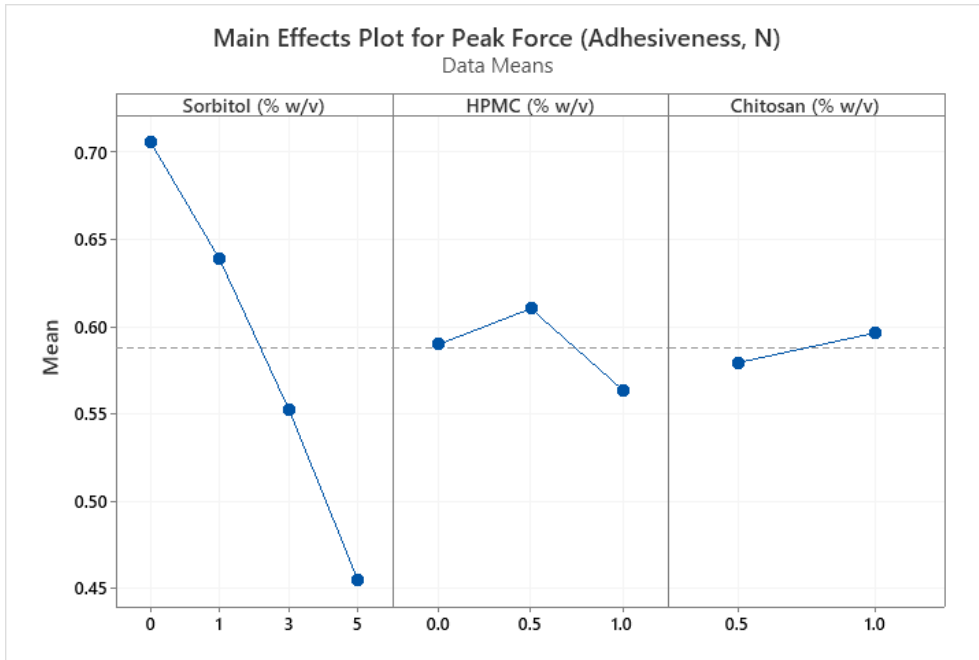
Figure 6.6 Main effect plot for peak force (adhesiveness, N) for LMW chitosan, HPMC and sorbitol tested on solidified gelatine (n= 3, Minitab).
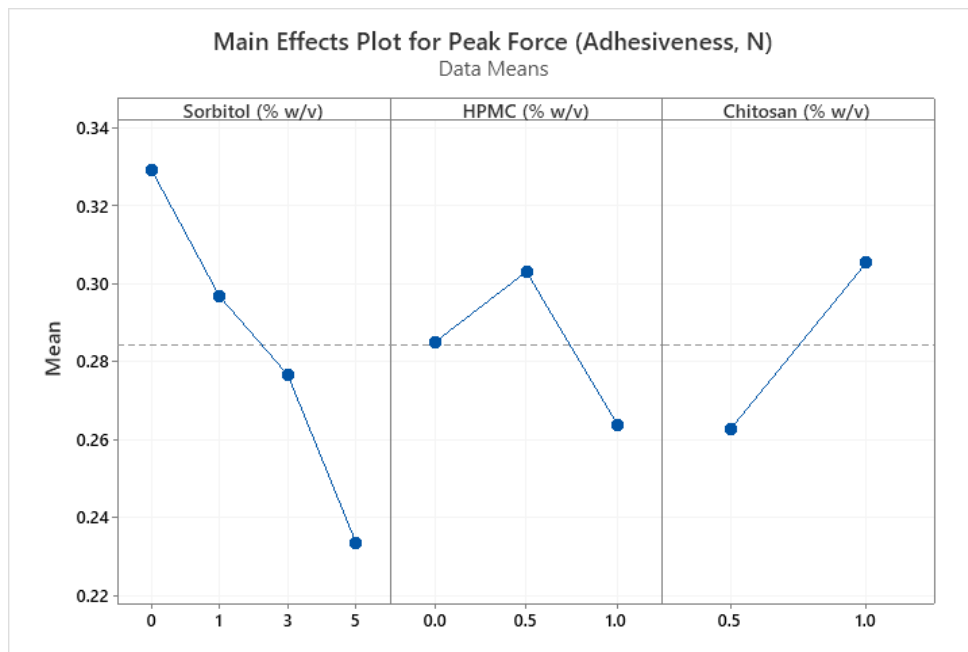
Figure 6.7: Main effect plot for peak force (adhesiveness, N) for LMW chitosan, HPMC and sorbitol tested on the porcine buccal mucosa (n= 3, Minitab).

It can be seen by comparison of both Figure 6.6 and Figure 6.7 that the trend in the results is very similar for both the porcine buccal mucosa and the solidified gelatine. Although the mean force is greater when using gelatine compared to porcine mucosa it is the overall trend comparison that is significant as it can be seen that although the porcine mucosa may not be entirely smooth and may vary slightly between batches, it does not affect the results in terms of testing mucoadhesiveness. Thus, it can be used as a reliable surface for testing of patch mucoadhesion.

As expected, an increase in the concentration of chitosan leads to an increase in the force of adhesion, possibly due to chitosan being cationic and hence at higher concentration results in greater electrostatic interactions with the anionic surfaces of the mucosa.

Remarkably, this was not the case with HPMC, as the optimum concentration appears to be 0.5% w/v. It can be observed from the results that the addition of HPMC greater than 0.5% w/v results in a decrease in mucoadhesion. A similar phenomenon was observed in another study working with chitosan and hydroxyethyl cellulose [241]. In this study, it was suggested increasing the concentration of hydroxyethyl cellulose, increased the elasticity of the film, which subsequently caused a reduction in the adhesive force between the porcine tissue.
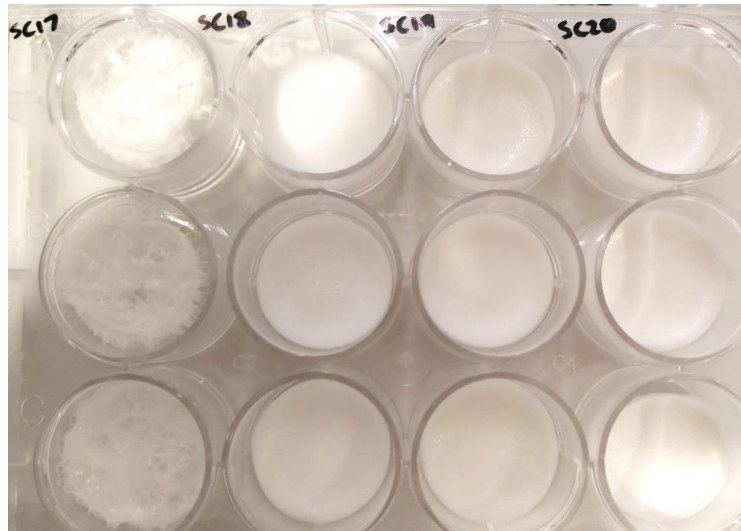
Figure 6.8: A sample 12-well plate containing the lyophilized patches of four different formulations of chitosan [column 1 (Sorbitol 5% w/v, HPMC 0% w/v & Chitosan 0.5% w/v), column 2 (Sorbitol 1% w/v, HPMC 1% w/v & chitosan 0.5% w/v), column 3 (Sorbitol 1% w/v, HPMC 1% w/v & chitosan 1% w/v) and column 4 (Sorbitol 3% w/v, HPMC 0.5% w/v & chitosan 1% w/v).

The results show an increase in sorbitol concentration leads to a decrease in the force of adhesion (Figure 6.6 and Figure 6.7). One reason for this occurrence is due to the increase in sorbitol concentration resulting in more significant interference with the mucoadhesive polymers, chitosan and HPMC, within the matrix. But in general, it was observed during the studies that patches that contained the higher concentrations of sorbitol (5% w/v) produced patches that were soft, porous, and fragile as can be seen in the first column of Figure 6.8. Whereas the lyophilized patches, containing low concentrations of sorbitol (0-1% w/v), formed the more robust, aesthetically appealing, and flexible patches that were easy to remove from the moulds (column 2-4). This outcome was possibly due to the hygroscopic nature of sorbitol, which at higher concentrations will initially incorporate more water molecules between the polymer matrix then once the water has evaporated there will be more air incorporated within the structure. It is known that an increase in porosity leads to lesser strength in

materials [240]. However, it was observed during the studies that the level of porosity and fragility because of the concentration of cryoprotectant differed depending on the type and ratios of the polymers used. Thus in further studies, the formulations were continually optimised in the polymer combinations (HPMC with either chitosan or sodium alginate) to accommodate higher concentrations of sorbitol, which will be a crucial ingredient for cryoprotection of insulin and the transfersomes within the patch in the final formulation [127].

6.6 Results and Discussion: Comparison of sodium alginate in the presence of different concentrations of sorbitol and HPMC

Factor	Name	Type	Levels	Level Values			
A	Sorbitol	Numeric ▼	4	0	1	5	10
B	HPMC	Numeric ▼	3	0.5	1	2	
C	S. alginate	Numeric ▼	3	0	1	2	

Figure 6.9: Image showing the level and level values of a general factorial design used for the formation of mucoadhesive patches with sorbitol, HPMC and sodium alginate.
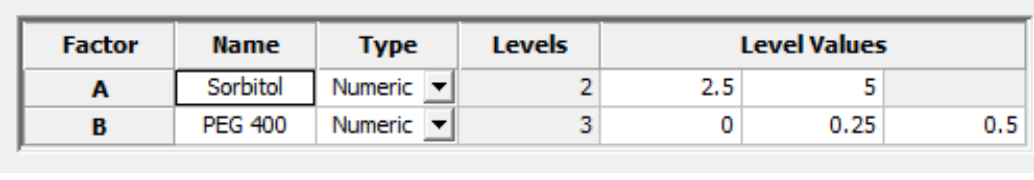
It was observed with chitosan that the presence of HPMC enhanced mucoadhesiveness of the patch at an optimum concentration of 0.5% w/v, but further increase resulted in a decline in mucoadhesiveness. Thus, to confirm whether or not the same effect would be observed with sodium alginate, a higher concentration of 2% w/v HPMC was also included in the factorial design (Figure 6.9).
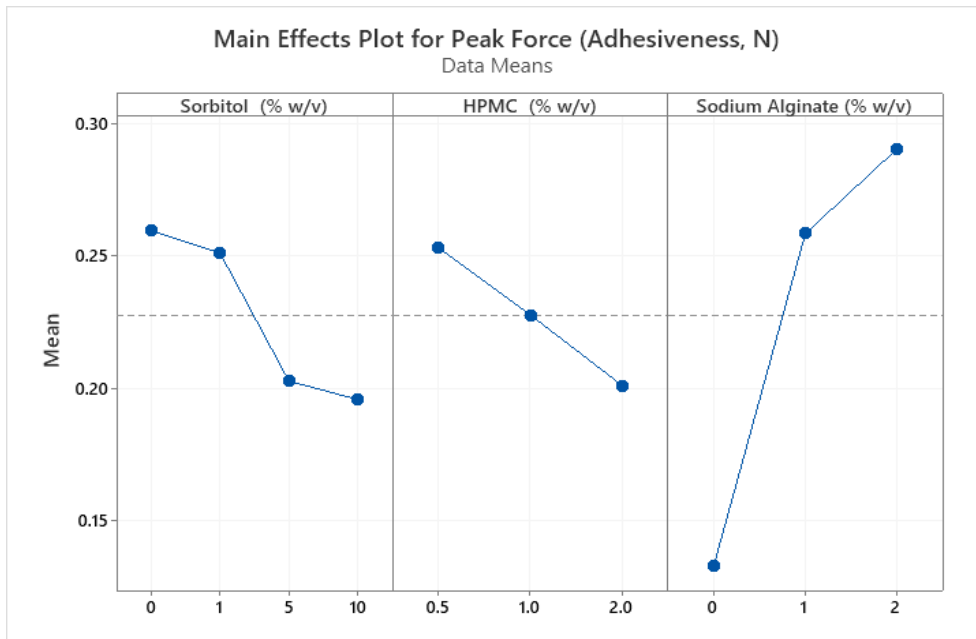
Figure 6.10: Main effect plot for peak force (adhesiveness, N) for sodium alginate, HPMC and sorbitol tested on porcine buccal tissue (n= 3).

It can be observed from Figure 6.10, likewise to results with chitosan, an increase in sorbitol concentration (1-10% w/v) led to a decrease in the force of adhesion. The optimum concentration of HPMC is again shown to be 0.5% w/v, with a further increase to 2% w/v resulting in a reduction of mucoadhesiveness. An increase in sodium alginate concentration leads to an increase in mucoadhesion, which can be expected as the higher concentration leads to more significant interaction of the ionized carboxyl groups with the mucosal tissue.

6.7 Results and Discussion: Comparison of the addition of PEG 400 as a plasticiser in the chitosan and sodium alginate formulations

Factor	Name	Type	Levels	Level Values		
A	Sorbitol	Numeric ▼	2	2.5	5	
B	PEG 400	Numeric ▼	3	0	0.25	0.5

Figure 6.11: Image showing the level and level values of a general factorial design used for the formation of mucoadhesive patches comparing sorbitol and PEG 400. Patches with HPMC 0.5% w/v and either LMW Chitosan or Sodium alginate 2% w/v

It was observed during studies increasing concentrations of sorbitol (2.5-5% w/v), which generally can also act as a plasticiser, leads to unfavourable outcomes in terms of repeatability of aesthetically appealing patches. Thus, as a manner of improving flexibility, PEG 400 was tested as a second plasticiser, which has enhanced the flexibility of freeze-dried patches in the literature (Figure 6.11) [107]. The concentration of chitosan was also increased to 2% to see if such an increase will also make a positive influence on the formulation both in terms of mucoadhesion and aesthetics of the patches.

a.

b.
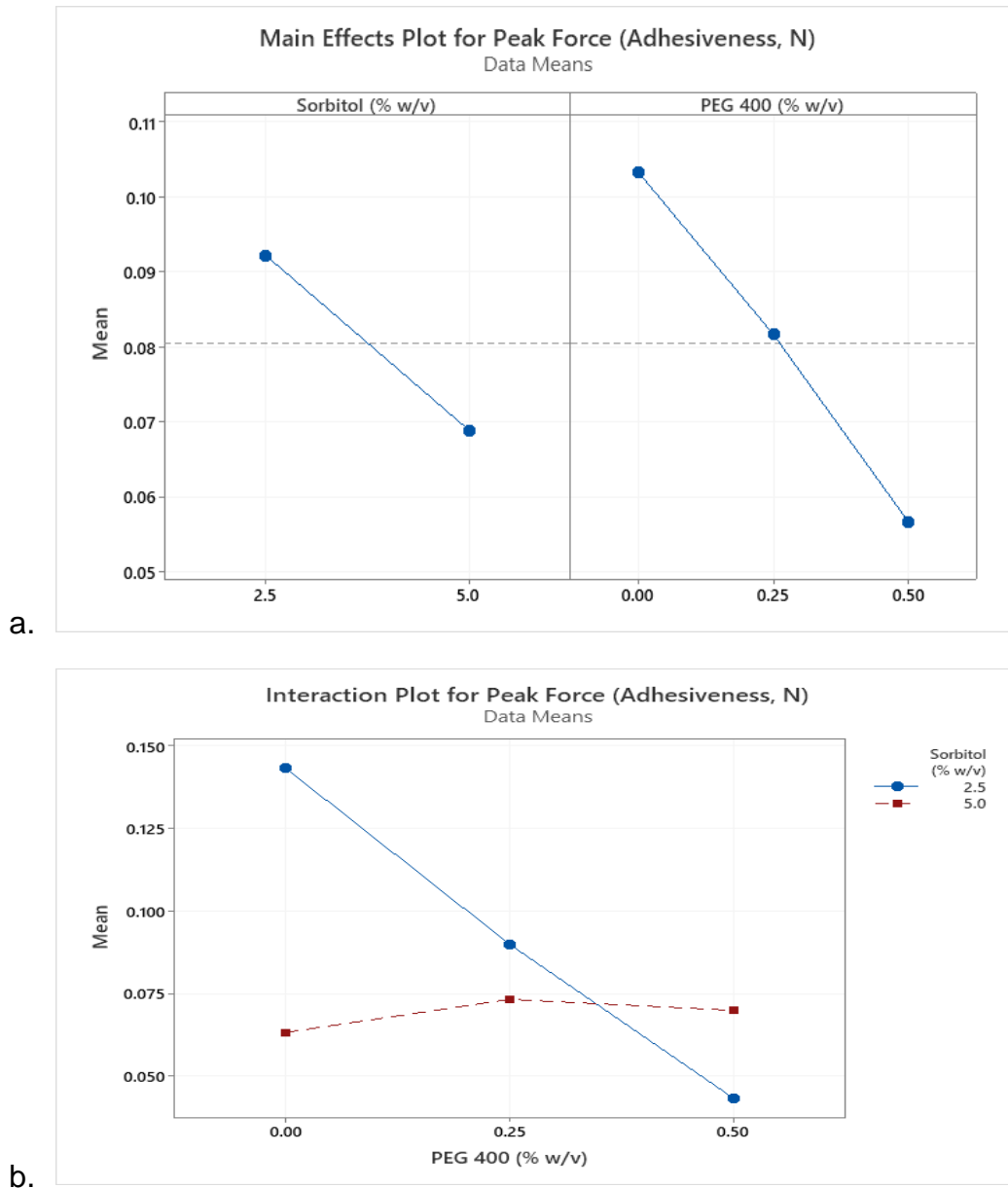
Figure 6.12: Chitosan, HPMC, sorbitol and PEG 400 (a) Main effect plot for peak force (adhesiveness, N) and (b) Interaction plot for peak force (adhesiveness, N) (n=3, Minitab).

Comparing the results both the main effect plot and the specific interaction plot for chitosan in Figure 6.12, the addition of PEG 400 in the formulation at both concentrations (0.25 and 0.5% w/v) resulted in a decrease in the force of mucoadhesion. Thus, it was decided the chitosan formulation would be taken forward without PEG 400, and the best combination for further studies was chosen to be

chitosan 2% w/v, with sorbitol 2.5% w/v and HPMC 0.5% w/v (patch C in Table 6.1 and Figure 6.14).

a.

b.
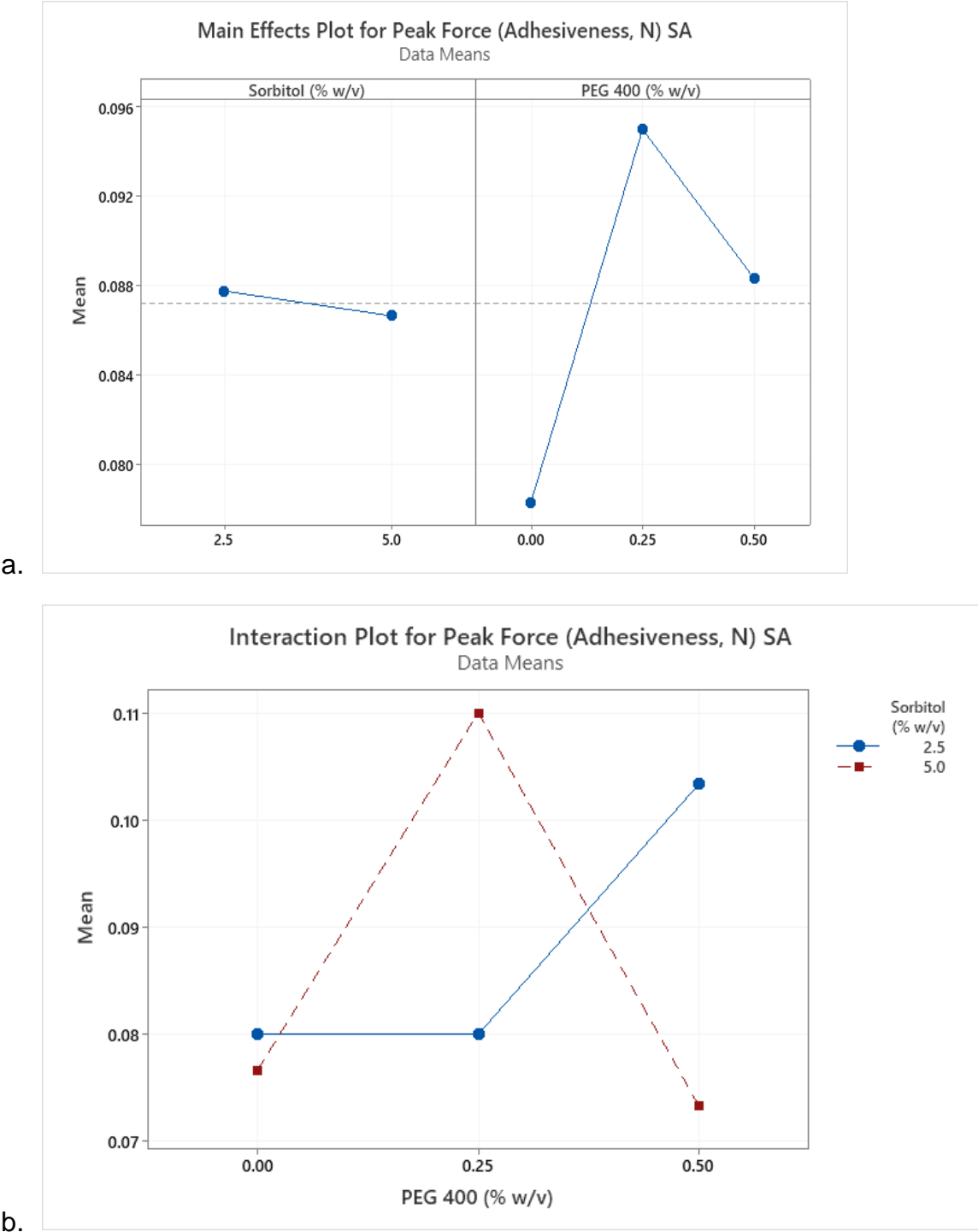
Figure 6.13: Sodium alginate, HPMC, sorbitol and PEG 400 (a) Main effect plot for peak force (adhesiveness, N) and (b) Interaction plot for peak force (adhesiveness, N) (n=3, Minitab).

The results for the main effect plot in Figure 6.13, shows the addition of PEG 400 in the formulation at concentrations of 0.25% w/v results in an increase in the mucoadhesion whereas a further increase to 0.5% w/v results in a decrease in mucoadhesion. In the main effect plot for sorbitol a decrease in mucoadhesion is seen with an increase in sorbitol concentration from 2.5% to 5% w/v, however, examining the interaction plot of the individual components it can be observed that the mucoadhesion is highest when sorbitol concentration is at 5% concentration and PEG 400 at 0.25% w/v. Thus, the best combination for further studies was chosen to be sodium alginate 2% w/v, sorbitol 5% w/v, PEG 400 0.25% w/v and HPMC 0.5% w/v (patch S in Table 6.1 and Figure 6.13).

Table 6.1: Ingredients in the finalised buccal patch formulations labelled S (main component sodium alginate) and C (main component Low MW chitosan).

Formulation	S	C
Sodium Alginate (% w/v)	2	0
Low MW Chitosan (% w/v)	0	2
HPMC (% w/v)	0.5	0.5
Sorbitol (% w/v)	5	2.5
PEG 400 (% w/v)	0.25	0
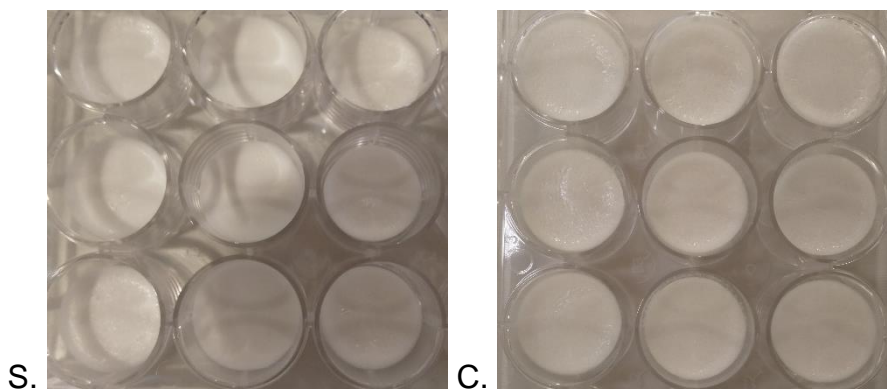
Figure 6.14: Images of the final patches S and C.

Notes: Content of patches detailed in Table 6.1.

Table 6.2: Percentage of the different components in each transfersomal formulation (total 60 µmoles/mL).

Formulation	Cholesterol (% mol)	Span 60 (% mol)	DPPE (% mol)	Tween 80 (% mol)	DCP (% mol)	SGDC (% mol)
D5E	15	40	20	20	5	
S5E	15	40	20	20		5

Abbreviations: 1,2-dipalmitoyl-3-sn-phosphatidylethanolamine (DPPE), dicetyl phosphate (DCP), and sodium glycodeoxycholate (SGDC)

Overall, the study showed good improvement on the formulations with minimum sorbitol content of 2.5% for (patch C) and 5% for (patch S) with both final formulations being aesthetically appealing, flexible, easy to remove from the moulds, no fractured surfaces, and no or very little bubbles formed above or below the patch surface. This enables a good comparison for further studies, including release studies, as the final transfersomes detailed in Table 6.2 are embedded in the patch formulations (S and C). The shortcodes representing the content embedded in the patches are detailed in Table 6.3.

Table 6.3: Shortcodes for content embedded in buccal patches.

Code	S or C patch
I	+ 0.36mg Insulin
TED	+ Transfersomes D5E Empty
TID	+ Transfersome D5E with Insulin (0.467 mg)
TES	+ Transfersomes S5E Empty
TIS	+ Transfersomes S5E with Insulin (0.353 mg)

Patches S and C are detailed in Table 6.1. Transfersomes D5E and S5E are detailed in Table 6.2

200 μm* EHT = 20.00 kV WD = 8.5 mm

C.

200 μm EHT = 15.00 kV WD = 6.0 mm

CI.

200 μm* EHT = 20.00 kV WD = 7.5 mm

CTED.

200 μm* EHT = 20.00 kV WD = 7.5 mm
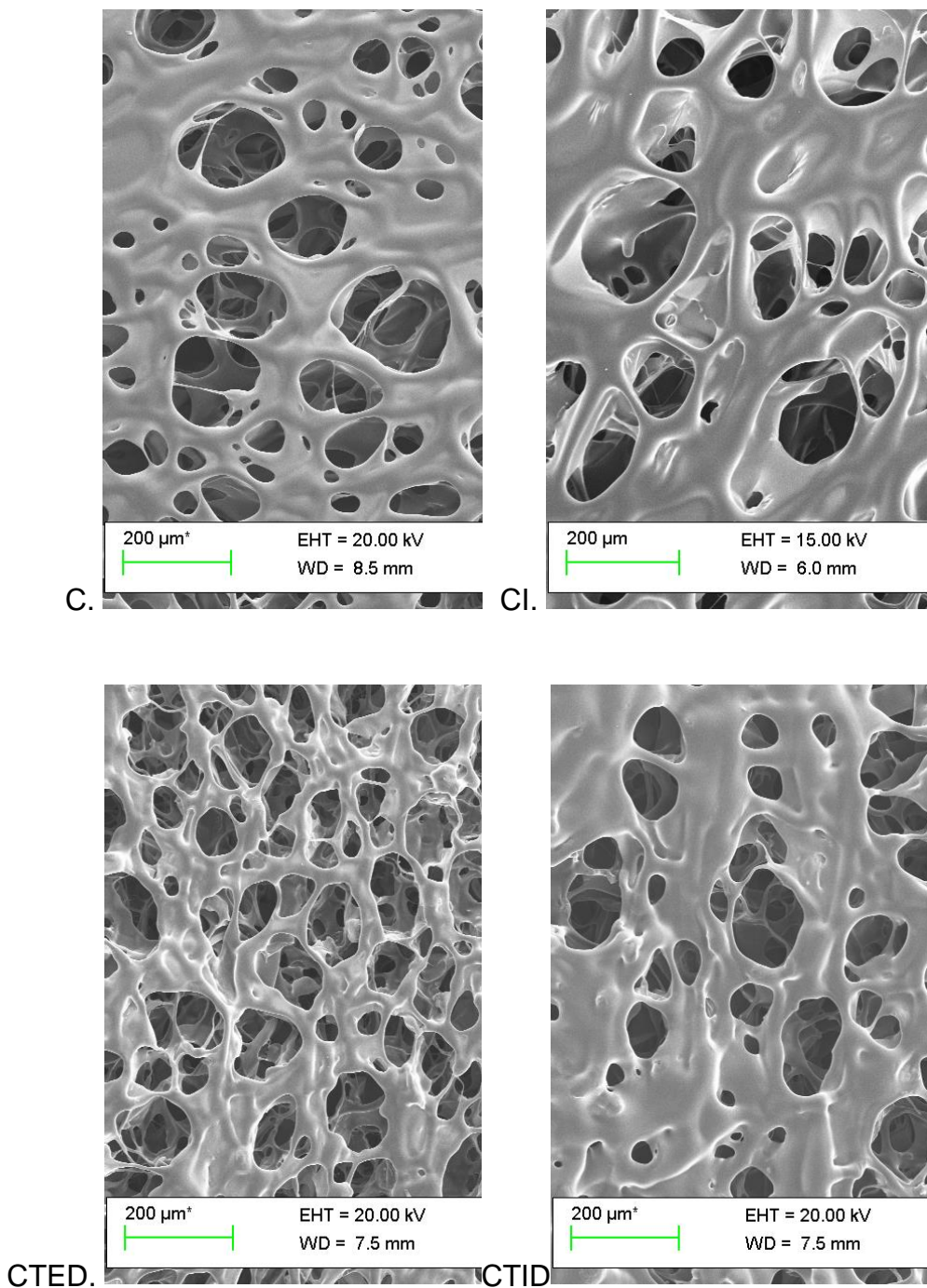
CTID

Figure 6.15: SEM images of chitosan containing buccal patches: empty (C); with insulin (CI); with the unloaded transfersome (CTED); and with the loaded transfersomes (CTID).

The SEM images of the C patches, shown in Figure 6.15, demonstrate the porous nature of the patches as seen in another study working on lyophilised patches of

chitosan [242]. However, compared to the SEM images, seen in the other study, the surface of the C patches with combined HPMC and sorbitol, are much smoother in the network of polymers. The incorporation of insulin in the patches (CI), does not seem to alter the morphology of the surface. Still, the incorporation of the unloaded (CTED) and loaded (CTID) transfersomes appear to have made the surface of the patches more granular in morphology.

6.7.2 X-ray diffraction analysis

Figure 6.16: XRD spectra of raw ingredients: insulin, sorbitol, sodium alginate and low MW chitosan.
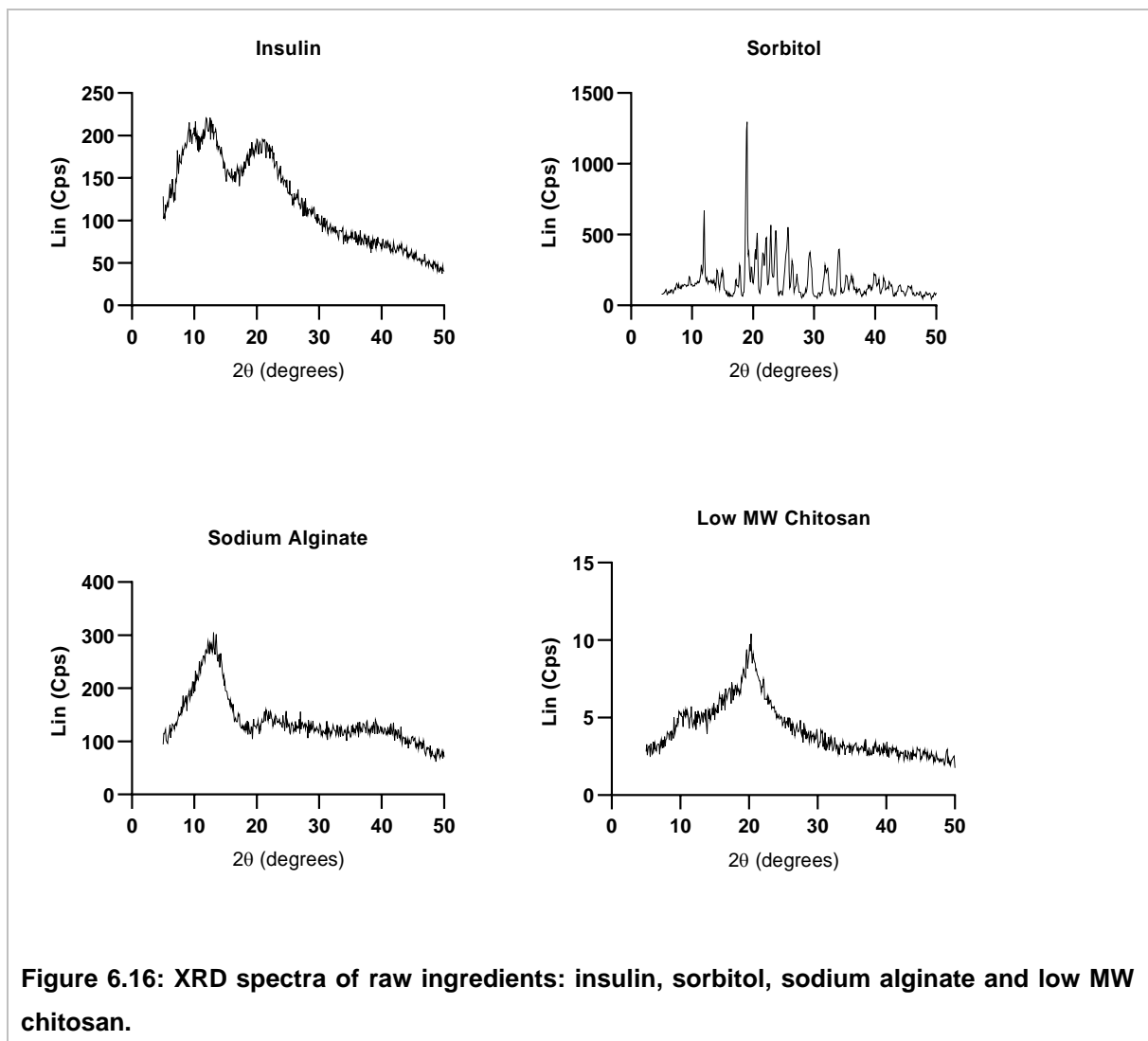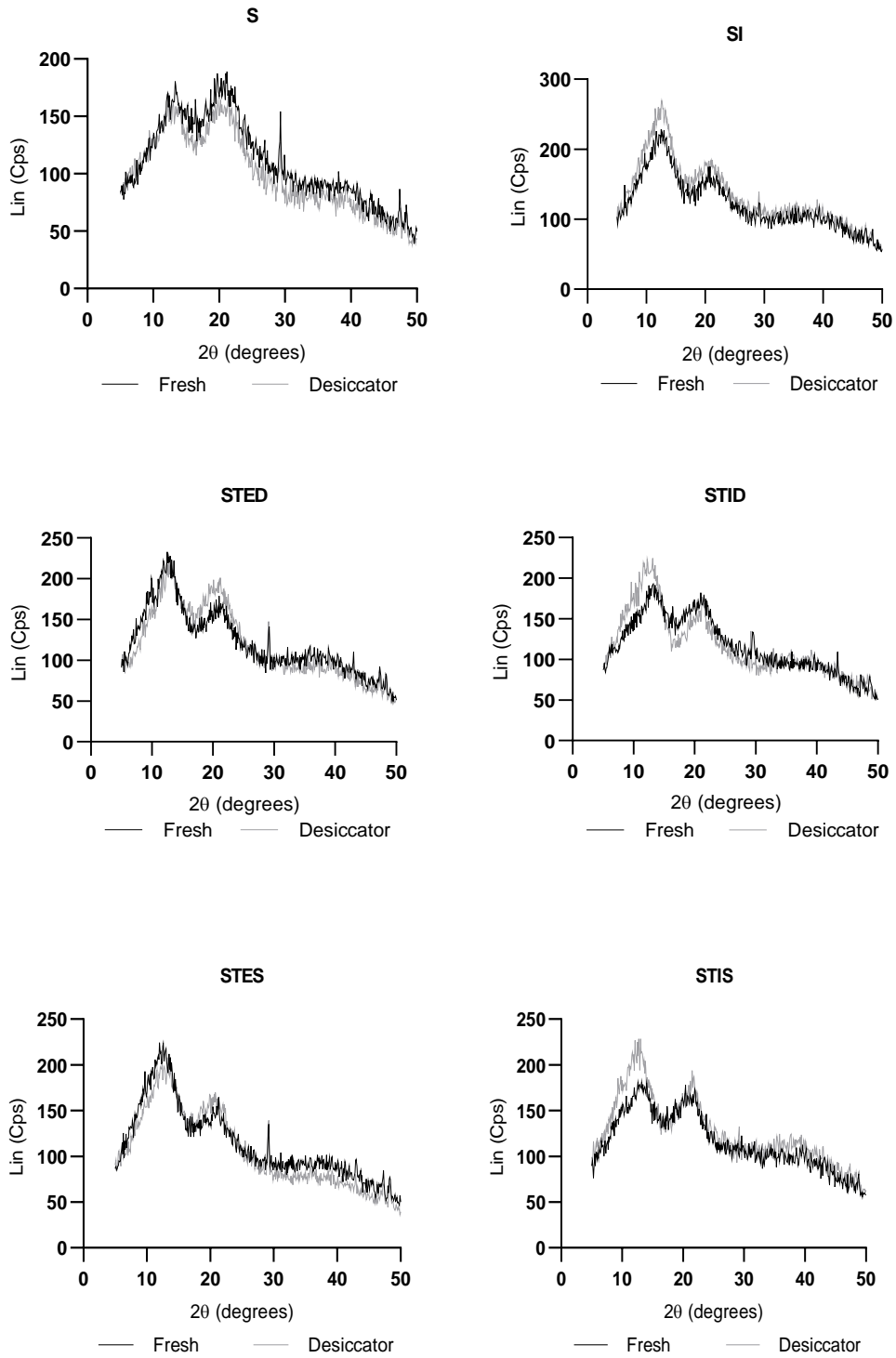
Figure 6.17: XRD spectra for sodium alginate containing buccal patches: fresh and stored in a desiccator (2 months).
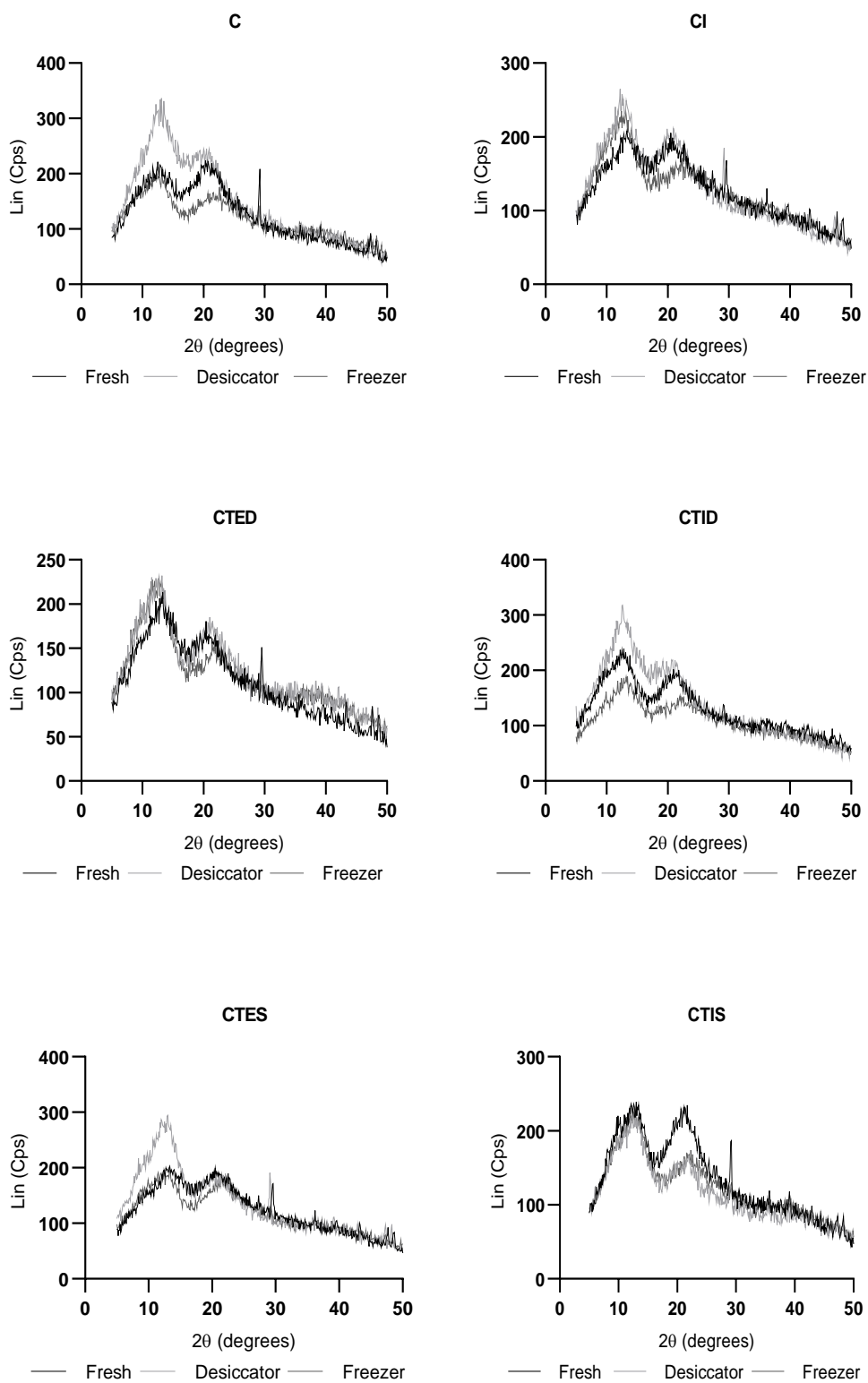
Figure 6.18: XRD spectra of chitosan containing buccal patches: fresh, stored in a desiccator (2 months) or stored in a freezer (-20°C, three months).

XRD studies have often been used to study materials to determine their crystal structure as well as size [201]. They are also used to determine if a material is amorphous or crystalline in structure. Looking at the XRD spectra of the raw ingredients, used to form the buccal patches, most except for sorbitol are predominantly amorphous (Figure 6.16). The spectra for sodium alginate and chitosan are comparable to the results obtained in several other studies, with two characteristic crystalline peaks obtained at 10° (2θ) and 20° (2θ) (Figure 6.16) [243]–[245]. HPMC, based on literature, is also amorphous with a broad peak present around 22.5° (2θ) [246]. The amorphous nature of the raw powders was expected as insulin, and the natural polymers (chitosan, sodium alginate and HPMC) all have high molecular weights. Thus, it is difficult for these molecules to arrange themselves into repeating and orderly patterns, which is the case with crystalline material [247].

As anticipated, the spectra obtained from the XRD data demonstrated that the freeze-dried patches of both the S and C patches are highly amorphous, with some crystallinity present within the formulation (Figure 6.17 & Figure 6.18). In both the S and C patches, there are two strong, broad peaks around 10° (2θ) and 20° (2θ), the similarity possibly being related to the spectra of sodium alginate and chitosan, but also the common ingredients sorbitol and HPMC. In the S and C patches, the strong crystalline peak that is present at 29°(2θ) is likely to be due to sorbitol, as it is present in the presence and absence of insulin and the transfersomes. Also, comparison of the patches, in the presence and absence of transfersomes and insulin, do not display any major changes in the broadness of the peaks, or appearances of new peaks, in the spectra, indicating an unlikely occurrence of chemical reactions or complexing

between the polymers and the drug and the vesicles as seen in some studies when complexing does occur [243].

Amorphous material, due to their unstable nature, can offer advantages such as higher solubility and faster dissolution rates [247]. However, amorphous materials are unstable, due to lack of lattice energy, and thus over time can transform to a crystalline form [247]. A study investigating buccal films of several types of polymers (including HPMC and sodium alginate), which were initially amorphous, found after six months storage in a petri dish that the XRD data showed several crystalline peaks [248]. This was attributed to the possible recrystallization of the originally crystalline drug fluconazole due to absorption of moisture during storage. Hence, the XRD of the patches in our study was repeated after storage to see if a similar situation may occur in this study with possible recrystallisation of sorbitol or formation of new crystalline structures. But the XRD patterns of the patches stored in a desiccator (2 months both S & C patches) and in the freezer (-20°C, three months C patches) showed no significant difference in the XRD patterns after storage in these conditions, possibly due to these methods providing adequate protection from moisture (Figure 6.17 & Figure 6.18). Thus, based on these results, both forms of storage provide conditions sufficient to maintain the stability of the hygroscopic patches for at least 2 months.

6.7.3 Differential scanning calorimetry
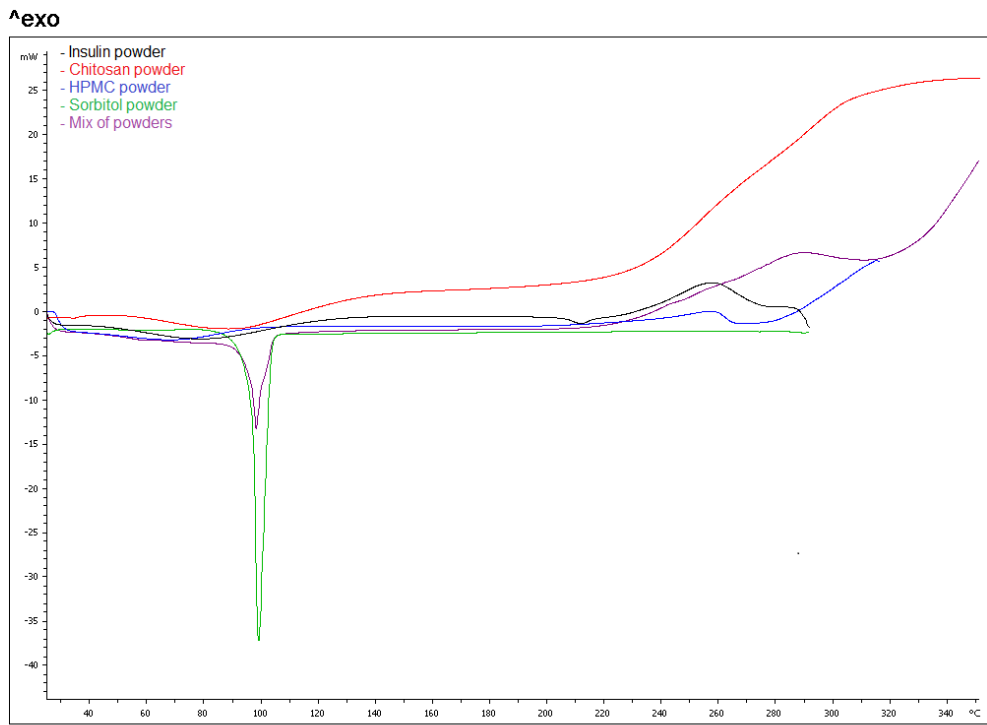
a.
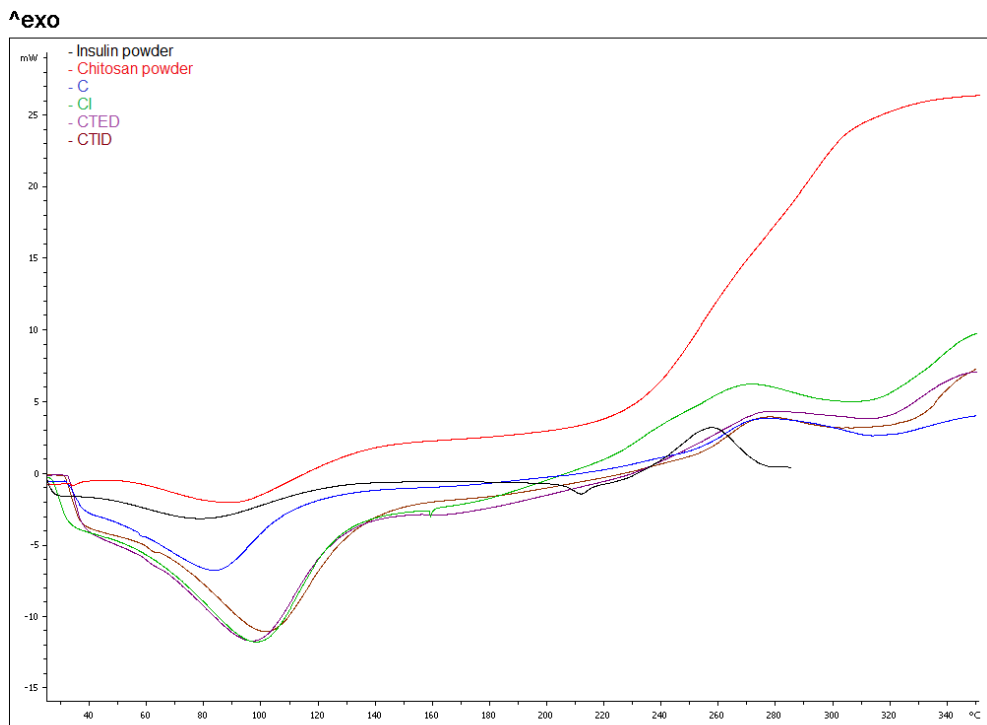
b.
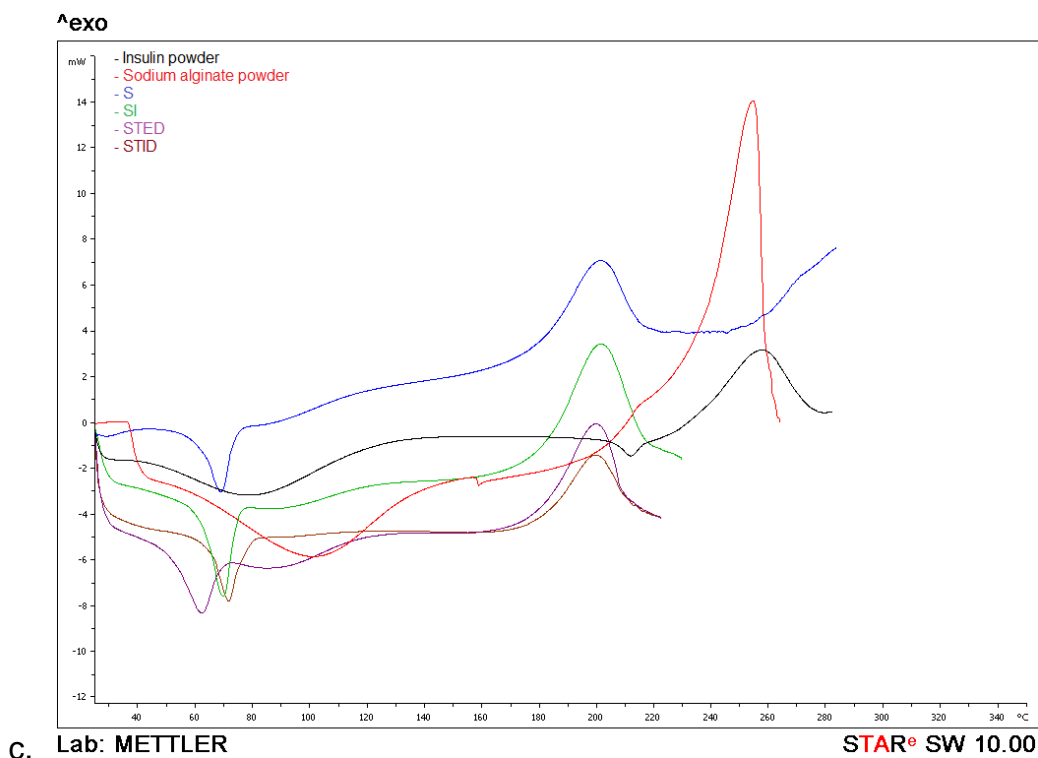
Figure 6.19: DSC thermogram of (a) Insulin powder, Low MW chitosan powder, HPMC powder, Sorbitol powder, Mix of all the powders (the composition of patch C), (b) Insulin powder, Low MW chitosan, C, CI, CTED, CTID, and (c) Insulin powder, Sodium alginate powder, S, SI, STED, STID.

It was identified by XRD analysis that sorbitol is a crystalline material, and this is confirmed by the sharp endothermic peak at 99.2°C, which corresponds to its melting temperature, similar to the results in the literature [Figure 6.19 (a)] [249]. The other pure polymers are all amorphous, and this is confirmed by, the absence of sharp peaks, and the presence of broad endothermic peaks, indicating loss of water followed by a broad exothermic peak representing polymer degradation. The thermograms seen for chitosan and sodium alginate are similar to those observed in the literature [243], [250]. The deterioration of chitosan involves dehydration of saccharide ring, depolymerization as well as decomposition of deacetylated and acetylated chitosan units [250].

The endothermic peaks for the pure powders: HPMC (69.6°C), insulin has two peaks (79.6°C) and a second small endothermic peak at (211.8°C), chitosan (91.4°C), and sorbitol (99.2°C) [Figure 6.19 (a)]. The freeze-dried patches (C, containing sorbitol, HPMC and chitosan) the peak becomes broader and shifts to 84.3°C, in combination with insulin (CI, 98.8°C), with unloaded transfersomes (CTED, 97.3°C), and with insulin loaded transfersomes (CTID) it is 101.8°C [Figure 6.19 (b)]. Comparing the physical powder mixture of the composition of patch C (part a) it can be observed that the sharp endothermic peak representing sorbitol melting is still present in the powder mixture around 98.0°C, However, in the freeze-dried patches, the endothermic peak although around similar temperatures to the original excipients, is broad reflecting the conversion of sorbitol to the amorphous form and coalescence with the other amorphous components, as seen with drugs in previous literature [251]. As there is no significant shift in the peaks, it is unlikely for any new chemical entities to be produced after freeze-drying. This is also reflected with the exothermic peaks as insulin has a peak at 257.0°C, HPMC 257.2°C, the physical mixture of patch C at 290°C, C freeze-dried patches: 275.1°C (C), 266.9°C (CI), 274.1°C (CTED) and 274.7°C (CTID). Thus, the thermogram of the C patches indicates the drug and excipients are well mixed within the patches.

Based on literature PEG 400 has an endothermic peak at 58.2°C [251]. Pure sodium alginate has an endothermic peak around 100.0° C, in the freeze-dried patches (S, containing PEG 400, sorbitol, HPMC and sodium alginate) the peak becomes less broad and shifts to 68.9°C, in combination with insulin (SI, 69.6°C), with unloaded transfersomes (STED, 62.1°C), and with insulin loaded transfersomes (STID) it is 71.6°C [Figure 6.19 (c)]. The downward shift in peak is likely due to the presence of

PEG 400, which as a plasticiser, can lower the *glass transition temperature (Tg)* of amorphous material by becoming integrated into the polymer network [252]. Thus, for pure sodium alginate the exothermic peak is around 254.5°C whereas for the S patches they are lower at 200.9°C (S), 201.2°C (SI), 199.7°C (STED), and 199.1°C (STID).

6.7.4 Thickness and surface pH determination
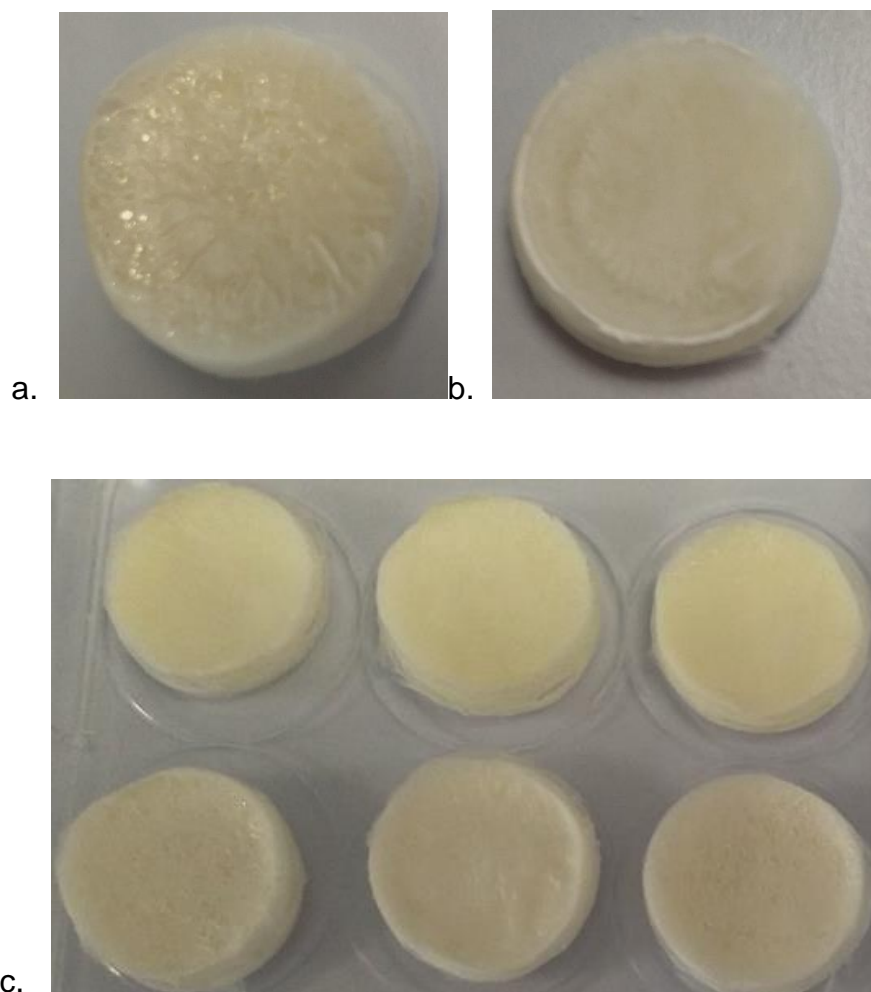
Figure 6.20: Examples of images of the final mucoadhesive patches with the impermeable backing layer. (a) Close up image of the front mucoadhesive layer containing the transfersomes, (b) Close up image of the back layer, and (c) Top row C patches and bottom row S patches.

In general, due to the controlled volumes poured into moulds, the thickness of the patches was relatively uniform throughout. The thickness of the final patches, examples shown in Figure 6.20, were found to be 0.40 ± 0.1 mm for the C patches and 0.45 ± 0.1 mm for the S patches. In water, the surface pH of the patches was found to be around 7.0 (S patches) and 5.0 (C patches). For the C patches, the lower pH is

likely as a result of the residual acetic acid, in which the polymer was initially dissolved. In PBS pH 7.4, as expected both patches had a surface pH of around 7.0-7.5.

6.7.5 Insulin release from buccal patches
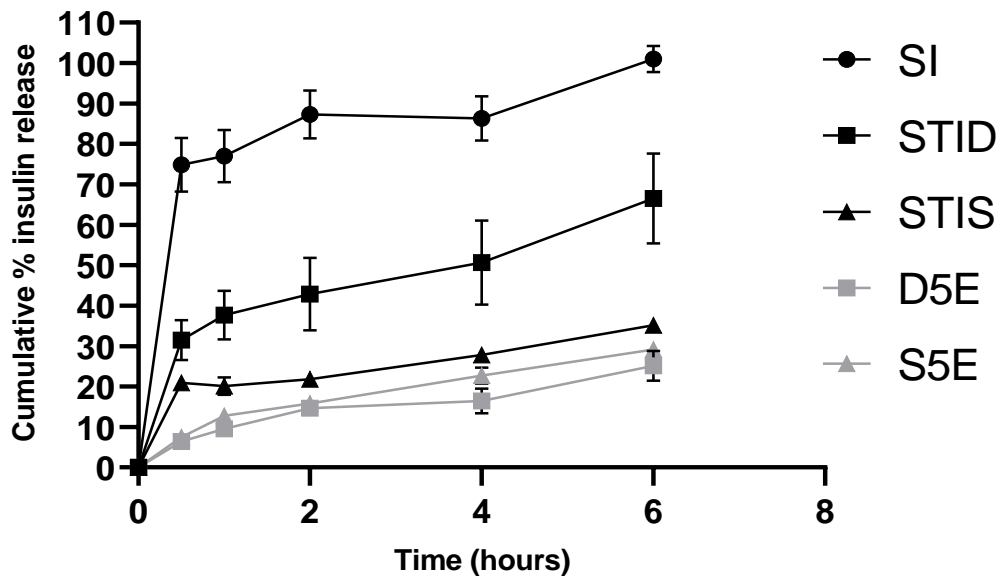
Figure 6.21: Comparison of cumulative % insulin release from SI, STID and STIS and transfersomes D5E and S5E (not embedded in patches).

Results represent mean ± SD (n=3). Two-way ANOVA analysis showed a significant difference ($p < 0.0001$) in the release of insulin between all systems. Tukey's multiple comparisons test showed significant difference ($p < 0.0001$) between the control SI and all the other formulations. The release from the transfersomal embedded formulation STID was also significantly higher ($p < 0.0001$) compared to STIS, D5E and S5E. The difference in the release from STIS and S5E were statistically insignificant ($p > 0.05$).
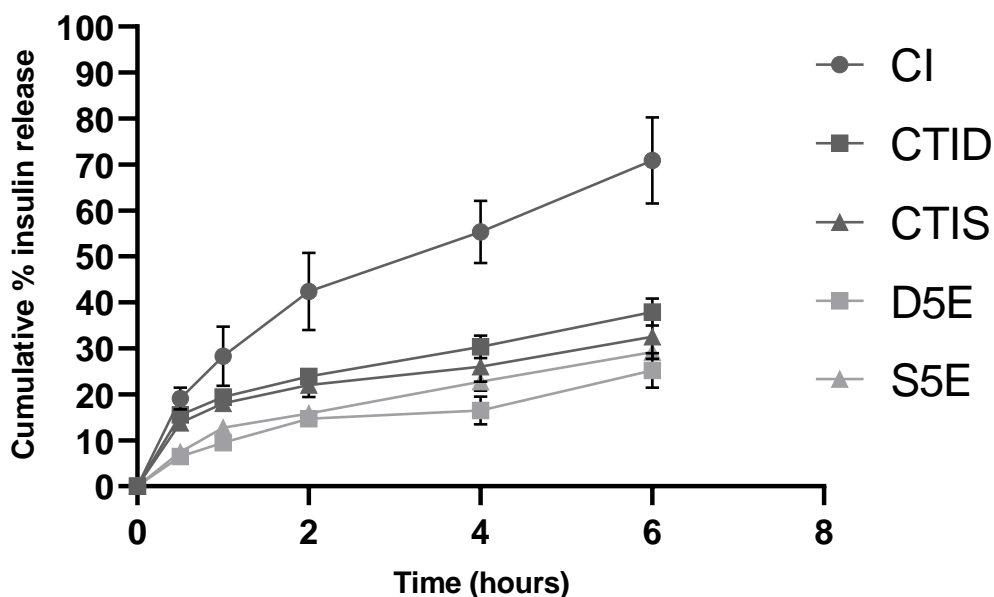
Figure 6.22: Comparison of cumulative % insulin release from CI, CTID and CTIS and transfersomes D5E and S5E (not embedded in patches).

Results represent mean ± SD (n=3). Two-way ANOVA analysis showed a significant difference ($p < 0.0001$) in the release of insulin between all systems. Tukey's multiple comparisons tests showed a significant difference ($p < 0.0001$) between the control CI and all the other formulations at 2, 4 and 6 hours. The difference in release from CTID and CTIS were statistically insignificant ($p > 0.05$). The difference in release from CTID was significantly higher ($p < 0.05$) compared to D5E across all time points. The difference in release from CTIS and S5E were statistically insignificant ($p > 0.05$).

A study looking at the release of fluconazole (dissolved in 10% w/w PEG) from buccal films found the drug release to be rapid and completed within 1 hour of initiation from the sodium alginate (1% w/w) film, 95% drug released within 2 hours for the chitosan (2% w/w) film and 90% of the drug content released by around 4 hours with the HPMC (3% w/w) film [248]. In this study, carried out at pH 6.8, it was also observed when either sodium alginate or chitosan was combined with other polymers, such as sodium carboxymethylcellulose or Carbopol, the release was more gradual compared to the individual polymers [248]. Another study found increased concentrations of HPMC led to prolongation of drug release [251].

As it can be seen from Figure 6.21 and Figure 6.22 the release of insulin from the control patch formulations S [sodium alginate (2%), HPMC (0.5%), Sorbitol (5%) and PEG 400 (0.25%)] and C [low MW chitosan (2%), HPMC (0.5%) and sorbitol (2.5%)] without transfersomes, showed significantly higher ($p < 0.0001$) cumulative percentage insulin release compared to the transfersome containing patches and the free transfersomes (S5E & D5E, not embedded in patches). Since both, the S and C patches are highly amorphous, observed in XRD studies, it was anticipated that dissolution process and drug release would be a quick process. The drug release from the formulation SI, was the highest among all the formulations, with 75% of the total insulin released in the first 30 minutes then slower release to completion. This was expected, both due to the previous release studies of sodium alginate films in literature, but also in our research when attempting to study the swelling characteristics of the patches, the S patches disintegrated soon after wetting. Additionally, the S patches contain PEG 400 and a higher percentage ratio of sorbitol, both of which are hydrophilic compounds (additives that can act as plasticisers), which enables water to penetrate faster within the patch to allow drug release. Furthermore, it was observed during patch production that patches containing higher percentage ratios of sorbitol were more porous in nature, and this also aids the dissolution process. Other than the absence of PEG 400 and a lower concentration of sorbitol, the slower release from the C patches may also be due to the solubility of chitosan, which is a pH-dependent polymer. Chitosan is soluble in water up to pH 6.2, above this pH, it forms a hydrated gel-like precipitate, which could hinder drug release, and the release study was carried out at pH 7.4 [122]. A study looking at chitosan freeze-dried buccal patches (labelled sponges in the study) with impermeable ethyl cellulose backing layer also found similar insulin

release results for the chitosan patches, which were initially formed in pH 2 media but release carried out at pH 7.4 [242].

The highest percentage drug release (66.5%) from a transfersomal containing formulation, in 6 hours, was from D5E embedded in patch S (labelled STID in Figure 6.21). One explanation for this is that the S patch formulation is overall faster at drug release and dissolution compared to the C patches, which can be observed with the release of insulin from the insulin only containing control patches SI and CI respectively. Another possible additive reason is that sodium alginate is an anionic polymer and based on the zeta potentials both transfersomes D5E (-30 mV) and S5E (-18 mV) are also negatively charged, thus as a result of electrical repulsion between the transfersomes and the polymer the drug is exposed and released faster in the media. Moreover, insulin has an isoelectric point of 5.3, thus above this pH (pH 7.4) the protein is negatively charged, and this also supports the same electrostatic repulsion theory in difference in release [242]. This can also explain why S5E, with the less negative surface charge, is released more slowly compared to D5E. Moreover, this can further explain why there is much slower, and lower drug release from the transfersomes in the C patches as chitosan is a cationic polymer. Thus, the electrical attraction will retain the transfersomes and insulin within the patch and hinder insulin release.

6.7.5.1 Mathematical modelling of insulin release from patches

Table 6.4: Mathematical modelling of insulin release from patches S and C containing insulin (control) or insulin-containing transfersomes initiated from 0.5 hours.

	Zero-order	First-order	Higuchi	Korsmeyer-Peppas	
	R^2	R^2	R^2	R^2	n
SI	0.883	0.801	NA	NA	NA
STID	0.978	0.960	NA	1.00	0.22
STIS	0.955	0.948	NA	0.998	0.24
CI	0.969	0.991	0.995	0.995	0.49
CTID	0.988	0.993	0.993	0.993	0.37
CTIS	0.967	0.974	0.984	0.991	0.33

Results represents mean (n=3)

Mathematical modelling was carried out to analyse the *in vitro* release data from all the six patch formulations, shown in **Error! Reference source not found.**. The S patches (SI, STID and STIS) cannot be modelled with the Higuchi model since the patches do not comply with one of the assumptions of the model, which is negligible polymer swelling and dissolution hence has been labelled as not applicable (NA). The SI patch also cannot be modelled with the Korsmeyer-Peppas model as the amount of drug release in 0.5 hours exceeds 60% of drug release [131]. R^2 is the correlation coefficient and indicates the level of fitting of insulin release to the various kinetic models, i.e. zero, first, Higuchi and sometimes Korsmeyer-Peppas. Drug release, as summarised by Mesnukul et al. (2009), is described as being; zero-order when the rate of drug release is independent of drug concentration and first-order when the rate is concentration-dependent [251]. For most of the patches, the Korsmeyer-Peppas model was the best fitting model with the highest correlation for all the patches except for SI, which could not be modelled and for CI the R^2 was equivalent for both Higuchi model and Korsmeyer-Peppas. All the patches containing the transfersomes displayed

n values below 0.45, which does not correspond to any defined categories for drug release mechanisms according to this model. Thus, the results are atypical and will need further investigations to determine the exact mechanism of release, which is understandable as these are relatively complicated systems consisting of the protein crossing the vesicle bilayer prior to diffusion out of the polymeric system. The CI patch has n value of 0.49, which falls into the category of anomalous (non-Fickian) transport, and this indicates insulin release from the patch formulation is a combination of diffusion and polymer relaxation [251]. However, for all the patch formulations, except the SI patch, the correlation coefficient for the first-order model is higher than the zero-order model, which indicates drug release is concentration-dependent.

6.8 Conclusion

This study has led to the production of a unique unidirectional mucoadhesive delivery system with novel transfersomes embedded within the patch as permeation enhancers. The most promising formulation, which achieved the highest percentage drug release (66.5%), in 6 hours, was from the transfersomal formulation D5E embedded in the sodium alginate containing patch S (STID). The study also demonstrated a direct link between increasing concentrations of sorbitol and reduction of mucoadhesiveness of lyophilised polymeric patches. It was also observed that the presence of HPMC only at an optimum concentration increases mucoadhesiveness and beyond this leads to a reduction in mucoadhesive forces in patches.

7. General conclusion and future works

In the 21st century, an array of insulin formulations and devices are in clinical practice. However, non-invasive insulin delivery systems remain a challenge. Pfizer's inhaled insulin product Exubera was approved by FDA in 2006 but was not successful, and this led to a few companies halting their developments of similar products [1], [23]. Although the product failed, it provided a good learning opportunity for other pharmaceutical companies and academic researchers, in terms considering product design and marketing in addition to the formulation. Thus, learning from Exubera, recently in 2014, Afrezza®, a newer and much smaller, non-invasive inhaled human insulin device, was approved by the FDA [22]. But the product still faces many obstacles to achieve success and worldwide acceptance. In the UK and the rest of Europe, it is still in phase 3 clinical trials [25], [26]. Another product of interest was the buccal insulin formulation, Generex Oral-lyn™ spray. Although it has been approved for clinical use in Ecuador and Lebanon, in the US and Europe, the product remains in phase 3 clinical trials [15], [30], [31]. It is formulated using GRAS excipients and insulin-containing micelles, are used as absorption enhancers [15], [32].

As summarised in the first chapter, the oral route for most individuals would be the preferred route for drug delivery. However, insulin is a protein with an MW of 5808 Da, and without any assistance, the permeability and bioavailability are very low [53]. Thus, oral insulin formulations would require absorption enhancers; however, the possible toxicity of such products can be a concern in the long-term. Although buccal formulations will also need some form of permeation enhancement, the cells in the buccal cavity have the advantage of the much shorter recovery time compared to the GIT [59], [60]. Thus, it will likely pose a lower risk. As the paracellular pathway is

suggested to be the main route utilised by proteins, the major hurdle to buccal mucosal permeation, is the intercellular lipids. However, factors such as enzymatic activity and saliva production, in the oral cavity, must also be taken into consideration in the formulation design. On completion of the initial research, the inspiration emerged to produce insulin-containing vesicles that will be embedded in a double-layered mucoadhesive buccal patch formulation. This motivation partially stemmed from the following two products; the MidaForm Insulin PharmFilm® in developed by MonoSol Rx and Midatech and HDV insulin produced by Diasome Pharmaceuticals [36], [43], [61].

Various vesicular systems have been studied to increase the permeability of proteins, such as insulin, via the buccal route. Transfersomes, are quite novel drug delivery systems, in which the bilayer consists of a combination of phospholipids and edge activators. The advantage of these vesicles in comparison to ordinary liposomes and niosomes is that they are ultra-deformable. Thus, it can squeeze through pores, under non-occlusive conditions, up to one-tenth smaller than their size. As a result, particles of 200-300 nm can enter the intact skin [98]–[101]. A considerable number of studies are associated with the use of transfersomes in enhancing drug delivery across the skin. Still, only a small number of studies can be found that have explored the mechanism of such vesicles for improving drug delivery in the buccal cavity. Theoretically, the structure of the skin is in close resemblance to the buccal membrane, but with improved permeability, thus greater enhancement of insulin delivery may be possible [102]. The capability of transfersomes to enhance drug delivery is indicated to be due to the synergistic effect of the vesicles being permeation enhancers and ultradeformable carriers [78].

Formulating a patch for delivery of proteins via the buccal cavity requires numerous considerations, although the most critical factors are the projected time of action and the bioavailability. However, other factors also need to be taken into account, including physical appearance and drug stability [107]. For a buccal formulation, ideally, the duration for the formulation to remain in the mouth should be as short as possible, but the maximum would be around 4-6 hours [77]. This is because maintaining the patch for longer than 6 hours would likely cause discomfort for the patient and may give rise to problems such as reduced patient compliance. The central purpose of using a patch is to both deliver and increase contact time for the drug at the site of absorption.

The second chapter of the thesis was designated to the development and validation of an analytical method for the detection and quantification of insulin. It was important for the method to be robust and stability-indicating to detect insulin degradation during product development. Also, the specificity of the method to insulin was critical, as many other excipients and impurities were to be involved in the overall formulation, including surfactants, phospholipids, cholesterol, and polymers (e.g. chitosan, HPMC and sodium alginate). Thus, the chromatographic method RP-HPLC, combined with UV detection, was chosen for this purpose. The method was validated according to ICH guidelines, which consist of specificity, accuracy, precision, repeatability, intermediate precision, detection limit, quantification limit, linearity, and range [147], [148]. In the final method, adapted from previous literature, 2-nitrophenol was used as an internal standard [143]. Samples were run for 10 minutes, and the peak for insulin was observed between 3.5-4.5 minutes while 2-nitrophenol was observed between 7.5-8.5 minutes. To aid peak separation, TFA was used in the mobile phases as an ion-pairing agent. As expected, based on previous literature, insulin was observed to degrade

much more rapidly in acidic conditions compared to neutral or alkaline environments [152], [153] as a protein insulin is known to face stability issues, particularly in liquids. Although the final formulation is in a solid patch formulation, the freeze-dried patches are hygroscopic and are likely to be affected by humidity and temperature. Due to time constraint, it was not monitored but to optimise storage conditions and shelf-life, it would be essential to analyse insulin content using HPLC, over several months, after incorporation in the buccal patch.

Chapter 3 was dedicated to preliminary studies by forming niosomes and looking at optimisation of the necessary components of vesicles as well as the method of vesicle production (thin film hydration technique). The initial focus was on the choice of surfactant (Span 20, 40, 60, 80), the effect of cholesterol and the presence of charged molecule on particle size, zeta-potential, and EE (%). Safety of the formulation was taken into consideration throughout the project. Hence the Spans, and most of the other components of the preparation, were selected based on the fact that they are already used in the food and pharmaceutical industry and are on the FDA GRAS ingredients list [104]. Typically EE (%) is affected by both the HLB of surfactants as well as the hydrophobicity or hydrophilicity of the drug to be entrapped [79], [174]. It is suggested that using surfactants with high HLB values achieves greater entrapment with hydrophilic drugs [79]. Nevertheless, there are conflicting results in this regard, as a study found the EE (%) to be the highest with Span based vesicles even though they have low HLB values [175]. Furthermore, the physical state of the surfactant could affect the EE (%). For example in some studies, the gel-type surfactants, Span 40 and Span 60 accomplished niosomes with better EE (%) compared to liquid state surfactants (Span 20 and Span 80) [79], [162]. Particle size is also a critical factor

regarding both the physical properties of vesicles and that of the encapsulated drug as well as their biological fate [187], [188]. For example, a study looking at oral administration of griseofulvin loaded liposomes found liposomes of the smaller size of less than 400 nm were able to achieve greater bioavailability compared to vesicles above 800 nm [189]. After these early studies it was confirmed that a cholesterol content of 30% molar ratio was the best to take forward, based on particle size results, and Span 60 containing 10% DCP, was able to achieve one of the highest in terms of EE (51 ± 1%). Consequently, the Span 60 niosomal formulation comprising of 60:30:10 ratio of surfactant: cholesterol: DCP respectively were carried forward for further studies. During the initial studies, it was observed particle size reproducibility, i.e. PDI was high, and thus required further improvement.

The ingredients of transfersomes can be designed and developed specifically for particular drugs, taking into consideration the complete formulation and route of delivery [78]. The main aim in chapter 4 was to develop transfersomal formulations with excellent characteristics such as particle size, PDI and EE (%), but also have favourable outcomes in release studies. Concurrently, the formulations were also tested for toxicity and permeability studies using TR146 buccal cells (see Chapter 5). After experimentation with the incorporation of different ratios of phospholipid (DPPE), the results demonstrated the highest percentage encapsulation (> 42.5) was obtained when phospholipid concentration was between 60-72 µmoles, and Span 60 concentration was between 108-120 µmoles. The data on EE (45 ± 6%) and particle size (~900 nm) indicated the formulation P60S120 containing DCP (30 µmoles), DPPE (60 µmoles), cholesterol (90 µmoles), and Span 60 (120 µmoles) to be the best combination to be considered for further studies. This formulation was tested for

release studies and permeation across TR146 buccal cells, and the results showed the release and permeation to be undetectable after 6 hours of study. This could have been due to the large particles size but also the possibility that both phosphatidylethanolamine and cholesterol can increase the rigidity of the bilayer, and this rigidity could be to the degree that the insulin molecule is not able to penetrate across the vesicle bilayer [83], [182].

Thus, manual extrusion was included as a downsizing method to reduce particle size further and form more homogenous vesicles. The effect of reducing cholesterol content was also investigated. Additionally, Span 60 (C_{18}) is one of the least leaky surfactants, as a result of the high phase transition temperature, which can benefit EE (%) but can impede drug release [83], [104]. Hence the inclusion of more hydrophilic surfactant, such as Tween 80 (HLB 15), could aid drug release as it has been found in studies to enhance release or permeability of the encapsulated drugs [195], [196]. Furthermore, Tween 80 compared to bile salts and the more lipophilic Spans, has also been found to have the highest level of deformability [175]. This was attributed to the presence of the hydrophilic surfactant forming transient holes within the bilayer and thus enhancing membrane fluidity [175]. Moreover, the concentration of insulin was increased from 0.73 mg/mL to 1.5 mg/mL in the hydration stage, and the effect on EE (%) and LC (%) analysed. As expected, a decrease in cholesterol content, comparing compositions with 90 µmoles (C90T0 and C90T45) and those with 45 µmoles (C45T0 and C45T45) resulted in a significant reduction in the particle size. The formulation with Tween 80 and the lowest concentration of cholesterol (C45T45), resulted in producing the smallest vesicle size of 206.7 nm ± 2.69 nm, which was used for further studies. After extrusion, the PDI also became less than 0.5 across all the formulations, indicating an

increase in homogeneity compared to earlier studies. Usually, for electrostatic stabilisation of vesicles, the zeta potential is ideally above +30 mV or below -30 mV [194]. Although all the formulations were indicated to be stable based on the results for the zeta potential it was noticeable that a significant reduction in zeta potential occurred in formulations containing Tween 80 (C90T45 and C45T45). Increasing concentration of insulin from 0.73 mg/mL to 1.5 mg/mL led to a significant decrease in EE (%) but significant increase in LC (%). This is understandable as simply a certain volume or space is available within the aqueous compartment of the vesicles, thus only a certain amount of insulin can be accommodated within the volume. These results, together with the results from the toxicity studies, indicated the formulation C45T45, consisting of Span 60 (40%), DPPE (20%), cholesterol (15%), Tween 80 (15%) and DCP (10%) should be taken forward for further studies.

The formulation C45T45 was then further manipulated to consist of either lecithin or DPPE with DCP or SGDC or both. In studies, the bile salt SGDC has been shown to have the ability to increase the permeability of insulin and other hydrophilic macromolecules across TR146 buccal cells and porcine mucosa, respectively [60], [64]. Thus, it was chosen as a possible supplementary permeation enhancer, to be incorporated within the transfersomal formulation. After extrusion, the newer formulations (Table 4.3) all except (D10E) formed particles < 400 nm, however, the lecithin containing formulations were found to be overall much smaller in size compared to the formulations with DPPE. The zeta potential was optimal (-30 mV or below surface charge) for most formulations, except for S5E, S10E, D5S5E and S5L. In terms of EE (%) and LC (%), all compositions achieved between 26-47% and 1-1.9%, respectively. Nevertheless, the promising formulations in terms of EE (%), were

D5S5L (46.8%), D10E (39.2%) and D5E (39.0%). However, after carrying out viability assays, the safest formulations were discovered to be D5E and S5E. Although D5E was the more favourable formulation, due to the higher EE and optimal zeta potential, S5E (29.4% EE) was also selected as the presence of the bile salt (SGDC) would offer good comparison for permeability studies. Thus, these two formulations were then taken forward for morphological, permeation, toxicity, and release studies as well as for incorporation in the final buccal patches. Morphological analysis, using SEM, revealed the transfersomes to be relatively consistent in size and spherical in shape. The release studies carried out at pH 7.4 showed insulin release, after 6 hours, to be 25.2 ± 3.8% (D5E) and 29.2 ± 0.3% (S5E) and after 24 hours 30.9 ± 4.8 (D5E) and 39.9 ± 2.1% (S5E). Based on these results S5E transfersomes overall achieved significantly higher percentage drug release compared to D5E; possibly due to the higher leakage offered by the hydrophilic bile salts, through the formation of transient pores within the bilayer, compared to DCP containing vesicles [175]. The difference in release, between 6 hours and 24 hours, resembled prolonged drug release. This phenomenon has been observed in other studies investigating liposomal drug release, and particularly Span 60-based vesicles carrying drugs such as doxorubicin and ketoprofen [205], [206]. This form of release can be of therapeutic benefit if an extended release is desired.

Chapter 5 was dedicated to cell culture studies and mainly focused on the toxicity of the formulations and permeability of insulin across the cells from the formulation. For *in vitro* tests, TR146 buccal cells were selected, as they can form stratified squamous epithelium similar to normal human buccal epithelium [209], [210]. Growth and viability studies were imaged using the novel CytoSMART Omni system. The SRB toxicity

studies demonstrated that the presence of Tween 80 in transfersomal formulations has some protective effect on the cell viability, which may not be surprising as Tween 80 is sometimes used as a stabilising agent for proteins in *in vivo* studies [215]. The initial testing of the Tween containing formulations showed, similar to other studies on surfactants, concentration-dependent cell toxicity, particularly for C45T45, which at 5 mg/mL and 10 mg/mL was insignificantly different to the viability of the control (cells only). Still, at the higher concentrations, the viability is significantly lower than the control [217]. Thus, the *in vitro* cell viability of the ten-insulin loaded transfersomes was tested at two different concentrations (5 and 10 mg/mL) on TR146 buccal cells. Actinomycin D, which is a potent inducer of cell apoptosis, was used as a positive control, and the results demonstrated concentration-dependent cytotoxicity [219], [220]. Only two formulations, D5E and S5E, were found to have % viability not significantly different from the control (cells only) and were taken forward for permeation studies. In the permeation studies atenolol (Mw 266 Da) was used as a control as it is a small hydrophilic drug and has been previously tested for permeability across the TR146 cells. FITC-Dextran (Mw 20,000 Da) was used as a second control as it is a large hydrophilic molecule, compared to insulin (Mw 5808 Da) [98]. In a study looking at the permeation of FITC-Dextran molecules (4,000 to 40,000 Da), a linear decrease in K_p was exhibited with increasing Mw [212]. As anticipated, FITC-Dextran attained significantly lower K_p than both insulin and atenolol. But unexpectedly insulin and atenolol both achieved high K_p with no significant difference between the two, possibly due to the low initial TEER of ~ 55 of the TR146 cells, enabling the greater crossing of bigger molecules. The two final transfersomes (D5E and S5E), neither managed to enhance the permeability of insulin compared to the control within the 6 hours of the study. This could be because when applied on the skin the penetration

occurs as a result of the difference in osmotic gradient between the surface of the skin and the intercellular lipids but with the TR146 cell model the cells have to be maintained hydrated with HBSS throughout the study. Thus, the hydration gradient is absent, and this would be similar to applying drug-containing transfersomes under occlusion, which has been suggested to disable these ultradeformable carriers by eliminating the main driving force in crossing membranes [177]. Moreover, the hydration of cells can loosen the interstices, which could result in accumulation of insulin and the vesicles within the cell layers and thus prolonging the permeation of the drug [228]. Although the results for permeability are not as hoped, they may not represent the *in vivo* conditions and either of the formulations (D5E or S5E) could still be capable of enhancing insulin permeation.

Chapter 6 encompasses the formation and development of the mucoadhesive patches, in which the final transfersomal formulations (D5E and S5E) was then incorporated and tested for release studies. Freeze-drying was chosen as the method to form the patches as both insulin and lipid vesicles can have stability issues, such as the formation of aggregates and sometimes drug leakage [229]. Although a cryoprotectant is usually required to minimise such drawbacks in the formulation. Sorbitol has been found to offer some level of protection for preventing structural changes to insulin during freeze-drying and also improving formulation stability in storage conditions [39]. Minitab DOE was used to evaluate and study the influence of several polymers (HPMC, sodium alginate and Low MW chitosan), the cryoprotectant sorbitol, and the plasticiser PEG 400 on mucoadhesion. Mucoadhesion was tested using a texture analyser and, similar to other studies, porcine buccal tissue was used to represent the human buccal mucosa [238], [239]. Analysis of the results for mucoadhesion showed both for sodium

alginate, and chitosan containing patches, increasing concentrations of sorbitol decreased mucoadhesion. The optimum concentration of HPMC, in both chitosan and sodium alginate containing patches, was found to be 0.5% w/v, with the further increase resulting in a reduction of mucoadhesiveness. Similar to increasing concentrations of chitosan, an increase in the concentration of sodium alginate led to an increase in mucoadhesion, which can be expected as the greater concentration leads to greater interaction of the ionized carboxyl groups with the mucosal tissue.

It was observed during studies that higher concentrations of sorbitol (2.5-5% w/v), which normally can act as a plasticiser, leads to unfavourable outcomes in terms of producing consistently aesthetically appealing patches. Thus, as a manner of improving flexibility, PEG 400 was tested as a second plasticiser, which in literature has been shown to improve the flexibility of freeze-dried patches [107]. The addition of PEG 400, in the chitosan containing patches, at both concentrations (0.25 and 0.5% w/v) resulted in a decrease in the force of mucoadhesion. Hence, it was decided the chitosan formulation would be taken forward without PEG 400 and consisted of chitosan 2% w/v, with sorbitol 2.5% w/v and HPMC 0.5% w/v (i.e. patch C). In sodium alginate containing patches, the addition of PEG 400 in the formulation at concentrations of 0.25% w/v resulted in an increase in the mucoadhesion but a further increase to 0.5% w/v resulted in a decrease in mucoadhesion. Mucoadhesion was found to be highest when sorbitol concentration was 5%, and PEG 400 was 0.25% w/v. Thus, the sodium alginate (2% w/v) patch chosen for further studies was the combination with sorbitol 5% w/v, PEG 400 0.25% w/v and HPMC 0.5% w/v (i.e. patch S). Additionally, both final formulations were found to be aesthetically appealing, flexible, easy to remove from the moulds, no fractured surfaces, and no or very little

bubbles formed above or below the surfaces of the patches. Morphological studies, with SEM, demonstrated the porous nature of the patches and incorporation of the transfersomes could be observed within the polymer network.

As anticipated, the XRD data demonstrated the freeze-dried patches to be highly amorphous, with some crystallinity, most likely attributable to sorbitol, present within the formulations. Amorphous material, due to their unstable nature, can offer advantages such as higher solubility and faster dissolution rates but can also have disadvantages including hygroscopicity, and due to lack of lattice energy, they can over time transform to a crystalline form [247]. But the XRD patterns of the patches stored in a desiccator (2 months both S & C patches) and in the freezer (-20°C, three months C patches) showed no significant difference in the XRD patterns after storage in these conditions. Analysing the DSC data of the physical powder mixture, of the composition of patch C, it was observed that the sharp endothermic peak representing sorbitol melting was still present around 98.0°C. However, in the freeze-dried patches, the endothermic peak although around similar temperatures to the original excipients was found to be very broad reflecting the conversion of sorbitol to the amorphous form and coalescence with the other amorphous components, as seen with drugs in previous literature [251]. As no significant shift in the peaks was observed it was assumed unlikely for any new chemical entities to be produced after freeze-drying. The thickness of the final patches was found to be 0.40 ± 0.1 mm for the C patches and 0.45 ± 0.1 mm for the S patches. Also, in water, the surface pH of the patches was observed to be around 7.0 (S patches) and 5.0 (C patches).

The release of insulin from the control patch formulations S and C containing free insulin without transfersomes, showed significantly higher cumulative percentage

insulin release over 6 hours, in comparison to the transfersome containing patches and the free transfersomes (S5E & D5E, not embedded in patches). Since both, the S and C patches are highly amorphous; it was anticipated that the dissolution process and drug release would be quick. The drug release from the formulation SI was found to be the highest among all the formulations, with 75% of the total insulin released in the first 30 minutes then slower release to completion. The S patches contain PEG 400 and a greater percentage ratio of sorbitol, both of which are hydrophilic compounds and enable water to penetrate faster within the patch, leading to faster drug release. Also, the release study was carried out at pH 7.4, and the slower release from the C patches can also be due to the solubility of chitosan, which is soluble in water up to pH 6.2, above this pH, it forms a hydrated gel-like precipitate, which could hinder drug release [122]. The maximum percentage drug release (66.5%) in 6 hours from a transfersomal formulation was D5E embedded in the sodium alginate containing patch S (labelled STID). This can be explained by the fact that sodium alginate is an anionic polymer and based on the negative zeta potential of both transfersomes D5E (-30 mV) and S5E (-18 mV), as a result of electrical repulsion between the transfersomes and the polymer the drug is exposed and released faster in the media. Also, the isoelectric point of insulin is 5.3, and in environments above this pH (pH 7.4), the protein is negatively charged, which further supports the same electrostatic repulsion theory in release [242]. Additionally, this explains why S5E, with the less negative surface charge, is released more slowly compared to D5E. Moreover, this can explain why there is much slower, and lower drug release from the transfersomes in the C patches as chitosan is a cationic polymer thus the electrical attraction can retain the transfersomes and insulin within the patch and impede insulin release.

For future studies, it would be particularly helpful to study insulin permeation from the patches using an animal model such as a rabbit. As this would enable the patches to be tested in the presence of saliva, and consequently determine how long they can remain intact or get washed off [253]. Thus, it will be essential to investigate the influence of different sorbitol concentrations (1-5%) on the stability of insulin in the formulation and on mucoadhesion *in vivo* conditions. Also, due to the likely presence of the hydration gradient, it will provide a better environment for studying permeation compared to TR146 buccal cells. Further investigations are also required to examine the exact permeation pathway of both insulin and the transfersomes. Additionally, during insulin release studies the amount of release did not reach 100%, and since the insulin EE was indirectly calculated, throughout the studies, it would be useful if a second method is developed to directly disrupt the vesicles and analyse the insulin content. This would be a way to ensure the exact amount of insulin present in the vesicles and if there is a difference to the indirect calculations it can affect the release and permeation studies, thus would be useful information for further studies.

This thesis has led to the development of original unidirectional immobilized delivery systems consisting of a mucoadhesive layer, with transfersomes (D5E or S5E) embedded, and an outer impermeable layer for the buccal delivery of insulin. The results so far appear promising and with further studies could lead to a possibly successful non-invasive insulin delivery system. Achievement of such a formulation that can replace subcutaneous injections would not only be a great accomplishment scientifically, in terms of delivering a protein safely for chronic use non-invasively but also a significant contribution to easing the lives of millions of patients and reducing healthcare costs worldwide.

8. References

[1]   N. Easa, R. G. Alany, M. Carew, and A. Vangala, "A review of non-invasive insulin delivery systems for diabetes therapy in clinical trials over the past decade," *Drug Discov. Today*, 2018.

[2]   N. H. Cho *et al.*, "IDF Diabetes Atlas: Global estimates of diabetes prevalence for 2017 and projections for 2045.," *Diabetes Res. Clin. Pract.*, vol. 138, pp. 271–281, 2018.

[3]   World Health Organization, "Definition, Diagnosis and Classification of Diabetes Mellitus and its Complications," Geneva, 1999.

[4]   World Health Organization, "Global report on diabetes," France, 2016.

[5]   F. Ashcroft and S. Ashcroft, "Insulin synthesis," in *Insulin: Molecular Biology to Pathology*, USA: Oxford University Press, 1992, pp. 64–87.

[6]   Z. Fu, E. R. Gilbert, and D. Liu, "Regulation of insulin synthesis and secretion and pancreatic Beta-cell dysfunction in diabetes," *Curr. Diabetes Rev.*, vol. 9, no. 1, pp. 25–53, 2013.

[7]   J. A. Galloway and R. E. Chance, "Improving insulin therapy: achievements and challenges," *Horm. Metab. Res.*, vol. 26, no. 12, pp. 591–598, 1994.

[8]   D. J. A. Crommelin, "Insulin," in *Pharmaceutical Biotechnology: Fundamentals and Applications*, 3rd ed., R. D. Sindelar and B. Meibohm, Eds. Hoboken: Taylor and Francis, 2007, pp. 265–278.

[9]   J. Hyllested-Winge, K. H. Jensen, and J. Rex, "A Review of 25 Years' Experience with the NovoPen® Family of Insulin Pens in the Management of Diabetes Mellitus," *Clin. Drug Investig.*, vol. 30, no. 10, pp. 643–674, 2010.

[10]   Joint Formulary Committee, "Chapter 6: Endocrine System," in *British National Formulary 72*, London: BMJ Group & Pharmaceutical Press, 2016, pp. 640–646.

[11]   U.S. National Library of Medicine, "Insulin Interventional Studies Diabetes," 2017. [Online]. Available: https://clinicaltrials.gov/. [Accessed: 23-Dec-2017].

[12]   D. Harris and J. R. Robinson, "Drug Delivery via the Mucous Membranes of the Oral Cavity," *J. Pharm. Sci.*, vol. 81, no. 1, pp. 1–10, 1992.

[13]   A. H. Shojaei, "Buccal mucosa as a route for systemic drug delivery: a review," *J. Pharm. Sci.*, vol. 1, no. 1, pp. 15–30, 1998.

[14]   T. Tanner and R. Marks, "Delivering drugs by the transdermal route: review and comment," *Ski. Res. Technol.*, vol. 14, no. 3, pp. 249–260, 2008.

[15]   L. Heinemann and Y. Jacques, "Oral insulin and buccal insulin: a critical reappraisal," *J. Diabetes Sci. Technol.*, vol. 3, no. 3, pp. 568–584, 2009.

[16]   R. I. Henkin, "Inhaled insulin—Intrapulmonary, intranasal, and other routes of administration: Mechanisms of action," *Nutrition*, vol. 26, no. 1, pp. 33–39, 2010.

[17]   T. S. Cavaiola and S. Edelman, "Inhaled insulin: a breath of fresh air? A review of inhaled insulin," *Clin. Ther.*, vol. 36, no. 8, pp. 1275–1289, 2014.

[18]   M. Hultstrom, N. Roxhed, and L. Nordquist, "Intradermal insulin delivery: a

promising future for diabetes management," *J. Diabetes Sci. Technol.*, vol. 8, no. 3, pp. 453–457, May 2014.

[19] M. J. Rathbone, I. Pather, and S. Şenel, "Overview of Oral Mucosal Delivery," in *Oral Mucosal Drug Delivery and Therapy*, M. J. Rathbone, I. Pather, and S. Şenel, Eds. Boston: Springer, 2015, pp. 17–29.

[20] B. M. A. Silva, A. F. Borges, C. Silva, J. F. J. Coelho, and S. Simões, "Mucoadhesive oral films: The potential for unmet needs," *Int. J. Pharm.*, vol. 494, no. 1, pp. 537–551, 2015.

[21] U.S. National Library of Medicine, "ClinicalTrials.gov," 2017. [Online]. Available: https://clinicaltrials.gov/ct2/results?cond=Diabetes Mellitus. [Accessed: 23-Dec-2017].

[22] FDA, "AFREZZA® (insulin human) Inhalation Powder," 2014. [Online]. Available: https://www.accessdata.fda.gov/drugsatfda_docs/nda/2014/022472Orig1s000TOC.cfm. [Accessed: 21-Jan-2018].

[23] L. Heinemann, "The failure of exubera: are we beating a dead horse?," *J. Diabetes Sci. Technol.*, vol. 2, no. 3, pp. 518–529, 2008.

[24] J. B. Fink *et al.*, "Good Things in Small Packages: an Innovative Delivery Approach for Inhaled Insulin," *Pharm. Res.*, vol. 34, no. 12, pp. 2568–2578, 2017.

[25] Specialist Pharmacy Service, "Insulin Inhaled," 2017. [Online]. Available: https://www.sps.nhs.uk/medicines/insulin-inhaled/. [Accessed: 15-Oct-2018].

[26] D. C. Klonoff, "Afrezza Inhaled Insulin," *J. Diabetes Sci. Technol.*, vol. 8, no. 6, pp. 1071–1073, 2014.

[27] T. Goldberg and E. Wong, "Afrezza (Insulin Human) Inhalation Powder: A New Inhaled Insulin for the Management Of Type-1 or Type-2 Diabetes Mellitus.," *P T*, vol. 40, no. 11, pp. 735–741, 2015.

[28] E. S. Kim and G. L. Plosker, "AFREZZA® (insulin human) Inhalation Powder: A Review in Diabetes Mellitus," *Drugs*, vol. 75, no. 14, pp. 1679–1686, 2015.

[29] L. W. Fleming, J. W. Fleming, and C. S. Davis, "Afrezza: An inhaled approach to insulin delivery," *J. Am. Assoc. Nurse Pract.*, vol. 27, no. 10, pp. 597–601, 2015.

[30] Specialist Pharmacy Service, "Insulin Buccal," 2018. [Online]. Available: https://www.sps.nhs.uk/medicines/insulin-buccal/. [Accessed: 15-Oct-2018].

[31] J. O. Morales and J. D. Brayden, "Buccal delivery of small molecules and biologics: of mucoadhesive polymers, films, and nanoparticles," *Curr. Opin. Pharmacol.*, vol. 36, pp. 22–28, 2017.

[32] K. Park, I. C. Kwon, and K. Park, "Oral protein delivery: Current status and future prospect," *React. Funct. Polym.*, vol. 71, no. 3, pp. 280–287, 2011.

[33] G. Bernstein, "Delivery of insulin to the buccal mucosa utilizing the RapidMist™ system," *Expert Opin. Drug Deliv.*, vol. 5, no. 9, pp. 1047–1055, 2008.

[34] P. Modi, M. Mihic, and A. Lewin, "The evolving role of oral insulin in the treatment of diabetes using a novel RapidMist™ system," *Diabetes. Metab. Res. Rev.*, vol. 18, no. 1, pp. 38–42, 2002.

[35] Midatech Pharma, "News Release: Initiation of Phase IIa study of insulin delivery via buccal strip for type 1 diabetes," 2015. [Online]. Available: http://www.midatechpharma.com/news/49/143/Initiation-of-Phase-IIa-study-of-insulin-delivery-via-buccal-strip-for-type-1-diabetes.html. [Accessed: 20-Mar-2017].

[36] J. O. Morales *et al.*, "Challenges and Future Prospects for the Delivery of Biologics: Oral Mucosal, Pulmonary, and Transdermal Routes," *AAPS J.*, vol. 19, no. 3, pp. 652–668, 2017.

[37] Midatech Pharma, "Midatech's primary platform technology is based on carbohydrate-coated gold nanoparticle (GNP) drug conjugates.," 2017. [Online]. Available: http://www.midatechpharma.com/gnp-technology. [Accessed: 20-Mar-2017].

[38] Midatech Pharma, "News Release: Midatech Pharma announces clinical pipeline update," 2016. [Online]. Available: http://www.midatechpharma.com/news/69/143/Midatech-Pharma-announces-clinical-pipeline-update.html. [Accessed: 21-Mar-2017].

[39] P. Fonte, F. Araujo, S. Reis, and B. Sarmento, "Oral insulin delivery: how far are we?," *J. Diabetes Sci. Technol.*, vol. 7, no. 2, pp. 520–531, 2013.

[40] Novo Nordisk, "Company announcement: Financial report for the period 1 January 2015 to 30 June 2015," 2015.

[41] Oramed Pharmaceuticals, "Technology," 2016. [Online]. Available: http://www.oramed.com/technology/. [Accessed: 05-Feb-2017].

[42]   R. Eldor, E. Arbit, A. Corcos, and M. Kidron, "Glucose-reducing effect of the ORMD-0801 oral insulin preparation in patients with uncontrolled type 1 diabetes: a pilot study," *PLoS One*, vol. 8, no. 4, p. e59524, 2013.

[43]   W. B. Geho, H. C. Geho, J. R. Lau, and T. J. Gana, "Hepatic-directed vesicle insulin: a review of formulation development and preclinical evaluation," *J. Diabetes Sci. Technol.*, vol. 3, no. 6, pp. 1451–1459, 2009.

[44]   Diasome   Pharmaceuticals,   "Pipeline,"   2016.   [Online].   Available: http://diasomepharmaceuticals.com/pipeline/. [Accessed: 11-Feb-2017].

[45]   S. D. Luzio, G. Dunseath, A. Lockett, T. P. Broke-Smith, R. R. New, and D. R. Owens, "The glucose lowering effect of an oral insulin (Capsulin) during an isoglycaemic clamp study in persons with type 2 diabetes," *Diabetes, Obes. Metab.*, vol. 12, no. 1, pp. 82–87, 2010.

[46]   O. Gribova and A. Vol, "Methods and compositions for oral administration of insulin," 20100278922, Apr-2010.

[47]   E. Zijlstra, L. Heinemann, and L. Plum-Mörschel, "Oral Insulin Reloaded: A Structured Approach," *J. Diabetes Sci. Technol.*, vol. 8, no. 3, pp. 458–465, 2014.

[48]   Biocon,   "Active   Discovery   Programs,"   2016.   [Online].   Available: http://www.biocon.com/biocon_research_discovery.asp.   [Accessed: 19-Feb-2017].

[49]   A. Khedkar *et al.*, "A dose range finding study of novel oral insulin (IN-105) under

fed conditions in type 2 diabetes mellitus subjects," *Diabetes, Obes. Metab.*, vol. 12, no. 8, pp. 659–664, 2010.

[50] Diabetology, "Capsulin," 2017. [Online]. Available: http://www.diabetology.co.uk/projects/capsulin/. [Accessed: 31-Mar-2018].

[51] Diabetology, "Axcess Oral Delivery System," 2017. [Online]. Available: http://www.diabetology.co.uk/technology/. [Accessed: 31-Mar-2018].

[52] A. Muheem *et al.*, "A review on the strategies for oral delivery of proteins and peptides and their clinical perspectives," *Saudi Pharm. J.*, vol. 24, no. 4, pp. 413–428, 2016.

[53] S. E. Swenson and W. J. Curatolo, "(C) Means to enhance penetration: (2) Intestinal permeability enhancement for proteins, peptides and other polar drugs: mechanisms and potential toxicity," *Adv. Drug Deliv. Rev.*, vol. 8, no. 1, pp. 39–92, 1992.

[54] CPEX Pharmaceuticals, "Permeation Enhancement Technology," 2011. [Online]. Available: http://www.cpexpharmaceuticals.com/permeation-technology.html. [Accessed: 19-Feb-2017].

[55] R. Stote, M. Miller, T. Marbury, L. Shi, and P. Strange, "Enhanced absorption of Nasulin™, an ultrarapid-acting intranasal insulin formulation, using single nostril administration in normal subjects," *J. Diabetes Sci. Technol.*, vol. 5, no. 1, pp. 113–119, 2011.

[56] A. C. Leary, M. Dowling, K. Cussen, J. O'Brien, and R. M. Stote,

"Pharmacokinetics and pharmacodynamics of intranasal insulin spray (Nasulin™) administered to healthy male volunteers: influence of the nasal cycle," *J. Diabetes Sci. Technol.*, vol. 2, no. 6, pp. 1054–1060, 2008.

[57] B. K. Redding, "Designing an ultrasound enabled patch for Insulin," *ONdrugDelivery*, pp. 22–26, May-2014.

[58] S. Shahani and L. Shahani, "Use of insulin in diabetes: a century of treatment.," *Hong Kong Med. J. = Xianggang yi xue za zhi*, vol. 21, no. 6, pp. 553–9, 2015.

[59] S. I. Pather, M. J. Rathbone, and S. Şenel, "Current status and the future of buccal drug delivery systems," *Expert Opinion on Drug Delivery*, vol. 5, no. 5. Taylor & Francis, pp. 531–542, May-2008.

[60] S. Bashyal, J. E. Seo, T. Keum, G. Noh, Y. W. Choi, and S. Lee, "Facilitated permeation of insulin across TR146 cells by cholic acid derivatives-modified elastic bilosomes," *Int. J. Nanomedicine*, vol. 13, pp. 5173–5186, 2018.

[61] M. Montenegro-Nicolini and J. O. Morales, "Overview and Future Potential of Buccal Mucoadhesive Films as Drug Delivery Systems for Biologics," *AAPS PharmSciTech*, vol. 18, no. 1, pp. 3–14, Feb. 2017.

[62] V. F. Patel, F. Liu, and M. B. Brown, "Advances in oral transmucosal drug delivery," *Journal of Controlled Release*, vol. 153, no. 2. pp. 106–116, 30-Jul-2011.

[63] T. P. Johnston, "Anatomy and Physiology of the Oral Mucosa," in *Oral Mucosal Drug Delivery and Therapy*, M. J. Rathbone, I. Pather, and S. Şenel, Eds.

Springer, Boston, MA, 2015, pp. 1–15.

[64] T. Caon, L. Jin, C. M. O. Simões, R. S. Norton, and J. A. Nicolazzo, "Enhancing the buccal mucosal delivery of peptide and protein therapeutics," *Pharmaceutical Research*, vol. 32, no. 1. Springer New York LLC, pp. 1–21, 2015.

[65] C. A. Squier and P. W. Wertz, "Structure and function of the oral mucosa and implications for drug delivery," *New York Marcel Dekker*, pp. 1–26, 1996.

[66] P. W. Wertz, D. C. Swartzendruber, and C. A. Squier, "Regional variation in the structure and permeability of oral mucosa and skin," *Advanced Drug Delivery Reviews*, vol. 12, no. 1–2. Elsevier, pp. 1–12, 1993.

[67] S. Law, P. W. Wertz, D. C. Swartzendruber, and C. A. Squier, "Regional variation in content, composition and organization of porcine epithelial barrier lipids revealed by thin-layer chromatography and transmission electron microscopy," *Arch. Oral Biol.*, vol. 40, no. 12, pp. 1085–1091, 1995.

[68] I. Diaz-Del Consuelo, Y. Jacques, G. P. Pizzolato, R. H. Guy, and F. Falson, "Comparison of the lipid composition of porcine buccal and esophageal permeability barriers," *Arch. Oral Biol.*, vol. 50, no. 12, pp. 981–987, 2005.

[69] M. J. Rathbone and I. G. Tucker, "Mechanisms, barriers and pathways of oral mucosal drug permeation," *Adv. Drug Deliv. Rev.*, vol. 12, no. 1–2, pp. 41–60, 1993.

[70] E. C. I. Veerman, P. A. M. Keybus, A. Vissink, and A. V. N. Amerongen, "Human glandular salivas: their separate collection and analysis," *Eur. J. Oral Sci.*, vol.

104, no. 4, pp. 346–352, 1996.

[71]   A. Bardow, J. Madsen, and B. Nauntofte, "The bicarbonate concentration in human saliva does not exceed the plasma level under normal physiological conditions," *Clin. Oral Investig.*, vol. 4, no. 4, pp. 245–253, 2000.

[72]   N. Salamat-Miller, M. Chittchang, and T. P. Johnston, "The use of mucoadhesive polymers in buccal drug delivery," *Advanced Drug Delivery Reviews*, vol. 57, no. 11. pp. 1666–1691, 2005.

[73]   K. Edsman and H. Hägerström, "Pharmaceutical applications of mucoadhesion for the non-oral routes," *J. Pharm. Pharmacol.*, vol. 57, no. 1, pp. 3–22, 2005.

[74]   D. S. Jones, A. D. Woolfson, J. Djokic, and W. A. Coulter, "Development and mechanical characterization of bioadhesive semi-solid, polymeric systems containing tetracycline for the treatment of periodontal diseases," *Pharm. Res.*, vol. 13, no. 11, pp. 1734–1738, 1996.

[75]   J. C. McElnay and C. M. Hughes, "Drug Delivery: Buccal route," in *Encyclopedia of Pharmaceutical Technology*, Third Edit., J. Swarbrick, Ed. Pinehurst, North Carolinia: Informa Healthcare USA, Inc., 2007, pp. 1071–1081.

[76]   R. B. Gandhi and J. R. Robinson, "Oral cavity as a site for bioadhesive drug delivery," *Advanced Drug Delivery Reviews*, vol. 13, no. 1–2. Elsevier, pp. 43–74, 1994.

[77]   S. Verma, M. Kaul, A. Rawat, and S. Saini, "An overview on buccal drug delivery system," *Int. J. Pharm. Sci. Res.*, vol. 2, no. 6, pp. 1303–1321, 2011.

[78]   J. Chen, W. L. Lu, W. Gu, S. S. Lu, Z. P. Chen, and B. C. Cai, "Skin permeation behavior of elastic liposomes: Role of formulation ingredients," *Expert Opin. Drug Deliv.*, vol. 10, no. 6, pp. 845–856, 2013.

[79]   R. Bnyan *et al.*, "Formulation and optimisation of novel transfersomes for sustained release of local anaesthetic," *J. Pharm. Pharmacol.*, vol. 71, no. 10, pp. 1508–1519, 2019.

[80]   A. Sharma, L. Kumar, P. Kumar, N. Prasad, and V. Rastogi, "Niosomes: A Promising Approach in Drug Delivery Systems," *J. Drug Deliv. Ther.*, vol. 9, no. 4, pp. 635–642, 2019.

[81]   A. Bagheri, B.-S. S. Chu, H. Yaakob, A. Bagheri, and B.-S. S. Chu, "Niosomal Drug Delivery Systems: Formulation, Preparation and Applications," *World Appl. Sci. J.*, vol. 32, no. 8, pp. 1671–1685, 2014.

[82]   P. Yeo, C. Lim, S. Chye, and A. Ling, "Niosomes: a review of their structure, properties, methods of preparation, and medical applications," *Asian Biomed.*, vol. 11, no. 4, pp. 301–314, 2018.

[83]   I. F. Uchegbu and S. P. Vyas, "Non-ionic surfactant based vesicles (niosomes) in drug delivery," *Int. J. Pharm.*, vol. 172, no. 1–2, pp. 33–70, 1998.

[84]   P. . Gadhiya, S. . Shukla, D. . Modi, and P. Bharadia, "Niosomes in Targeted Drug Delivery – A Review ," *Int. J. Pharm. Res. Sch.*, vol. 1, no. 2, pp. 59–72, 2012.

[85]   A. Pardakhty, J. Varshosaz, and A. Rouholamini, "In vitro study of

polyoxyethylene alkyl ether niosomes for delivery of insulin," *Int. J. Pharm.*, vol. 328, no. 2, pp. 130–141, 2007.

[86] F. Szoka and D. Papahadjopoulos, "Procedure for preparation of liposomes with large internal aqueous space and high capture by reverse-phase evaporation," *Proc. Natl. Acad. Sci. U. S. A.*, vol. 75, no. 9, pp. 4194–4198, 1978.

[87] A. J. Baillie, A. T. Florence, L. R. Hume, G. T. Muirhead, and A. Rogerson, "The preparation and properties of niosomes-non-ionic surfactant vesicles," *J. Pharm. Pharmacol.*, vol. 37, no. 12, pp. 863–868, 1985.

[88] K. M. Kazi *et al.*, "Niosome: A future of targeted drug delivery systems," *J. Adv. Pharm. Technol. Res.*, vol. 1, no. 4, pp. 374–380, 2010.

[89] A. D. Bangham, M. M. Standish, and J. C. Watkins, "Diffusion of univalent ions across the lamellae of swollen phospholipids," *J. Mol. Biol.*, vol. 13, no. 1, pp. 238–252, Aug. 1965.

[90] U. Bulbake, S. Doppalapudi, N. Kommineni, and W. Khan, "Liposomal formulations in clinical use: An updated review," *Pharmaceutics*, vol. 9, no. 2. MDPI AG, 2017.

[91] B. Z. Jin, X. Q. Dong, X. Xu, and F. H. Zhang, "Development and in vitro evaluation of mucoadhesive patches of methotrexate for targeted delivery in oral cancer," *Oncol. Lett.*, vol. 15, no. 2, pp. 2541–2549, 2018.

[92] Y. Barenholz, "Doxil® - The first FDA-approved nano-drug: Lessons learned," *Journal of Controlled Release*, vol. 160, no. 2. pp. 117–134, 2012.

[93]   R. Rajera, K. Nagpal, S. K. Singh, and D. N. Mishra, "Niosomes: a controlled and novel drug delivery system," *Biol. Pharm. Bull.*, vol. 34, no. 7, pp. 945–953, 2011.

[94]   M. Gharbavi, J. Amani, H. Kheiri-Manjili, H. Danafar, and A. Sharafi, "Niosome: A Promising Nanocarrier for Natural Drug Delivery through Blood-Brain Barrier," *Adv. Pharmacol. Sci.*, 2018.

[95]   J. Malakar, S. O. Sen, A. K. Nayak, and K. K. Sen, "Formulation, optimization and evaluation of transferosomal gel for transdermal insulin delivery," *Saudi Pharm. J.*, vol. 20, no. 4, pp. 355–363, 2012.

[96]   T. Goswami, B. R. Jasti, and X. Li, "Estimation of the theoretical pore sizes of the porcine oral mucosa for permeation of hydrophilic permeants," *Arch. Oral Biol.*, vol. 54, no. 6, pp. 577–582, Jun. 2009.

[97]   H. Abdelkader, A. W. G. Alani, and R. G. Alany, "Recent advances in non-ionic surfactant vesicles (niosomes): Self-assembly, fabrication, characterization, drug delivery applications and limitations," *Drug Deliv.*, vol. 21, no. 2, pp. 87–100, 2014.

[98]   G. Cevc, D. Gebauer, J. Stieber, A. Schätzlein, and G. Blume, "Ultraflexible vesicles, Transfersomes, have an extremely low pore penetration resistance and transport therapeutic amounts of insulin across the intact mammalian skin," *Biochim. Biophys. Acta - Biomembr.*, vol. 1368, no. 2, pp. 201–215, 1998.

[99]   A. Gupta, G. Aggarwal, S. Singla, and R. Arora, "Transfersomes: A novel vesicular carrier for enhanced transdermal delivery of sertraline: Development, characterization, and performance evaluation," *Sci. Pharm.*, vol. 80, no. 4, pp.

1061–1080, 2012.

[100] T. Garg, S. Jain, H. P. Singh, A. Sharma, and A. K. Tiwary, "Elastic liposomal formulation for sustained delivery of antimigraine drug: In vitro characterization and biological evaluation," *Drug Dev. Ind. Pharm.*, vol. 34, no. 10, pp. 1100–1110, 2008.

[101] D. Mishra, M. Garg, V. Dubey, S. Jain, and N. K. Jain, "Elastic liposomes mediated transdermal delivery of an anti-hypertensive agent: Propranolol hydrochloride," *J. Pharm. Sci.*, vol. 96, no. 1, pp. 145–155, 2007.

[102] W. M. Haschek, C. G. Rousseaux, and M. A. Wallig, "Skin and Oral Mucosa," in *Fundamentals of Toxicologic Pathology*, Elsevier, 2010, pp. 135–161.

[103] S. Raahulan, B. K. R. Sanapalli, V. V. S. R. Karri, and S. K. S. S. Pindiprolu, "Transfersome vs liposomes as drug delivery vehicle for the treatment of skin cancers," *Int. J. Res. Pharm. Sci.*, vol. 10, no. 3, pp. 1795–1807, 2019.

[104] T. Yoshioka, B. Sternberg, and A. T. Florence, "Preparation and properties of vesicles (niosomes) of sorbitan monoesters (Span 20, 40, 60 and 80) and a sorbitan triester (Span 85)," *Int. J. Pharm.*, vol. 105, no. 1, pp. 1–6, 1994.

[105] E. A. Essa, "Effect of formulation and processing variables on the particle size of sorbitan monopalmitate niosomes," *Asian J. Pharm. Free full text Artic. from Asian J Pharm*, vol. 4, no. 4, 2014.

[106] T. Yang *et al.*, "Enhanced solubility and stability of PEGylated liposomal paclitaxel: In vitro and in vivo evaluation," *Int. J. Pharm.*, vol. 338, no. 1–2, pp.

317–326, 2007.

[107] K. Bin Liew, M. A. Odeniyi, and K.-K. Peh, "Application of freeze-drying technology in manufacturing orally disintegrating films," *Pharm. Dev. Technol.*, vol. 21, no. 3, pp. 346–353, 2016.

[108] S. Verma and N. Kumar, "Buccal Film: An Advance Technology for Oral Drug Delivery," *Adv. Biol. Res. (Rennes).*, vol. 8, no. 6, pp. 260–267, 2014.

[109] M. Maniruzzaman, J. S. Boateng, M. J. Snowden, and D. Douroumis, "A Review of Hot-Melt Extrusion: Process Technology to Pharmaceutical Products," *ISRN Pharm.*, pp. 1–9, 2012.

[110] A. Portero, C. Remuñán-López, and H. M. Nielsen, "The potential of chitosan in enhancing peptide and protein absorption across the TR146 cell culture model - An in vitro model of the buccal epithelium," *Pharm. Res.*, vol. 19, no. 2, pp. 169–174, 2002.

[111] I. Ayensu, J. C. Mitchell, and J. S. Boateng, "Effect of membrane dialysis on characteristics of lyophilised chitosan wafers for potential buccal delivery of proteins," *Int. J. Biol. Macromol.*, vol. 50, no. 4, pp. 905–909, 2012.

[112] J. O. Morales and J. T. McConville, "Manufacture and characterization of mucoadhesive buccal films," *European Journal of Pharmaceutics and Biopharmaceutics*, vol. 77, no. 2. pp. 187–199, 2011.

[113] J. D. Smart, "The basics and underlying mechanisms of mucoadhesion," *Advanced Drug Delivery Reviews*, vol. 57, no. 11. pp. 1556–1568, 2005.

[114] R. Shaikh, T. Raj Singh, M. Garland, A. Woolfson, and R. Donnelly, "Mucoadhesive drug delivery systems," *Journal of Pharmacy and Bioallied Sciences*, vol. 3, no. 1. pp. 89–100, 2011.

[115] S. A. Mortazavi and J. D. Smart, "An investigation of some factors influencing the in vitro assessment of mucoadhesion," *Int. J. Pharm.*, vol. 116, no. 2, pp. 223–230, 1995.

[116] M. M. Patel, J. D. Smart, T. G. Nevell, R. J. Ewen, P. J. Eaton, and J. Tsibouklis, "Mucin/poly(acrylic acid) interactions: A spectroscopic investigation of mucoadhesion," *Biomacromolecules*, vol. 4, no. 5, pp. 1184–1190, 2003.

[117] E. Russo *et al.*, "A focus on mucoadhesive polymers and their application in buccal dosage forms," *J. Drug Deliv. Sci. Technol.*, vol. 32, pp. 113–125, 2016.

[118] N. A. Nafee, F. A. Ismail, N. A. Boraie, and L. M. Mortada, "Mucoadhesive delivery systems. I. Evaluation of mucoadhesive polymers for buccal tablet formulation.," *Drug Dev. Ind. Pharm.*, vol. 30, no. 9, pp. 985–93, 2004.

[119] L. Illum, "Chitosan and its use as a pharmaceutical excipient.," *Pharm. Res.*, vol. 15, no. 9, pp. 1326–31, 1998.

[120] N. Islam, I. Dmour, and M. O. Taha, "Degradability of chitosan micro/nanoparticles for pulmonary drug delivery," *Heliyon*, vol. 5, no. 5. p. e01684, 2019.

[121] M. A. Mohammed, J. T. M. Syeda, K. M. Wasan, and E. K. Wasan, "An overview of chitosan nanoparticles and its application in non-parenteral drug delivery,"

Pharmaceutics, vol. 9, no. 4. 2017.

[122] K. Kumar, N. Dhawan, H. Sharma, S. Vaidya, and B. Vaidya, "Bioadhesive polymers: Novel tool for drug delivery," *Artif. Cells, Nanomedicine, Biotechnol.*, vol. 42, no. 4, pp. 274–283, 2014.

[123] B. Menchicchi *et al.*, "Biophysical Analysis of the Molecular Interactions between Polysaccharides and Mucin," *Biomacromolecules*, vol. 16, no. 3, pp. 924–935, 2015.

[124] A. K. Singla, M. Chawla, and A. Singh, "Potential Applications of Carbomer in Oral Mucoadhesive Controlled Drug Delivery System: A Review," *Drug Dev. Ind. Pharm.*, vol. 26, no. 9, p. 913, 2000.

[125] G. Bonacucina, S. Martelli, and G. F. Palmieri, "Rheological, mucoadhesive and release properties of Carbopol gels in hydrophilic cosolvents," *Int. J. Pharm.*, vol. 282, no. 1–2, pp. 115–130, 2004.

[126] M. Aulton and S. Somavarapu, "Dosage form design and manufacture: Drying," in *Aulton's Pharmaceutics E-Book: The Design and Manufacture of Medicines*, 5th ed., M. E. Aulton and K. M. G. Taylor, Eds. Elsevier, 2017, p. 514.

[127] I. F. Uchegbu and A. G. Schätzlein, "Dosage form design and manufacture: Delivery of biopharmaceuticals," in *Aulton's Pharmaceutics E-Book: The Design and Manufacture of Medicines*, 5th ed., M. E. Aulton and K. M. G. Taylor, Eds. Elsevier, 2017, p. 776.

[128] P. Fonte *et al.*, "Stability study perspective of the effect of freeze-drying using

cryoprotectants on the structure of insulin loaded into PLGA nanoparticles," *Biomacromolecules*, vol. 15, no. 10, pp. 3753–3765, 2014.

[129] P. York, "Design of dosage forms," in *Aulton's Pharmaceutics E-Book: The Design and Manufacture of Medicines*, 5th ed., M. E. Aulton and K. M. G. Taylor, Eds. Elsevier, 2017, pp. 12–17.

[130] G. Radhakant, B. Himankar, and Z. Qing, "Application of Mathematical Models in Drug Release Kinetics of Carbidopa and Levodopa ER Tablets," *J. Dev. Drugs*, vol. 6, no. 2, pp. 1–6, 2017.

[131] S. Dash, N. P. Murthy, L. Nath, and P. Chowdhury, "Kinetic modeling on drug release from controlled drug delivery systems.," *Acta Pol. Pharm.*, vol. 67, no. 3, pp. 217–223, 2010.

[132] A. Jain and S. K. Jain, "In vitro release kinetics model fitting of liposomes: An insight," *Chemistry and Physics of Lipids*, vol. 201. pp. 28–40, 2016.

[133] H. K. Shaikh, R. V. Kshirsagar, and S. G. Patil, "Mathematical models for drug release characterization: a review," *World J. Pharm. Pharm. Sci.*, vol. 4, no. 4, pp. 324–338, 2015.

[134] T. Higuchi, "Mechanism of sustained-action medication. Theoretical analysis of rate of release of solid drugs dispersed in solid matrices," *J. Pharm. Sci.*, vol. 52, no. 12, pp. 1145–1149, 1963.

[135] R. W. Korsmeyer, R. Gurny, E. Doelker, P. Buri, and N. A. Peppas, "Mechanisms of solute release from porous hydrophilic polymers," *Int. J. Pharm.*, vol. 15, no.

1, pp. 25–35, 1983.

[136] P. L. Ritger and N. A. Peppas, "A simple equation for description of solute release I. Fickian and non-fickian release from non-swellable devices in the form of slabs, spheres, cylinders or discs," *J. Control. Release*, vol. 5, no. 1, pp. 23–36, 1987.

[137] S. M. Darby, M. L. Miller, R. O. Allen, and M. LeBeau, "A Mass Spectrometric Method for Quantitation of Intact Insulin in Blood Samples," *J. Anal. Toxicol.*, vol. 25, no. 1, pp. 8–14, 2001.

[138] Y. Shen, W. Prinyawiwatkul, and Z. Xu, "Insulin: A review of analytical methods," *Analyst*, vol. 144, no. 14. Royal Society of Chemistry, pp. 4139–4148, 2019.

[139] T. Waritani, J. Chang, B. McKinney, and K. Terato, "An ELISA protocol to improve the accuracy and reliability of serological antibody assays," *MethodsX*, vol. 4, pp. 153–165, 2017.

[140] I. A. Darwish, "Immunoassay Methods and their Applications in Pharmaceutical Analysis: Basic Methodology and Recent Advances.," *Int. J. Biomed. Sci.*, vol. 2, no. 3, pp. 217–35, 2006.

[141] S. Sakamoto *et al.*, "Enzyme-linked immunosorbent assay for the quantitative/qualitative analysis of plant secondary metabolites," *Journal of Natural Medicines*, vol. 72, no. 1. Springer Tokyo, pp. 32–42, 2018.

[142] H. Li, X. Liu, L. Li, X. Mu, R. Genov, and A. J. Mason, "CMOS electrochemical instrumentation for biosensor microsystems: A review," *Sensors (Switzerland)*,

vol. 17, no. 1. MDPI AG, pp. 1–26, 2017.

[143] A. Najjar, M. Alawi, N. AbuHeshmeh, and A. Sallam, "A Rapid, Isocratic HPLC Method for Determination of Insulin and Its Degradation Product," *Hindawi Publ. Corp.*, pp. 1–6, 2014.

[144] M. I. Aguilar, "Reversed-phase high-performance liquid chromatography.," in *HPLC of Peptides and Proteins. Methods in molecular biology.*, vol. 251, Springer, Totowa, NJ, 2004, pp. 9–22.

[145] J. G. Dorsey and K. A. Dill, "The Molecular Mechanism of Retention in Reversed-Phase Liquid Chromatography," *Chem. Rev.*, vol. 89, no. 2, pp. 331–346, 1989.

[146] M. I. Aguilar and M. T. W. Hearn, "High-resolution reversed phase high-performance liquid chromatography of peptides and proteins," *Methods in Enzymology*, vol. 270. Academic Press Inc., pp. 3–26, 1996.

[147] ICH, "ICH Q2 (R1) Validation of analytical procedures: text and methodology," London, 1995.

[148] ICH, "ICH Q2(R1) Validation of Analytical Procedures: Text and Methodology," 2005.

[149] B. Sarmento, A. Ribeiro, F. Veiga, and D. Ferreira, "Development and validation of a rapid reversed-phase HPLC method for the determination of insulin from nanoparticulate systems," *Biomed. Chromatogr.*, vol. 20, no. 9, pp. 898–903, 2006.

[150] S. Ravi, K. K. Peh, Y. Darwis, B. Krishna Murthy, and T. Raghu Raj Singh,

"Development and validation of an HPLC-UV method for the determination of insulin in rat plasma: Application to pharmacokinetic study," *Chromatographia*, vol. 66, no. 9–10, pp. 805–809, 2007.

[151] R. Rayasam, "Oral delivery of insulin for diabetes therapy : the design, fabrication and characterisation of a modified-chitosan based nanoparticle system," Kingston University, London, 2017.

[152] J. Brange, L. Langkj\sgmaelig;r, S. Havelund, and A. Vølund, "Chemical Stability of Insulin. 1. Hydrolytic Degradation During Storage of Pharmaceutical Preparations," *Pharm. Res. An Off. J. Am. Assoc. Pharm. Sci.*, vol. 9, no. 6, pp. 715–726, 1992.

[153] J. Brange and L. Langkjoer, "Insulin structure and stability.," *Pharmaceutical biotechnology*, vol. 5. pp. 315–350, 1993.

[154] A. Oliva, J. B. Fariña, and M. Llabrés, "Influence of temperature and shaking on stability of insulin preparations: Degradation kinetics," *Int. J. Pharm.*, vol. 143, no. 2, pp. 163–170, 1996.

[155] S. Ruiz, M. Bernad, S. Chacon, and D. Estrada, "Glucose Response in Animals Induced With Experimental Diabetes Type 1 after Treatment with Human Insulin Exposed To High Temperatures," *Transylvanian Rev.*, vol. 25, no. 23, pp. 6189–6196, 2017.

[156] Z. Al-Kurdi, B. Chowdhry, S. Leharne, M. Al Omari, and A. Badwan, "Low Molecular Weight Chitosan–Insulin Polyelectrolyte Complex: Characterization and Stability Studies," *Mar. Drugs*, vol. 13, no. 4, pp. 1765–1784, 2015.

[157] B. Moussa, F. Farouk, and H. Azzazy, "A validated RP-HPLC method for the determination of recombinant human insulin in bulk and pharmaceutical dosage form," *J. Chem.*, pp. 449–457, 2010.

[158] G. P. Kumar and P. Rajeshwarrao, "Nonionic surfactant vesicular systems for effective drug delivery—an overview," *Acta Pharm. Sin. B*, vol. 1, no. 4, pp. 208–219, 2011.

[159] D. Ag Seleci, M. Seleci, J.-G. Walter, F. Stahl, and T. Scheper, "Niosomes as Nanoparticular Drug Carriers: Fundamentals and Recent Applications," *Hindawi Publ. Corp.*, pp. 1–13, 2016.

[160] A. Shahiwala and A. Misra, "Studies in topical application of niosomally entrapped Nimesulide," *J. Pharm. Pharm. Sci.*, vol. 5, no. 3, pp. 220–225, 2002.

[161] J. N. Israelachvili, D. J. Mitchell, and B. W. Ninham, "Theory of self-assembly of hydrocarbon amphiphiles into micelles and bilayers," *Journal of the Chemical Society, Faraday Transactions 2: Molecular and Chemical Physics*, vol. 72, no. 0. The Royal Society of Chemistry, pp. 1525–1568, 1976.

[162] J. Varshosaz, A. Pardakhty, V. I. Hajhashemi, and A. R. Najafabadi, "Development and physical characterization of sorbitan monoester niosomes for insulin oral delivery," *Drug Deliv.*, vol. 10, no. 4, pp. 251–262, 2003.

[163] K. Sahil, S. Premjeet, B. Ajay, A. Middha, and B. Kapoor, "Stealth liposomes: a review," *Artic. Int. J. Res. Ayurveda Pharm.*, vol. 2, no. 5, pp. 1534–1538, 2011.

[164] S. Naeem, L. V. Kiew, L. Y. Chung, V. R. E. Suk, A. Mahmood, and M. Bin

Misran, "Optimization of Phospholipid Nanoparticle Formulations Using Response Surface Methodology," *J. Surfactants Deterg.*, vol. 19, no. 1, pp. 67–74, 2016.

[165] T. J. McIntosh, "The effect of cholesterol on the structure of phosphatidylcholine bilayers," *BBA - Biomembr.*, vol. 513, no. 1, pp. 43–58, 1978.

[166] N. Mali, S. Darandale, and P. Vavia, "Niosomes as a vesicular carrier for topical administration of minoxidil: Formulation and in vitro assessment," *Drug Deliv. Transl. Res.*, vol. 3, no. 6, pp. 587–592, 2013.

[167] S. Taymouri and J. Varshosaz, "Effect of different types of surfactants on the physical properties and stability of carvedilol nano-niosomes," *Adv. Biomed. Res.*, vol. 5, no. 1, p. 48, 2016.

[168] V. C. Okore, A. A. Attama, K. C. Ofokansi, C. O. Esimone, and E. B. Onuigbo, "Formulation and evaluation of niosomes," *Indian J. Pharm. Sci.*, vol. 73, no. 3, pp. 323–328, 2011.

[169] F. Nowroozi, A. Almasi, J. Javidi, A. Haeri, and S. Dadashzadeh, "Effect of surfactant type, cholesterol content and various downsizing methods on the particle size of niosomes," *Iran. J. Pharm. Res.*, vol. 17, no. 2, pp. 1–11, 2018.

[170] A. S. Yagoubi, F. Shahidi, M. Mohebbi, M. Varidi, and S. Golmohammadzadeh, "Preparation, characterization and evaluation of physicochemical properties of phycocyanin-loaded solid lipid nanoparticles and nanostructured lipid carriers," *J. Food Meas. Charact.*, pp. 1–8, 2017.

[171] A. Barhoum, M. L. García-Betancourt, H. Rahier, and G. Van Assche, "Physicochemical characterization of nanomaterials: Polymorph, composition, wettability, and thermal stability," in *Emerging Applications of Nanoparticles and Architectural Nanostructures: Current Prospects and Future Trends*, Elsevier Inc., 2018, pp. 255–278.

[172] C. J. Chirayil, J. Abraham, R. K. Mishra, S. C. George, and S. Thomas, "Instrumental Techniques for the Characterization of Nanoparticles," in *Thermal and Rheological Measurement Techniques for Nanomaterials Characterization*, vol. 3, Elsevier, 2017, pp. 1–36.

[173] Z. Sezgin-Bayindir, M. N. Antep, and N. Yuksel, "Development and Characterization of Mixed Niosomes for Oral Delivery Using Candesartan Cilexetil as a Model Poorly Water-Soluble Drug," *AAPS PharmSciTech*, vol. 16, no. 1, pp. 108–117, 2014.

[174] S. Jain, P. Jain, R. B. Umamaheshwari, and N. K. Jain, "Transfersomes--a novel vesicular carrier for enhanced transdermal delivery: development, characterization, and performance evaluation.," *Drug Dev. Ind. Pharm.*, vol. 29, no. 9, pp. 1013–26, 2003.

[175] G. M. El Zaafarany, G. A. S. Awad, S. M. Holayel, and N. D. Mortada, "Role of edge activators and surface charge in developing ultradeformable vesicles with enhanced skin delivery," *Int. J. Pharm.*, vol. 397, no. 1–2, pp. 164–172, 2010.

[176] R. N. Shamma and I. Elsayed, "Transfersomal lyophilized gel of buspirone HCl: Formulation, evaluation and statistical optimization," *J. Liposome Res.*, vol. 23,

no. 3, pp. 244–254, 2013.

[177] G. Cevc, S. Mazgareanu, M. Rother, and U. Vierl, "Occlusion effect on transcutaneous NSAID delivery from conventional and carrier-based formulations," *Int. J. Pharm.*, vol. 359, no. 1–2, pp. 190–197, Jul. 2008.

[178] T. A. Khan, H. C. Mahler, and R. S. K. Kishore, "Key interactions of surfactants in therapeutic protein formulations: A review," *European Journal of Pharmaceutics and Biopharmaceutics*, vol. 97, no. Pt A. Elsevier, pp. 60–67, 2015.

[179] A. Hillgren, J. Lindgren, and M. Aldén, "Protection mechanism of Tween 80 during freeze-thawing of a model protein, LDH," *Int. J. Pharm.*, vol. 237, no. 1–2, pp. 57–69, 2002.

[180] C. Sinico and A. M. Fadda, "Vesicular carriers for dermal drug delivery," *Expert Opinion on Drug Delivery*, vol. 6, no. 8. pp. 813–825, 2009.

[181] P. Prakash *et al.*, "Candesertan niosomes-formulation and evaluation using Span 60 as non-ionic surafactant," *J. Chem. Pharm. Res.*, vol. 7, no. 7, pp. 940–949, 2015.

[182] R. Dawaliby *et al.*, "Phosphatidylethanolamine is a key regulator of membrane fluidity in eukaryotic cells," *J. Biol. Chem.*, vol. 291, no. 7, pp. 3658–3667, 2016.

[183] R. Lipowsky, "Remodeling of membrane compartments: some consequences of membrane fluidity," *Biol. Chem.*, vol. 395, no. 3, pp. 253-274., 2014.

[184] P. L. Yeagle, "Cholesterol and the cell membrane," *BBA - Reviews on*

Biomembranes, vol. 822, no. 3–4. Elsevier, pp. 267–287, 1985.

[185] J. N. van der Veen, J. P. Kennelly, S. Wan, J. E. Vance, D. E. Vance, and R. L. Jacobs, "The critical role of phosphatidylcholine and phosphatidylethanolamine metabolism in health and disease," *Biochimica et Biophysica Acta - Biomembranes*, vol. 1859, no. 9. Elsevier B.V., pp. 1558–1572, 2017.

[186] M. Rahbarian, E. Mortazavian, F. A. Dorkoosh, and M. Rafiee Tehrani, "Preparation, evaluation and optimization of nanoparticles composed of thiolated triethyl chitosan: A potential approach for buccal delivery of insulin," *J. Drug Deliv. Sci. Technol.*, vol. 44, pp. 254–263, 2018.

[187] D. C. Litzinger, A. M. J. Buiting, N. van Rooijen, and L. Huang, "Effect of liposome size on the circulation time and intraorgan distribution of amphipathic poly(ethylene glycol)-containing liposomes," *BBA - Biomembr.*, vol. 1190, no. 1, pp. 99–107, 1994.

[188] P. Goyal, K. Goyal, S. G. V. Kumar, A. Singh, O. P. Katare, and D. N. Mishra, "Liposomal drug delivery systems - Clinical applications," *Acta Pharmaceutica*, vol. 55, no. 1. pp. 1–25, 2005.

[189] S. G. M. Ong, L. C. Ming, K. S. Lee, and K. H. Yuen, "Influence of the encapsulation efficiency and size of liposome on the oral bioavailability of griseofulvin-loaded liposomes," *Pharmaceutics*, vol. 8, no. 3, 2016.

[190] F. C. Szoka, D. Milholland, and M. Barza, "Effect of lipid composition and liposome size on toxicity and in vitro fungicidal activity of liposome-intercalated amphotericin B," *Antimicrob. Agents Chemother.*, vol. 31, no. 3, pp. 421–429,

1987.

[191] M. Danaei *et al.*, "pharmaceutics Impact of Particle Size and Polydispersity Index on the Clinical Applications of Lipidic Nanocarrier Systems," *Pharm. MDPI*, pp. 1–17, 2018.

[192] S. Hua, "Lipid-based nano-delivery systems for skin delivery of drugs and bioactives," *Frontiers in Pharmacology*, vol. 6, no. 219. Frontiers Media S.A., pp. 1–5, 2015.

[193] M. Ramezani, M. Khoshhamdam, A. Dehshahri, and B. Malaekeh-Nikouei, "The influence of size, lipid composition and bilayer fluidity of cationic liposomes on the transfection efficiency of nanolipoplexes," *Colloids Surfaces B Biointerfaces*, vol. 72, no. 1, pp. 1–5, 2009.

[194] X. Ge, M. Wei, S. He, and W. E. Yuan, "Advances of non-ionic surfactant vesicles (niosomes) and their application in drug delivery," *Pharmaceutics*, vol. 11, no. 2. MDPI AG, 2019.

[195] M. M. A. Elsayed, O. Y. Abdallah, V. F. Naggar, and N. M. Khalafallah, "Deformable liposomes and ethosomes as carriers for skin delivery of ketotifen.," *Pharmazie*, vol. 62, no. 2, pp. 133–7, 2007.

[196] S. N. Kang, S. S. Hong, S. Y. Kim, H. Oh, M. K. Lee, and S. J. Lim, "Enhancement of liposomal stability and cellular drug uptake by incorporating tributyrin into celecoxib-loaded liposomes," *Asian J. Pharm. Sci.*, vol. 8, no. 2, pp. 138–148, Apr. 2013.

[197] A. K. Sahu, J. Mishra, and A. K. Mishra, "Introducing Tween-curcumin niosomes: Preparation, characterization and microenvironment study," *Soft Matter*, vol. 16, no. 7, pp. 1779–1791, 2020.

[198] A. H. Al Shuwaili, B. K. A. Rasool, and A. A. Abdulrasool, "Optimization of elastic transfersomes formulations for transdermal delivery of pentoxifylline," *Eur. J. Pharm. Biopharm.*, vol. 102, pp. 101–114, 2016.

[199] H. M. El-Laithy, O. Shoukry, and L. G. Mahran, "Novel sugar esters proniosomes for transdermal delivery of vinpocetine: Preclinical and clinical studies," *Eur. J. Pharm. Biopharm.*, vol. 77, no. 1, pp. 43–55, 2011.

[200] N. Berger, A. Sachse, J. Bender, R. Schubert, and M. Brandl, "Filter extrusion of liposomes using different devices: Comparison of liposome size, encapsulation efficiency, and process characteristics," *Int. J. Pharm.*, vol. 223, no. 1–2, pp. 55–68, 2001.

[201] G. M. Shashidhar and B. Manohar, "Nanocharacterization of liposomes for the encapsulation of water soluble compounds from Cordyceps sinensis CS1197 by a supercritical gas anti-solvent technique," *RSC Adv.*, vol. 8, no. 60, pp. 34634–34649, 2018.

[202] A. Priprem, K. Janpim, S. Nualkaew, and P. Mahakunakorn, "Topical Niosome Gel of Zingiber cassumunar Roxb. Extract for Anti-inflammatory Activity Enhanced Skin Permeation and Stability of Compound D," *AAPS PharmSciTech*, vol. 17, no. 3, pp. 631–639, 2016.

[203] M. Han, S. Watarai, K. Kobayashi, and T. Yasuda, "Application of liposomes for

development of oral vaccines: Study of in vitro stability of liposomes and antibody response to antigen associated with liposomes after oral immunization," *J. Vet. Med. Sci.*, vol. 59, no. 12, pp. 1109–1114, 1997.

[204] M. C. Taira, N. S. Chiaramoni, K. M. Pecuch, and S. Alonso-Romanowski, "Stability of Liposomal Formulations in Physiological Conditions for Oral Drug Delivery," *Drug Deliv.*, vol. 11, no. 2, pp. 123–128, 2004.

[205] I. F. Uchegbu, J. A. Double, J. A. Turton, and A. T. Florence, "Distribution, metabolism and tumoricidal activity of doxorubicin administered in sorbitan monostearate (Span 60) niosomes in the mouse.," *Pharm. Res.*, vol. 12, no. 7, pp. 1019–24, 1995.

[206] A. Rajnish and S. Ajay, "Release studies of Ketoprofen niosome formulation," *J. Chem. Pharm. Res.*, vol. 2, no. 1, pp. 79–82, 2010.

[207] M. Hussain, N. Forbes, and Y. Perrie, "Comparative Analysis of Protein Quantification Methods for the Rapid Determination of Protein Loading in Liposomal Formulations," *Pharmaceutics*, vol. 11, no. 1, p. 39, 2019.

[208] P. Chinna Reddy, K. S. C. Chaitanya, and Y. Madhusudan Rao, "A review on bioadhesive buccal drug delivery systems: Current status of formulation and evaluation methods," *DARU, Journal of Pharmaceutical Sciences*, vol. 19, no. 6. pp. 385–403, 2011.

[209] C. Sander, H. M. Nielsen, and J. Jacobsen, "Buccal delivery of metformin: TR146 cell culture model evaluating the use of bioadhesive chitosan discs for drug permeability enhancement," *Int. J. Pharm.*, vol. 458, no. 2, pp. 254–261, 2013.

[210] H. M. Nielsen and M. R. Rassing, "TR146 cells grown on filters as a model of human buccal epithelium: IV. Permeability of water, mannitol, testosterone and β-adrenoceptor antagonists. Comparison to human, monkey and porcine buccal mucosa," *Int. J. Pharm.*, vol. 194, no. 2, pp. 155–167, 2000.

[211] J. Jacobsen, B. van Deurs, M. Pedersen, and M. R. Rassing, "TR146 cells grown on filters as a model for human buccal epithelium: I. Morphology, growth, barrier properties, and permeability," *Int. J. Pharm.*, vol. 125, no. 2, pp. 165–184, 1995.

[212] H. M. Nielsen, J. C. Verhoef, M. Ponec, and M. R. Rassing, "TR146 cells grown on filters as a model of human buccal epithelium: Permeability of fluorescein isothiocyanate-labelled dextrans in the presence of sodium glycocholate," *J. Control. Release*, vol. 60, no. 2–3, pp. 223–233, 1999.

[213] C. Technologies, "CytoSMART | CytoSMART Omni." [Online]. Available: https://www.cytosmart.com/products/omni. [Accessed: 15-Mar-2020].

[214] D. H. Oh, K. H. Chun, S. O. Jeon, J. W. Kang, and S. Lee, "Enhanced transbuccal salmon calcitonin (sCT) delivery: Effect of chemical enhancers and electrical assistance on in vitro sCT buccal permeation," *Eur. J. Pharm. Biopharm.*, vol. 79, no. 2, pp. 357–363, 2011.

[215] M. Johnson, "Detergents: Triton X-100, Tween-20, and More," *Mater. Methods*, vol. 3, p. 163, 2013.

[216] B. Arechabala, C. Coiffard, P. Rivalland, L. J. M. Coiffard, and Y. De Roeck-Holtzhauer, "Comparison of cytotoxicity of various surfactants tested on normal human fibroblast cultures using the neutral red test, MTT assay and LDH

release," *J. Appl. Toxicol.*, vol. 19, no. 3, pp. 163–165, 1999.

[217] D. DIMITRIJEVIC, A. J. SHAW, and A. T. FLORENCE, "Effects of Some Non-ionic Surfactants on Transepithelial Permeability in Caco-2 Cells," *J. Pharm. Pharmacol.*, vol. 52, no. 2, pp. 157–162, 2000.

[218] G. K. Srivastava *et al.*, "Comparison between direct contact and extract exposure methods for PFO cytotoxicity evaluation," *Sci. Rep.*, vol. 8, no. 1, pp. 1–9, 2018.

[219] J. Kleeff, M. Kornmann, H. Sawhney, and M. Korc, "Actinomycin D induces apoptosis and inhibits growth of pancreatic cancer cells," *Int. J. Cancer*, vol. 86, no. 3, pp. 399–407, 2000.

[220] R. P. Perry and D. E. Kelley, "Inhibition of RNA synthesis by actinomycin D: Characteristic dose-response of different RNA species," *J. Cell. Physiol.*, vol. 76, no. 2, pp. 127–139, 1970.

[221] T. Imura *et al.*, "Preparation and physicochemical properties of various soybean lecithin liposomes using supercritical reverse phase evaporation method," *Colloids Surfaces B Biointerfaces*, vol. 27, no. 3/2, pp. 133–140, 2003.

[222] R. P. Perry and D. E. Kelley, "Persistent synthesis of 5S RNA when production of 28S and 18S ribosomal RNA is inhibited by low doses of actinomycin D," *J. Cell. Physiol.*, vol. 72, no. 3, pp. 235–245, 1968.

[223] J. A. Nicolazzo, B. L. Reed, and B. C. Finnin, "Buccal penetration enhancers - How do they really work?," *Journal of Controlled Release*, vol. 105, no. 1–2. pp. 1–15, 2005.

[224] C.-M. Lehr, *Cell culture models of biological barriers : in vitro test systems for drug absorption and delivery*, 1st editio. CRC Press, 2019.

[225] H. M. Nielsen and M. R. Rassing, "TR146 cells grown on filters as a model of human buccal epithelium: IV. Permeability of water, mannitol, testosterone and beta-adrenoceptor antagonists. Comparison to human, monkey and porcine buccal mucosa.," *Int. J. Pharm.*, vol. 194, no. 2, pp. 155–67, 2000.

[226] A. Iyire, M. Alayedi, and A. R. Mohammed, "Pre-formulation and systematic evaluation of amino acid assisted permeability of insulin across in vitro buccal cell layers," *Sci. Rep.*, vol. 6, 2016.

[227] M. Kirjavainen *et al.*, "Interaction of liposomes with human skin in vitro - The influence of lipid composition and structure," *Biochim. Biophys. Acta - Lipids Lipid Metab.*, vol. 1304, no. 3, pp. 179–189, 1996.

[228] T. Z. Yang, X. T. Wang, X. Y. Yan, and Q. Zhang, "Phospholipid deformable vesicles for buccal delivery of insulin," *Chem. Pharm. Bull. (Tokyo).*, vol. 50, no. 6, pp. 749–753, 2002.

[229] S. Franze, F. Selmin, E. Samaritani, P. Minghetti, and F. Cilurzo, "Lyophilization of Liposomal Formulations: Still Necessary, Still Challenging.," *Pharm. MDPI*, vol. 10, no. 3, pp. 1–23, 2018.

[230] P. A. McCarron, R. F. Donnelly, A. Zawislak, A. D. Woolfson, J. H. Price, and R. McClelland, "Evaluation of a water-soluble bioadhesive patch for photodynamic therapy of vulval lesions," *Int. J. Pharm.*, vol. 293, no. 1–2, pp. 11–23, 2005.

[231] P. A. McCarron, A. D. Woolfson, R. F. Donnelly, G. P. Andrews, A. Zawislak, and J. H. Price, "Influence of plasticizer type and storage conditions on properties of poly(methyl vinyl ether-co-maleic anhydride) bioadhesive films," *J. Appl. Polym. Sci.*, vol. 91, no. 3, pp. 1576–1589, 2004.

[232] P. Rana and R. S. R. Murthy, "Drug Delivery Formulation and evaluation of mucoadhesive buccal films impregnated with carvedilol nanosuspension: a potential approach for delivery of drugs having high first-pass metabolism Formulation and evaluation of mucoadhesive buccal films impregna," *Drug Deliv*, vol. 20, no. 5, pp. 224–235, 2013.

[233] V. M. Patel, B. G. Prajapati, and M. M. Patel, "Formulation, evaluation, and comparison of bilayered and multilayered mucoadhesive buccal devices of propranolol hydrochloride," *AAPS PharmSciTech*, vol. 8, no. 1, pp. E147–E154, 2007.

[234] K. Wasilewska and K. Winnicka, "Ethylcellulose-a pharmaceutical excipient with multidirectional application in drug dosage forms development," *Materials*, vol. 12, no. 20. MDPI AG, 2019.

[235] H. Hamishehkar *et al.*, "The effect of formulation variables on the characteristics of insulin-loaded poly(lactic-co-glycolic acid) microspheres prepared by a single phase oil in oil solvent evaporation method," *Colloids Surfaces B Biointerfaces*, vol. 74, no. 1, pp. 340–349, 2009.

[236] N. Thirawong, J. Nunthanid, S. Puttipipatkhachorn, and P. Sriamornsak, "Mucoadhesive properties of various pectins on gastrointestinal mucosa: An in

vitro evaluation using texture analyzer," *Eur. J. Pharm. Biopharm.*, vol. 67, no. 1, pp. 132–140, 2007.

[237] V. Sluzky, A. M. Klibanov, and R. Langer, "Mechanism of insulin aggregation and stabilization in agitated aqueous solutions," *Biotechnol. Bioeng.*, vol. 40, no. 8, pp. 895–903, 1992.

[238] C. A. Squier, "The permeability of oral mucosa," *Critical Reviews in Oral Biology and Medicine*, vol. 2, no. 1. International and American Associations for Dental Research, pp. 13–32, 1991.

[239] V. F. Patel, F. Liu, and M. B. Brown, "Modeling the oral cavity: In vitro and in vivo evaluations of buccal drug delivery systems," *J. Control. Release*, vol. 161, no. 3, pp. 746–756, 2012.

[240] A. B. Nair, R. Kumria, S. Harsha, M. Attimarad, B. E. Al-Dhubiab, and I. A. Alhaider, "In vitro techniques to evaluate buccal films," *J. Control. Release*, vol. 166, no. 1, pp. 10–21, 2013.

[241] K. Luo, J. Yin, O. V. Khutoryanskaya, and V. V. Khutoryanskiy, "Mucoadhesive and Elastic Films Based on Blends of Chitosan and Hydroxyethylcellulose," *Macromol. Biosci.*, vol. 8, no. 2, pp. 184–192, 2008.

[242] A. Portero, D. Teijeiro-Osorio, M. J. Alonso, and C. Remuñán-López, "Development of chitosan sponges for buccal administration of insulin," *Carbohydr. Polym.*, vol. 68, no. 4, pp. 617–625, 2007.

[243] M. S. Pendekal and P. K. Tegginamat, "Hybrid drug delivery system for

oropharyngeal, cervical and colorectal cancer - in vitro and in vivo evaluation," *Saudi Pharm. J.*, vol. 21, no. 2, pp. 177–186, 2013.

[244] E. M. A. Hejjaji, A. M. Smith, and G. A. Morris, "Designing chitosan-tripolyphosphate microparticles with desired size for specific pharmaceutical or forensic applications," *Int. J. Biol. Macromol.*, vol. 95, pp. 564–573, 2017.

[245] M. A. Moharram, F. M. Reicha, N. Kinawy, and W. Mosad, "Factors controlling the adsorption capacity of crosslinked chitosan beads and natural montmorillonite powder: Comparative study," *J. Appl. Sci. Res.*, vol. 8, no. 11, pp. 5425–5435, 2012.

[246] R. Somashekar, G. K. Gowtham, V. Hegde, S. Meshk, and S. K. Sukrutha, "Synthesis and Characterization of Carbon Soot Particles Doped HPMC Polymer Composites," *J. Res. Updat. Polym. Sci.*, vol. 4, no. 2, pp. 62–68, 2015.

[247] S. Gaisford, "Dosage form design and manufacture: Pharmaceutical preformulation," in *Aulton's Pharmaceutics E-Book: The Design and Manufacture of Medicines*, 5th ed., M. E. Aulton and K. M. G. Taylor, Eds. Elsevier, 2017, p. 403.

[248] S. Yehia, O. El-Gazayerly, and E. Basalious, "Fluconazole Mucoadhesive Buccal Films: In Vitro/In Vivo Performance," *Curr. Drug Deliv.*, vol. 6, no. 1, pp. 17–27, 2009.

[249] Á. Gombás, P. Szabó-Révész, G. Regdon, and I. Erös, "Study of thermal behaviour of sugar alcohols," *J. Therm. Anal. Calorim.*, vol. 73, no. 2, pp. 615–621, 2003.

[250] A. P. Bagre, K. Jain, and N. K. Jain, "Alginate coated chitosan core shell nanoparticles for oral delivery of enoxaparin: in vitro and in vivo assessment.," *Int. J. Pharm.*, vol. 456, no. 1, pp. 31–40, 2013.

[251] A. Mesnukul, K. Yodkhum, and T. Phaechamud, "Solid dispersion matrix tablet comprising indomethacin-PEG-HPMC fabricated with fusion and mold technique," *Indian J. Pharm. Sci.*, vol. 71, no. 4, pp. 413–420, 2009.

[252] G. Buckton, "Scientific principles of dosage form design: Surfaces and interfaces," in *Aulton's Pharmaceutics E-Book: The Design and Manufacture of Medicines*, 5th ed., M. E. Aulton and K. M. G. Taylor, Eds. Elsevier, 2017, p. 57.

[253] M. Koland, K. Vijayanarayana, Rn. Charyulu, and P. Prabhu, "In vitro and in vivo evaluation of chitosan buccal films of ondansetron hydrochloride," *Int. J. Pharm. Investig.*, vol. 1, no. 3, p. 164, 2011.